

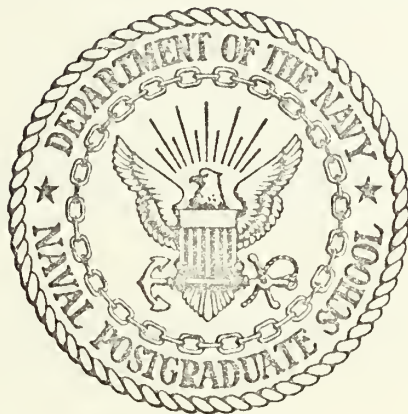
A HOT-WIRE ANEMOMETER STUDY OF
FREE TURBULENT MIXING IN
AXIAL PRESSURE GRADIENTS

Michael Erwin Kearney

Library
Naval Postgraduate School
Monterey, California 93940

NAVAL POSTGRADUATE SCHOOL

Monterey, California



THESIS

A HOT-WIRE ANEMOMETER STUDY OF
FREE TURBULENT MIXING IN
AXIAL PRESSURE GRADIENTS

by

Michael Erwin Kearney

Thesis Advisor:

G.J. Hokenson

December 1972

T153101

Approved for public release; distribution unlimited.



A Hot-Wire Anemometer Study of
Free Turbulent Mixing in
Axial Pressure Gradients

by

Michael Erwin Kearney
Lieutenant, United States Navy
B.S., Naval Postgraduate School, 1972

Submitted in partial fulfillment of the
requirements for the degree of

MASTER OF SCIENCE IN AERONAUTICAL ENGINEERING

from the

NAVAL POSTGRADUATE SCHOOL
December 1972

ABSTRACT

This report was prepared to describe the results of an experimental study of free turbulent mixing in axial pressure gradients. Both the pressure field and the velocity field were extracted using pitot-static probes and both a single normal wire and an X-array hot-wire anemometers. The resulting hot-wire data shown in Figures 1-80 present an excellent visual representation of the physical aspects of turbulent flow.

An analysis of the results of this experiment show conclusively that the Reynolds Stresses in the flow are related by some function to the turbulent kinetic energy; however, no specific function was found that would produce the relationship observed in this study.

TABLE OF CONTENTS

NOMENCLATURE -----	5
I. INTRODUCTION -----	7
II. EQUIPMENT -----	12
A. WIND TUNNEL -----	12
1. General Description -----	12
2. The Inlet -----	12
3. The Test Section -----	13
4. The Blower -----	14
B. DATA SENSORS -----	15
1. General Description -----	15
2. The Traverse -----	15
3. The Pitot-Static Sensor -----	16
4. The Normal Wire Anemometer Probe -----	16
5. The X-Array Anemometer Probe -----	17
III. EXPERIMENTAL PROCEDURE -----	18
A. GENERAL DESCRIPTION -----	18
B. PITOT-STATIC DATA -----	19
C. AXIAL FLOW ANEMOMETER DATA -----	20
D. TWO-DIMENSIONAL FLOW ANEMOMETER DATA -----	23
IV. DISCUSSION OF RESULTS -----	26
TABLES -----	29
FIGURES -----	44
APPENDIX A: DEVELOPMENT OF THE GOVERNING EQUATIONS OF MOTION FOR TURBULENT INCOMPRESSIBLE FLOW -----	141

APPENDIX B: DEVELOPMENT OF EQUATIONS FOR HOT- WIRE ANEMOMETER -----	147
APPENDIX C: DEVELOPMENT OF AN INTEGRATED FORM OF THE MOMENTUM EQUATION FOR THE CALCULATION OF THE LOCAL TURBULENT SHEAR COEFFICIENT -----	154
APPENDIX D: DATA CHECKS -----	160
APPENDIX E: DATA REDUCTION COMPUTER PROGRAM -----	169
APPENDIX F: COMPUTER PROGRAM OUTPUT -----	191
LIST OF REFERENCES -----	253
INITIAL DISTRIBUTION LIST -----	254
FORM DD 1473 -----	255

NOMENCLATURE

A_τ	Boussinesq apparent viscosity
A	X-Array hot-wire lead (u+v)
B	X-Array hot-wire lead (u-v)
C	Constant in hot-wire calculations
C_l	Constant in apparent viscosity relation
C_τ	Local turbulent shear coefficient
C_{uv}	Correlation coefficient
d	Wake generator diameter
e	Linear output from hot-wire
H	Shape factor
i,j	Indicates i or j direction ($i=1,2,\dots$ $j=1,2,\dots$)
k	Turbulent kinetic energy
ℓ	Prandtl mixing length
p	Pressure
q	Dynamic pressure
r	General flow parameter
$S(x)$	Apparent viscosity constant
T	Characteristic time
t	Time
x,y,z	Spatial Coordinates
	x - Axial
	y - Lateral
u,v,w	Corresponding velocities
v^*	Characteristic velocity

β	Constant in hot-wire calculations
δ	Displacement thickness
δ_3	Energy thickness
ϵ	Mixing length parameter = $k^m \ell^n$
θ	Momentum thickness
μ	Laminar viscosity
μ_t	Apparent viscosity
ν	Laminar kinetic viscosity
ν_t	Apparent kinetic viscosity
ρ	Density
τ	Reynold's Stress
∇	Differential operator DEL
$\int_a^b dy$	Integral from a to b with respect to y
$\frac{\partial u}{\partial r}$	Partial derivative with respect to r
$\frac{du}{dr}$	Ordinary derivative with respect to r
$ $	Indicates absolute value

Subscripts

A	Parameter of lead A on hot-wire
B	Parameter of lead B on hot-wire
e	Local external flow conditions
x,y	Indicates partial differentiation with respect to x,y
τ	Shear related quantity

Superscripts

—	Indicates a time averaged quantity
'	Designates a fluctuating quantity

I. INTRODUCTION

In most real fluid flows the transition from laminar to turbulent flow carries the fluid mechanist from a situation where he can safely predict the values of the flow-field parameters from the solution of the Navier-Stokes Equations to one where predictions are obtainable only on the average, at best. Yet most practical applications require at least some consideration of turbulence and how it can be dealt with. In the past the engineer has assumed various plausible hypotheses in order to introduce a measure of order and predictability to turbulent flow. It is the intention of this study, then, to attempt to experimentally verify certain of these hypotheses. Before describing the currently accepted assumptions regarding turbulent flow, a general review of their history will be presented to provide the necessary background information.

A turbulent flow is defined as one in which an irregular fluctuation or mixing motion is superimposed on the principal fluid motion. Its onset is accompanied by a noticeable change in the law of resistance. In the case of laminar pipe flow, the longitudinal pressure gradient which maintains the motion is proportional to the first power of the velocity. By contrast, in turbulent flow this pressure gradient becomes nearly proportional to the square of the mean flow velocity. In order to calculate flow field values

in a turbulent field, then, some logical hypothesis must be made to account for this change in the apparent viscosity of the flow. First, it is generally assumed that the fluid motion can be separated into a mean and a fluctuating part which are linearly related to the total fluid motion in such a way that a flow parameter (r) can be defined

$$r = \bar{r} + r' \quad (I-1)$$

These definitions can be substituted into the equations of motion to produce a new set of equations involving mean and fluctuating terms and their cross products. Assuming that the time average of the fluctuations is zero, the equations may be averaged to get the following momentum equation for a two-dimensional mean flow (see Appendix A for the complete development):

$$\bar{u} \frac{\partial \bar{u}}{\partial x} + \bar{v} \frac{\partial \bar{u}}{\partial y} = u_e \frac{du_e}{dx} + v_t(x) \frac{\partial^2 \bar{u}}{\partial y^2} \quad (A-22)$$

where the apparent kinematic viscosity ($v_t(x)$) is a function of the turbulent flow field, and is calculated by using some logical empirical hypothesis for approximating its value.

Since only the mean values of the flow parameters are known, some means of relating these values to the Reynolds stresses produced by the fluctuating part of the flow is required. The first hypothesis for relating these quantities

was proposed by J. Boussinesq,

$$\tau_o = -\rho \overline{u'v'} = A_\tau \frac{\partial \bar{u}}{\partial y} \quad (I-2)$$

where A_τ is an apparent or eddy viscosity that is not a fluid property but depends on the structure of the flow field.

$$A_\tau = \rho v_t(x)$$

This apparent viscosity is generally assumed to be proportional to some characteristic velocity (v^*) times the mean velocity gradient:

$$A_\tau = v^* \frac{\partial \bar{u}}{\partial y} \quad (I-3)$$

In 1925 Prandtl made an important advance in turbulent theory by introducing the concept of mixing length and the relation,

$$\tau_t = \rho \ell^2 \left| \frac{d\bar{u}}{dy} \right| \frac{d\bar{u}}{dy} \quad (I-4)$$

$$v_t(x) = \ell^2 \left| \frac{du}{dy} \right|$$

where

ℓ = mixing length

$\ell \left| \frac{du}{dy} \right|$ = characteristic velocity

This relation has produced relatively accurate values for some limited cases. However, this definition of the kinematic viscosity implies that it should vanish where the velocity gradient is zero, which is contradictory to experimental evidence. Several subsequent hypotheses were proposed by Taylor, Von Karman, and Prandtl himself, but they were all limited in application to free turbulent flow.

Later, in an effort to develop a universally valid model for the function μ_t , Prandtl introduced an energy-based hypothesis which was subsequently improved on by Emmons (1954), and Glushko (1965),

$$\mu_t \propto \rho k^{1/2} \ell \quad (I-5)$$

$$k \equiv (\bar{u}^2 + \bar{v}^2)/2$$

Here k was found to be a better characteristic velocity than in the earlier mixing length hypothesis, but the length scales were difficult to ascertain. More modern theories, referred to as two-equation viscosity models, use sophisticated analytical methods to determine this length scale. The apparent viscosity is first assumed to be related to the kinetic energy. Then some hypothesis of the form

$$\epsilon = k^m \ell^n$$

is made to make it possible to calculate the characteristic length. One of the most accepted of these relations was introduced by Chou in 1945:

$$\epsilon \equiv k^{3/2}/\ell \quad (\text{I-6})$$

$$\mu_t = C_1 \rho k^2/\epsilon$$

Thus

$$\mu_t = C_1 \rho k^{1/2} \ell \quad (\text{I-7})$$

It was this type of assumption which initiated the project reported here. Using both pitot-static and hot-wire anemometer sensors, an attempt was made to validate the hypothesis that shear was predominantly a function of the turbulent kinetic energy.

II. EQUIPMENT

A. WIND TUNNEL

1. General Description

The tunnel consists essentially of three major components: the inlet, the test section, and the blower as shown in Figures 81-83. The inlet was designed to contract the slow moving inlet air to a high-velocity parallel flow at the entrance of the test section. At this point, a plexiglas cylinder was introduced into the flow to generate a wake velocity defect which was then subjected to a constant adverse pressure gradient. After leaving the test section, the flow was maintained at a constant area through a length of tubing, then diffused and directed into the centrifugal blower and exhausted vertically.

2. The Inlet

The inlet section of the tunnel was composed of the inlet bellmouth, the plenum chamber, and the nozzle. Incoming air was first contracted into a two-foot square plenum section. This contraction was accomplished by the inlet bellmouth constructed from eight-inch diameter aluminum pipe halves. The corner seams were filled with a sanded epoxy fillet to effect a smooth transition of the air into parallel flow. The plenum section consisted of four two-foot square by one-foot long steel sections bolted together. Cork gaskets were inserted between the sections to prevent the influx

of air at the joints and to allow for undisturbed air flow over these junctions. A four-inch thick section of quarter-inch honeycomb was installed to straighten the air flow and prevent swirling. Next, two copper screens were inserted to reduce the ambient turbulence level in the flow. Finally, the air passed from the plenum chamber to the test section through a two-foot long steel nozzle with an exit area of forty-nine square inches (seven inches square), and produced a contraction ratio of 11.76. Static pressure ports were located on the right side of the nozzle at the inlet and exit for determination of the exit dynamic pressure.

3. The Test Section

The test section consisted of two parallel, vertical side walls separated by flexible and adjustable top and bottom walls. The flexible walls were constructed from one-eighth inch Plexiglas fastened to the nozzle with piano hinges. As described in Reference 1, these walls could be varied to produce a variety of different pressure gradients, but for this experiment they were set to create a constant adverse pressure gradient followed by a constant favorable pressure gradient.

One vertical wall was provided with thirteen slots for inserting data sensors. These slots were nineteen inches high, three-eighths of an inch wide, and spaced five inches apart. A filler plug for each slot was carefully hand milled, and polished to prevent disturbing the flow along the wall when the slots were not in use. A thin

aluminum strip was wedged over each filler plug to ensure a tight fit. When these plugs were removed to insert probes, a sliding teflon seal was used to prevent an influx of air through the slot (see Figure 84).

The other vertical wall of the test section had three rectangular access holes along the axial centerline for adjustments and measurements. In addition, as one can see in Fig. 85, thirty-three static pressure ports were inserted along the axial centerline at one-and-one-half inch intervals. A manometer bank, shown in Fig. 86, connected to these static pressure ports provided a visual indication of the uniformity of the pressure distribution, as well as indicating the presence of any regions of separation. As an additional indication of possible flow separation, several rows of tufts were attached to the walls in critical areas.

Having produced the desired environment for the type of air flow that this study was initiated to investigate, a turbulent wake velocity defect was introduced into the tunnel by placing a one-inch diameter cylinder in the inlet of the test section. In order to ensure a turbulent boundary layer at separation from the cylinder, a thin strip of abrasive, shown in Fig. 87, was attached to the stagnation line of the cylinder.

4. The Blower

After exiting the test section, the air passed through two seven-inch square, four-foot long steel sections into a diffusor and then into the blower. A centrifugal

blower operating at three thousand revolutions per minute was utilized to pull air through the tunnel. The air was then exhausted vertically through 4 sections of steel pipe which contained two dampers for the control of the total mass flow through the tunnel.

B. DATA SENSORS

1. General Description

The data for this study were taken with the three different types of probes shown in Fig. 88: A pitot static probe, a single normal hot wire probe, and an x-wire hot wire probe. A detachable traversing mechanism was used to position the probes vertically, and the values were recorded by hand or on an x-y plotter.

2. The Traverse

This apparatus was equipped with two constant speed motors to drive the mechanism across the nineteen-inch vertical span of the tunnel. The probe was clamped to a movable support on the traverse, and the vertical position measured by indexing a reference mark on this mechanism to a scale fixed to the frame of the apparatus. This scale was readable to one one-hundreth of an inch. A rack-and-pinion gearing system drove a potentiometer that was also attached to the movable support to produce an electrical position signal for the abscissa of the x-y plotter.

3. The Pitot-Static Sensor

A Prandtl-type pitot-static pressure probe Model # PBA-12-F-11-KL, built by United Sensors and measuring 81 hundredths of an inch from stem to tip, was used to obtain dynamic and local static pressures at one-tenth of an inch intervals through the wake. These pressures were read on two variable angle, water-filled U-tube manometers referenced to atmospheric pressure. This reference was chosen to reduce the fluctuations in the water levels. As described in Reference 1, taking P-total minus P-static directly creates very large fluctuations that make accurate data taking difficult. By separating the two readings, the fluctuations in the manometer were significantly reduced, but not eliminated.

A third manometer was attached to the plenum chamber of the tunnel, and referenced to the last static pressure port on the test section. As one can see in Fig. 89, all of these manometers were equipped with portable plastic sights which restricted one's line of sight to a plane perpendicular to the manometer, thus precluding possible parallax and assuring consistent readings.

4. The Normal Wire

This sensor, shown in Fig. 90, was a single-wire anemometer probe, Model # 1150 built by Thermo-Systems Inc. (TSI), measuring 4 inches from stem to tip. Again the probe was fixed to the traverse for data collection. The lead

from the sensor was connected to a 1054A-30 anemometer module with a 1051-2 monitor and power supply, also built by Thermo-Systems Inc. (TSI) (See Fig. 91 & 92), which converted the voltage changes to readable data. Next these data were fed into a TSI 1015C correlator that was used to separate the alternating and D.C. signals (see Appendix B). The output of the correlator was connected to an analog data processing computer which indicated the mean square average output of the correlator. Finally, the output of this apparatus was connected to the ordinate of the X-Y plotter, recalling that a potentiometer on the traverse was connected to the abscissa.

5. The X-Wire Anemometer Probe

The last sensor, a Model # 1055 built by TSI, consisted of two hot wires oriented at 45° to the axis of the probe such that the output signals of the wires corresponded to $u + v$ and $u - v$ respectively (See Appendix B). These data were processed in the same manner as the normal wire data except for the use of several additional algebraic functions of the 1015C correlator.

III. EXPERIMENTAL PROCEDURE

A. GENERAL DESCRIPTION

The previous study described in Reference 1 had configured the test section to produce a constant, adverse-favorable pressure gradient. Since this was the environment required for this study, no changes were made in the test section except to ensure a tight seal between the vertical and the movable walls by the addition of strips of clay along the lines of contact.

The actual collection of data was carried out in three distinct steps. First, the pitot-static system was used to collect the total and static pressure data that were introduced into the computer program, described in Appendix E, and used to calculate the flow parameters. Next, a normal-wire anemometer was inserted in the test section to gather information on both the mean and fluctuating axial velocities. These hot-wire values were converted to velocities by equating the maximum voltage at each station to the maximum value of the velocity calculated from the pitot-static data. Finally, an X-array hot-wire anemometer probe was used to get both mean and fluctuating data for velocities in both the axial and the lateral directions, as well as Reynolds stresses. Throughout the experiment a constant wind tunnel speed was maintained by ensuring that the total pressure of the Plenum chamber, minus the static pressure from the test

section, was no less than 9.90 nor greater than 10.00 inches of water on a thirty-degree inclined manometer.

B. PITOT-STATIC DATA

In this phase of the experiment all data were recorded (to an estimated accuracy of one one-hundreth of an inch) from water-filled U-Tube manometers connected to the pitot-static probe. At each of eleven stations downstream from the cylinder the static and total pressures were recorded at intervals through the wake of one-tenth of an inch. At each station the probe was moved near the upper limit of the traverse and situated in the free stream, then the traverse was marched across the flow, recording the values of total and static pressure at each increment. The initial determination of the freestream was accomplished by observing that the manometer becomes almost totally insensitive to changes in the vertical direction in the undisturbed flow. A change in total pressure of less than three one-hundredths of an inch for three consecutive positions was taken to be the edge of the wake defect.

As the traverse approached the center of the wake the intensity of the turbulence became so large that accurate readings were difficult to obtain due to fluctuations in the water level. However, by observing the water levels for a long period of time one could determine an average height that is estimated to be accurate to three one-hundredths of one inch. The same criterion was used at the bottom of the

flow channel, as at the top, to determine when the freestream had been reached.

C. AXIAL FLOW ANEMOMETER DATA

The probe used in this phase was a single normal hot-wire anemometer designed to produce voltage changes corresponding to velocity fluctuations in the flow. When the tungsten wire was exposed to the air in the wind tunnel it was cooled by the flow over it, thus requiring additional voltage to maintain a constant temperature in the wire. It is apparent, then, that the velocity in the tunnel is proportional to the voltage required to maintain a constant temperature in the hot-wire. The probe is placed in a bridge circuit in the TSI module, and its output linearized to produce a linear function of velocity of the form:

$$e = c (\bar{u} + u') \quad (\text{III-1})$$

where,

$$u = \bar{u} + u'$$

$$\bar{u} = \text{mean flow velocity}$$

$$u' = \text{fluctuating velocity}$$

and

$$\int_0^T u' \, dT \equiv 0 \quad (\text{III-2})$$

Therefore if the DC output on the correlator is selected, the output would be

$$e = c(\bar{u} + u')$$

However, since this signal was a strong function of time, the data were averaged using a low pass filter with a time constant (T) equal to 0.6 secs. The final output of the averager was simply

$$\bar{e} = c\bar{u} \quad (\text{III-3})$$

and this quantity was plotted versus the traverse position.

The second type of data for this phase was taken with the selector switch of the correlator on AC, thus producing an output corresponding to the fluctuating portion of the flow:

$$e' = cu' \quad (\text{III-4})$$

This signal was also a strong function of time but, because of the nature of the term u' , as expressed in (III-2), the signal could not be directly averaged. Therefore, in order to provide a finite measure, u' was first squared and then averaged and plotted versus the traverse position, since

$$\frac{1}{T} \int_0^T (u')^2 d\tau \neq 0$$

Once a plot of \bar{e} and e' had been obtained, the velocity could be calculated by solving equations (III-3) and (III-4) to get

$$\bar{u} = 1/C \bar{e}$$

$$\overline{u'^2} = \frac{1}{C^2} \overline{e'^2}$$

where from equation (B-5) in Appendix B

$$C \equiv \frac{\overline{e_e}}{\overline{u_e}} \quad (\text{III-5})$$

In order to produce accurate values for \bar{u} and u' in the laboratory environment the equipment had to be carefully adjusted for each individual flow. Specific instructions for this procedure can be found in the TSI operational manual but, in general, the first step was to adjust the control resistance to balance the bridge circuit. This adjustment was accomplished by setting the control resistor to a value that would produce a specified voltage change on the monitor. At this point the system was ready to run and the next step was to select the linearized operational mode on the monitor, position the probe in the free stream, and maximize the frequency response of the wire by setting the inductance to the minimum value that would not cause the signal to oscillate. The stability of the system was

monitored during this step on a dual-beam oscilloscope to ensure no oscillations were present in the signal. When the probe had been adjusted to the flow a digital voltmeter was used to check the multiplier-averager for correct operation. Then the x-y plotter was set to record the signal on an appropriate scale.

Now that the system had been checked for correct operation, it was positioned as close to the upper wall as practicable and the pen was dropped on the plotter. The sensor was then driven across the wake to a point near the bottom wall, and the pen lifted. After changing the paper in the plotter, the same procedure was used to make a traverse back to the top of the test section. A total of four traverses were made at each station to record both the mean flow and the mean square of the fluctuating flow. Each of these quantities was recorded at two different scales in order to facilitate translation into digital data for the IBM-360.

D. TWO-DIMENSIONAL ANEMOMETER DATA

The basic operation and accuracy checks of the x-array hot wire are very similar to those of the single normal wire. However, some additional complications are created by having two separate wires on the probe. The terms are now defined,

$$e = \bar{e} + e'$$

$$u = \bar{u} + u'$$

$$v = \bar{v} + v'$$

As explained in Appendix B, the outputs of the two wires (A & B) were

$$e_A = C_A (u + v)$$

$$e_B = C_B (u - v)$$

Thus, for a given flow, the values of C_A and C_B cannot be determined easily. In order to find these constants one must have

$$C_A = C_B = C$$

In this study the author used a basic physical characteristic of pipe flow to set these constants equal, i.e., that the lateral velocity must be zero at the centerline. Recall that, at $y = 0$

$$e_A = C_A u = C_B u = e_B$$

Thus the value of $(e_A - e_B)$ was set equal to zero so the constant (C) could be defined as in (III-5). Note that this procedure is equivalent to setting $V = 0$ at the centerline since,

$$e_A - e_B = C(u + v) - C(u - v) = 2Cv$$

$$e_A + e_B = C(u + v) + C(u - v) = 2Cu$$

The actual position of the centerline was determined from the pitot-static data taken in phase 1.

Again, the wires were adjusted to the individual flow at each station and the data were taken in the same manner as described in the previous section. However, several more traverses were required to get all of the data available to the x-array hot wire. The settings on the correlator, and the corresponding flow parameters, are listed below. All barred quantities were taken with the correlator on DC, and averaged before plotting. The primed quantities were taken with the correlator on AC, and squared, averaged, and then plotted.

<u>SETTING</u>	<u>RESULT</u>	<u>SETTING</u>	<u>RESULT</u>
$(\overline{A+B})$	\overline{u}	$\overline{(A+B)'^2}$	$\overline{u'^2}$
$(\overline{A-B})$	\overline{v}	$\overline{(A-B)'^2}$	$\overline{v'^2}$
\overline{A}	$\overline{u+v}$	$\overline{A'^2}$	$\overline{(u+v)'^2}$
\overline{B}	$\overline{u-v}$	$\overline{B'^2}$	$\overline{(u-v)'^2}$

IV. DISCUSSION OF RESULTS

Since this study was intended to carry out an investigation of free turbulent mixing in a constant pressure gradient, it would be appropriate to discuss how close the actual experimental environment approached that desired for the study. It can be easily seen in Fig. 21 that a wake velocity defect was initially created by the cylinder as desired, and the magnitude of $\overline{u'^2}$ in Fig. 41 clearly shows that the flow was, in fact, turbulent. However, it can also be seen that the adverse pressure gradient encourages the formation of a large boundary layer which, as it mixes downstream, interacts with the wake defect, tending to raise some doubt that free turbulent mixing is still present downstream of Station 6. It is especially significant to note that the turbulence near the wall builds up from a negligible value at Station 1 (see Fig. 41-50) to a value greater than that induced into the wake by the cylinder midway down the test section. As expected, the wake defect eventually begins to mix out in the favorable pressure gradient.

By comparing the stress calculated from the pitot-static data with that from the hot-wire anemometer, one can easily see that in both cases the stress is zero on the centerline, then builds up to a maximum as the velocity gradient nears the region of its maximum. At the later stations, both

types of data show a shear stress sign reversal, and its magnitude begins to increase as the traverse approaches the edge of the test section. This trend in the data was probably reflecting the increasing interaction with the boundary layer as the air flowed downstream.

Due to the greater capabilities of the hot-wire probe, it was used to take data very near the wall, and the velocity can be seen to fall rapidly in the vicinity of the boundary layer. The hot-wire data (Figures 1-80) were then used to prepare Table I to display the value of the correlation coefficient (C_{uv}) and η in the turbulent flow field. Note that the correlation coefficient C_{uv} approaches zero at the centerline, and reaches its maximum where the shear is a maximum as predicted by Schlichting (See Fig. 18.4 Ref. 2).

Considering the relation between kinetic energy and the shear stress, it is easy to see in Table II that both parameters reach a maximum at nearly the same point in the flow. Comparing the anemometer with the pitot-static data in Appendix F, the maximum shear there also occurs at the lateral position corresponding to the kinetic energy maximum. Thus, it is clear that at least some significant functional relationship exists between them. The ideal relationship would be that postulated by the theory of eddy viscosity, that the two parameters differ only by a constant that is a function of x . The slight displacement of the two maximums in this case would imply that the relationship between

k and C_τ is, in reality, a more complex function. As an additional attempt to clarify the relation between kinetic energy and shear stress, equation (7) was approximated by taking the characteristic velocity as the square root of the kinetic energy, and

$$S = C_1 \ell = S(x) \quad (\text{IV-1})$$

As a result, the relation for Reynolds stress becomes,

$$\frac{\tau_k}{\rho} = \mu_t \frac{\partial \bar{u}}{\partial y} = S(x) k^{1/2} \frac{\partial \bar{u}}{\partial y} \quad (\text{IV-2})$$

The values for equation (IV-2) were calculated and plotted versus traverse position for several stations from the data in Table II, which was derived from Figures 21-80. The results of these plots are shown in Figures 93-97. Once again, there is a definite similarity between the results of the approximating equation, (7), and the calculation of $\overline{u'v'}$ from the hot wire data. In this case the shapes of the curves were exceptionally similar, but the maximums were still displaced by a small amount, preventing direct correlation by multiplication by a constant. The author feels that a more comprehensive analysis of the data in this report is warranted by the obvious visual relationship of the curves. An in-depth analysis might well uncover a significantly better model for calculating turbulent flow fields than are currently in use.

TABLE I

Calculation of The Correlation
Coefficient and Eta

$$C_{uv} = \frac{\overline{e_A'^2} - \overline{e_B'^2}}{\sqrt{(e_A + e_B)' ^2} \sqrt{(e_A - e_B)' ^2}} \quad \eta = \frac{2(\overline{e_A'^2} + \overline{e_B'^2})}{(e_A + e_B)' ^2 + (e_A - e_B)' ^2}$$

Station 1		
Position	C	η
10.5	-.6529	1.310
11.0	-.4881	1.341
11.5	-.4353	1.494
12.0	-.2092	1.745
12.5	-.0319	1.812
13.0	.1501	1.782
13.5	.2857	1.489
14.0	.3112	1.292
14.5	.1631	1.243
Station 2		
9.5	-.4045	.9032
10.0	-.4170	1.250
10.5	-.2029	1.012
11.0	-.2353	.9706
11.5	-.2470	1.058
12.0	-.3108	1.243

Position	C	17
12.5	-.0381	1.219
13.0	.1172	1.249
13.5	.1880	1.188
14.0	.2576	1.343
14.5	.0851	1.277
15.0	.0683	1.153
15.5	-.2887	.875
Station 3		
9.0	-.4544	.878
10.0	-.3404	.922
11.0	-.3661	1.122
12.0	-.2401	1.227
13.0	.0915	1.281
14.0	.1889	1.211
15.0	.1097	1.071
Station 4		
8.0	-.6876	1.108
9.0	-.5699	1.281
10.0	-.4562	1.361
11.0	-.3599	1.426
12.0	-.1709	1.472
13.0	.0983	1.474
14.0	.2615	1.485

	4 (cont.)	
Position	C	η
15.0	.2815	1.314
16.0	.2400	1.194
17.0	-.0423	1.036
	Station 5	
8.0	-.2750	1.083
9.0	-.3340	1.176
10.0	-.3470	1.317
11.0	-.3040	1.341
12.0	-.1508	1.388
13.0	.0582	1.427
14.0	.1907	1.390
15.0	.2584	1.317
16.0	.1848	1.161
17.0	-.0418	1.105
	Station 6	
7.0	-.0154	1.145
8.0	-.2951	1.125
9.0	-.2809	1.165
10.0	-.2711	1.269
11.0	-.4096	1.119
12.0	-.0900	1.254
13.0	.0295	1.374

6 (cont)		
Position	C	17
14.0	.2051	1.296
15.0	.2327	1.283
16.0	.1704	1.212
17.0	.0461	1.049
Station 7		
7.0	.0684	1.103
8.0	-.1341	1.109
9.0	-.2719	1.158
10.0	-.3906	1.291
11.0	-.2718	1.279
12.0	-.1534	1.228
13.0	.0857	1.264
14.0	.2013	1.306
15.0	.1845	1.243
16.0	.1131	1.176
17.0	.0246	1.048

Station 8		
Position	C	γ
7.0	.1517	1.144
8.0	-.1027	1.010
9.0	-.3392	1.138
10.0	-.7895	1.095
11.0	-.7298	1.194
12.0	-.3909	1.205
13.0	.1279	1.165
14.0	.4510	1.232
15.0	.2654	1.200
16.0	.0634	1.151
17.0	-.4360	1.185
Station 10		
9.0	.0454	1.095
10.0	-.7389	1.130
11.0	-.8439	1.079
12.0	-.3313	1.080
13.0	.2910	1.091
14.0	.4818	1.105
15.0	-.0229	1.145
16.0	-.0116	1.020

Station 9		
Position	C	<i>η</i>
9.0	-.3614	1.123
10.0	-.6485	1.063
11.0	-.7565	1.130
12.0	-.3710	1.091
13.0	.1835	1.143
14.0	.5674	1.146
15.0	.3130	1.140

TABLE II
Calculation of Kinetic Energy
And Shear Stress Parameters

$$\overline{u'v'} = \beta^2(\overline{e_A'^2} - \overline{e_B'^2}) \quad k = \beta^2[\overline{(e_A + e_B)'^2} + \overline{(e_A - e_B)'^2}]$$

Station 1		
Position	k	$\overline{u'v'}$
12.8	993.9	36.81
13.0	965.0	70.99
13.2	928.2	84.14
13.4	870.3	94.66
13.6	780.9	115.69
13.8	657.3	89.40
14.0	512.7	78.88
14.2	331.3	47.33
14.4	239.3	34.18
14.6	155.1	13.15
Station 2		
12.0	535.0	-83.0
12.5	545.0	10.4

Station 2 (cont.)

Position	k	$\overline{u'v'}$
12.8	534.0	20.74
13.0	531.4	31.11
13.2	521.0	36.29
13.4	505.5	31.11
13.6	466.6	20.74
13.8	414.8	7.78
14.0	362.9	5.18
14.2	311.1	2.59
14.4	267.0	5.18
14.6	223.0	5.18
14.8	189.3	7.78
15.0	153.0	5.18

Station 3

12.4	378.5	-22.08
12.6	376.9	-11.04
12.8	376.9	3.15
13.0	380.1	15.77
13.2	381.7	28.39
13.4	378.5	28.39
13.6	364.3	29.97
13.8	343.8	29.97

Station 3 (cont.)

Position	k	$\overline{u'v'}$
14.0	320.2	29.97
14.2	296.5	23.66
14.4	265.0	22.08
14.6	236.6	17.35
14.8	205.0	12.62
15.0	176.6	9.46
15.2	135.6	6.31
15.4	119.9	3.15

Station 4

13.0	235.9	11.53
13.2	237.5	16.14
13.4	238.2	21.52
13.6	237.5	25.36
13.8	235.1	27.66
14.0	232.8	29.97
14.2	226.7	32.28
14.4	219.0	30.74
14.6	209.8	25.36
14.8	199.0	23.05
15.0	186.0	19.98
15.2	172.9	16.91

Station 4 (cont.)

Position	k	$\overline{u'v'}$
15.4	156.8	16.91
15.6	139.9	12.30
15.8	139.1	10.76
16.0	101.4	8.45
16.2	86.1	7.69
16.4	72.2	6.15
16.6	61.5	3.84
16.8	52.3	3.84

Station 5

12.0	217.5	-14.32
12.2	214.8	- 8.05
12.4	213.0	- 3.58
12.6	213.0	0.90
12.8	215.7	4.48
13.0	217.5	7.16
13.2	221.0	11.63
13.4	224.6	14.32
13.6	228.2	17.00
13.8	230.0	19.69
14.0	232.7	21.48
14.2	231.8	24.16
14.4	229.1	25.95

Station 5 (cont.)

Position	k	$\overline{u'v'}$
14.6	226.4	25.95
14.8	221.9	25.95
15.0	214.8	26.85
15.2	208.5	26.85
15.4	197.8	26.85
15.6	187.9	24.16
15.8	176.3	21.48
16.0	166.5	17.90
16.2	152.1	14.32
16.4	137.8	11.63
16.6	125.3	8.95
16.8	107.4	1.79
17.0	93.97	- 1.79
17.2	85.0	- 2.69
17.4	78.8	- 3.58

Station 6

13.0	191.1	2.71
13.2	197.5	6.34
13.4	202.0	10.87
13.6	205.6	13.59
13.8	208.4	18.12
14.0	211.1	20.84

Station 6 (cont.)

Position	k	$\overline{u'v'}$
14.2	212.0	23.55
14.4	212.0	24.46
14.6	211.1	24.46
14.8	208.4	23.55
15.0	204.7	22.65
15.2	199.3	21.74
15.4	193.9	22.65
15.6	188.4	19.02
15.8	181.2	16.31
16.0	174.8	13.59
16.2	164.0	10.87
16.4	153.1	7.25
16.6	144.9	5.44
16.8	135.0	3.62
17.0	129.5	2.72
17.2	121.4	0.0
17.4	116.9	- 3.62

Station 7

13.0	169.3	10.87
13.2	173.9	14.49
13.4	178.4	17.21
13.6	182.9	18.11

Station 7 (cont.)		
Position	k	$\overline{u'v'}$
13.8	188.4	18.11
14.0	192.9	18.11
14.2	195.6	18.11
14.4	198.3	18.11
14.6	198.3	18.11
14.8	215.0	18.11
15.0	193.8	17.21
15.2	190.2	17.21
15.4	184.7	15.40
15.6	180.2	14.49
15.8	173.9	11.77
16.0	169.3	9.06
16.2	163.9	8.15
16.4	158.5	7.25
16.6	154.0	6.34
16.8	151.3	4.53
17.0	148.5	1.81
17.2	147.6	- 3.62
17.4	149.4	-10.87
17.6	154.9	-16.30

Station 8		
Position	k	$\overline{u'v'}$
15.0	171.8	11.34
15.2	170.1	9.60
15.4	166.6	9.60
15.6	164.0	7.85
15.8	159.6	5.23
16.0	156.1	2.62
16.2	151.8	- 1.75
16.4	148.3	- 5.23
16.6	147.4	- 9.60
16.8	150.0	- 14.83
17.0	160.5	- 18.32
Station 9		
12.0	136.4	-13.22
12.2	133.1	- 9.92
12.4	131.4	- 5.79
12.6	131.4	- 1.65
12.8	133.9	2.48
13.0	138.8	6.61
13.2	140.5	10.74
13.4	143.8	14.05
13.6	147.1	17.36
13.8	151.2	20.66

Station 9 (cont.)		
Position	k	u'v'
14.0	152.9	21.49
14.2	152.1	20.66
14.4	149.6	19.83
14.6	147.1	16.53
14.8	143.8	14.88
15.0	142.1	11.57
Station 10		
12.0	123.0	-10.66
12.2	119.7	- 6.56
12.4	119.7	- 1.64
12.6	121.4	2.46
12.8	124.6	6.56
13.0	126.3	9.84
13.2	132.0	13.94
13.4	135.3	16.40
13.6	138.6	18.04
13.8	141.1	19.68
14.0	140.2	17.22
14.2	138.6	15.58
14.4	138.6	12.30
14.6	137.8	7.38
14.8	136.1	3.28

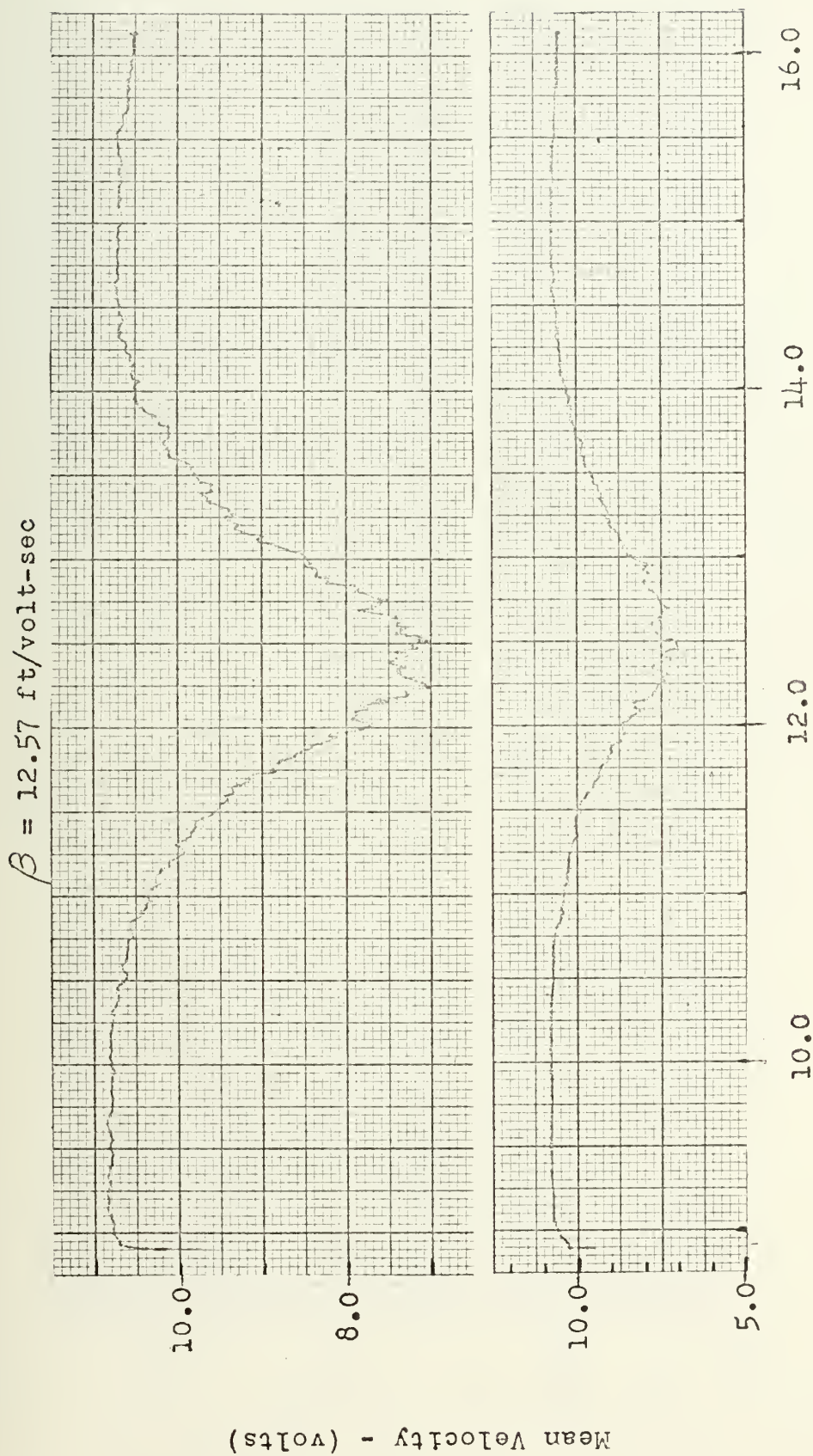


FIGURE 1
Station 1 Normal Wire Mean Velocity

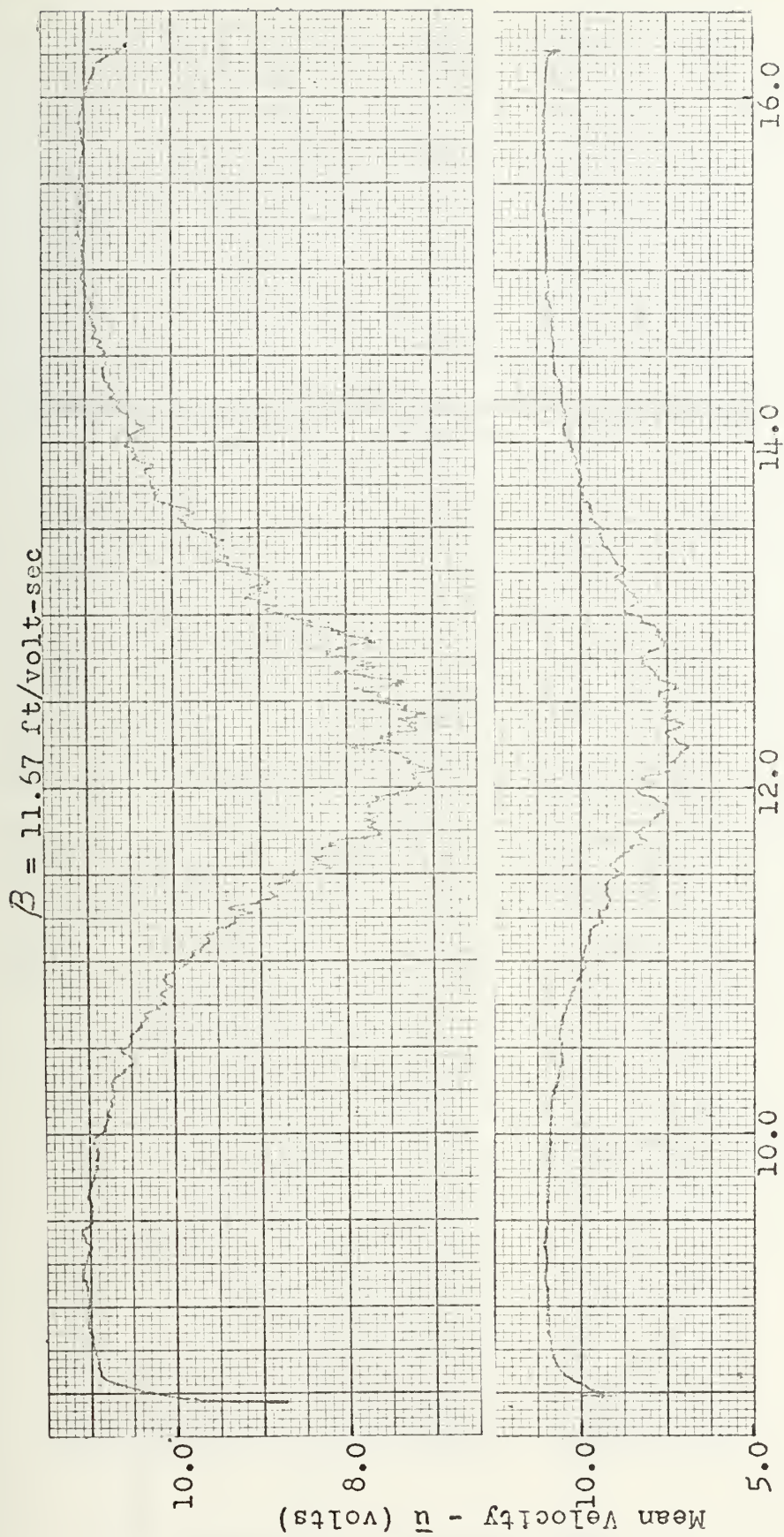
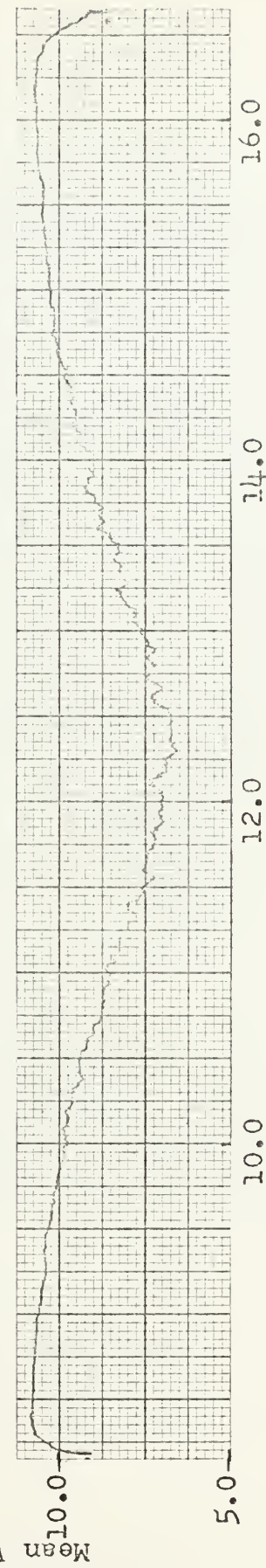
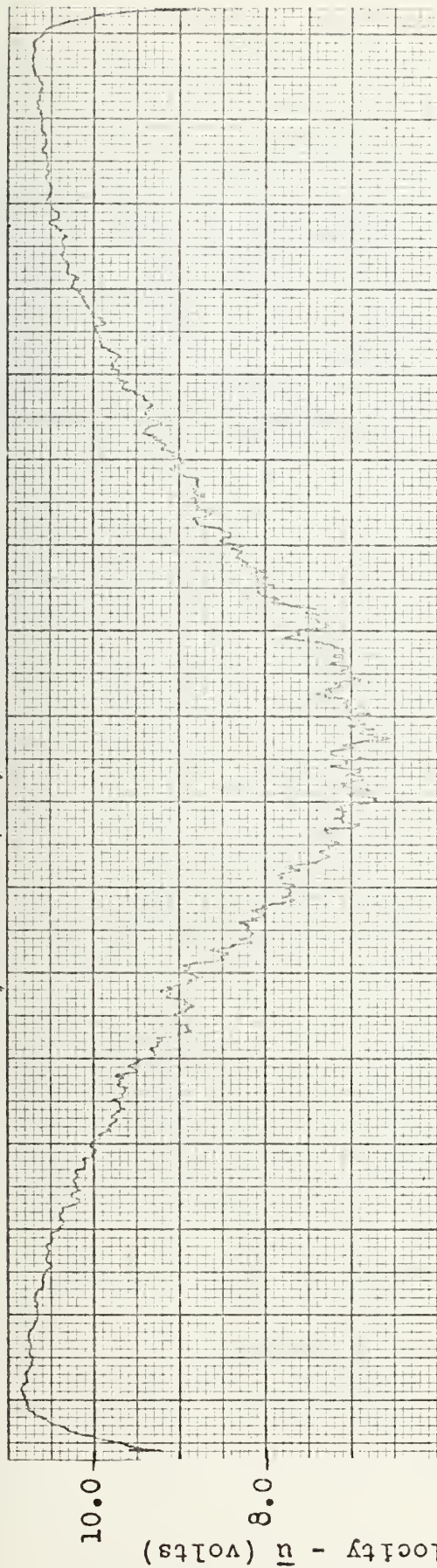


FIGURE 2

Station 2 Normal Wire Mean Velocity

$$\beta = 11.64 \text{ ft/volt-sec}$$



Station 3 Normal Wire Mean Velocity

FIGURE 3

Station 3 Normal Wire Mean Velocity

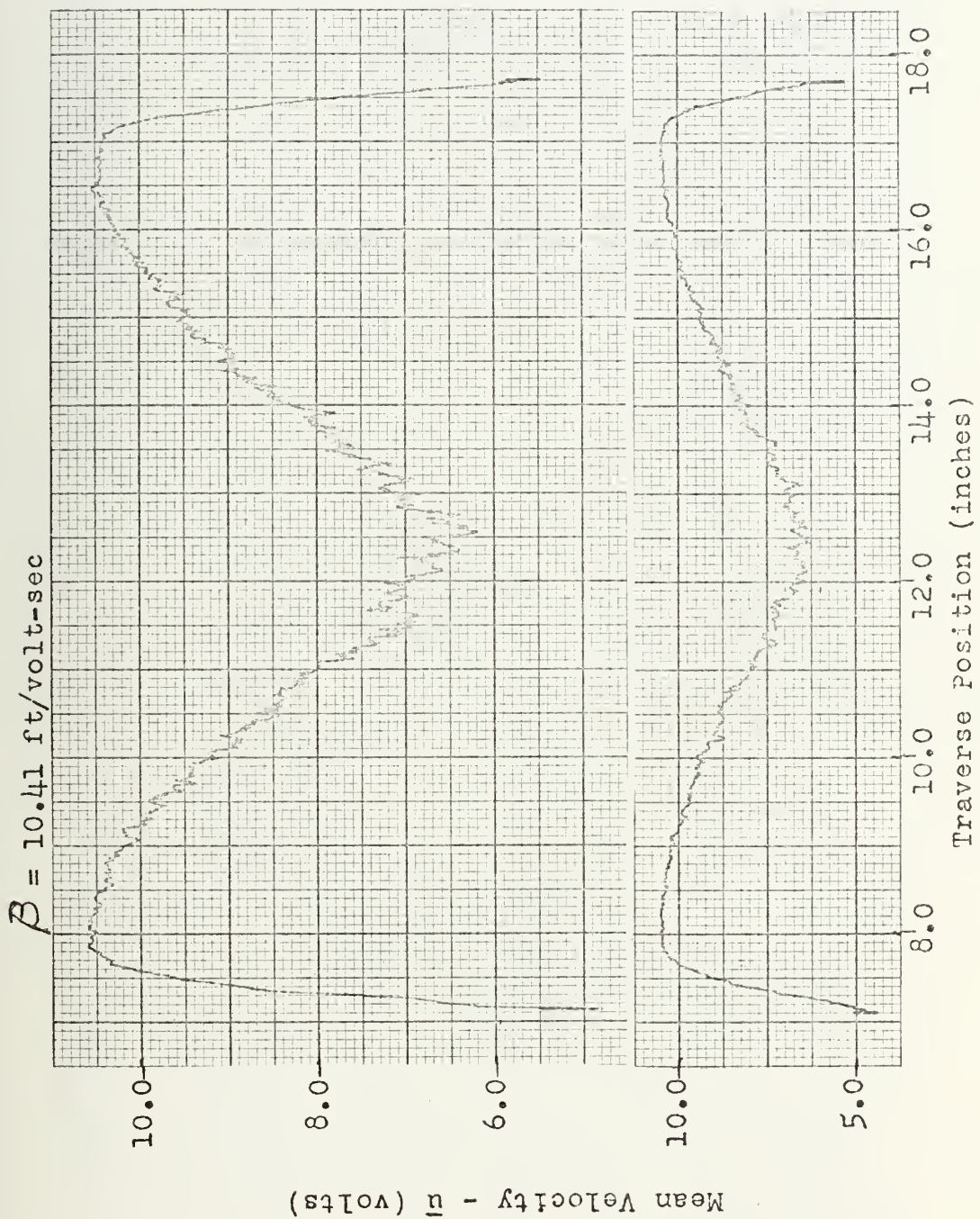


FIGURE 4

Station 4 Normal Wire Mean Velocity

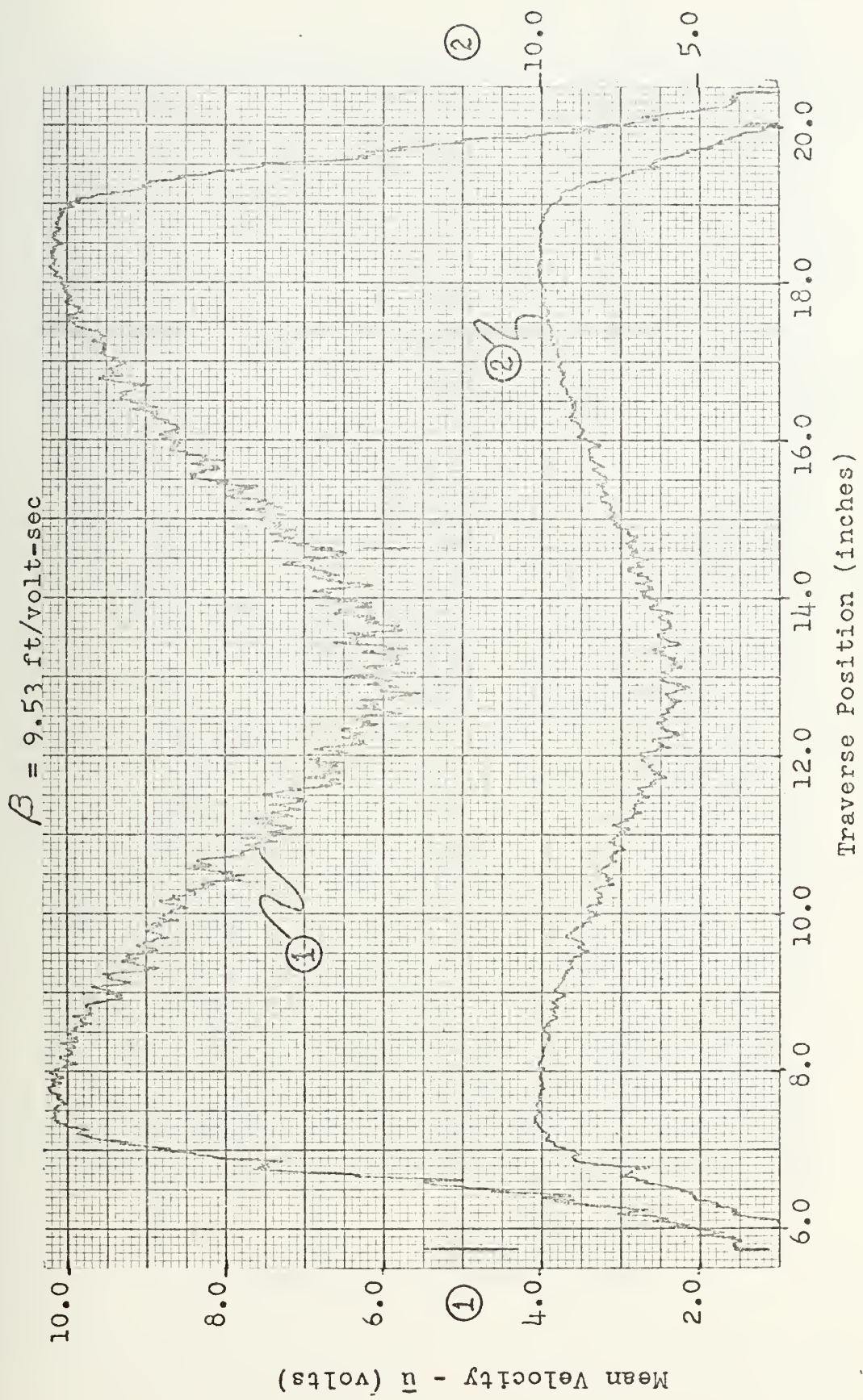


FIGURE 5
Station 5 Normal Wire Mean Velocity

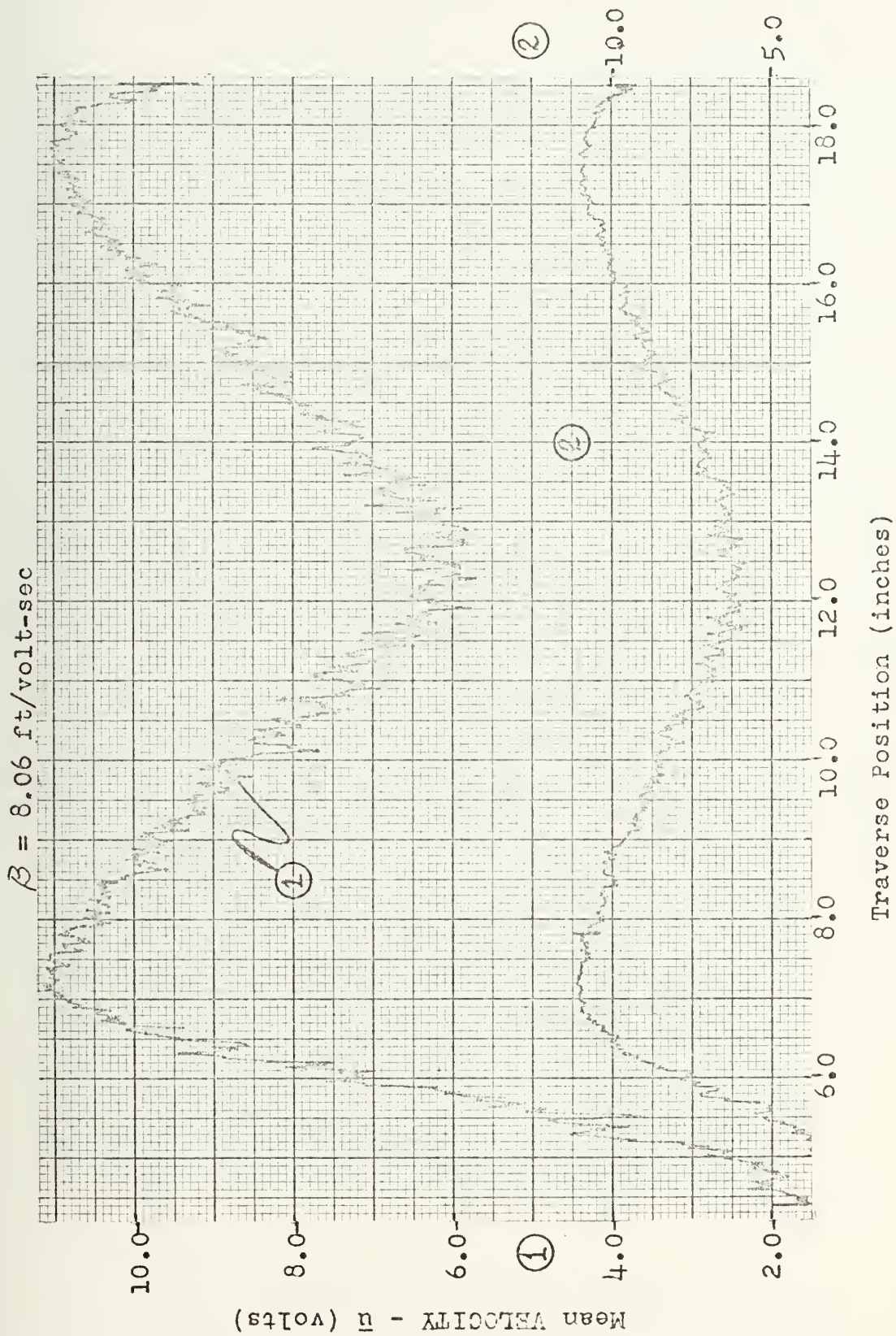


FIGURE 6
Station 6 Normal Wire Mean Velocity

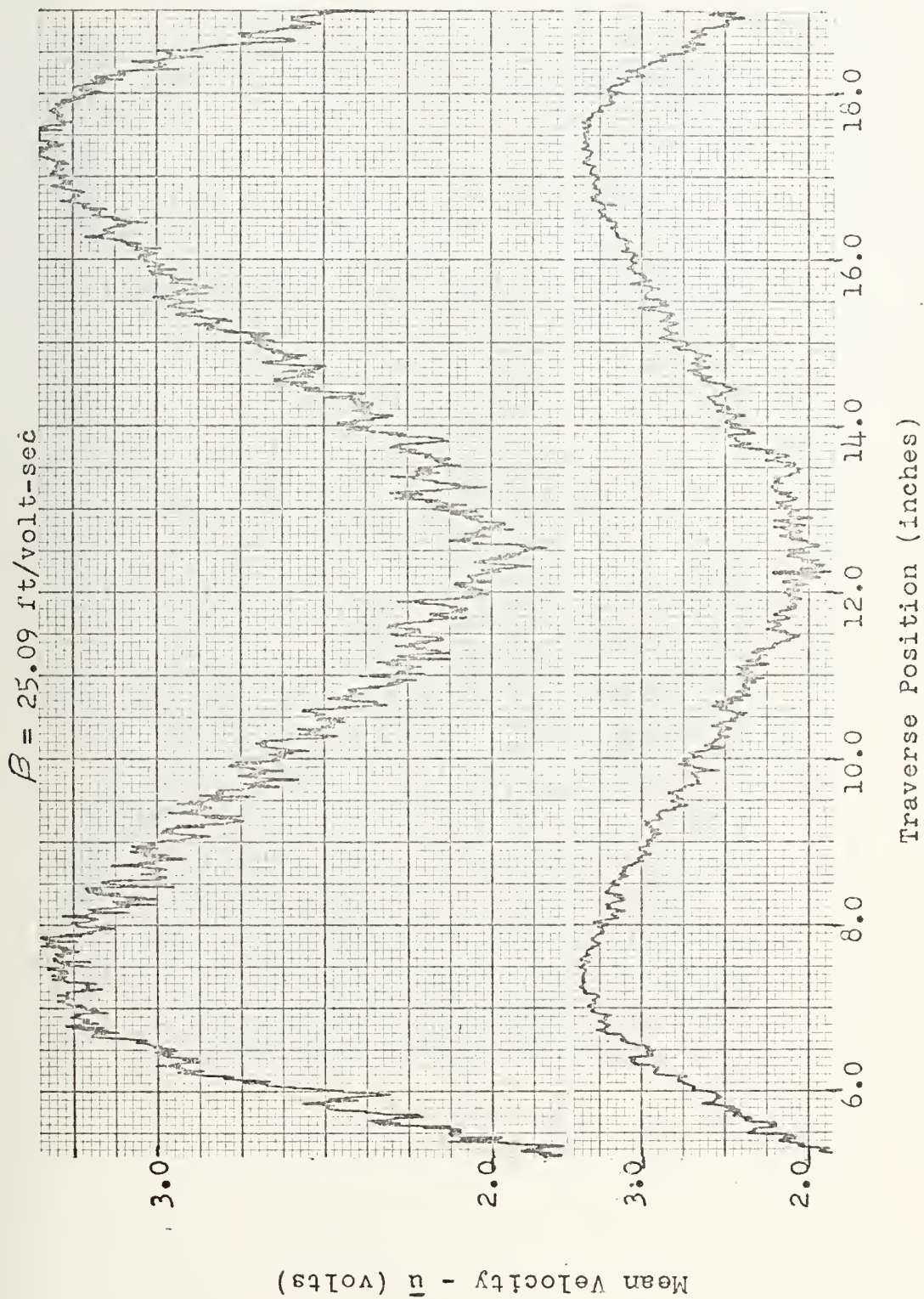


FIGURE 7
Station 7 Normal Wire Mean Velocity

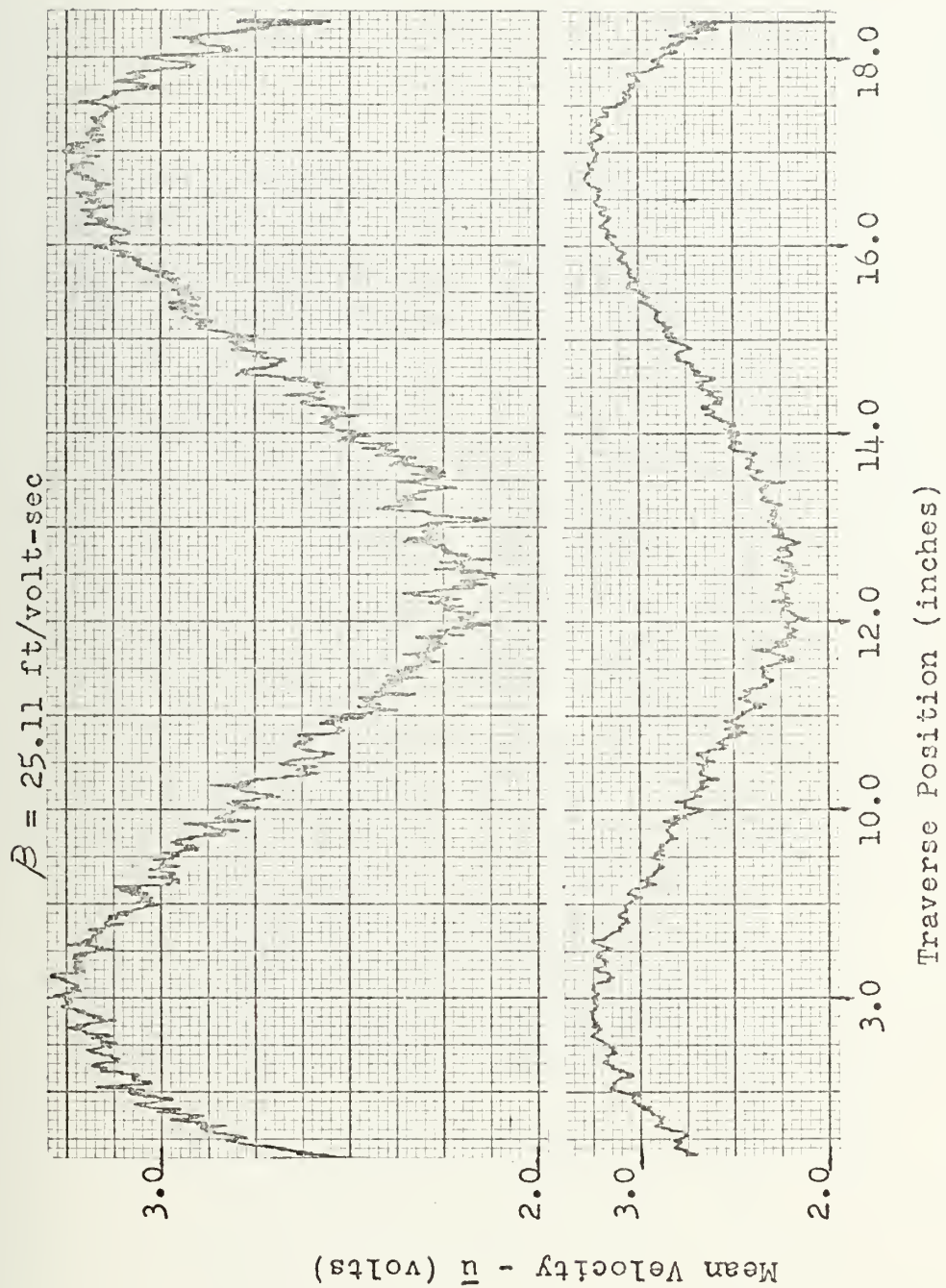


FIGURE 8

Station 8 Normal Wire Mean Velocity

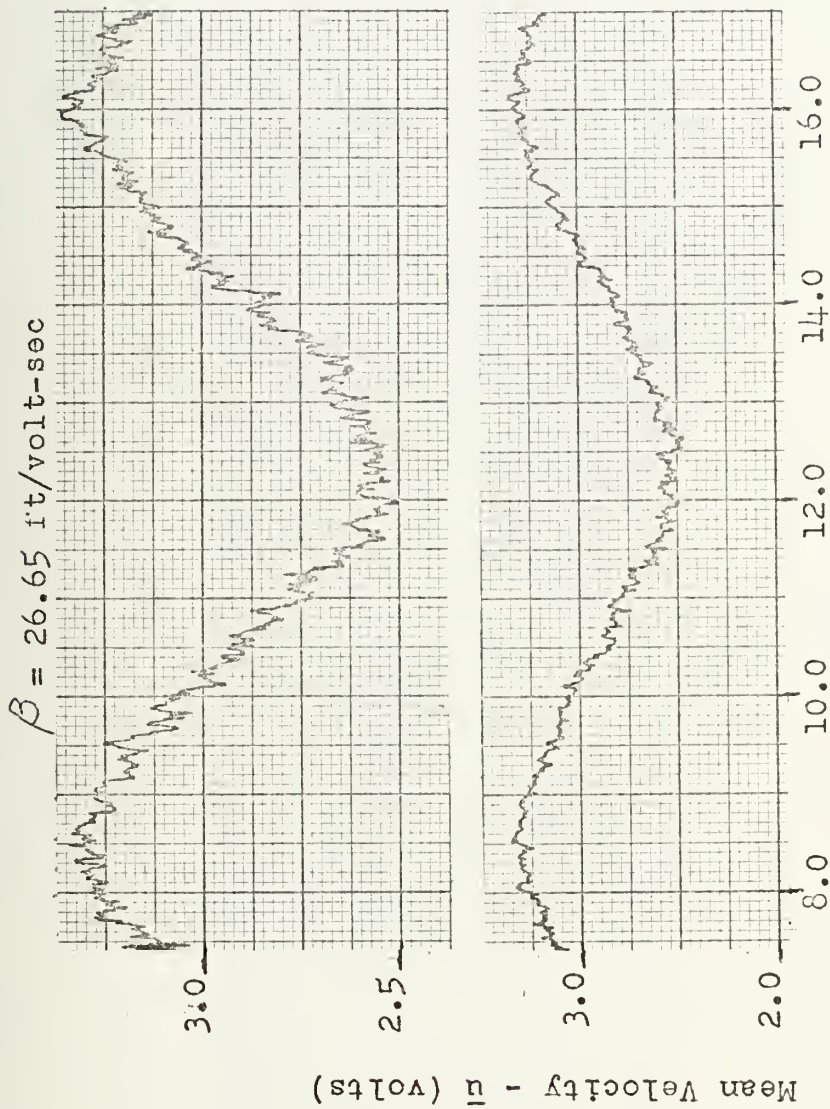
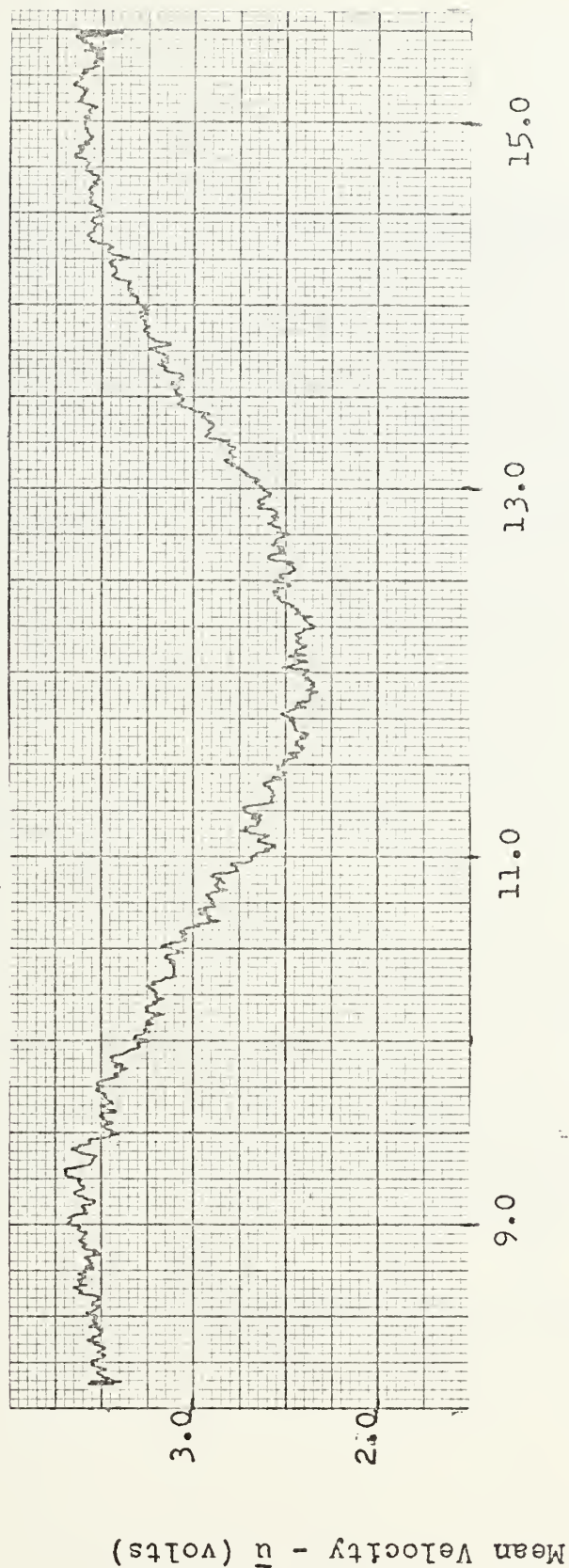


FIGURE 9
Station 9 Normal Wire Mean Velocity

$$\beta = 30.41 \text{ ft/volt-sec}$$



Traverse Position (inches)

FIGURE 10
Station 10 Normal Wire Mean Velocity

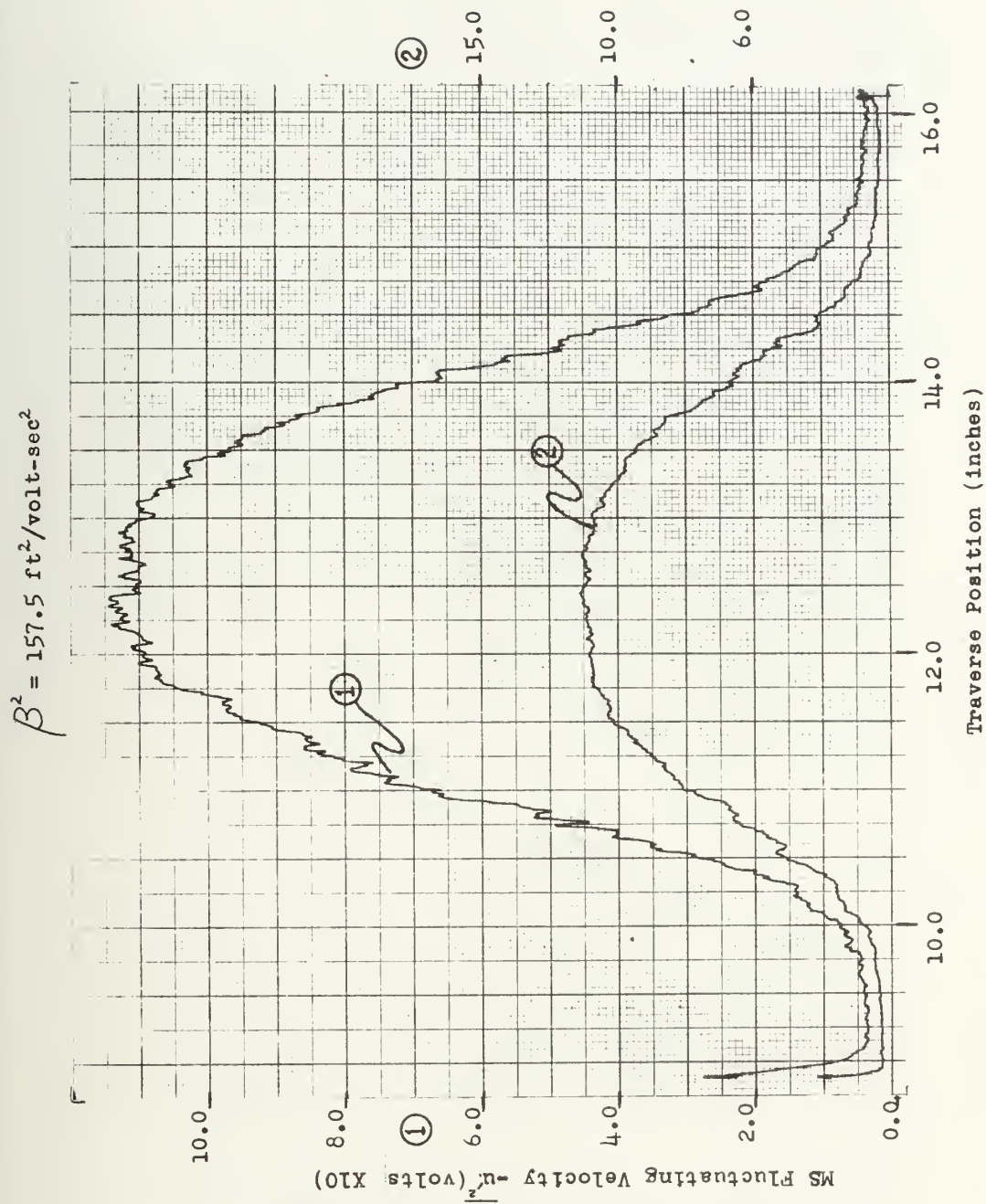


FIGURE 11
Station 1 MS Normal Wire Fluctuating Velocity

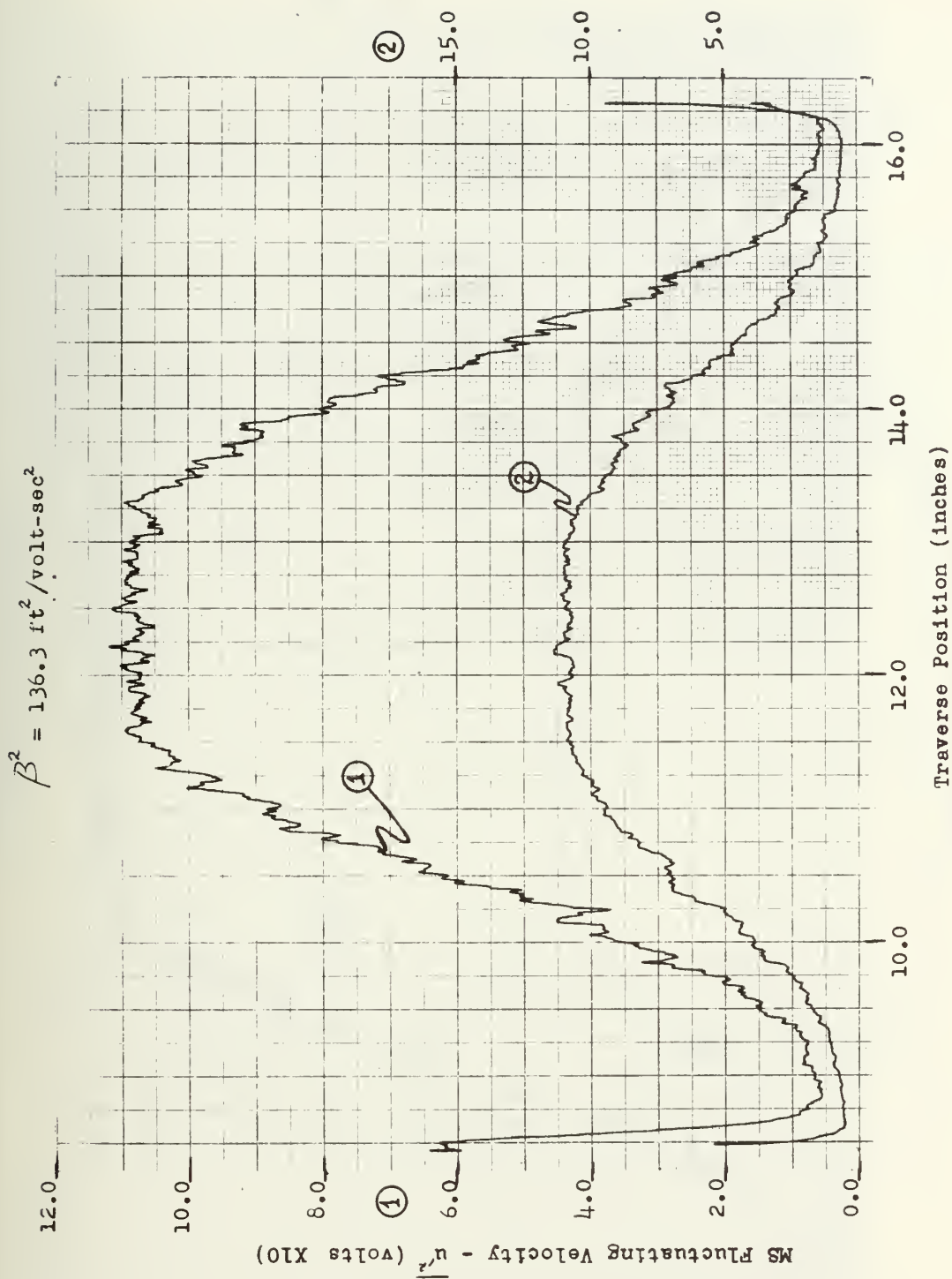


FIGURE 12
Station 2 MS Normal Wire Fluctuating Velocity

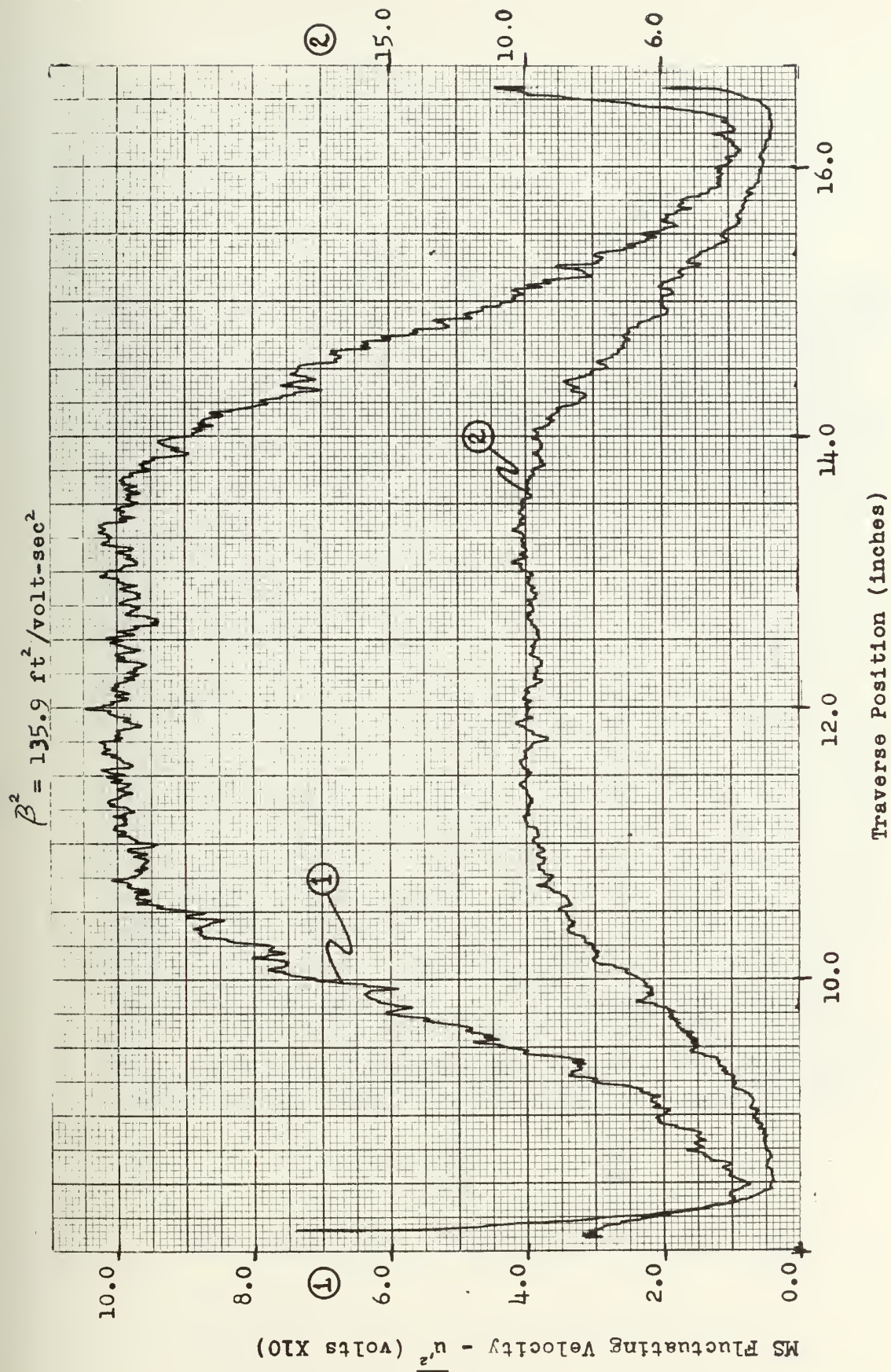


FIGURE 13
Station 3 MS Normal Wire Fluctuating Velocity

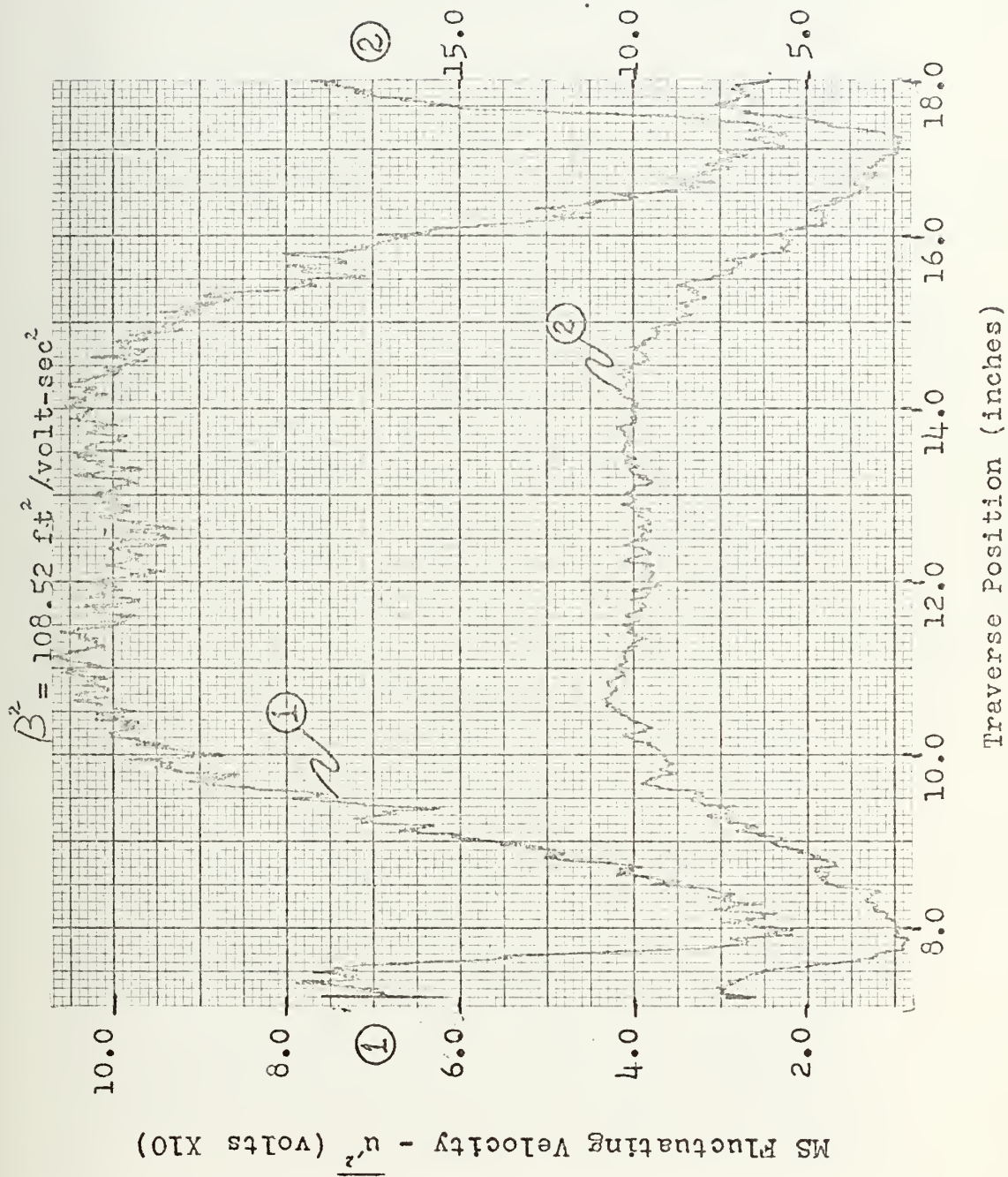


FIGURE 14
Station 4 MS Normal Wire Fluctuating Velocity

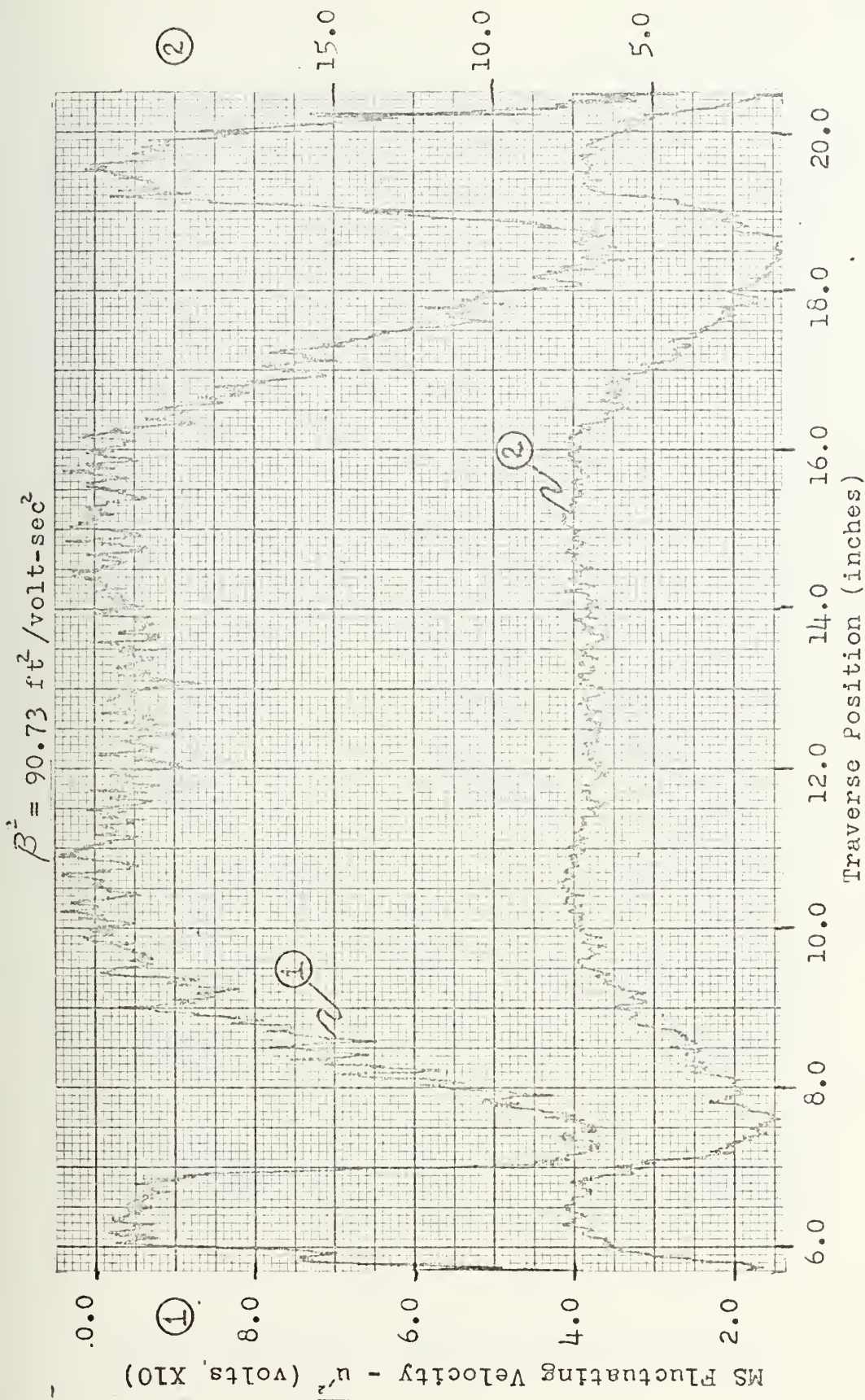


FIGURE 15
Station 5 MS Normal Wire Fluctuating Velocity

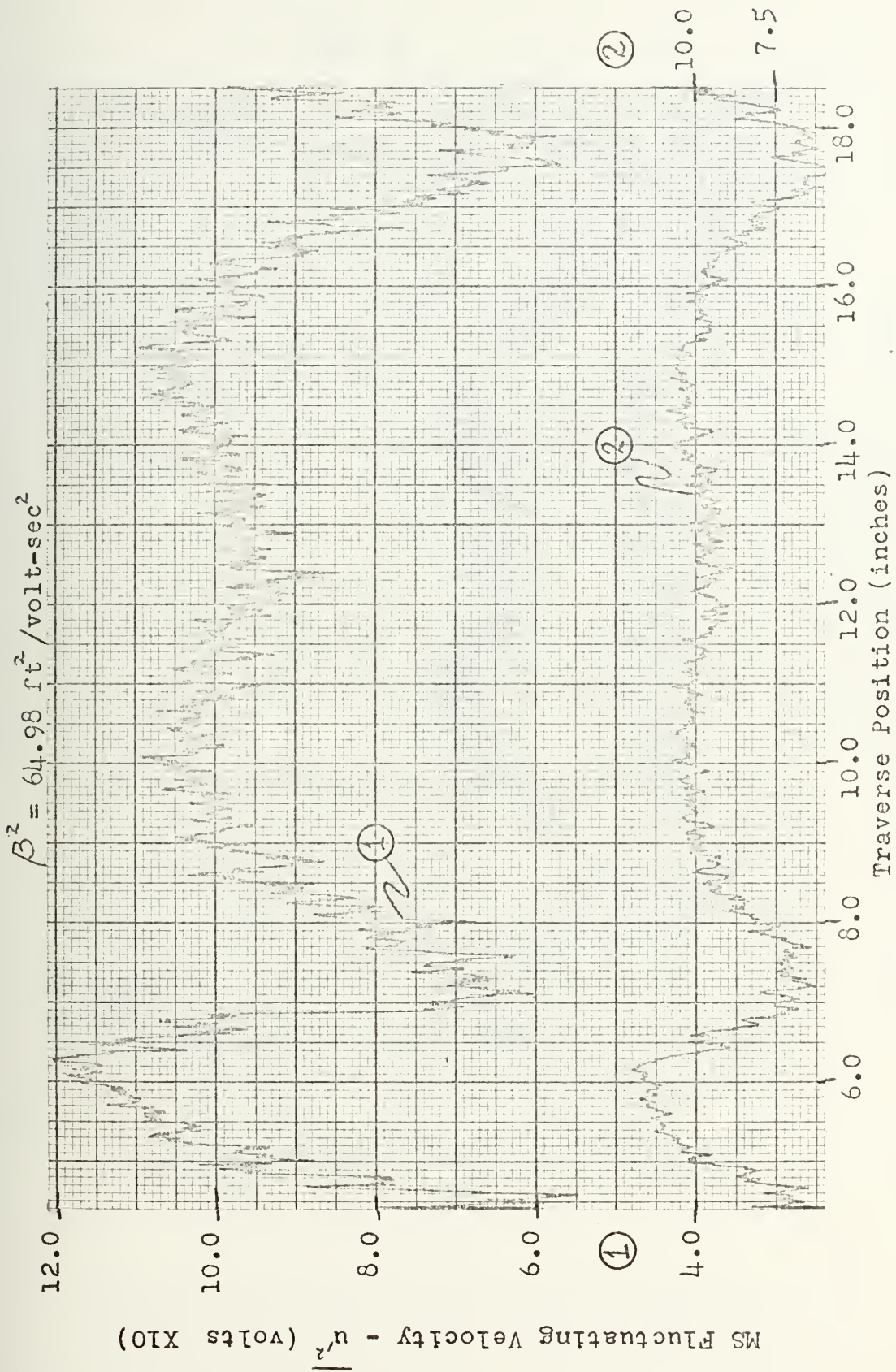


FIGURE 16
Station 6 MS Normal Wire Fluctuating Velocity

$$\beta^2 = 629.7 \text{ ft}^2/\text{volt-sec}^2$$

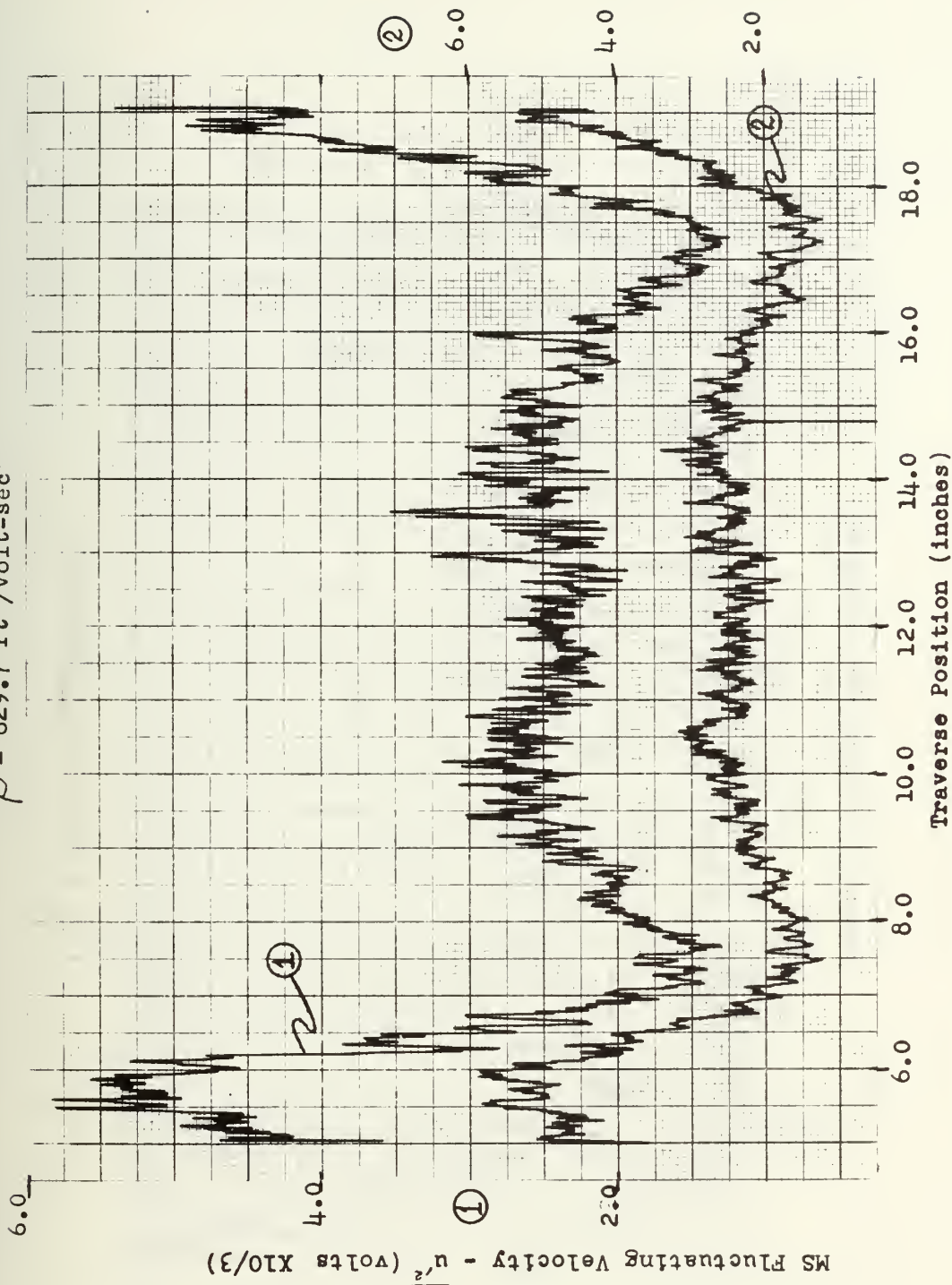


FIGURE 17

Station 7 MS Normal Wire Fluctuating Velocity

$$\beta^2 = 630.6 \text{ ft}^2/\text{volt-sec}^2$$

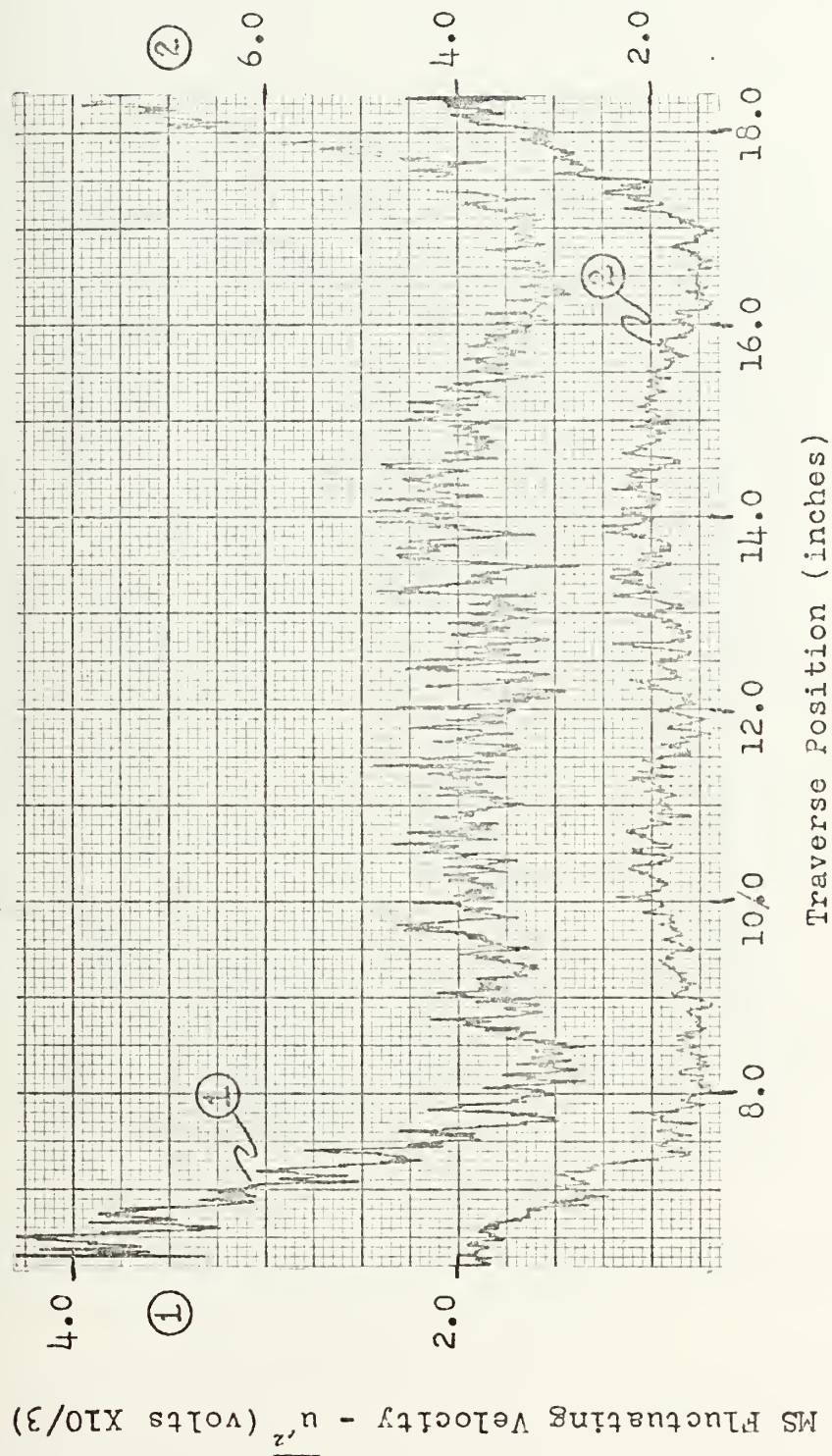


FIGURE 18
Station 8 MS Normal Wire Fluctuating Velocity

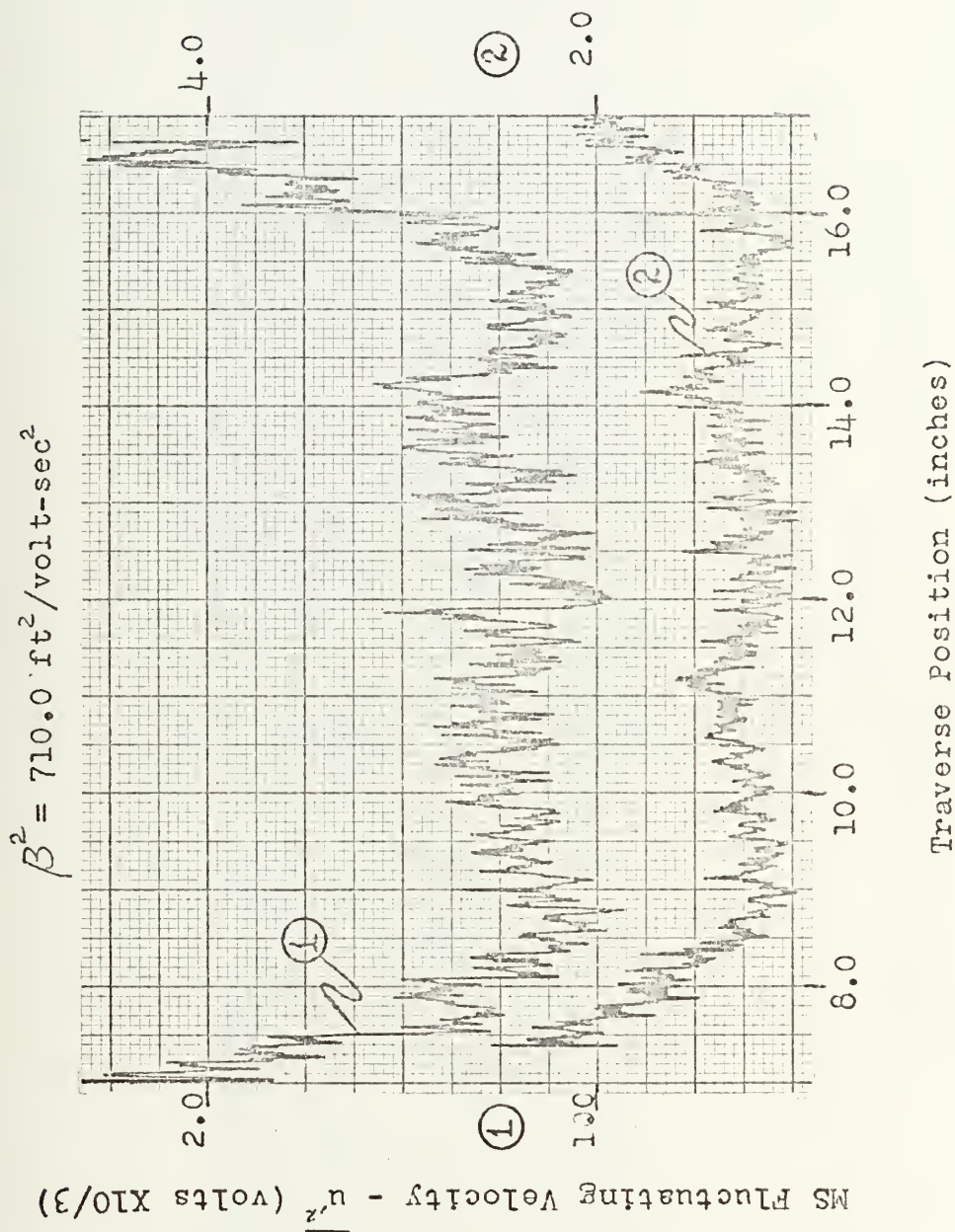


FIGURE 19
Station 9 MS normal Wire Fluctuating Velocity

MS Fluctuating Velocity - u'^2 (volts X10/3)

$$\beta^2 = 157.51 \text{ ft}^2/\text{volt-sec}^2$$

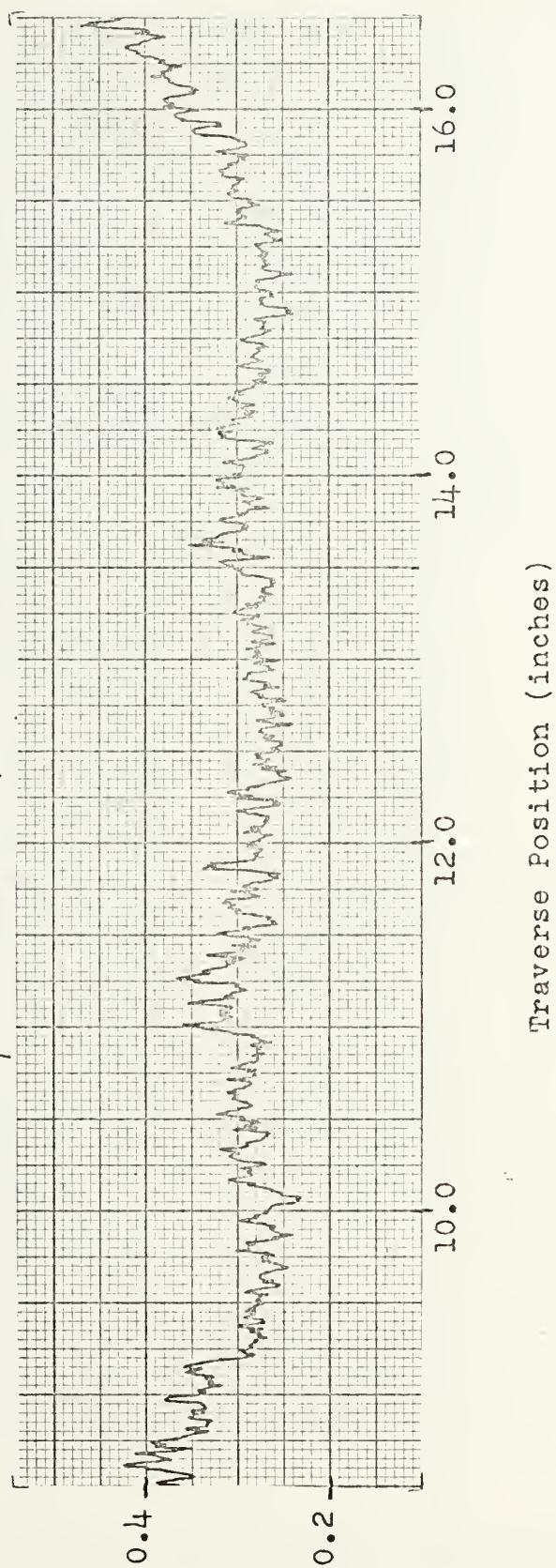


FIGURE 20
Station 10 MS Normal Wire Fluctuating Velocity

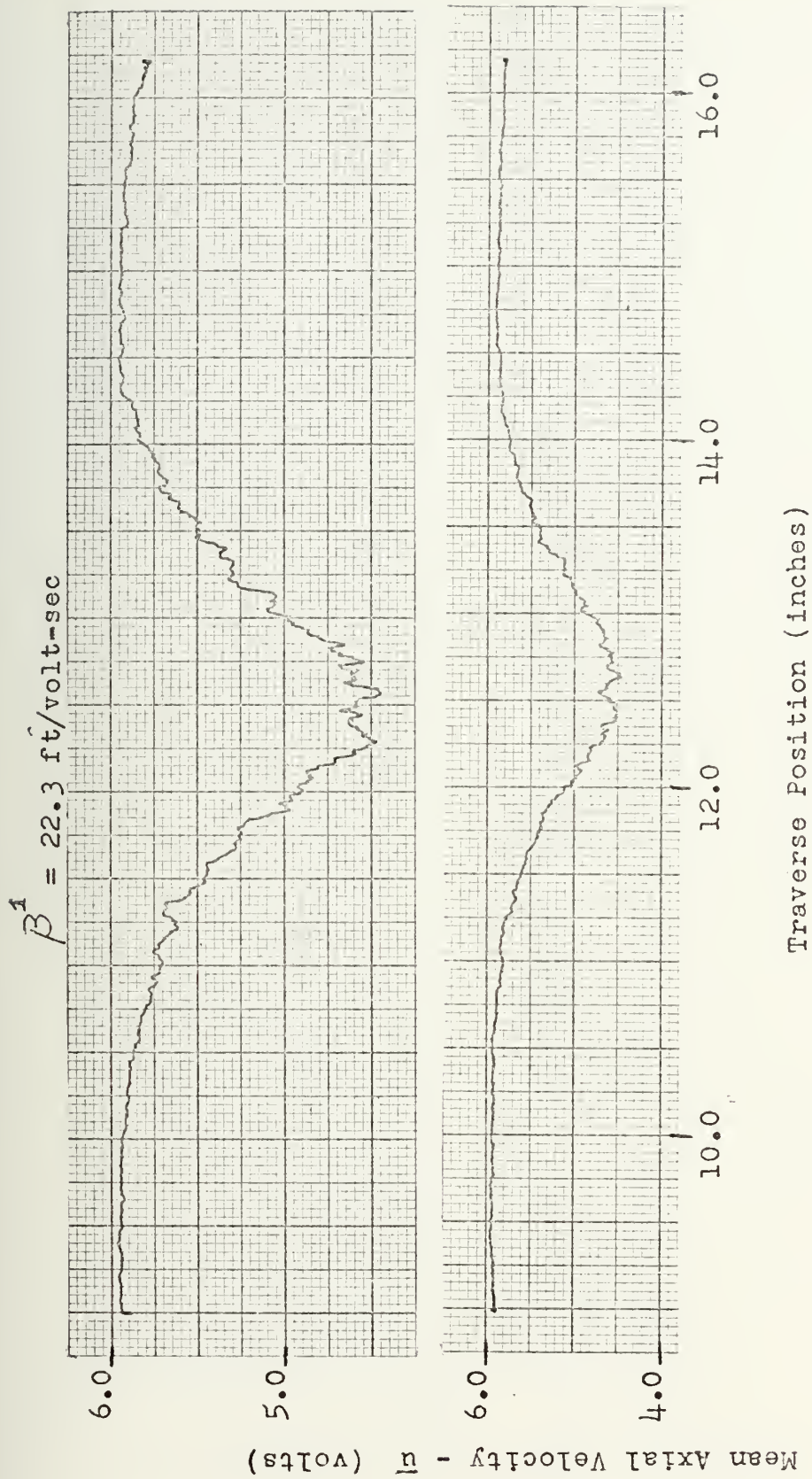


FIGURE 21
Station 1 X-Array Mean Axial Velocity

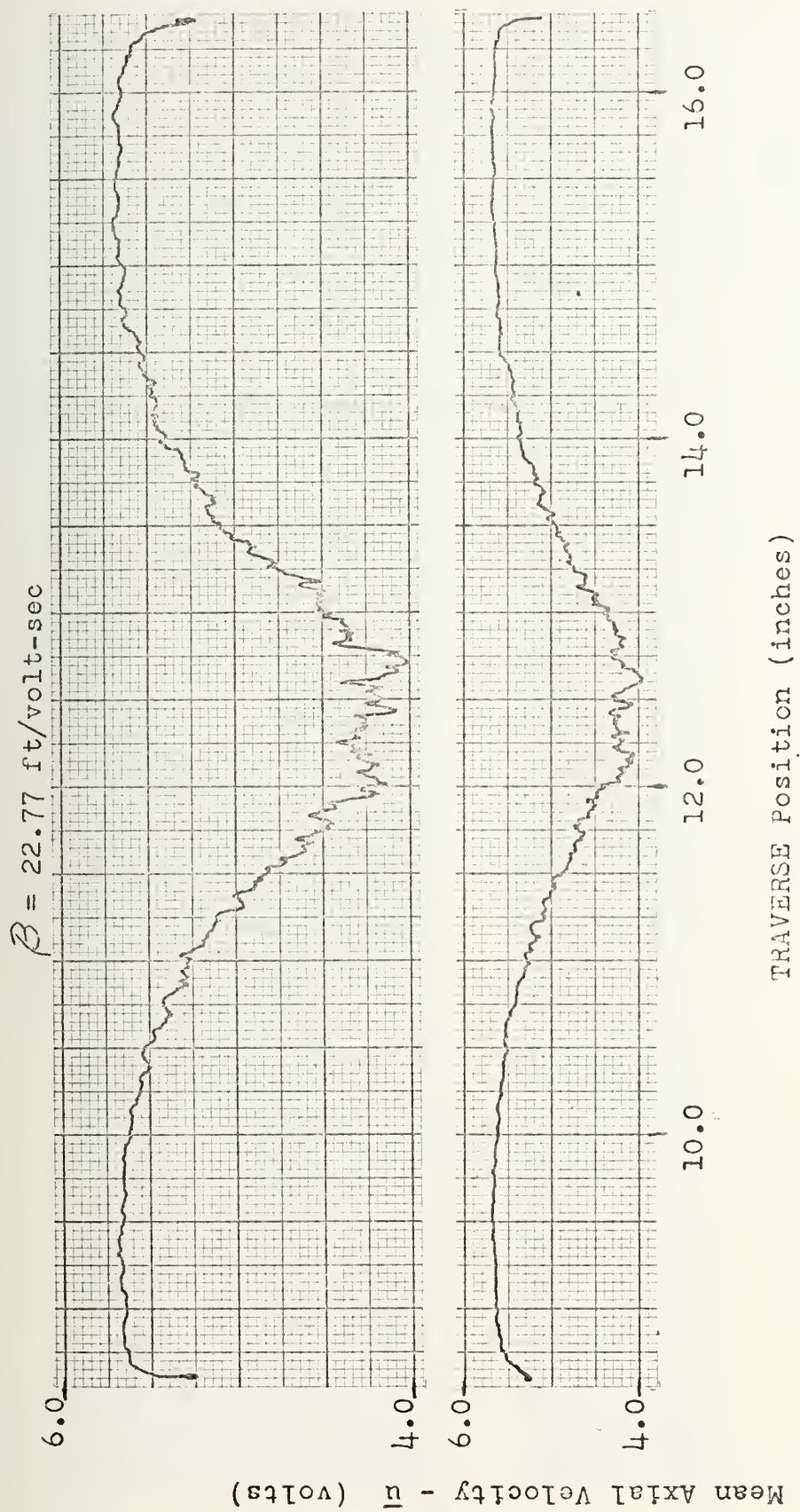
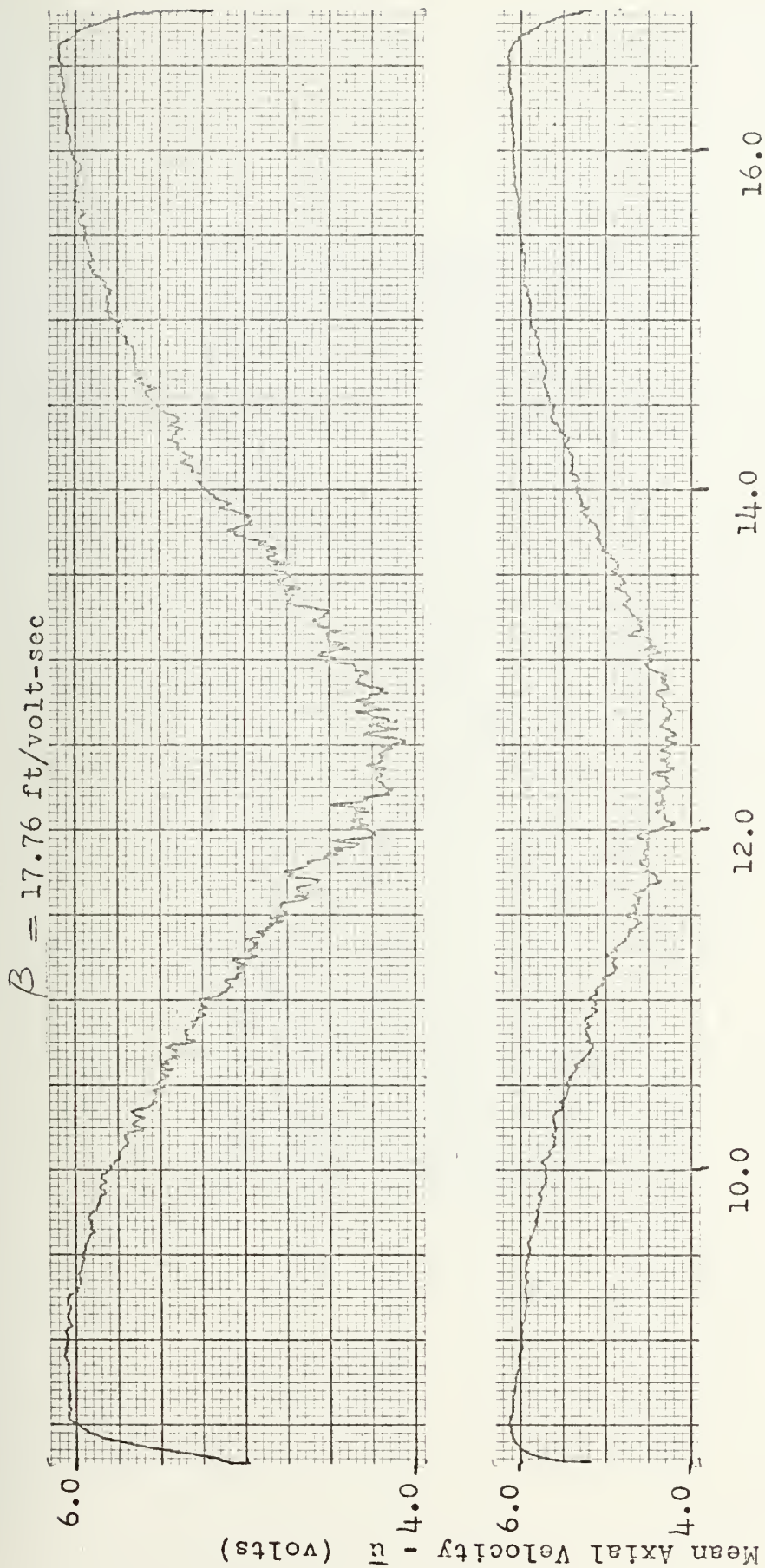


FIGURE 22
Station 2 X-Array Mean Axial Velocity



Traverse Position (inches)
 FIGURE 23
 Station 3 X-Array Mean Axial Velocity

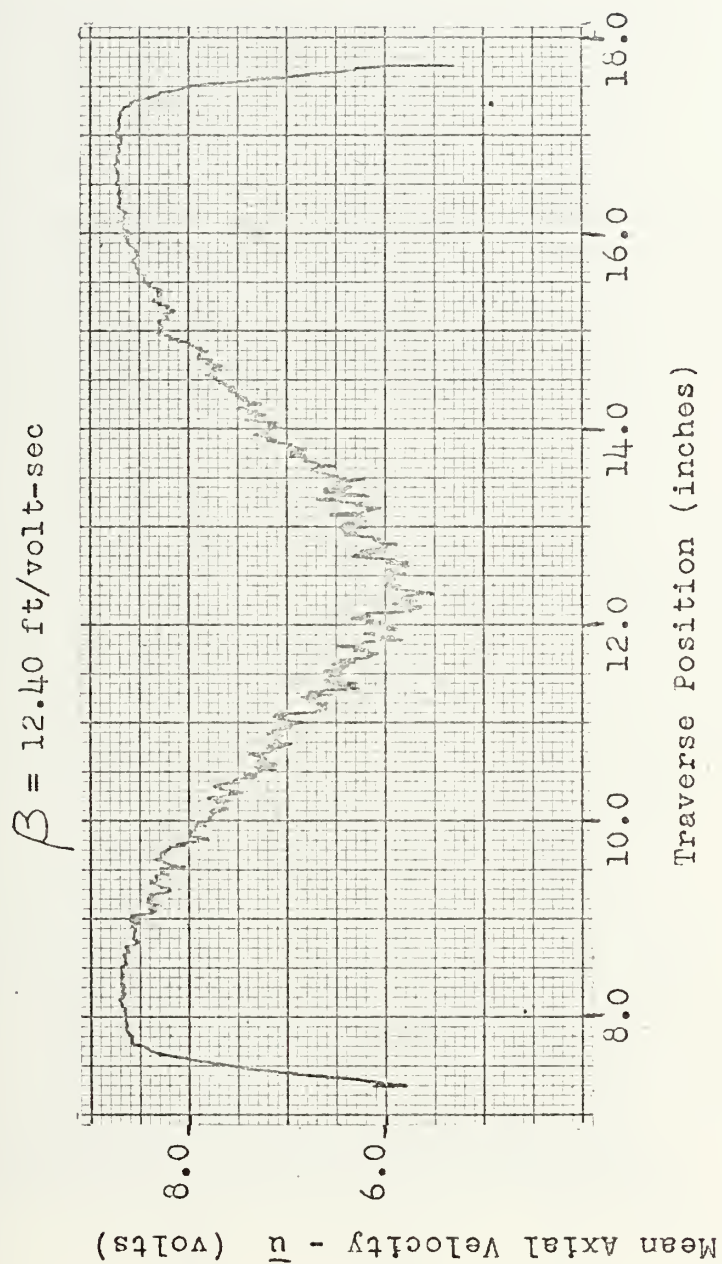


FIGURE 24
Station 4 X-Array Mean Axial Velocity

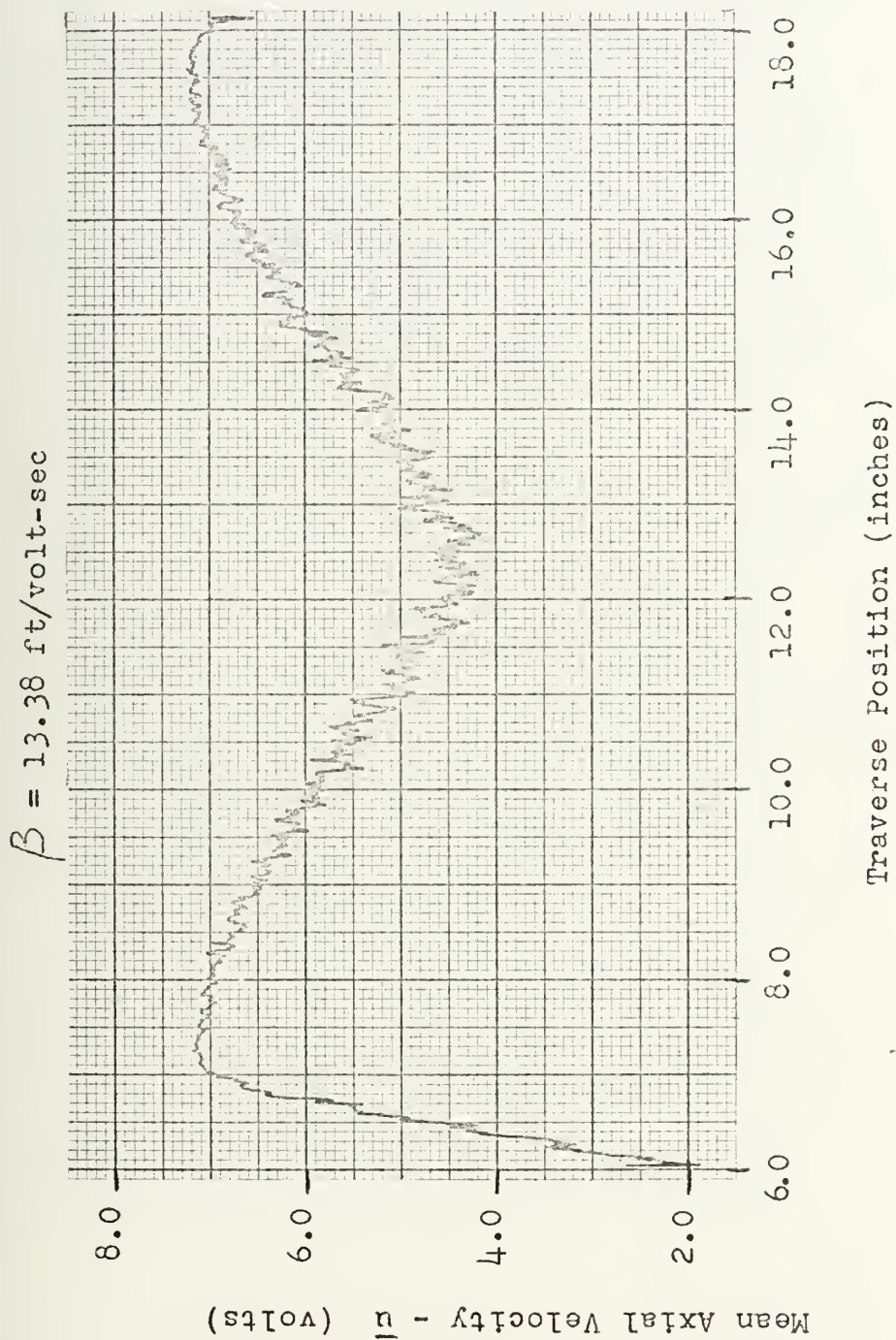


FIGURE 25
Station 5 X-Array Mean Axial Velocity

$$\beta = 13.46 \text{ ft/volt-sec}$$

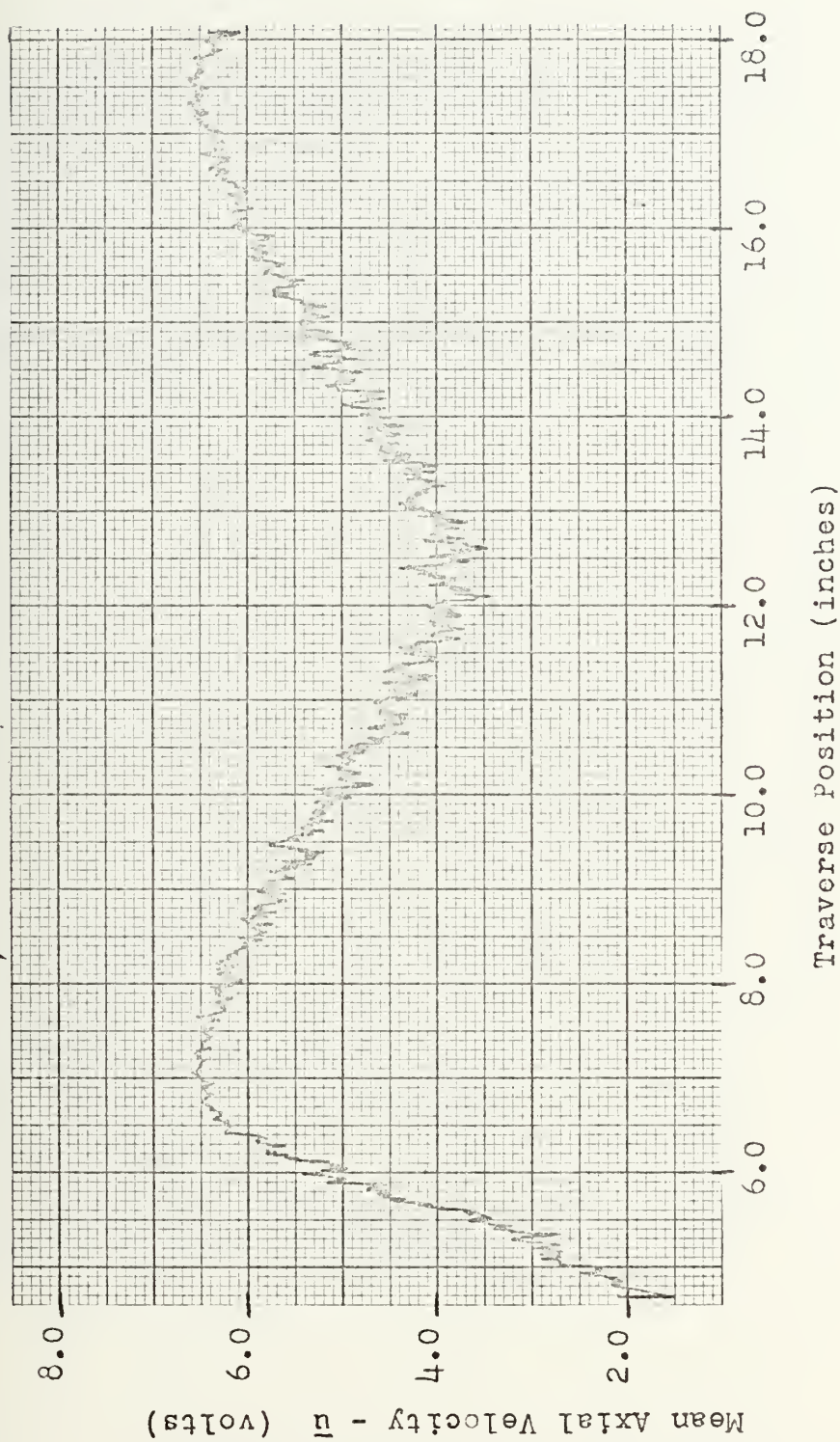


FIGURE 26
Station 6 X-Array Mean Axial Velocity

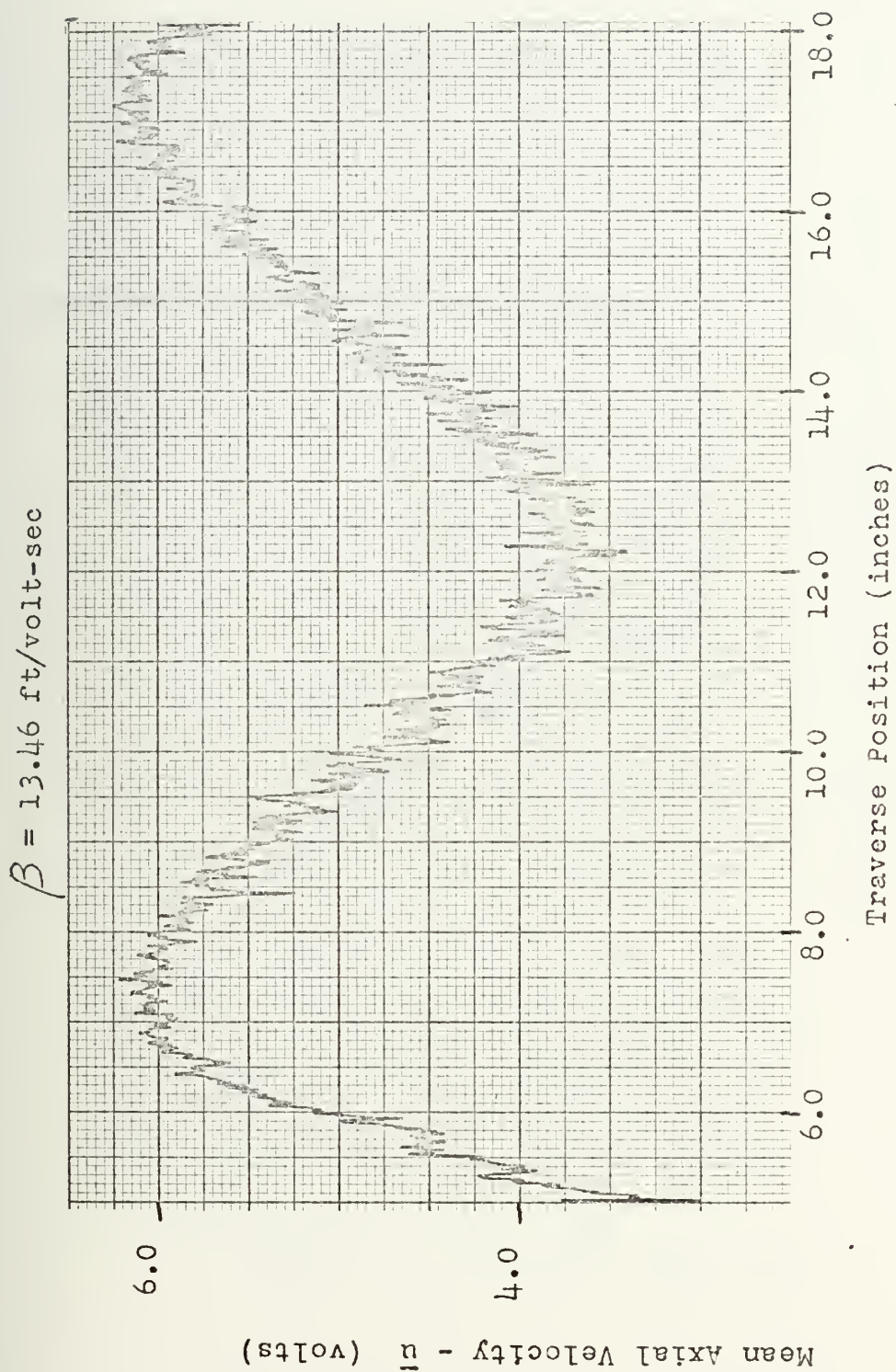
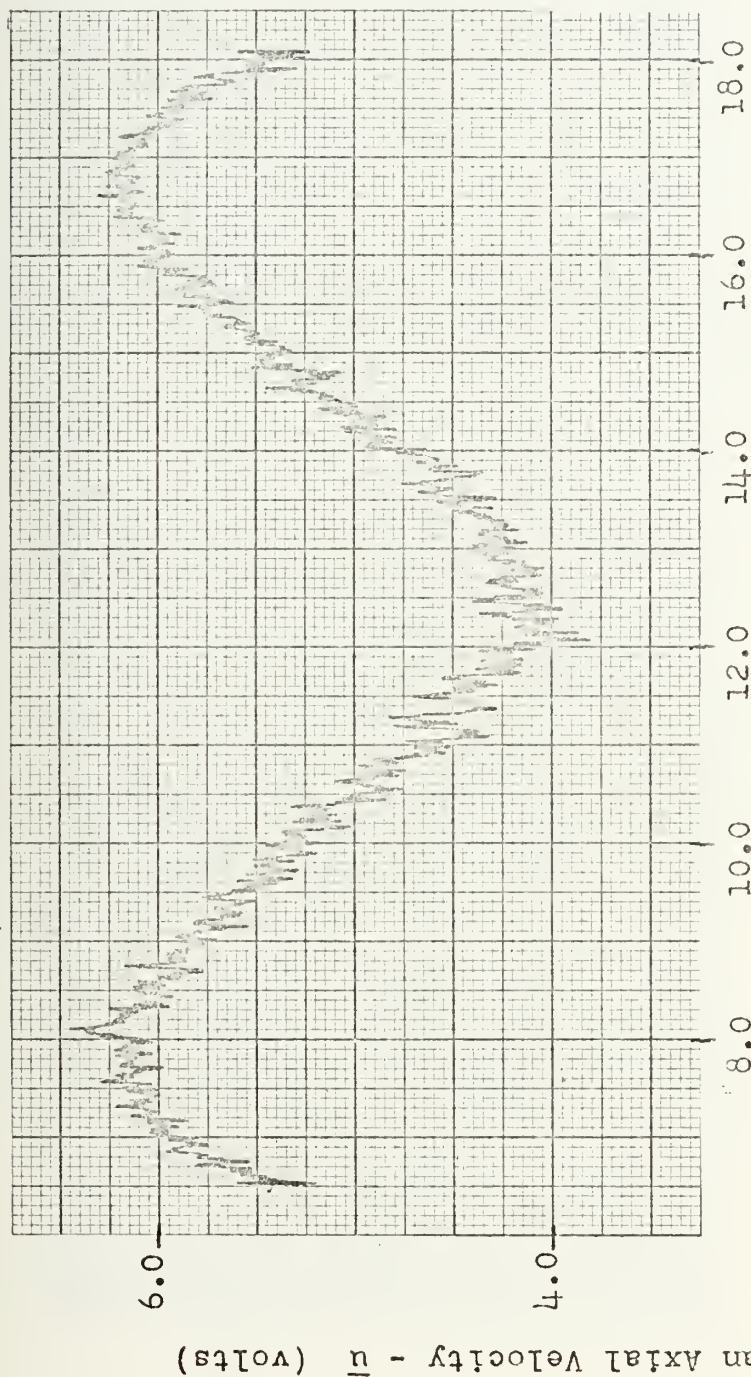


FIGURE 27
Station 7 X-Array Mean Axial Velocity

$$\beta = 13.21 \text{ ft/volt-sec}$$



Traverse Position (inches)

FIGURE 28
Station 8 X-Array Mean Axial Velocity

$$\beta = 12.86 \text{ ft/volt-sec}$$



Traverse Position (inches)

FIGURE 29
Station 9 X-Array Mean Axial Velocity

$$\beta = 12.81 \text{ ft/volt-sec}$$

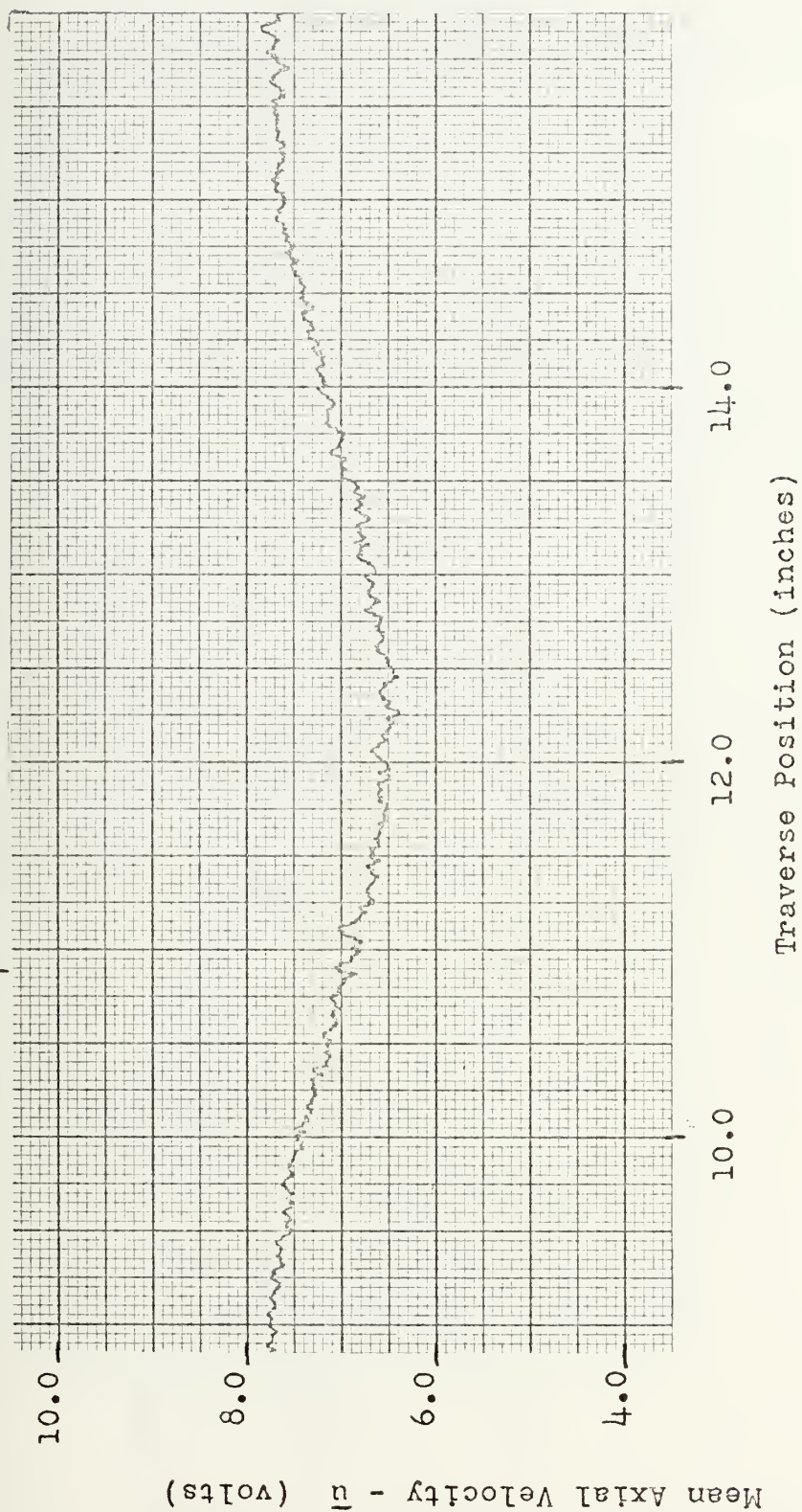


FIGURE 30
Station 10 X-Array Mean Axial Velocity

$$\beta = 22.93 \text{ ft/volt-sec}$$

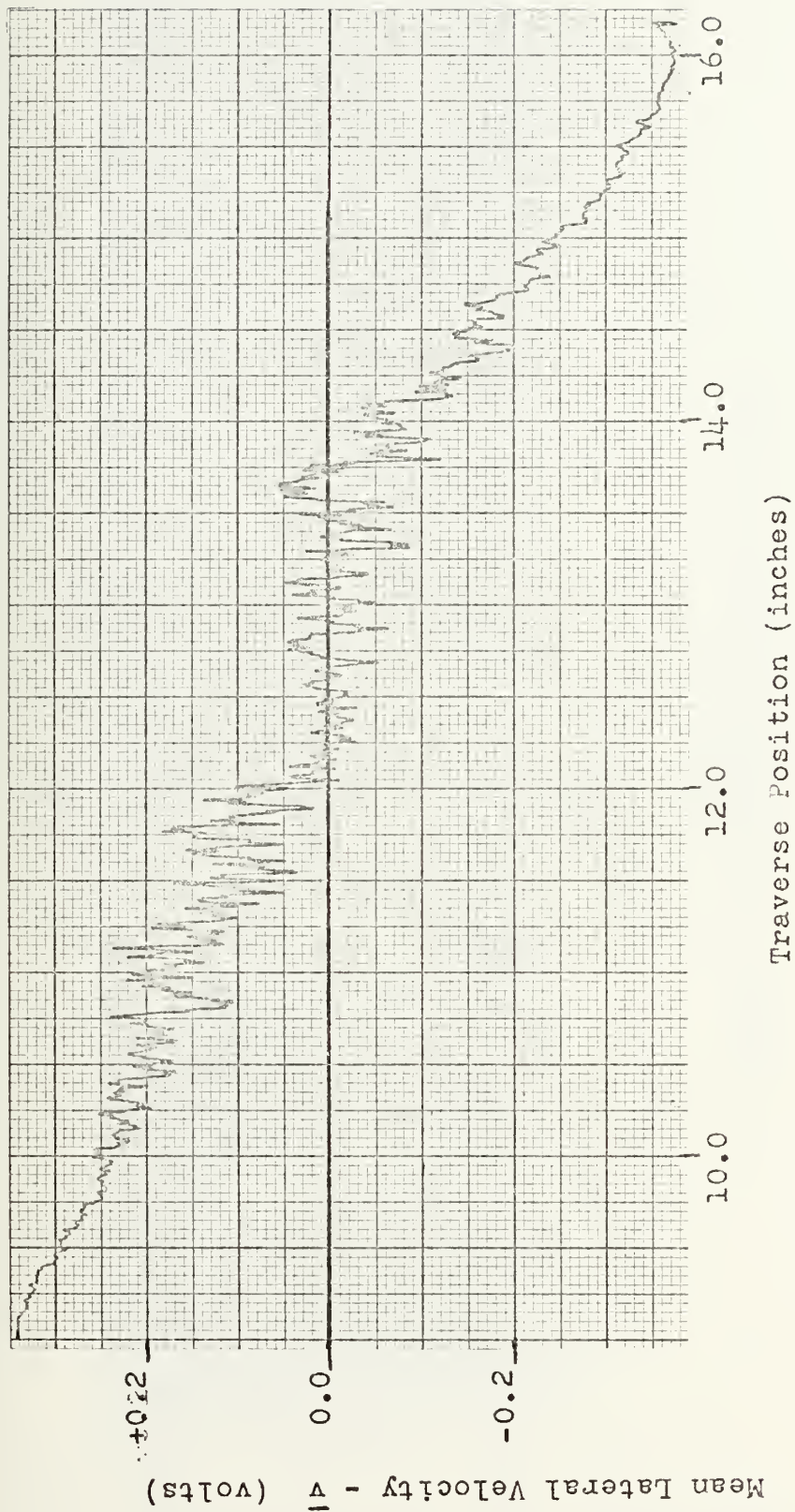


FIGURE 31
Station 1 X-Array Mean Lateral Velocity

$$\beta = 22.77 \text{ ft/volt-sec}$$

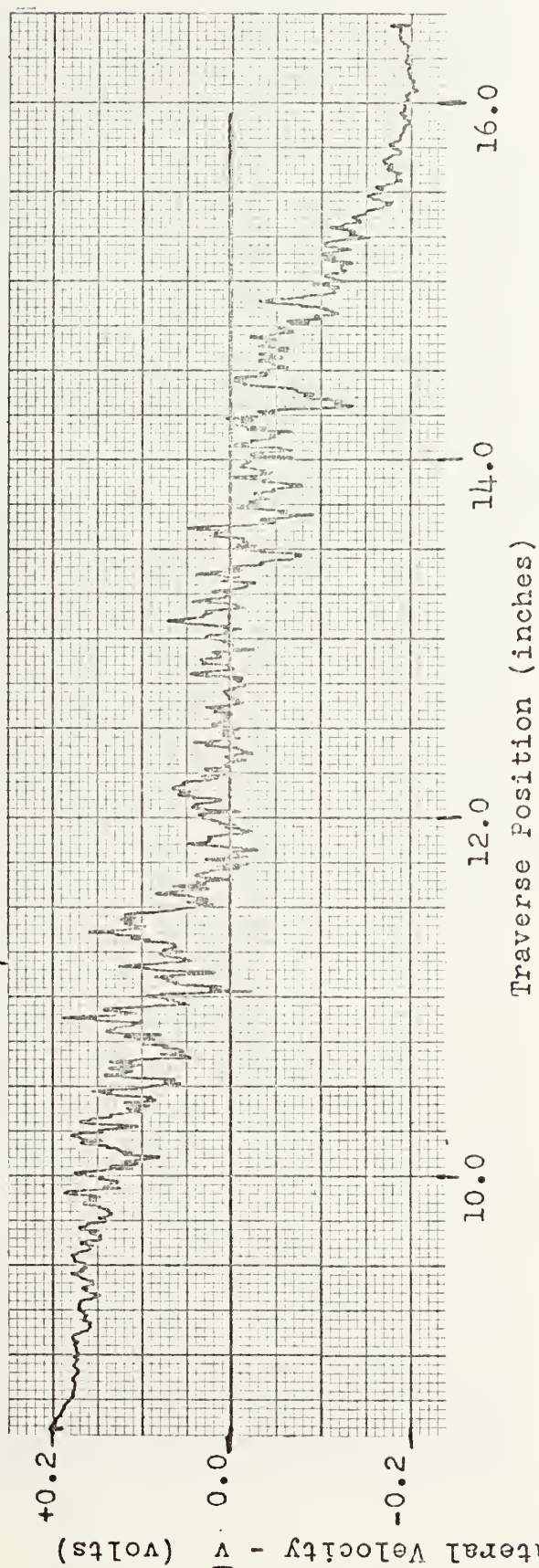


FIGURE 32
Station 2 X-Array Mean Lateral Velocity

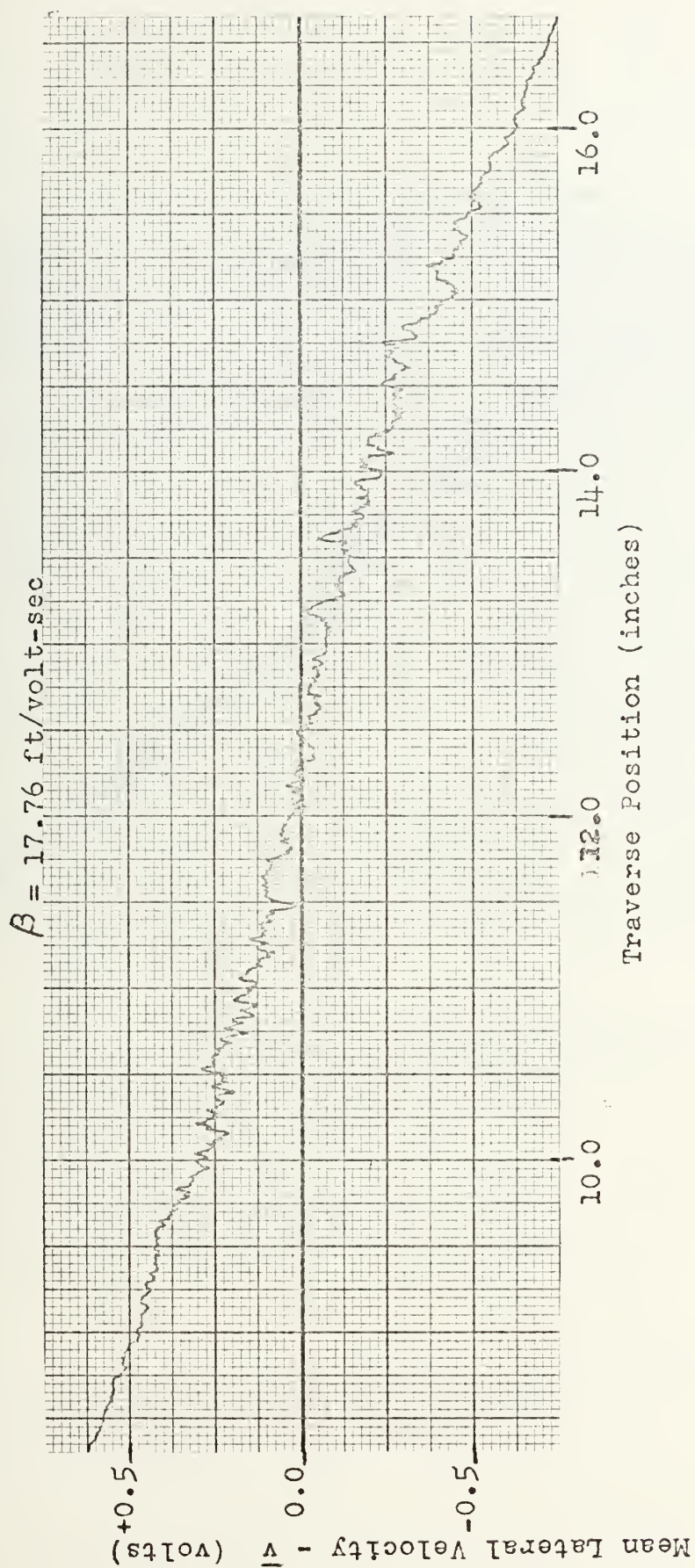


FIGURE 33
Station 3 X-Array Mean Lateral Velocity

$$\beta = 12.40 \text{ ft/volt-sec}$$

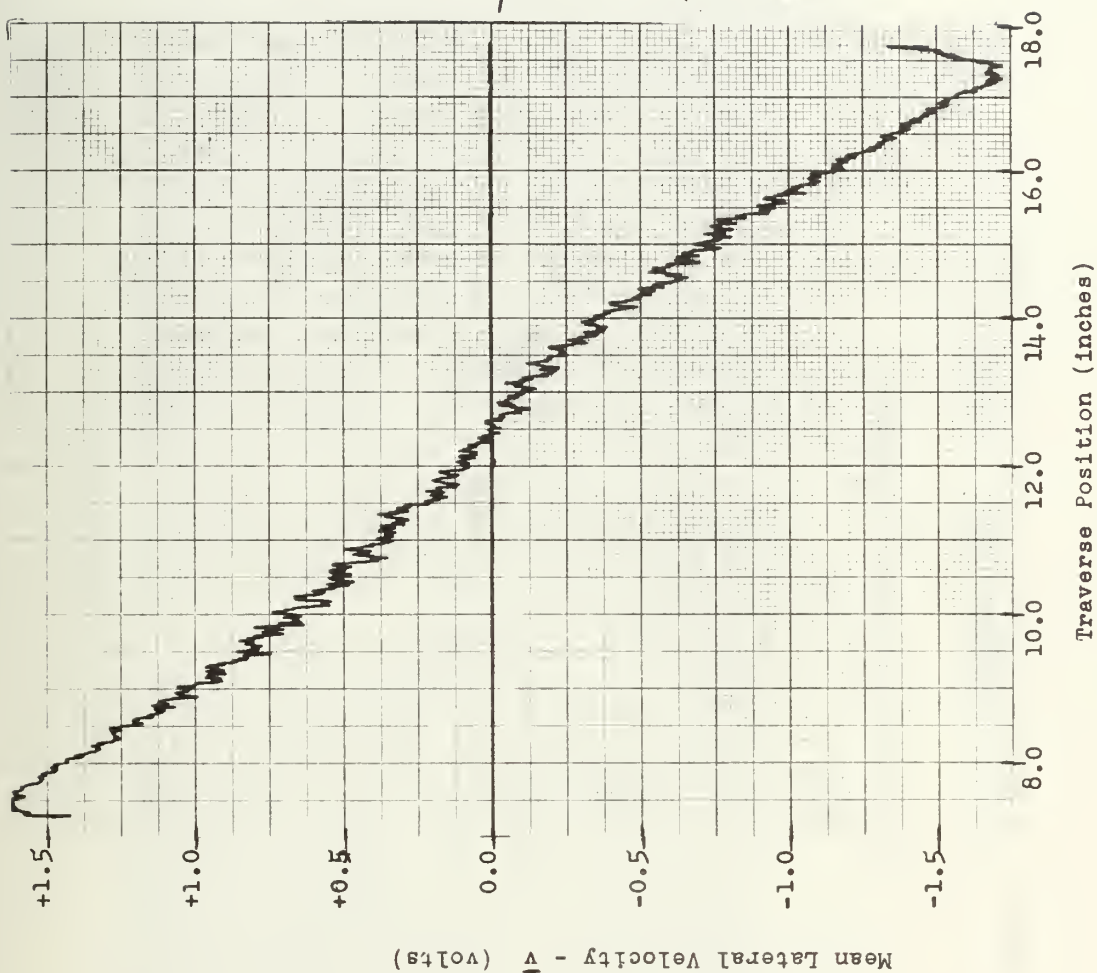


FIGURE 34
Station 4 X-Array Mean Lateral Velocity

$$\beta = 13.38 \text{ ft/volt-sec}$$

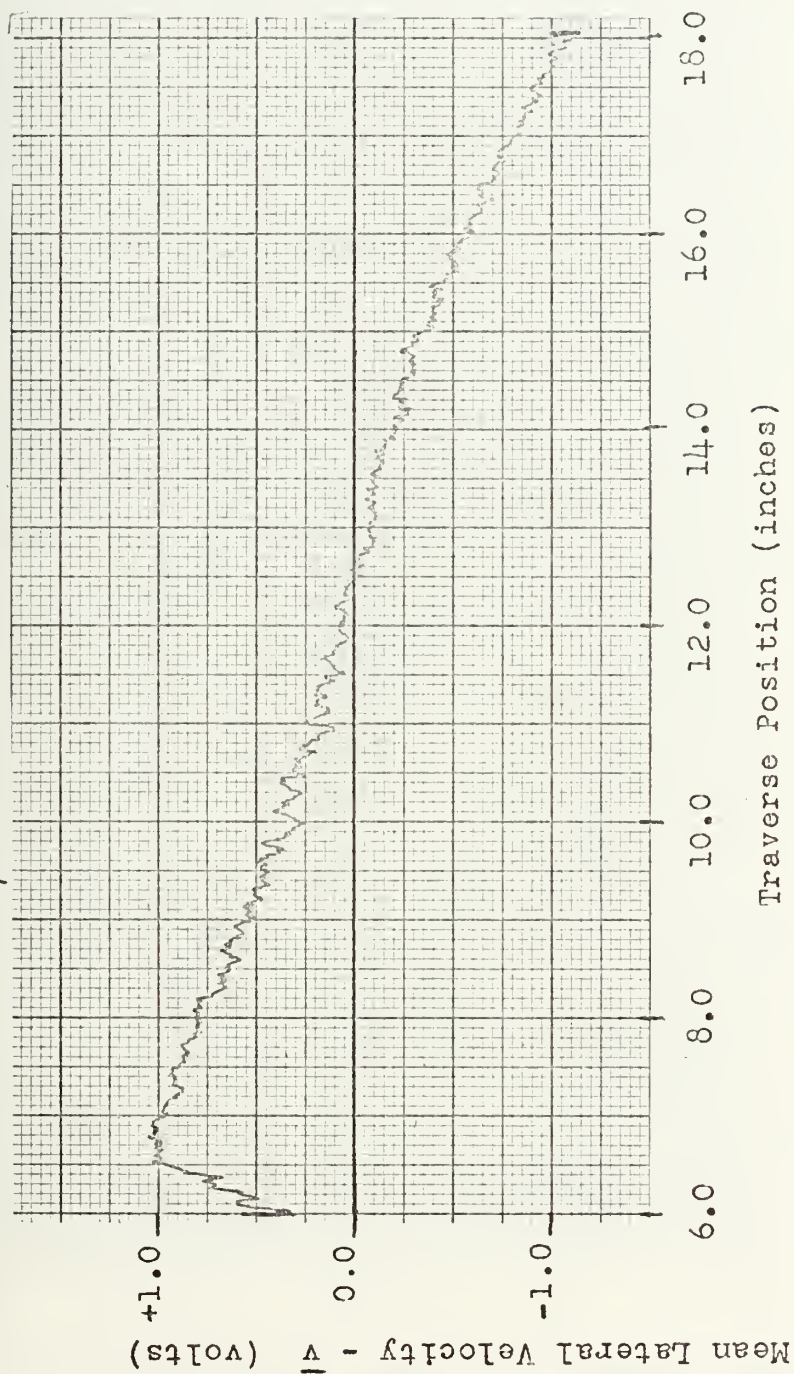


FIGURE 35
Station 5 X-Array Mean Lateral Velocity

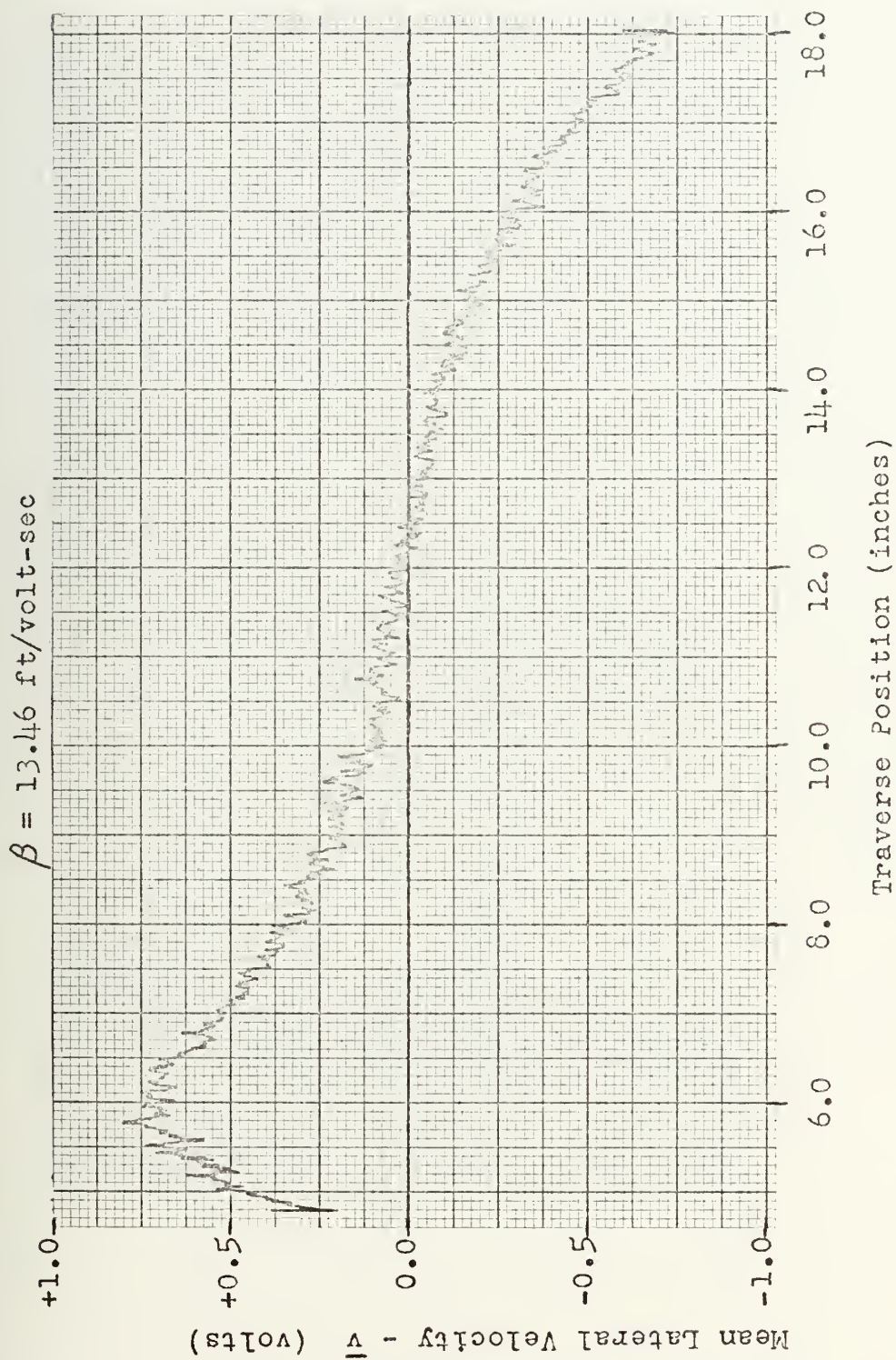


FIGURE 36
Station 6 X-Array Mean Lateral Velocity

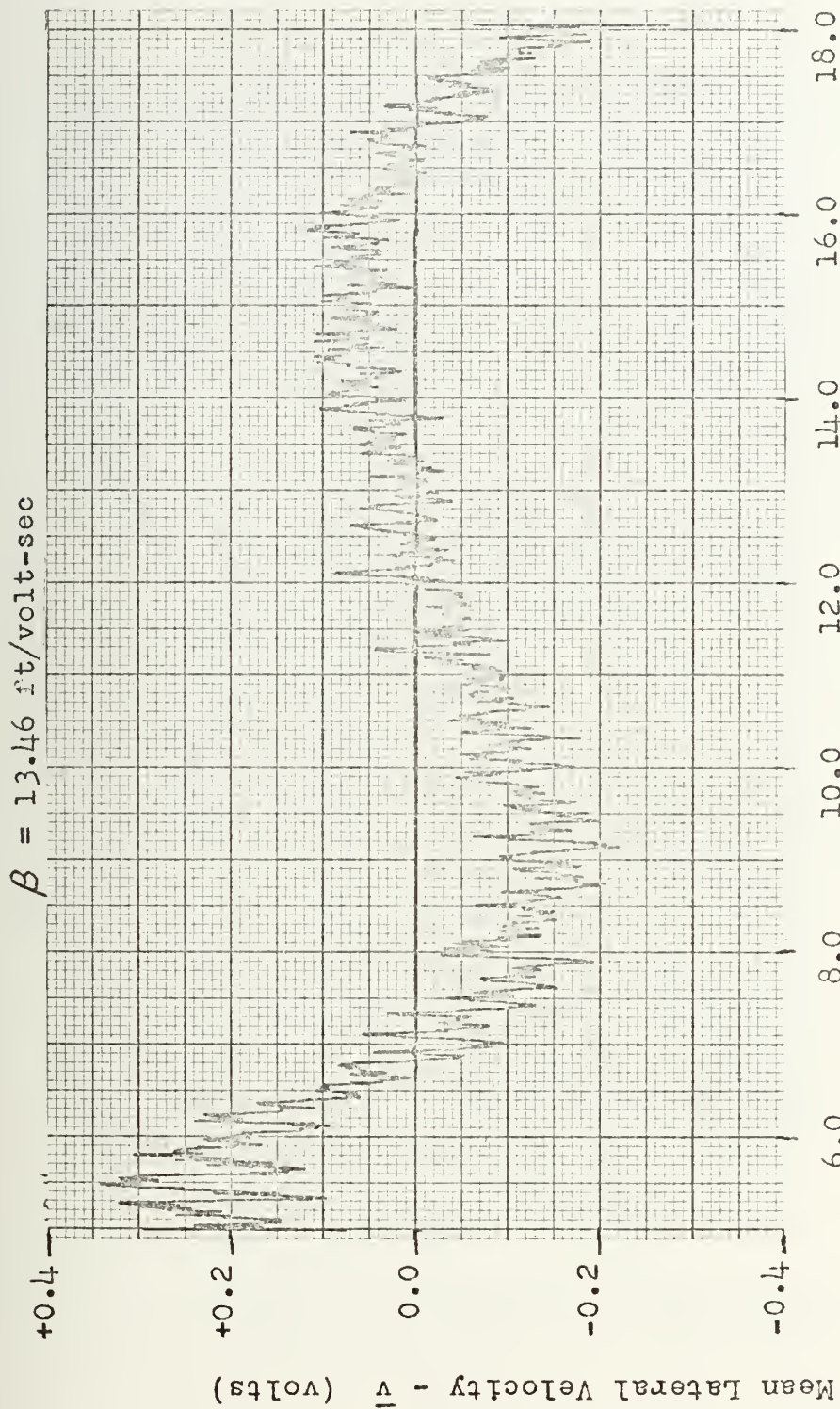


FIGURE 37
Station 7 X-Array Mean Lateral Velocity

$$\beta = 13.21 \text{ ft/volt-sec}$$



FIGURE 38
Station 8 X-Array Mean Lateral Velocity

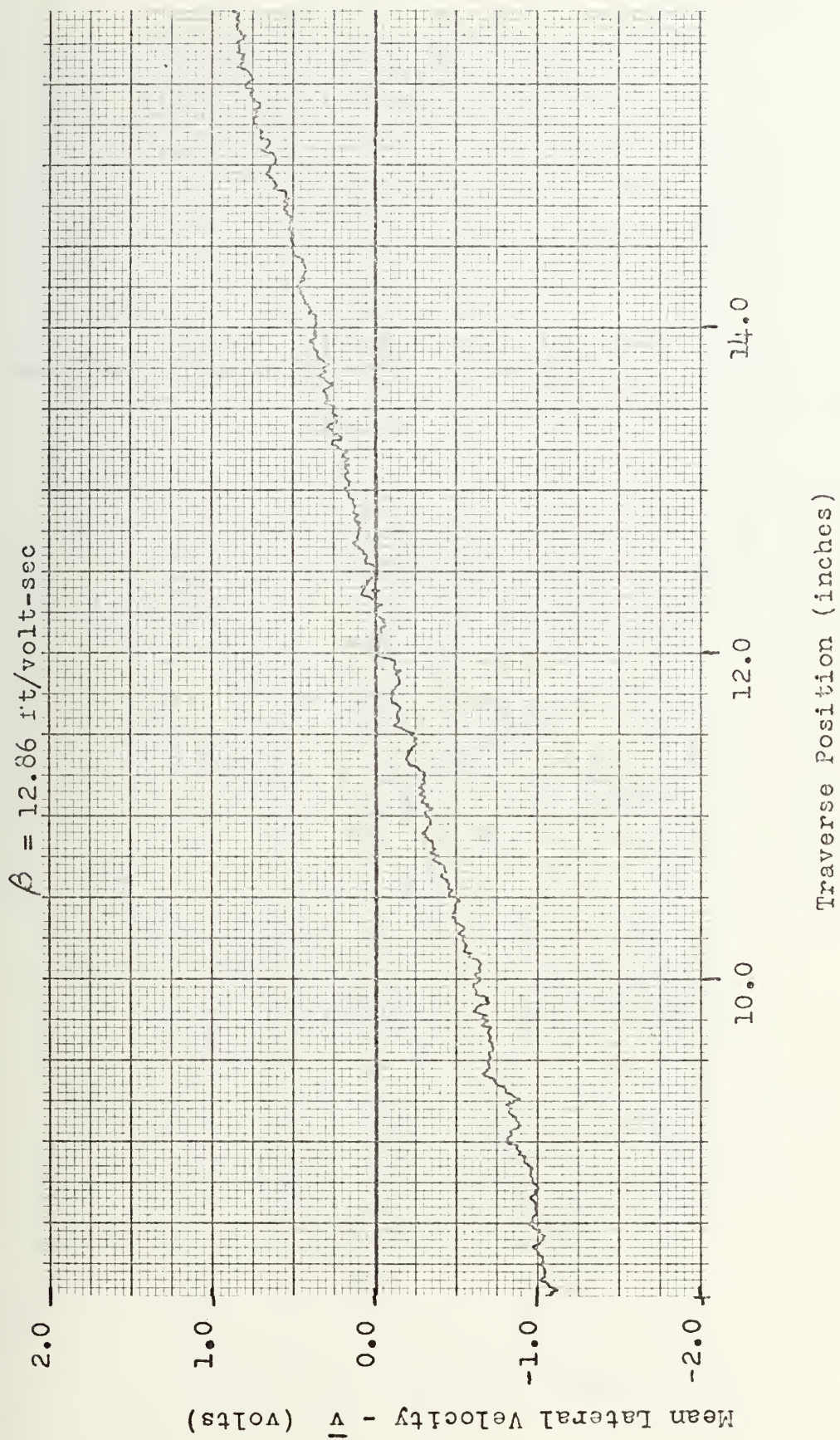


FIGURE 39
Station 9 X-Array Mean Lateral Velocity

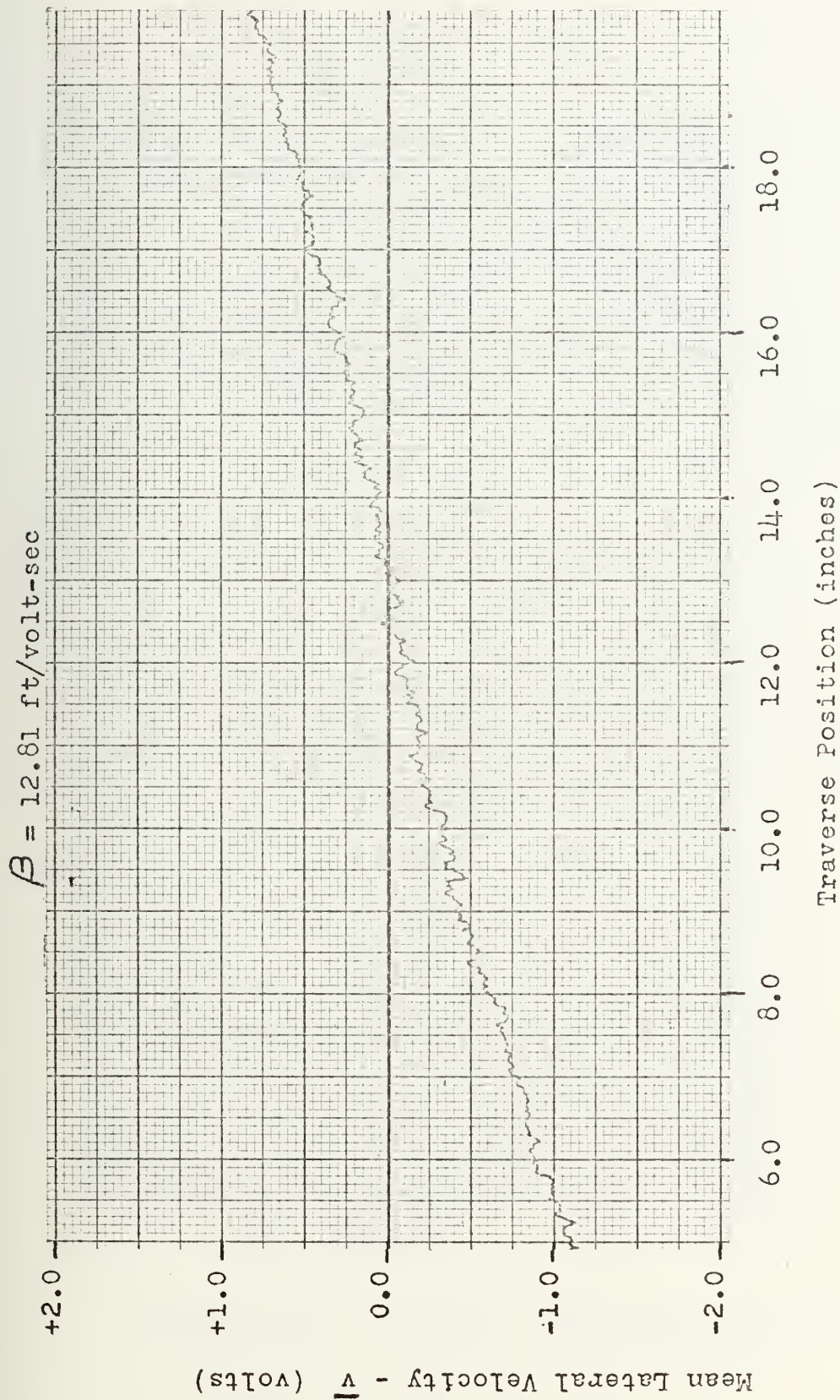


FIGURE 40
Station 10 X-Array Mean Lateral Velocity

$$\beta = 525.87 \text{ ft}^2/\text{volt-sec}^2$$

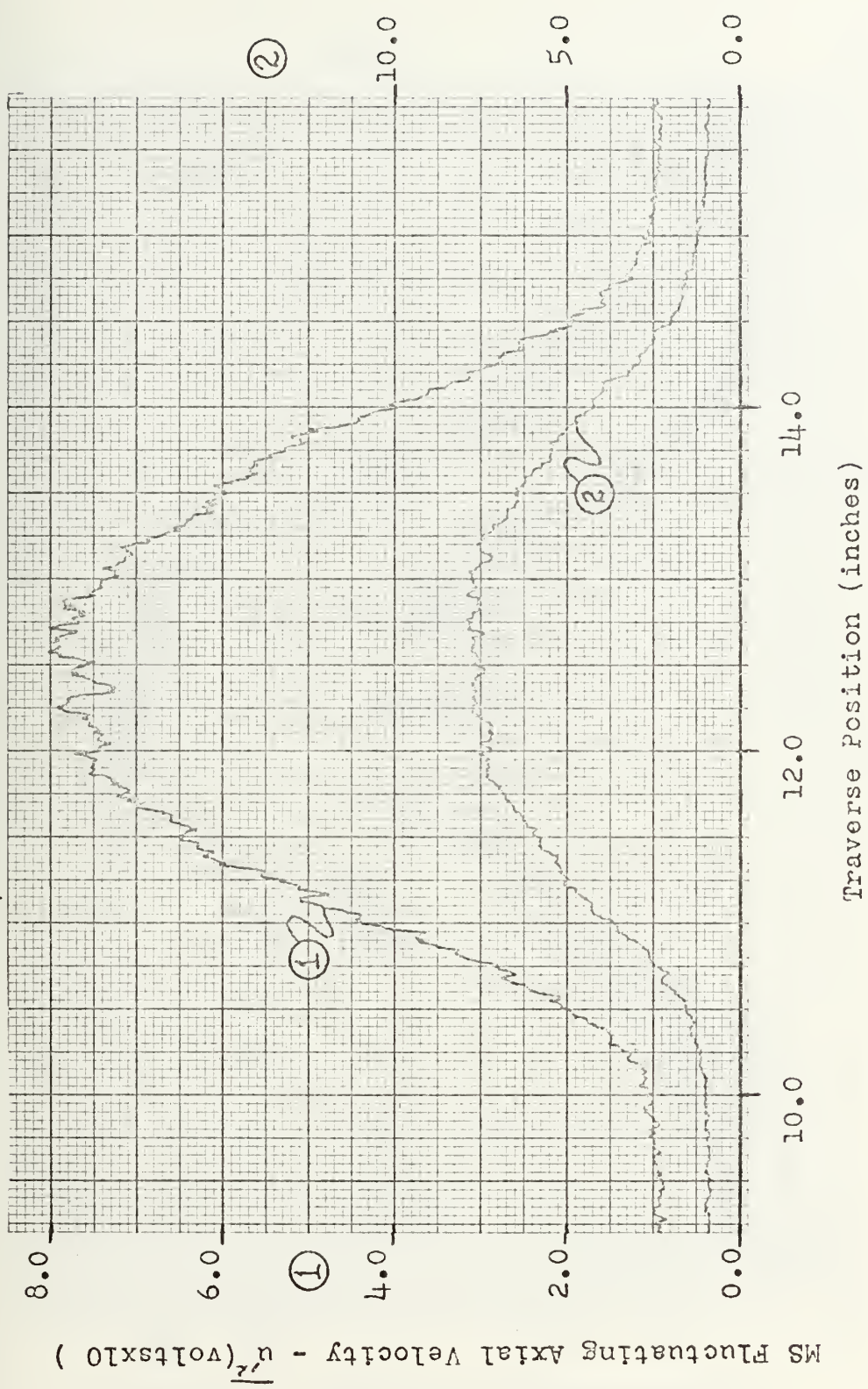
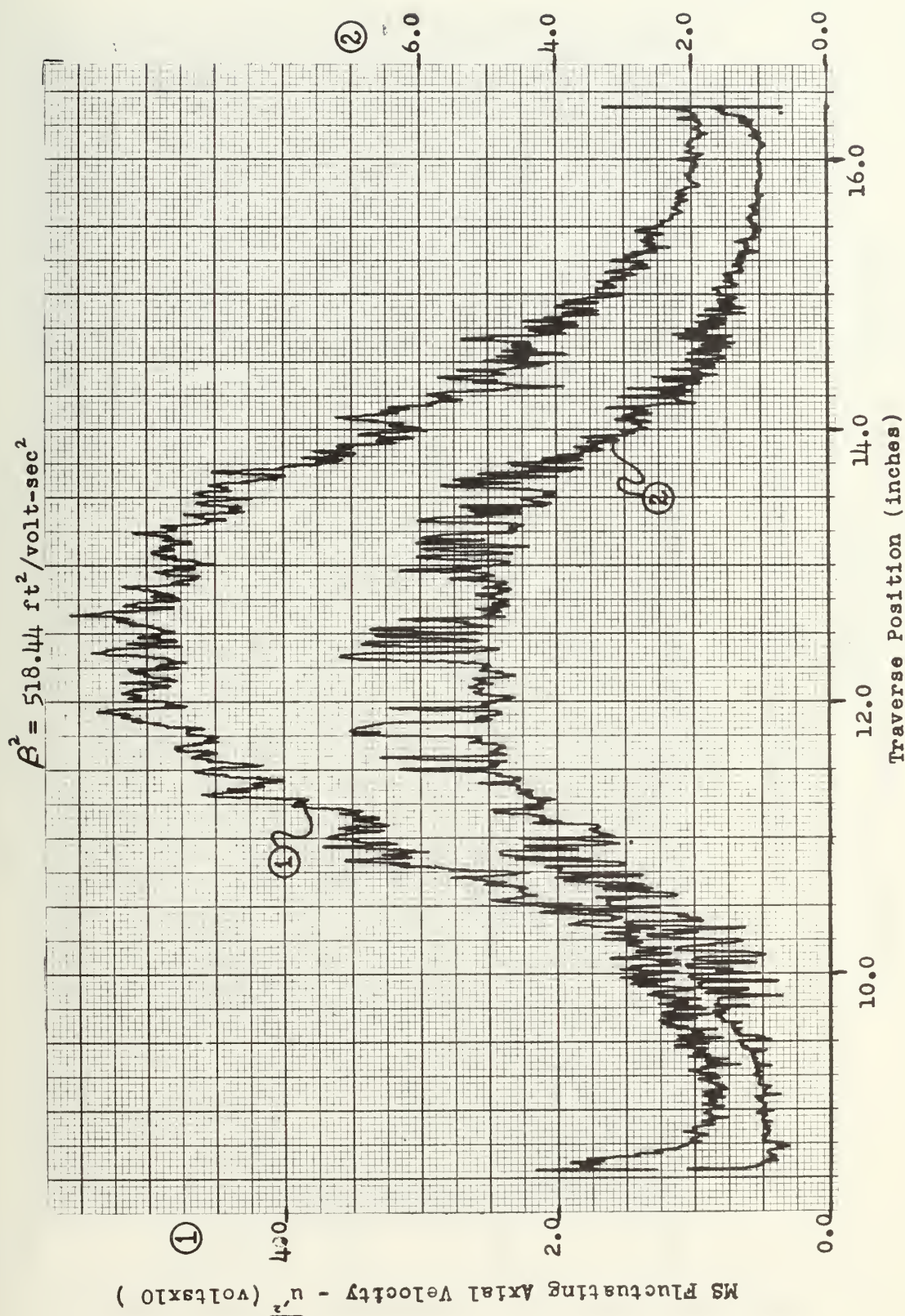


FIGURE 41
Station 1 X-Array MS Fluctuating Axial Velocity



Station 2 X-Array MS Fluctuating Axial Velocity
FIGURE 42

$$\beta = 315.43 \text{ ft}^2/\text{volt-sec}^2$$

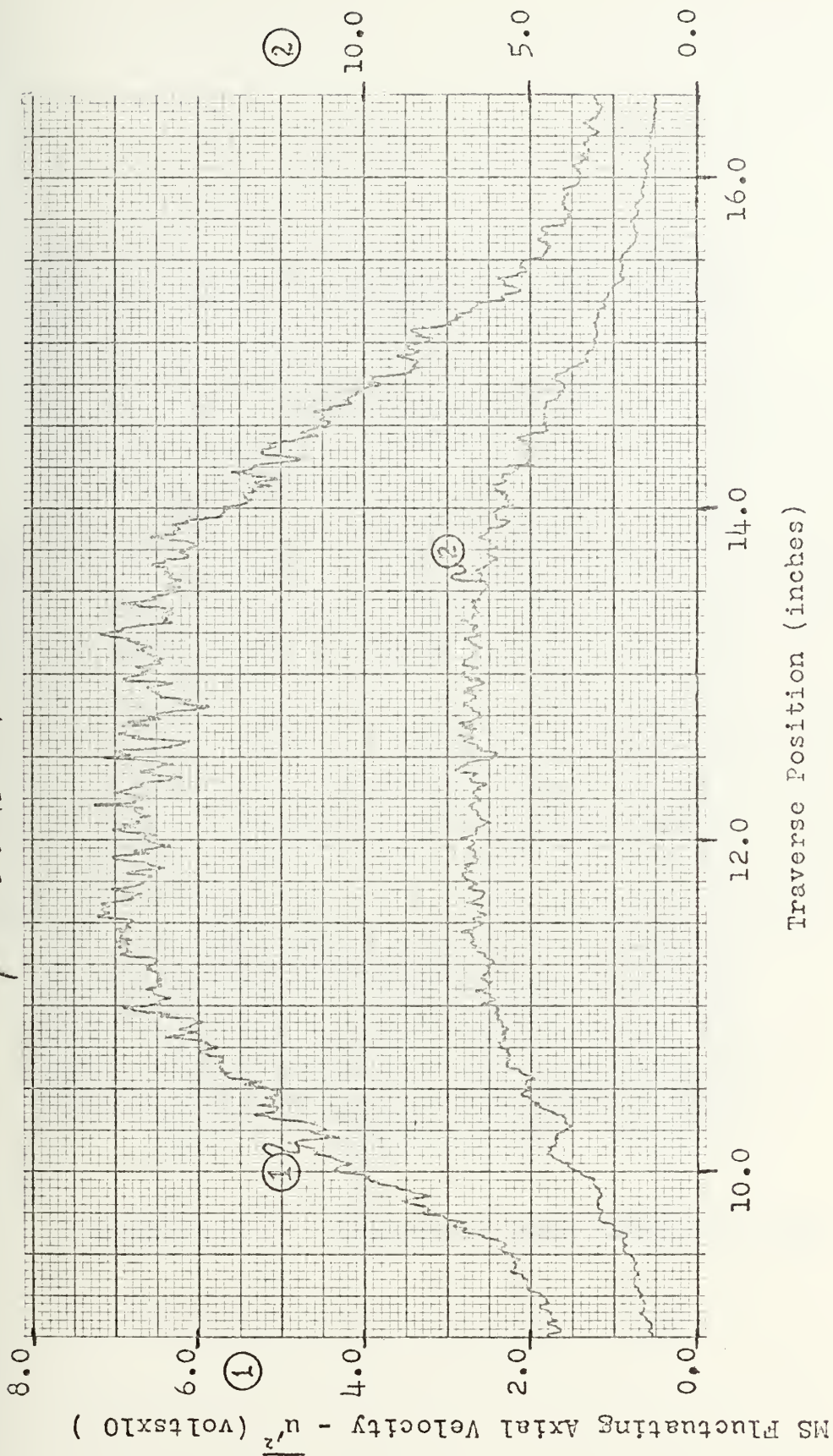


FIGURE 43
Station 3 X-Array MS Fluctuating Axial Velocity

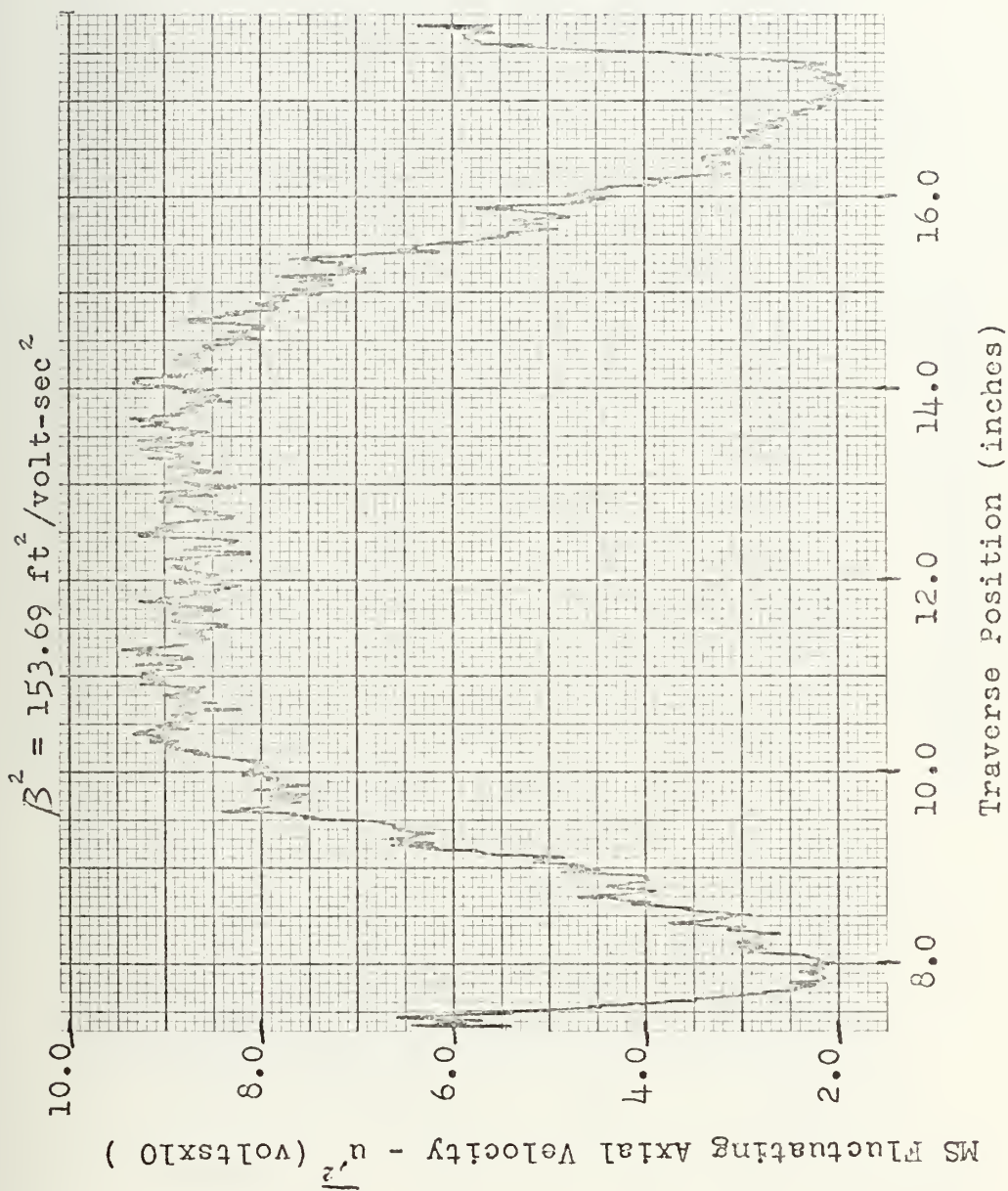


FIGURE 44
Station 4 X-Array MS Fluctuating Axial Velocity

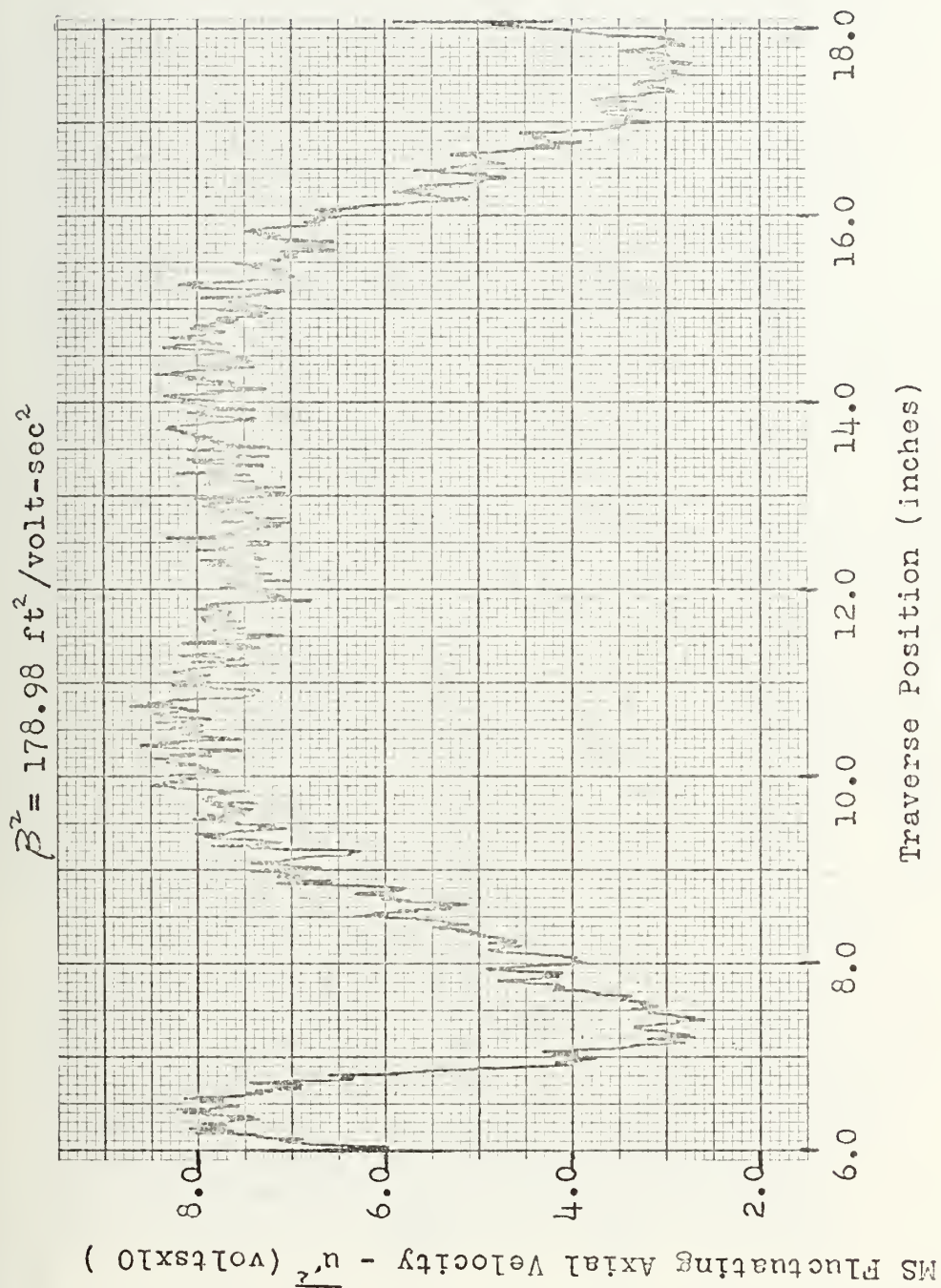


FIGURE 45
Station 5 X-Array MS Fluctuating Axial Velocity

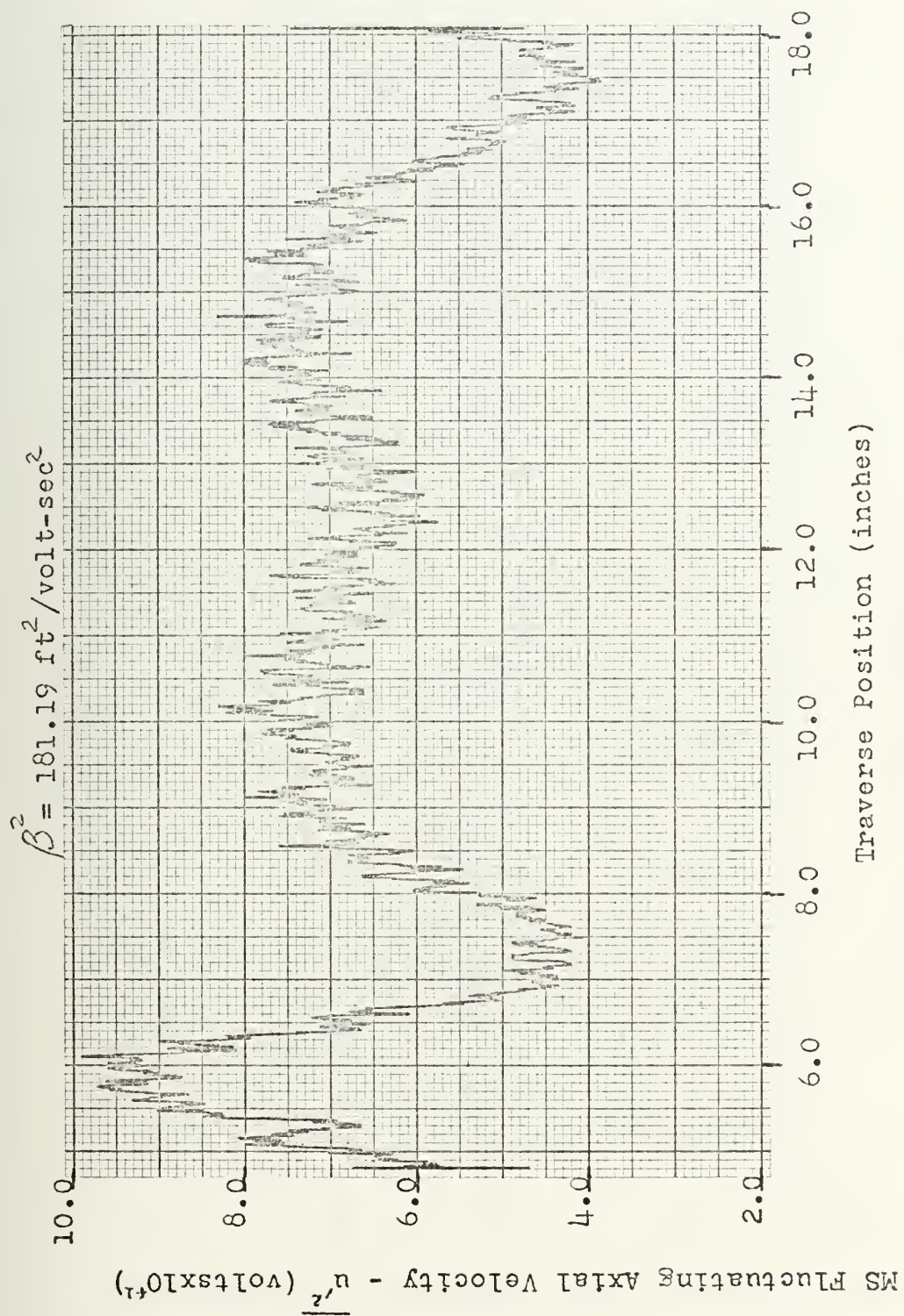


FIGURE 46
Station 6 X-Array MS Fluctuating Axial Velocity

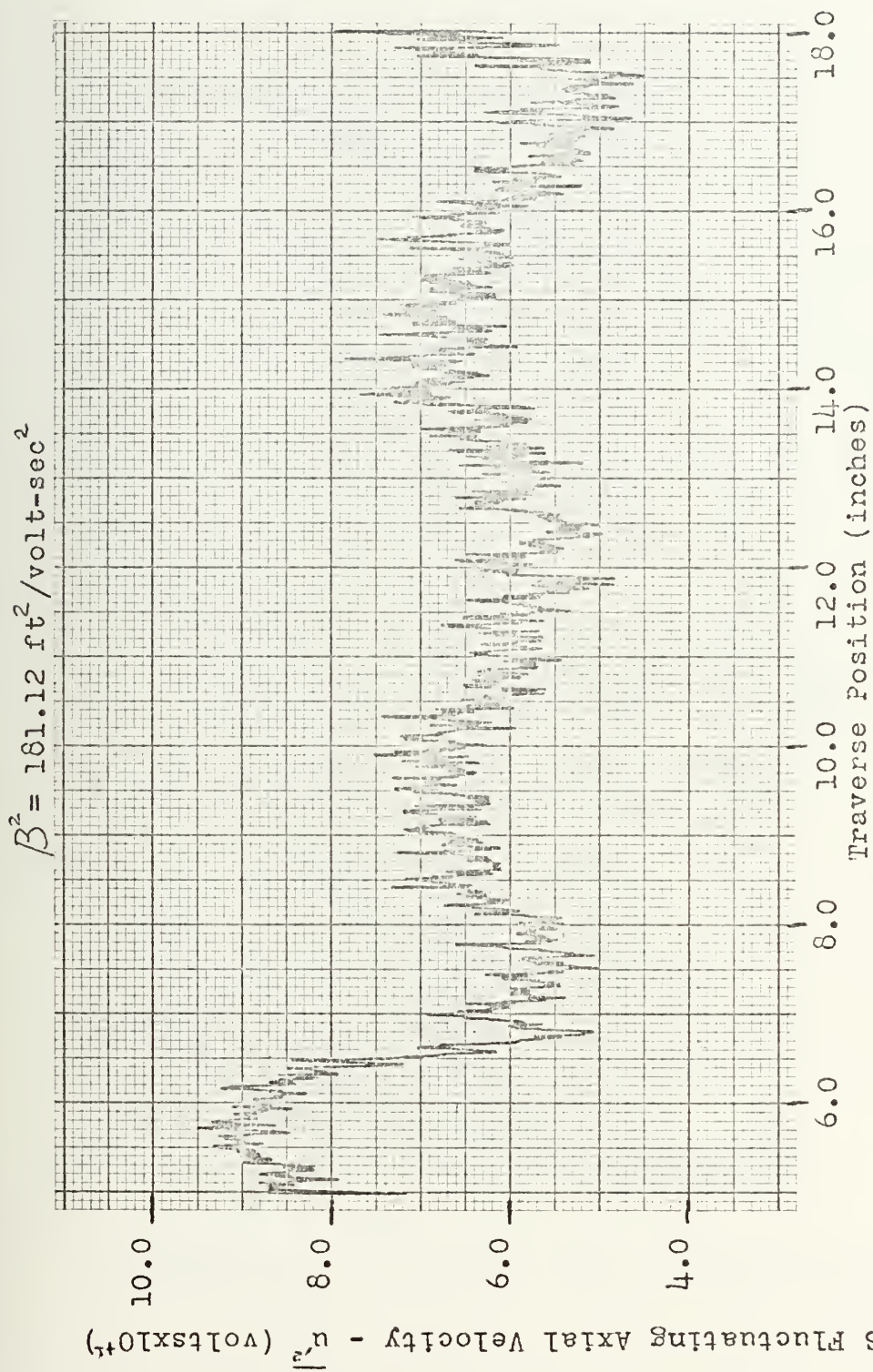


FIGURE 47
Station 7 X-Array MS Fluctuating Axial Velocity

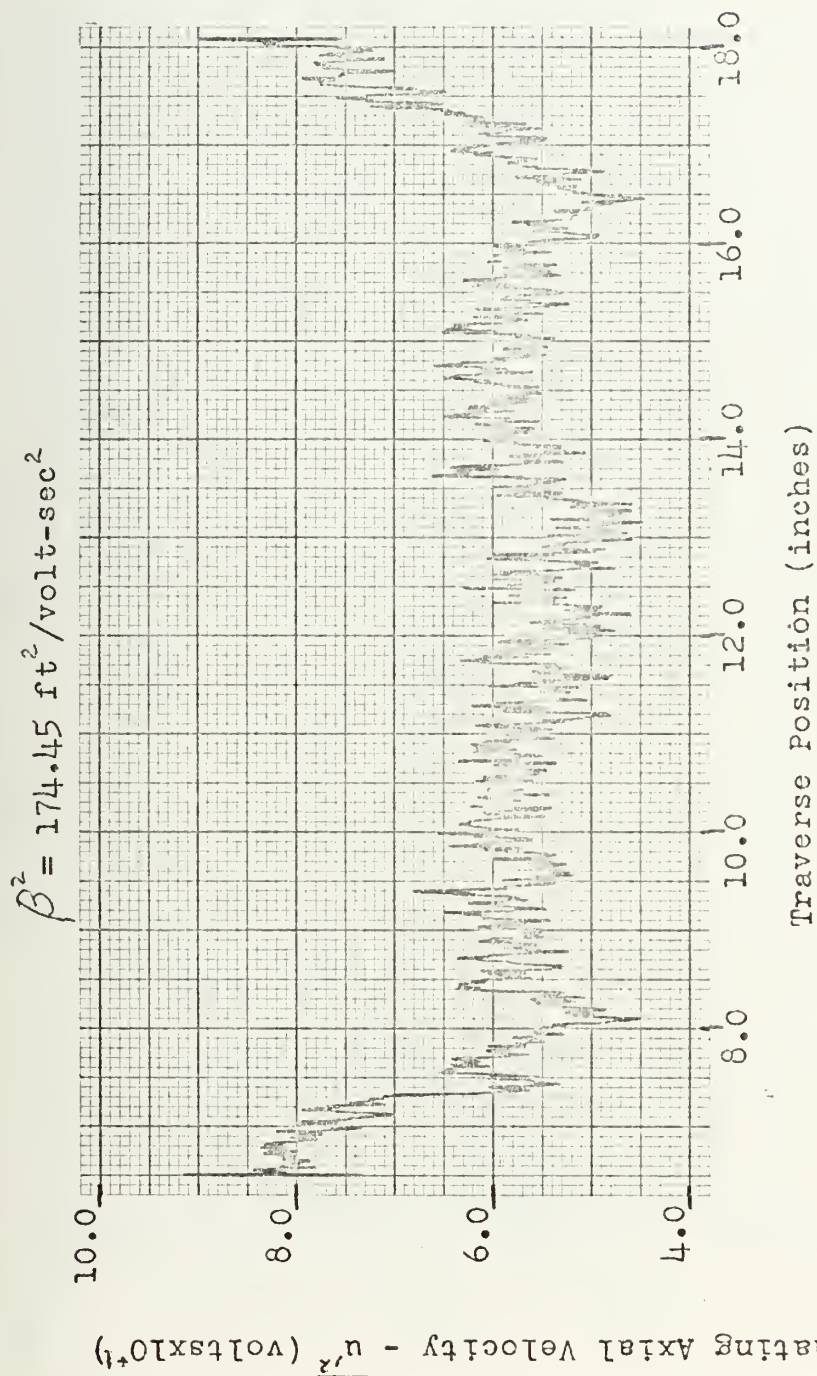


FIGURE 48
Station 8 X-Array MS Fluctuating Axial Velocity

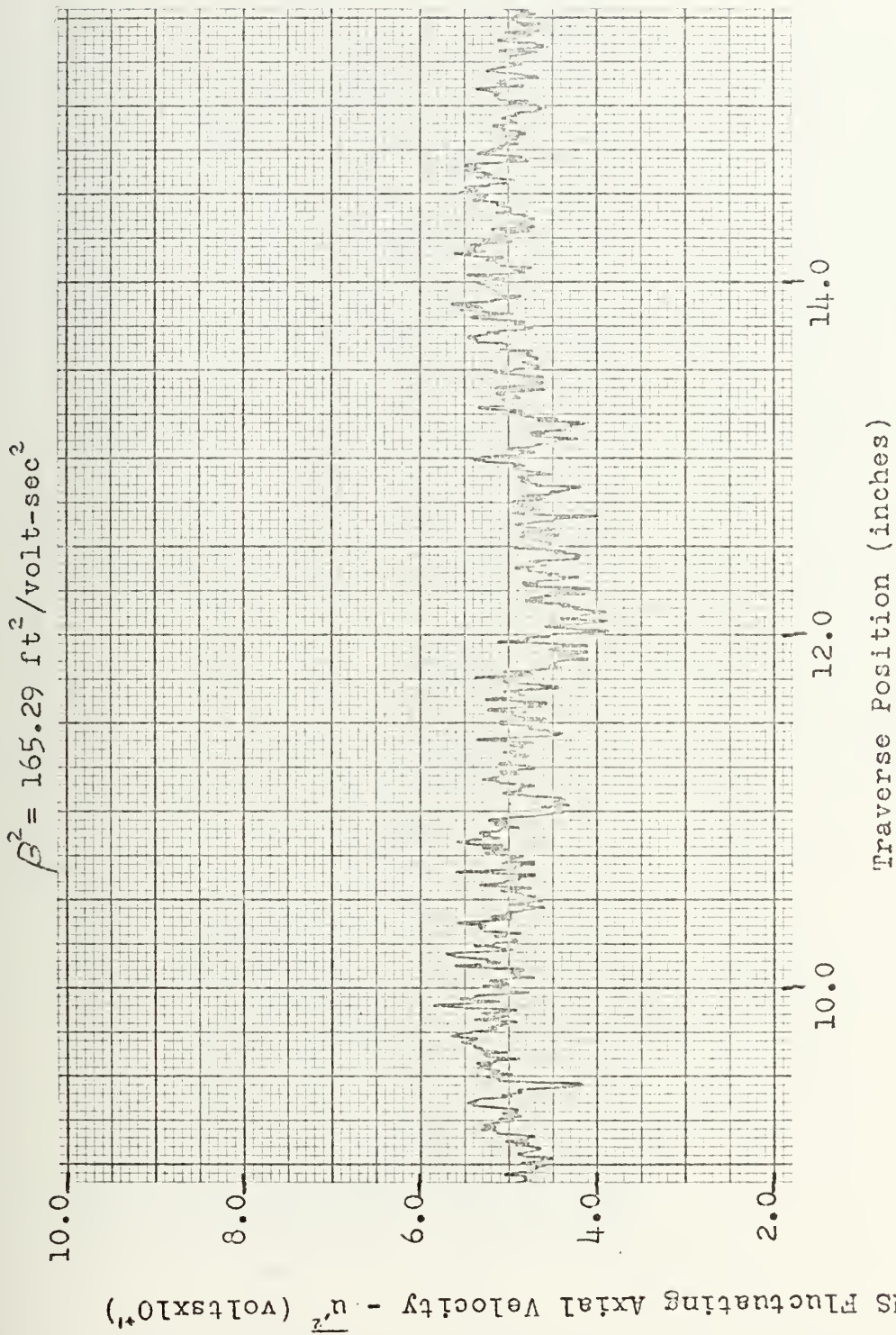


FIGURE 49
Station 9 X-Array MS Fluctuating Axial Velocity

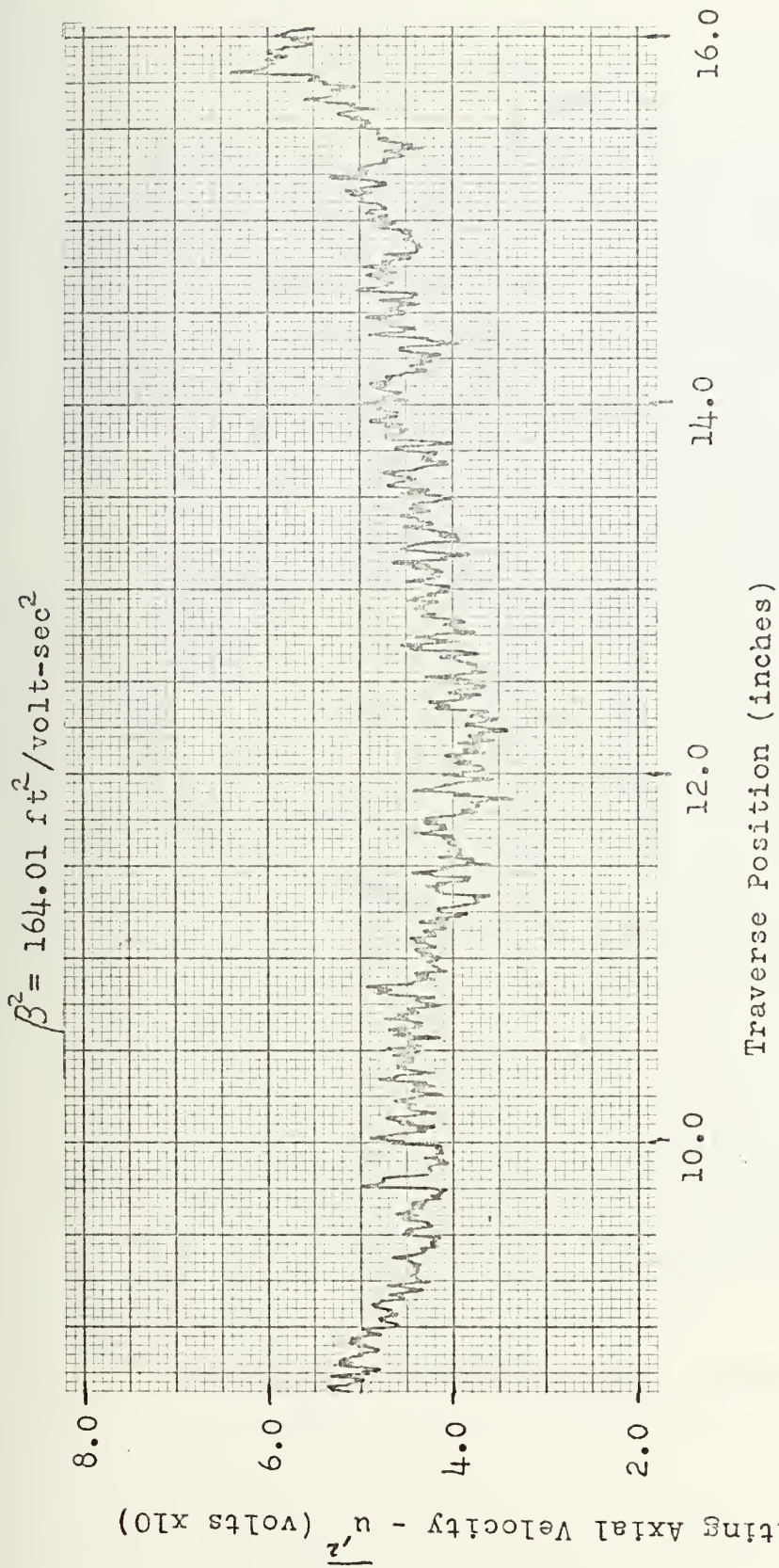


FIGURE 50
Station 10 X-Array MS Fluctuating Axial Velocity

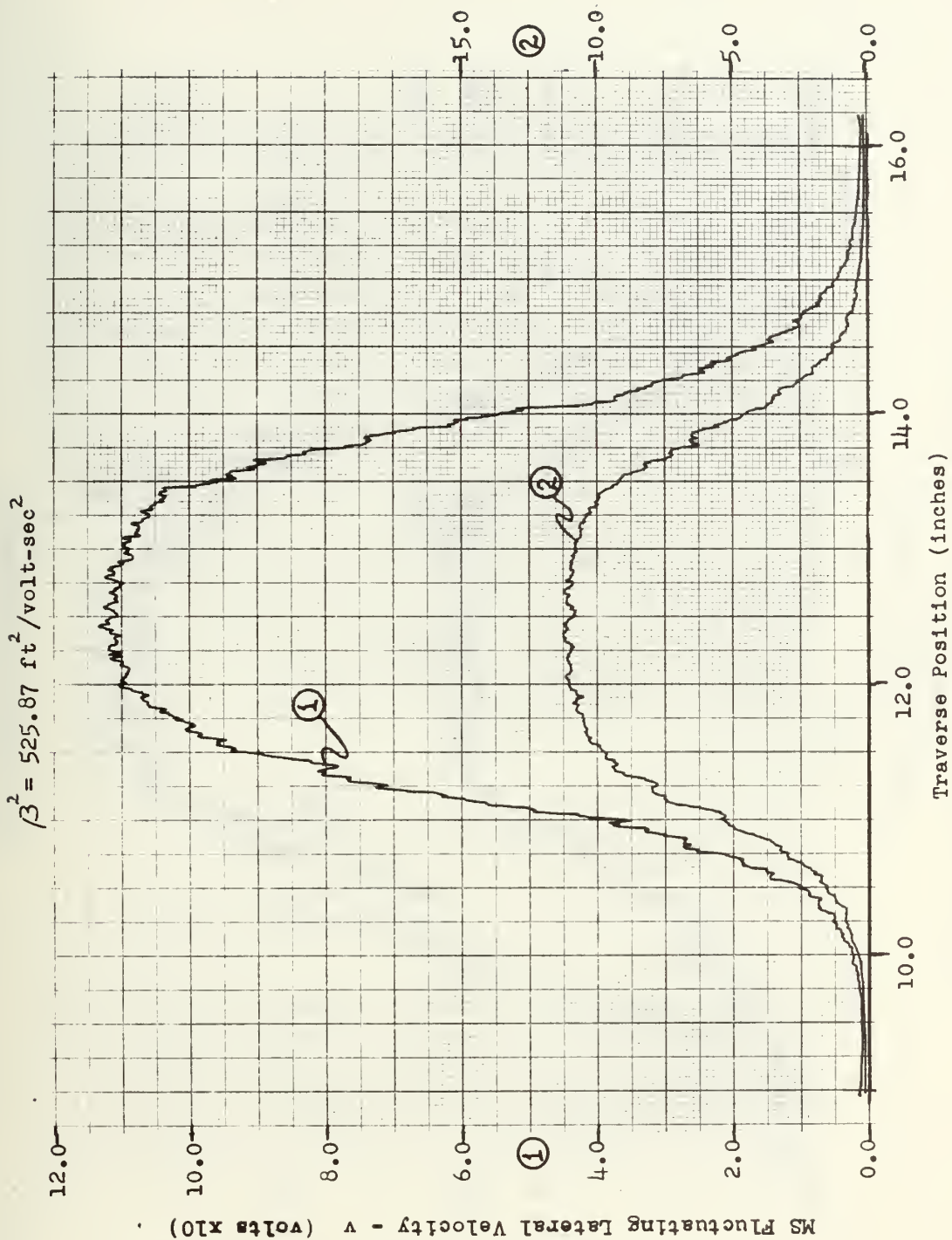


FIGURE 51
Station 1 X-Array MS Fluctuating Lateral Velocity

$$\beta^2 = 518.44 \text{ ft}^2/\text{volt-sec}^2$$

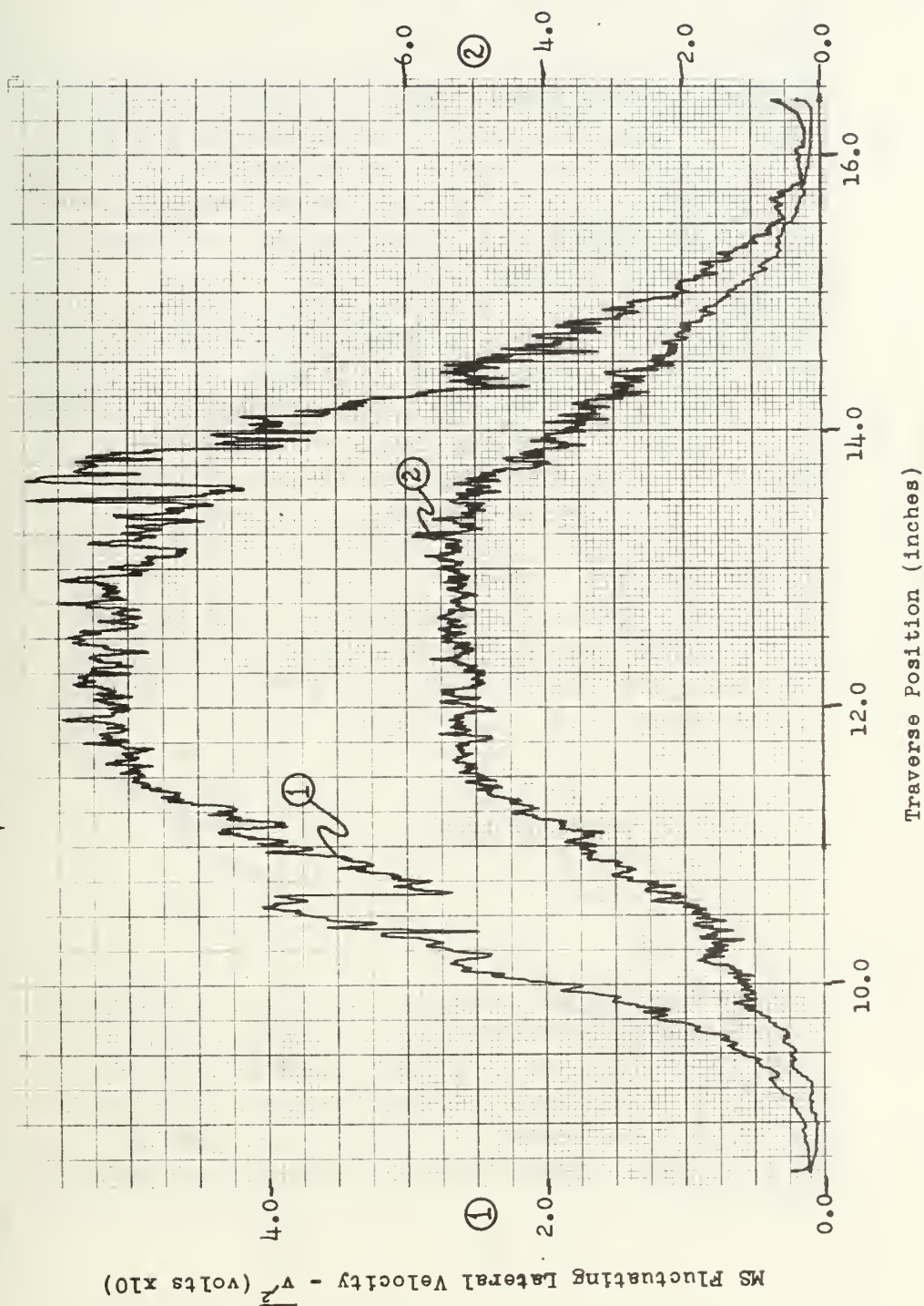


FIGURE 52
Station 2 X-Array MS Fluctuating Lateral Velocity

$$\beta^2 = 315.43 \text{ ft}^2 / \text{volt-sec}^2$$

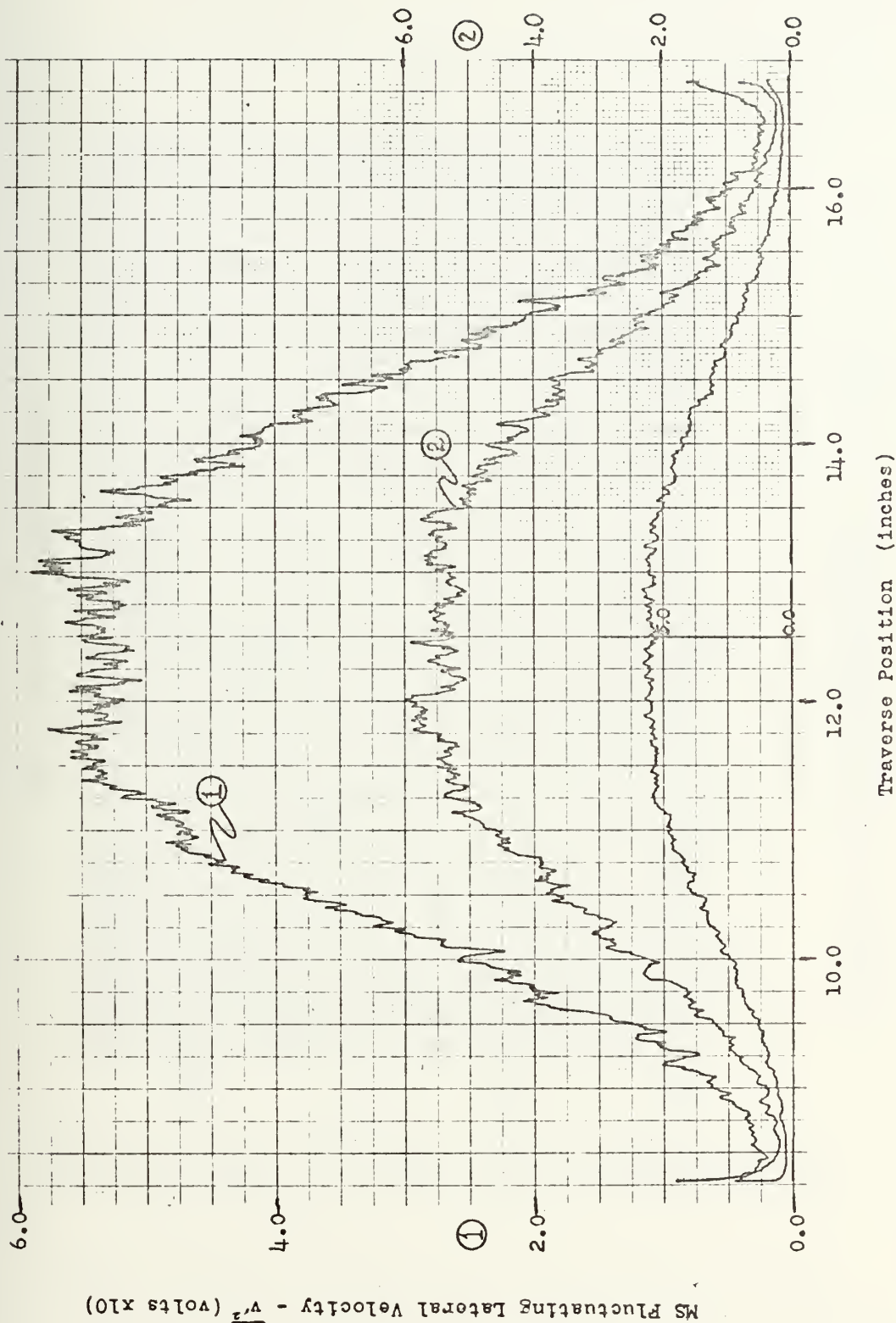
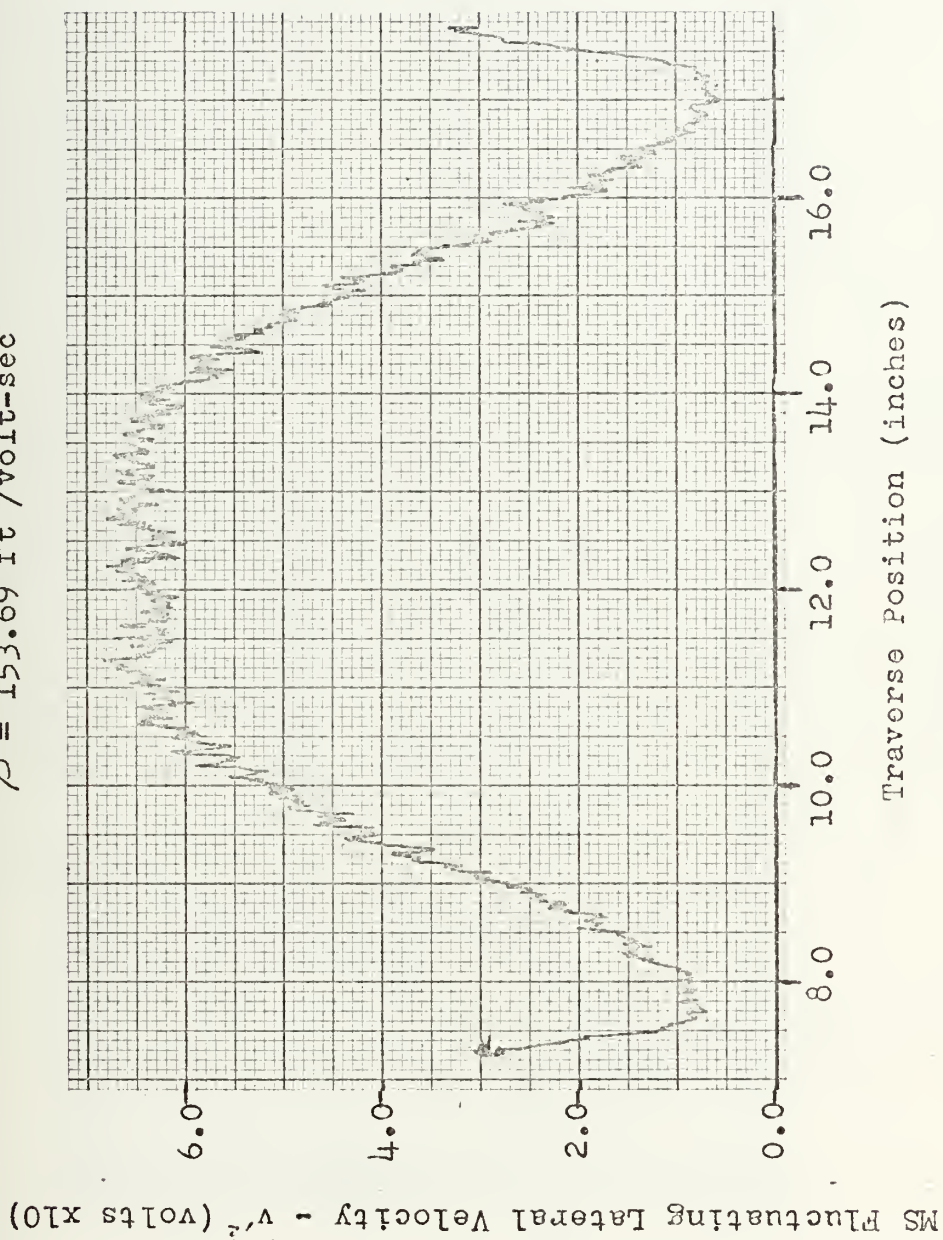


FIGURE 53
Station 3 X-Array MS Fluctuating Lateral Velocity

$$\beta^2 = 153.69 \text{ ft}^2/\text{volt-sec}^2$$



Traverse Position (inches)

FIGURE 54

Station 4 X-Array MS Fluctuating Lateral Velocity

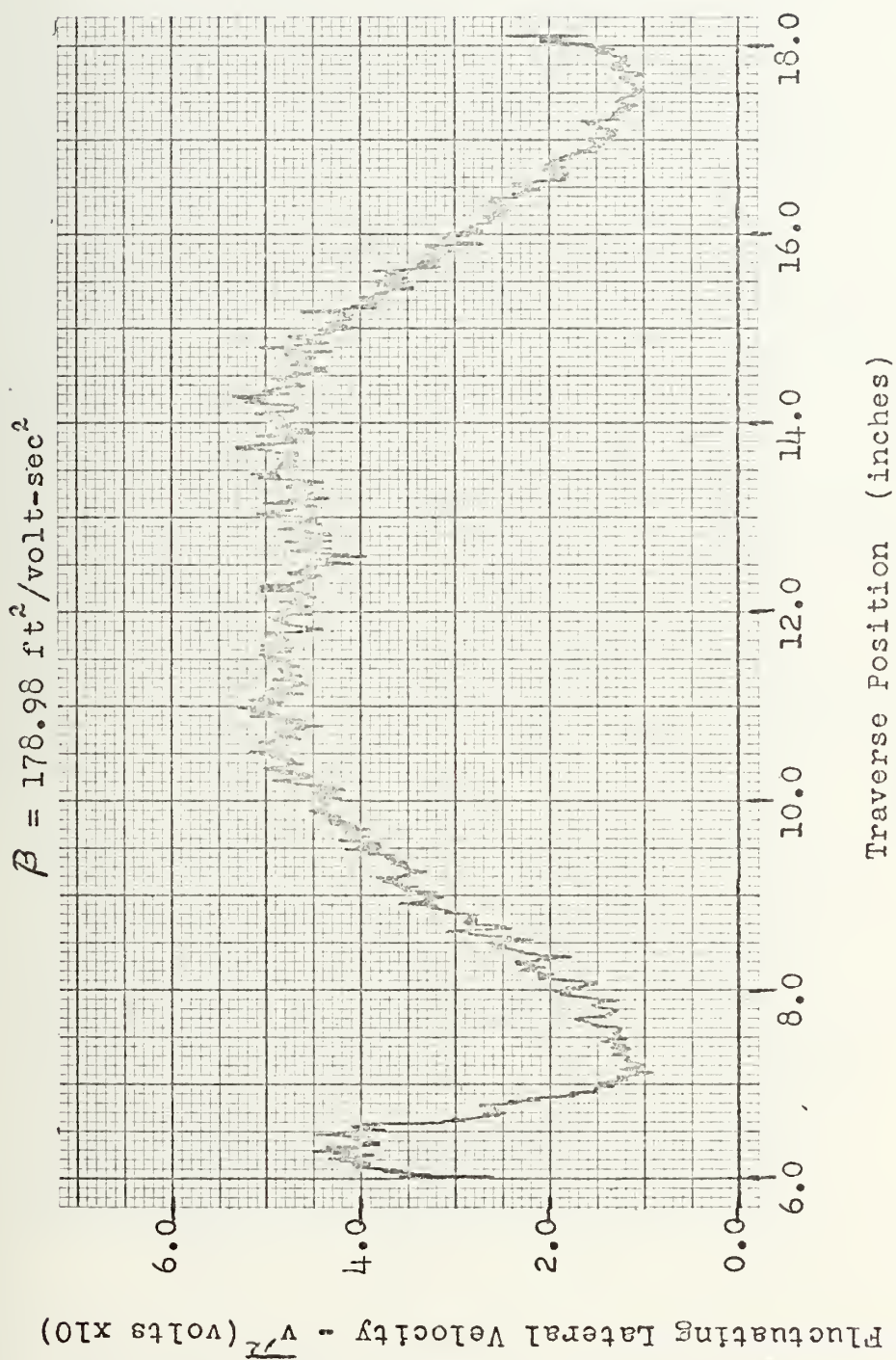
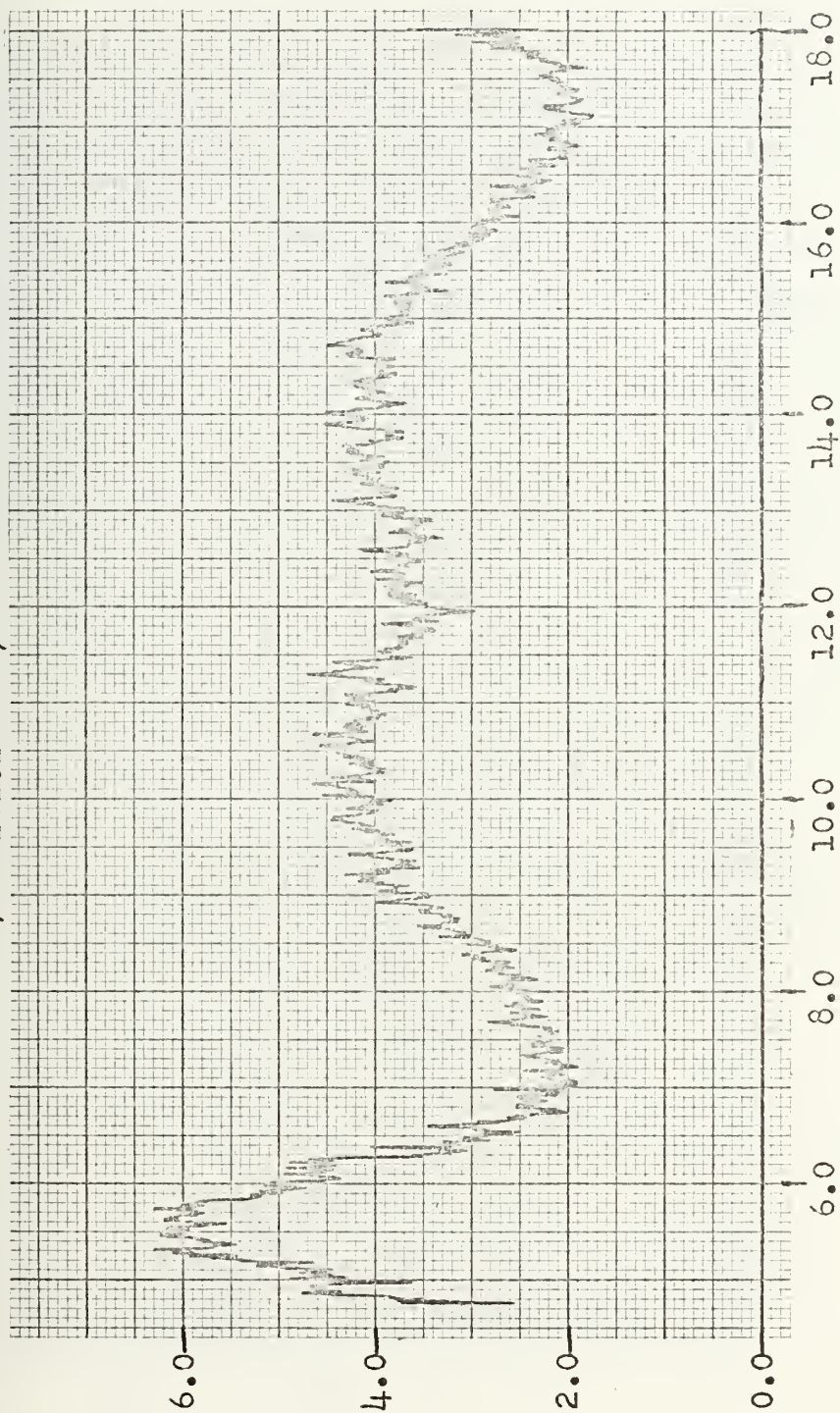


FIGURE 55
Station 5 X-Array MS Fluctuating Lateral Velocity

$$\beta^2 = 181.18 \text{ ft}^2/\text{volt-sec}^2$$



Traverse Position (inches)

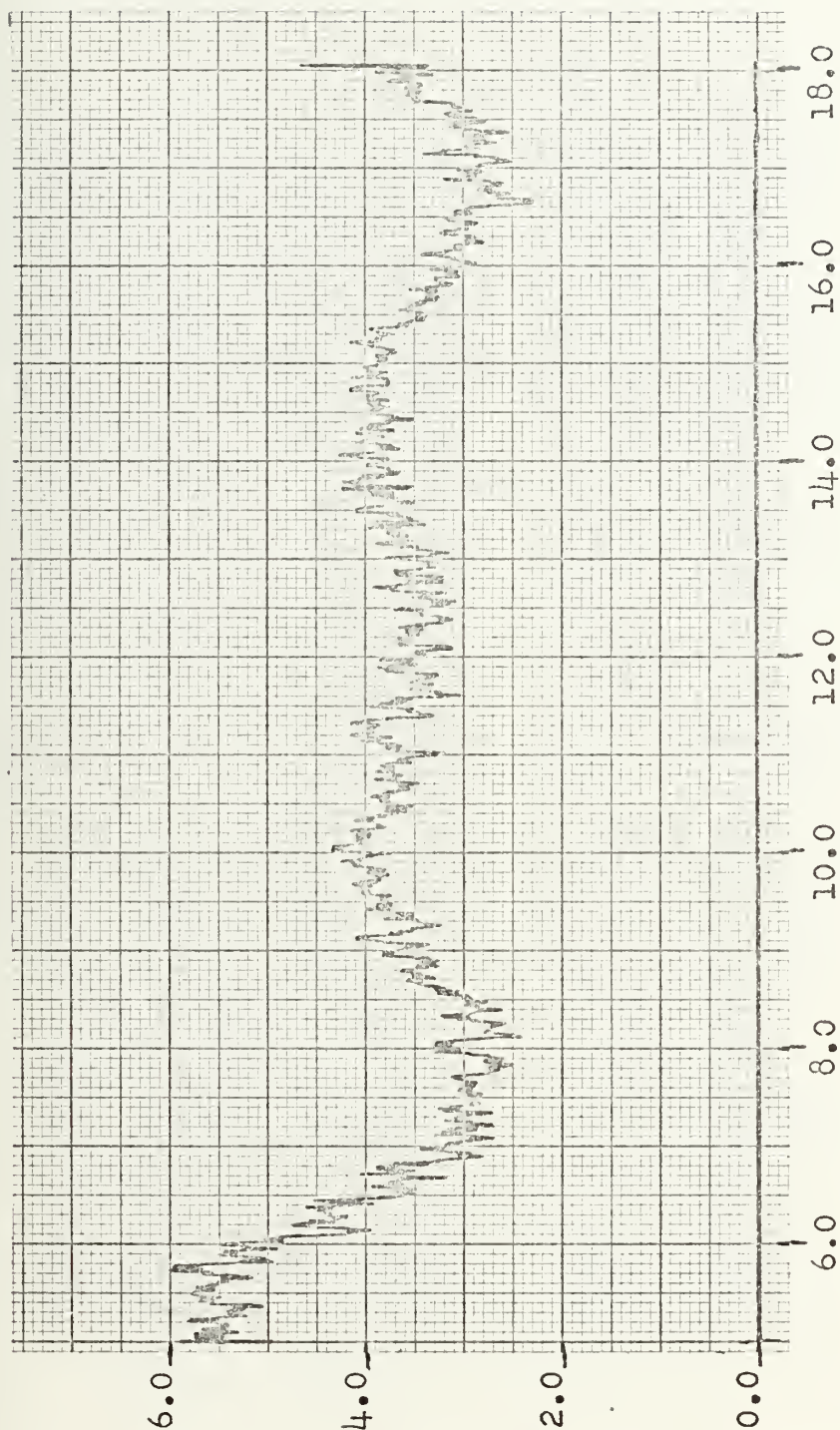
FIGURE 56

Station 6 X-Array MS Fluctuating Lateral Velocity

MS Fluctuating Lateral Velocity - v' (volts x 10)

$$\beta^2 = 181.12 \text{ ft}^2/\text{volt-sec}^2$$

MS Fluctuating Lateral Velocity - v_x^2 (volts x 10)



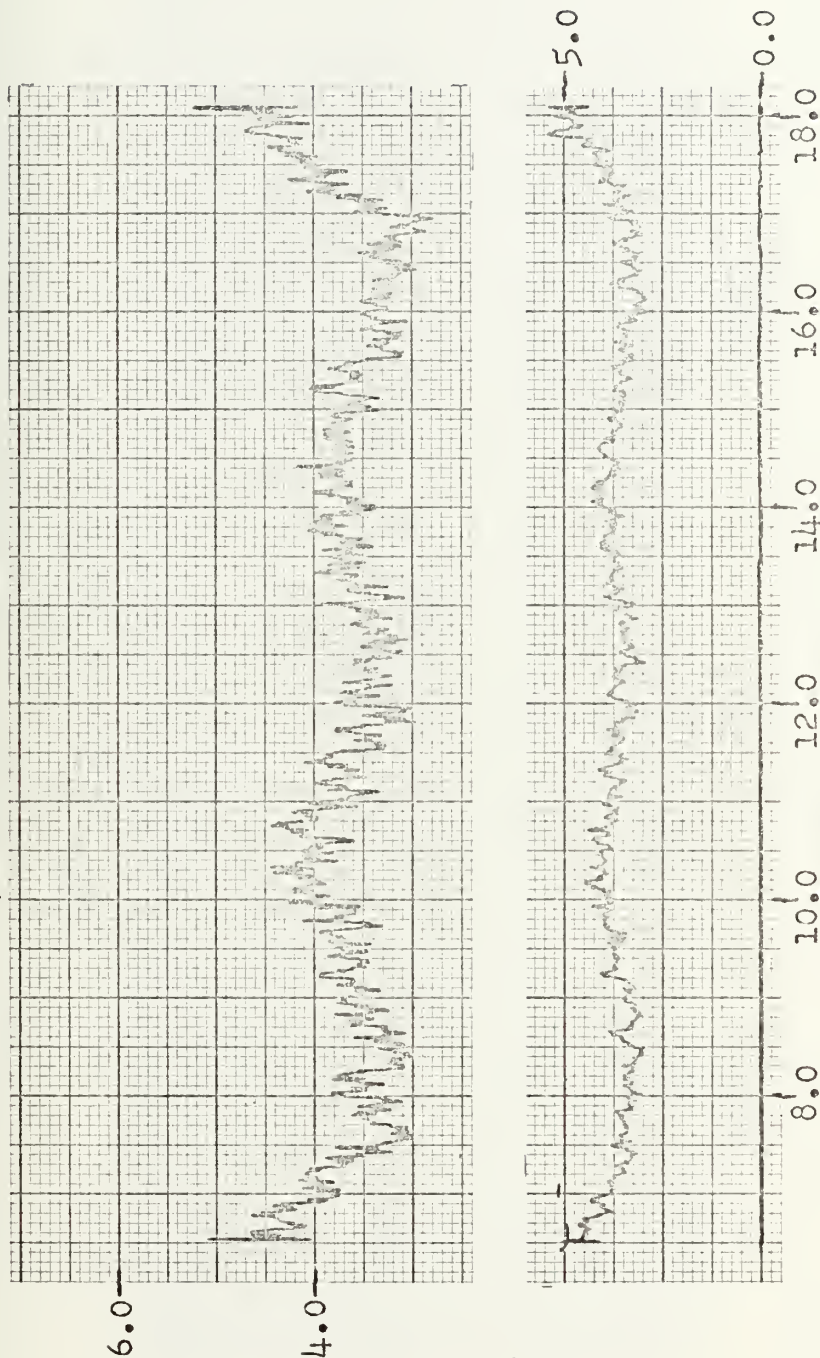
Traverse Position (inches)

FIGURE 57

Station 7 X-Array MS Fluctuating Lateral Velocity

$$\beta = 174.45 \text{ ft}^2/\text{volt-sec}^2$$

MS Fluctuating Lateral Velocity - $\sqrt{v^2}$ (volts x10)



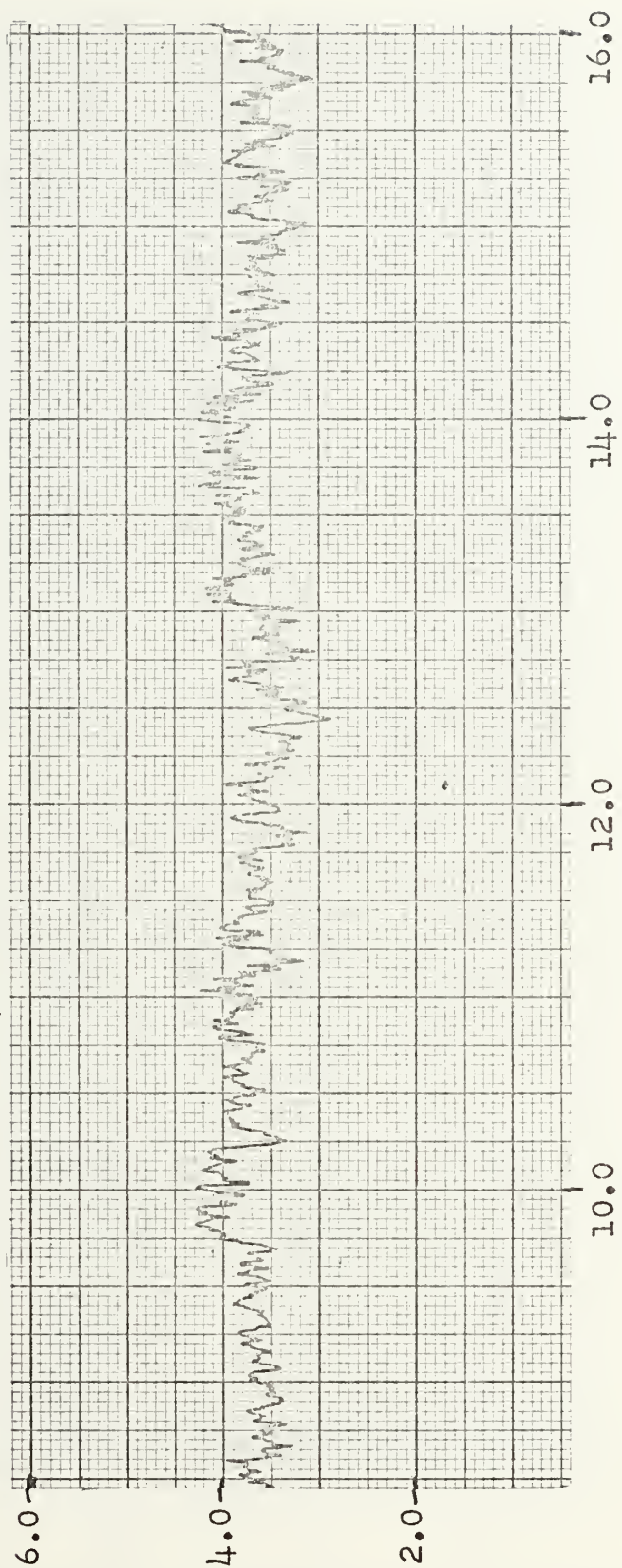
Traverse Position (inches)

FIGURE 58

Station 8 X-Array MS Fluctuating Lateral Velocity

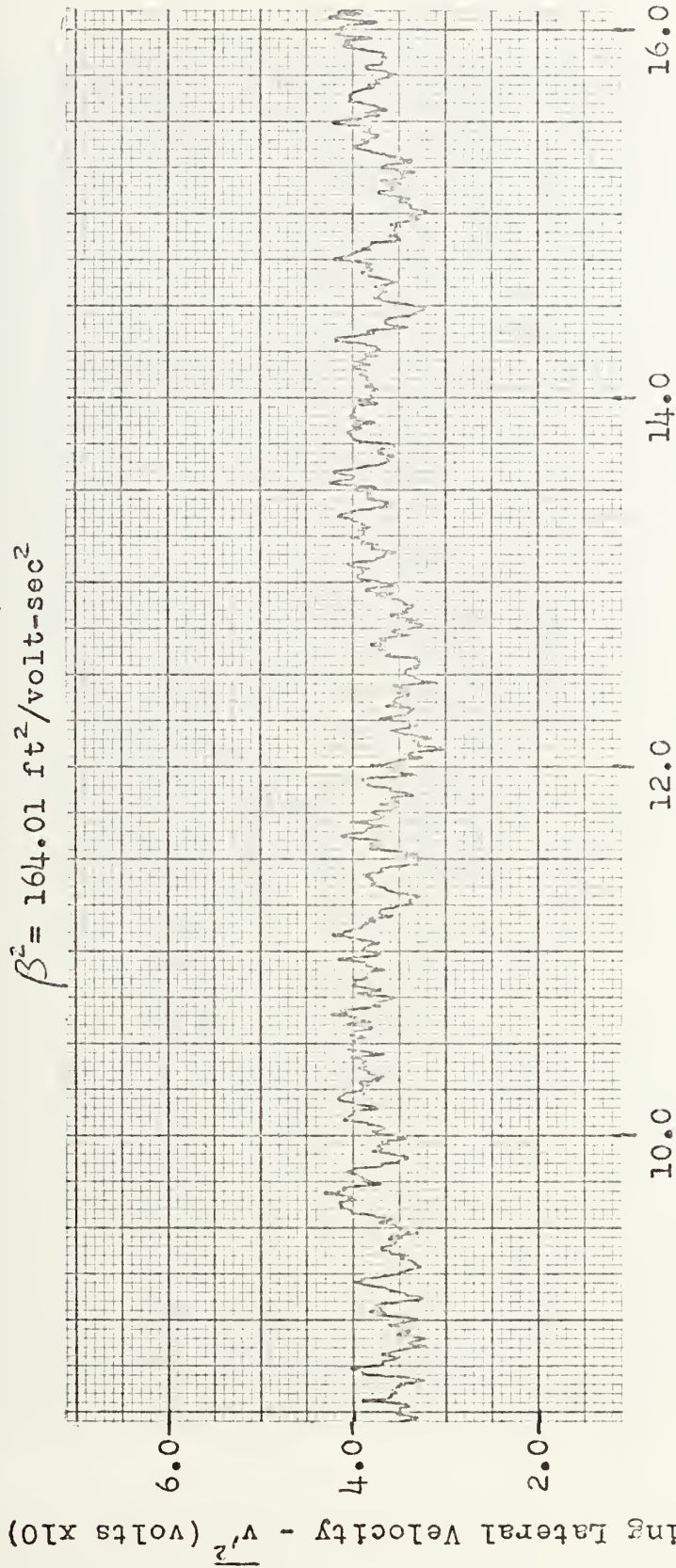
MS Fluctuating Lateral Velocity - v (volts x10)

$$\beta^2 = 165.29 \text{ ft}^2/\text{volt-sec}^2$$



Traverse Position (inches)

FIGURE 59
Station 9 X-Array MS Fluctuating Lateral Velocity



Traverse Position (inches)

FIGURE 60

Station 10 X-Array MS Fluctuating Lateral Velocity

$$\beta = 525.87 \text{ ft}^2/\text{volt-sec}^2$$

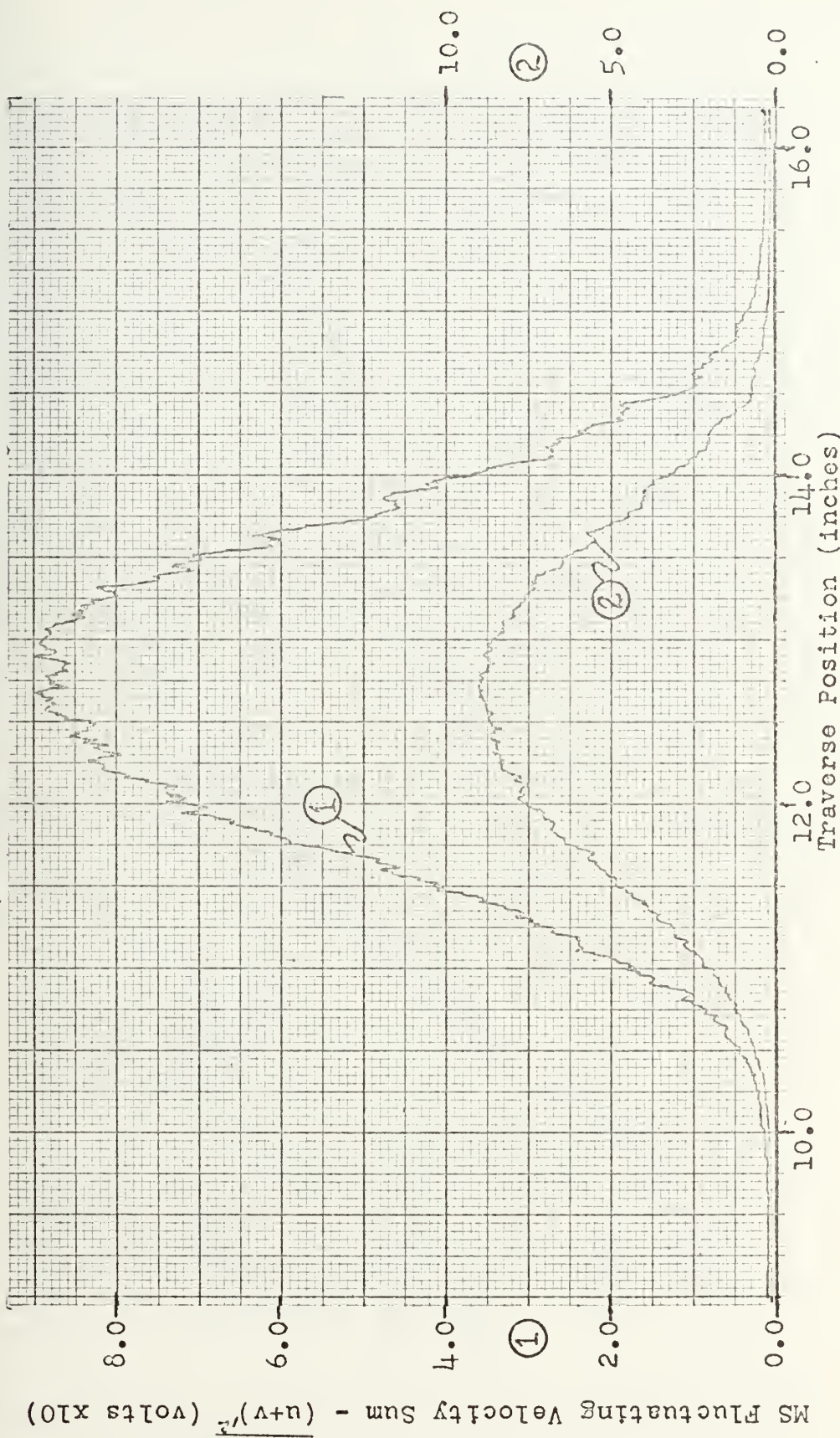


FIGURE 61

Station 1 X-Array MS Fluctuating Velocity Sum

$$\beta^2 = 518.44 \text{ ft}^2/\text{volt-sec}^2$$

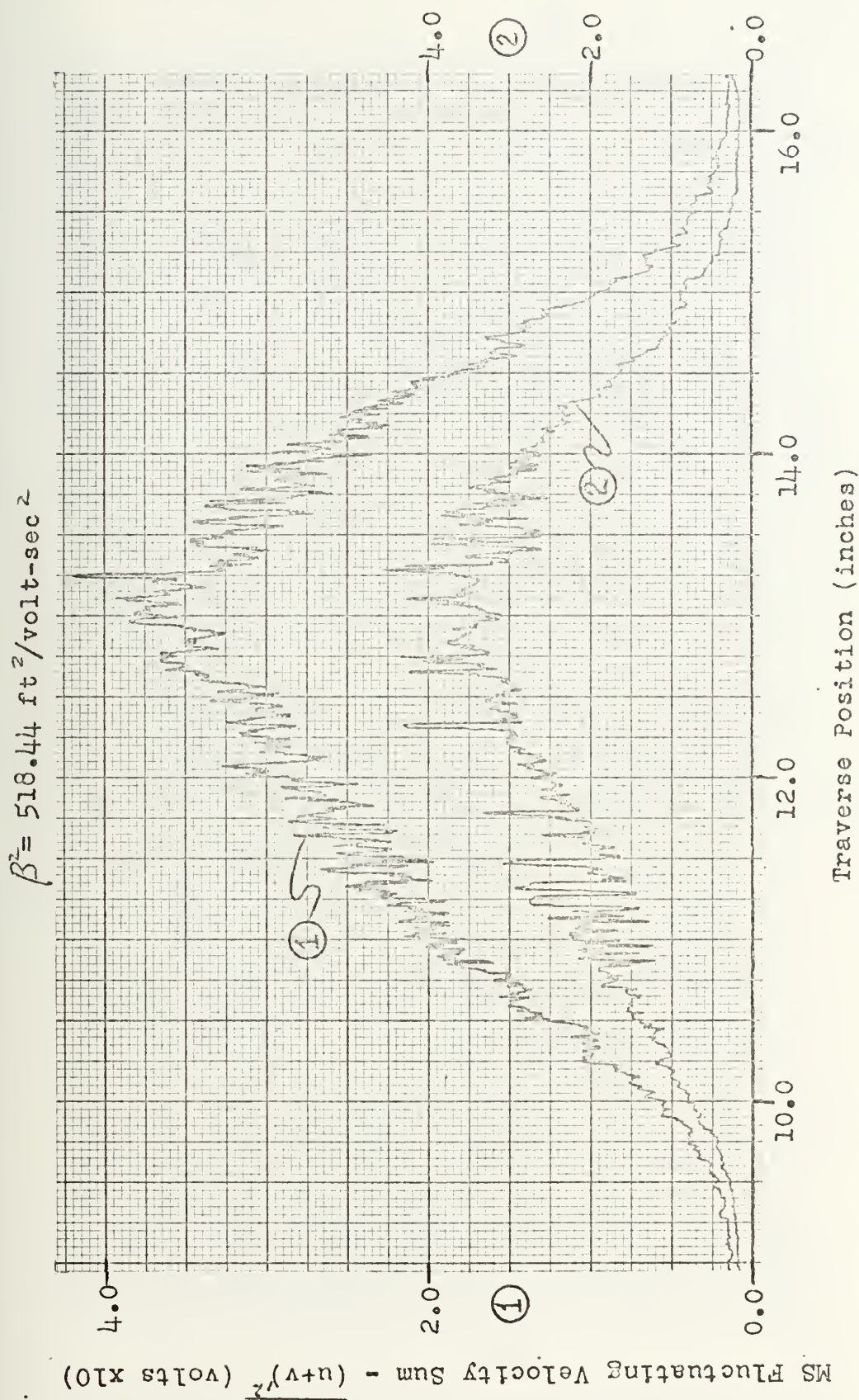


FIGURE 62

Station 2 X-Array MS Fluctuating Velocity Sum

$$\beta^2 = 315.43 \text{ ft}^2/\text{volt-sec}^2$$

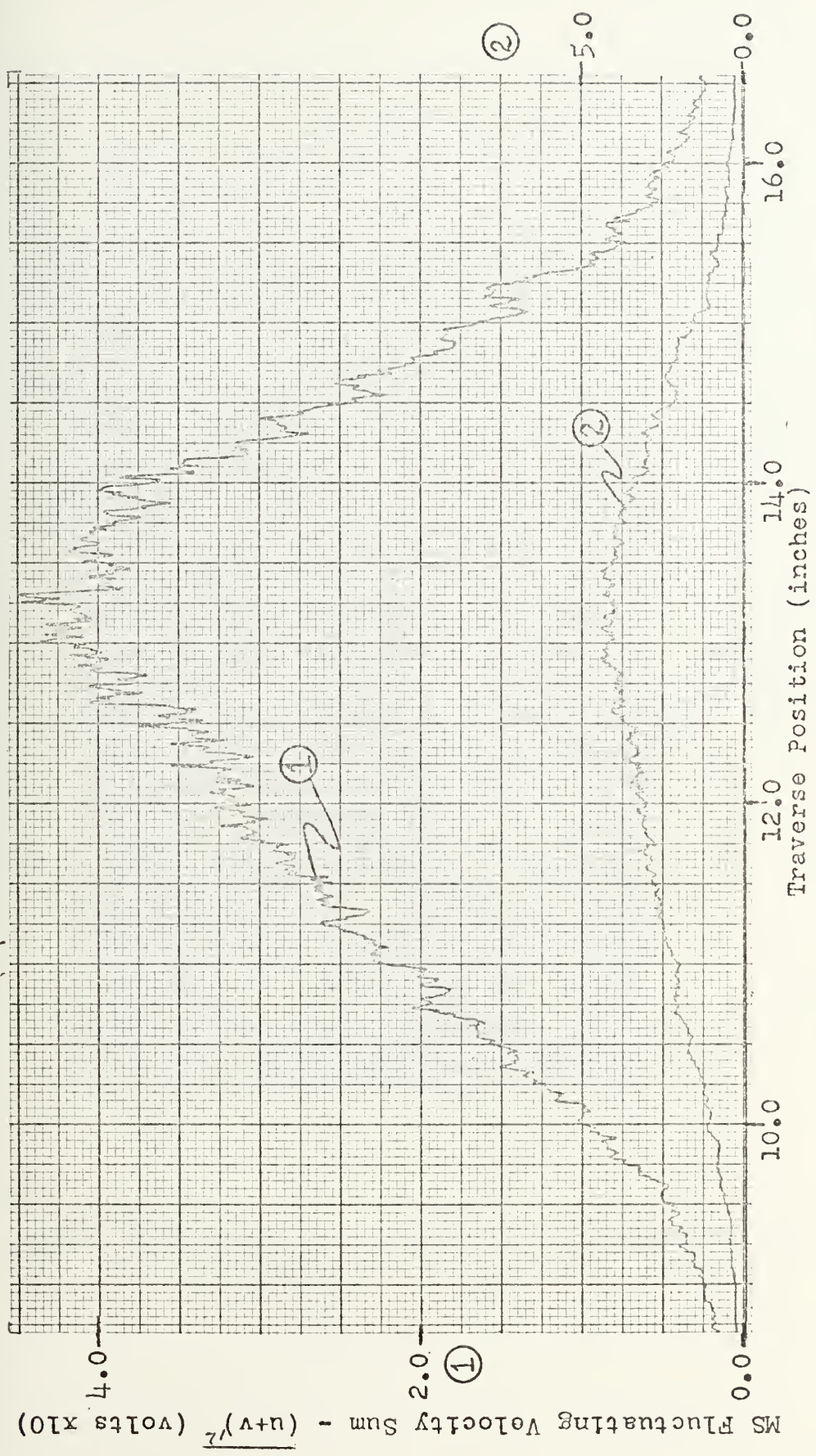


FIGURE 63

Station 3 X-Array MS Fluctuating Velocity Sum



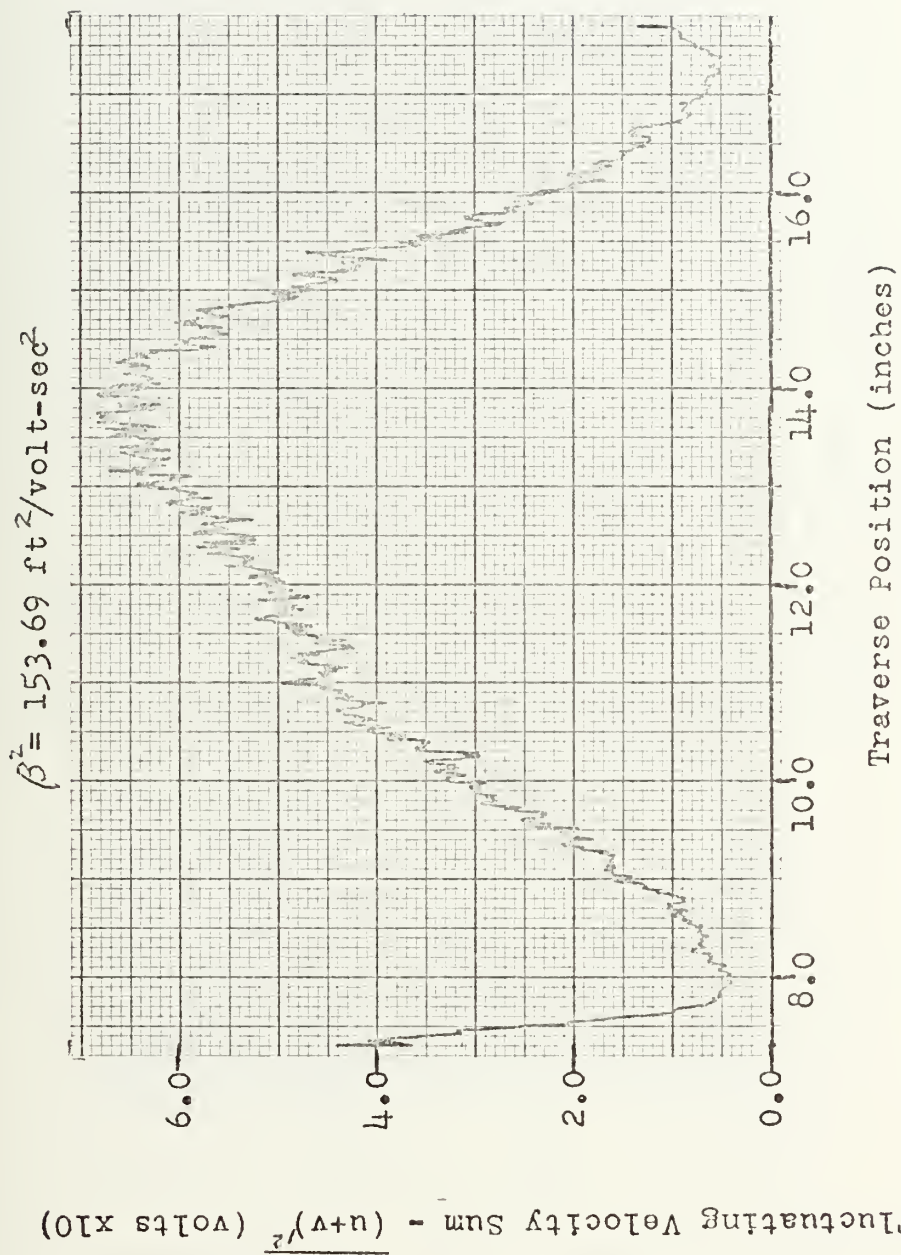
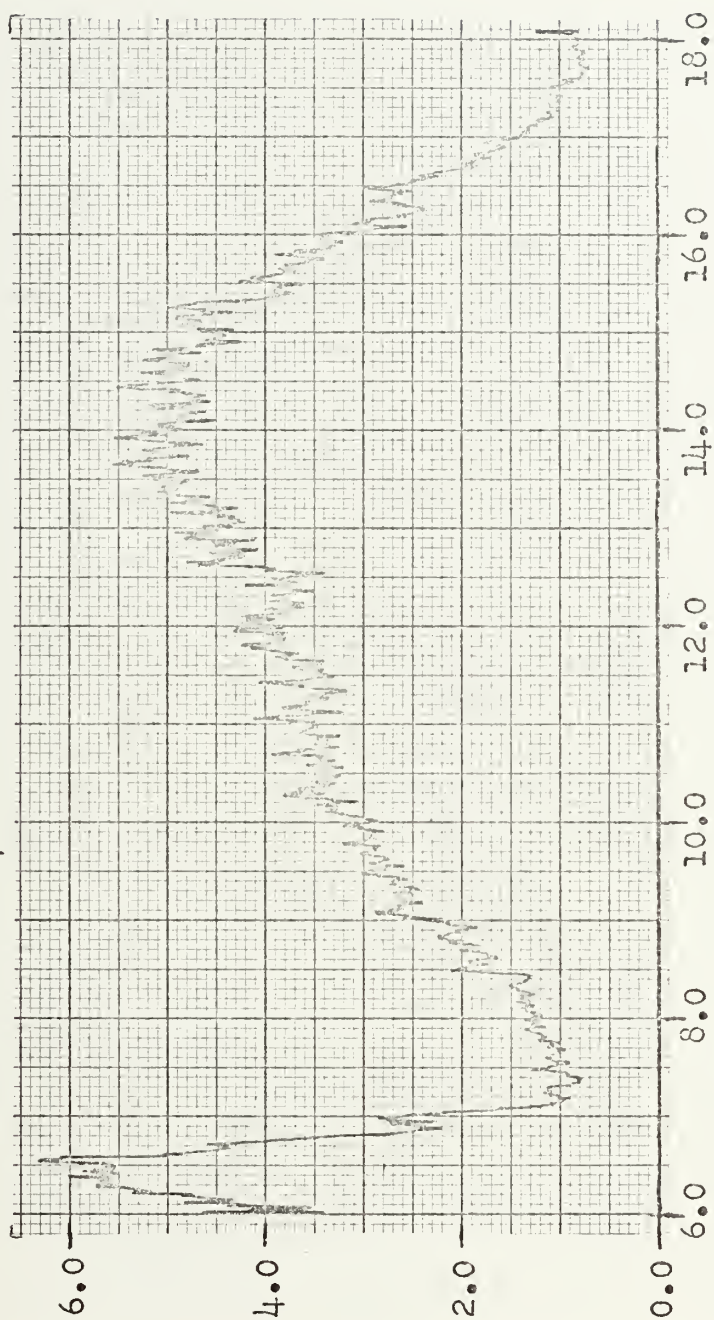


FIGURE 64

Station 4 X-Array MS Fluctuating Velocity Sum

MS Fluctuating Velocity Sum - $(u+v)^2$ (volts x10)

$$\beta^2 = 178.98 \text{ ft}^2/\text{volt-sec}^2$$



Traverse Position (inches)

FIGURE 65

Station 5 X-Array MS Fluctuating Velocity Sum

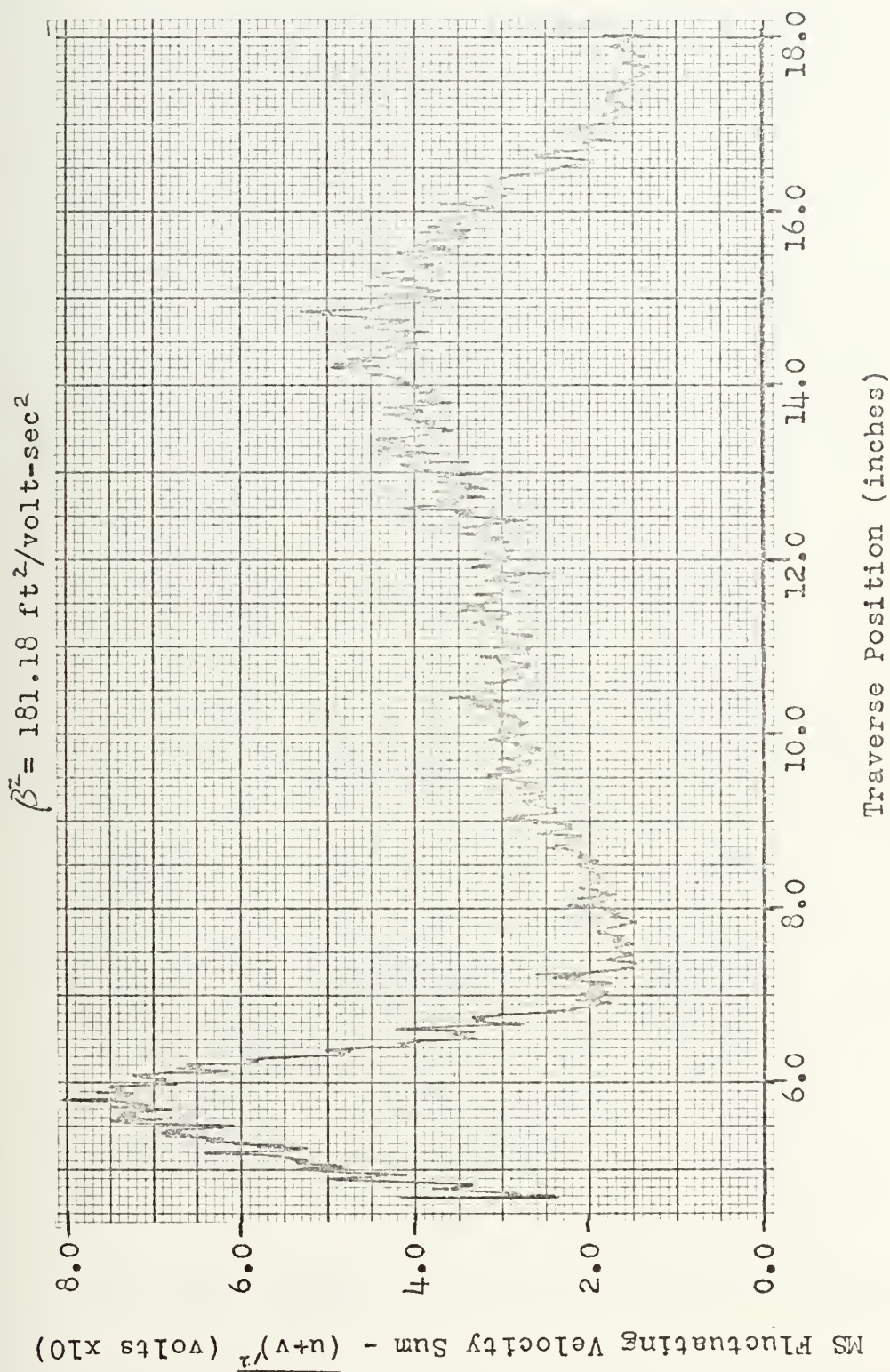


FIGURE 66

Station 6 X-Array MS Fluctuating Velocity Sum

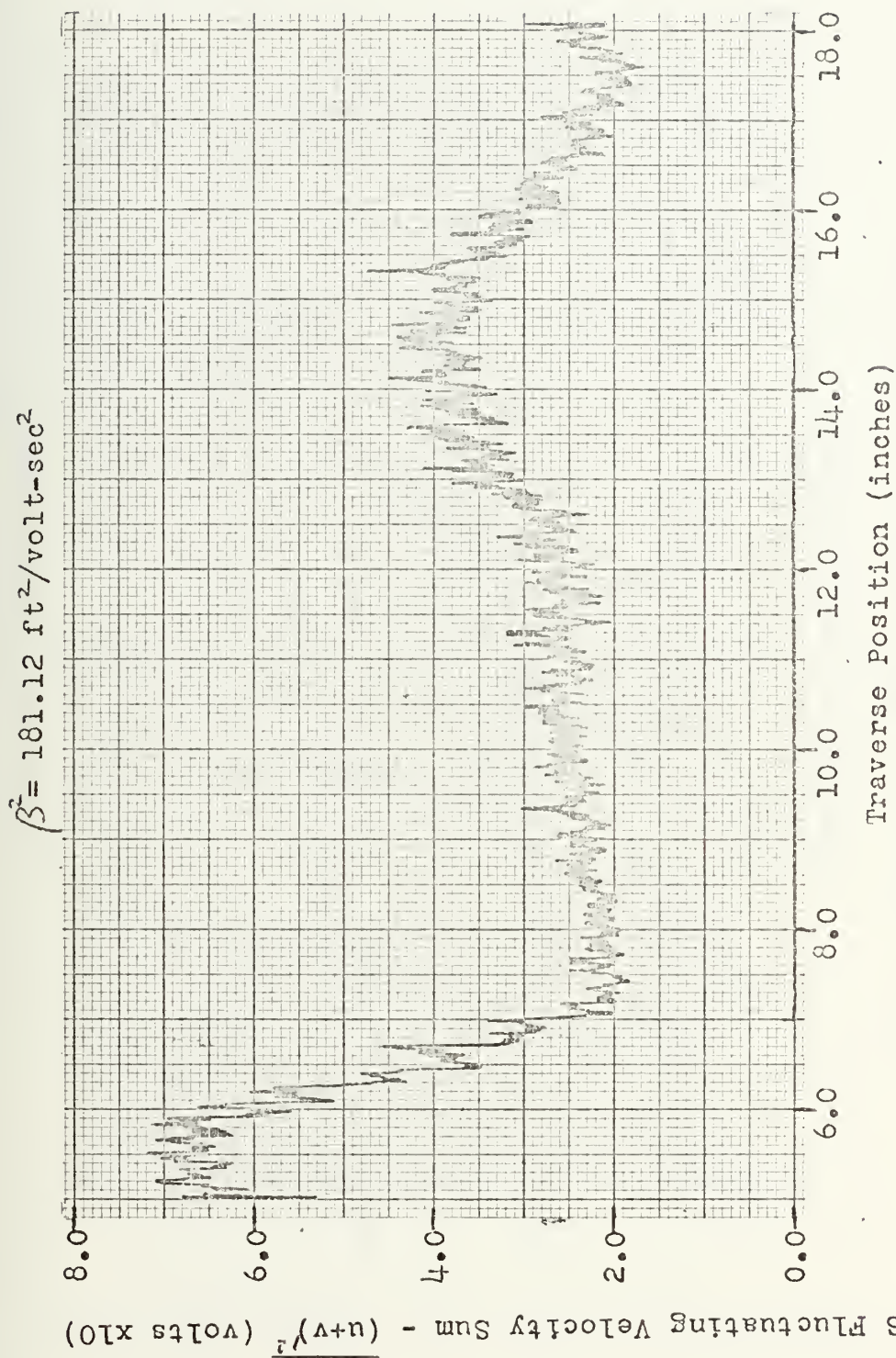
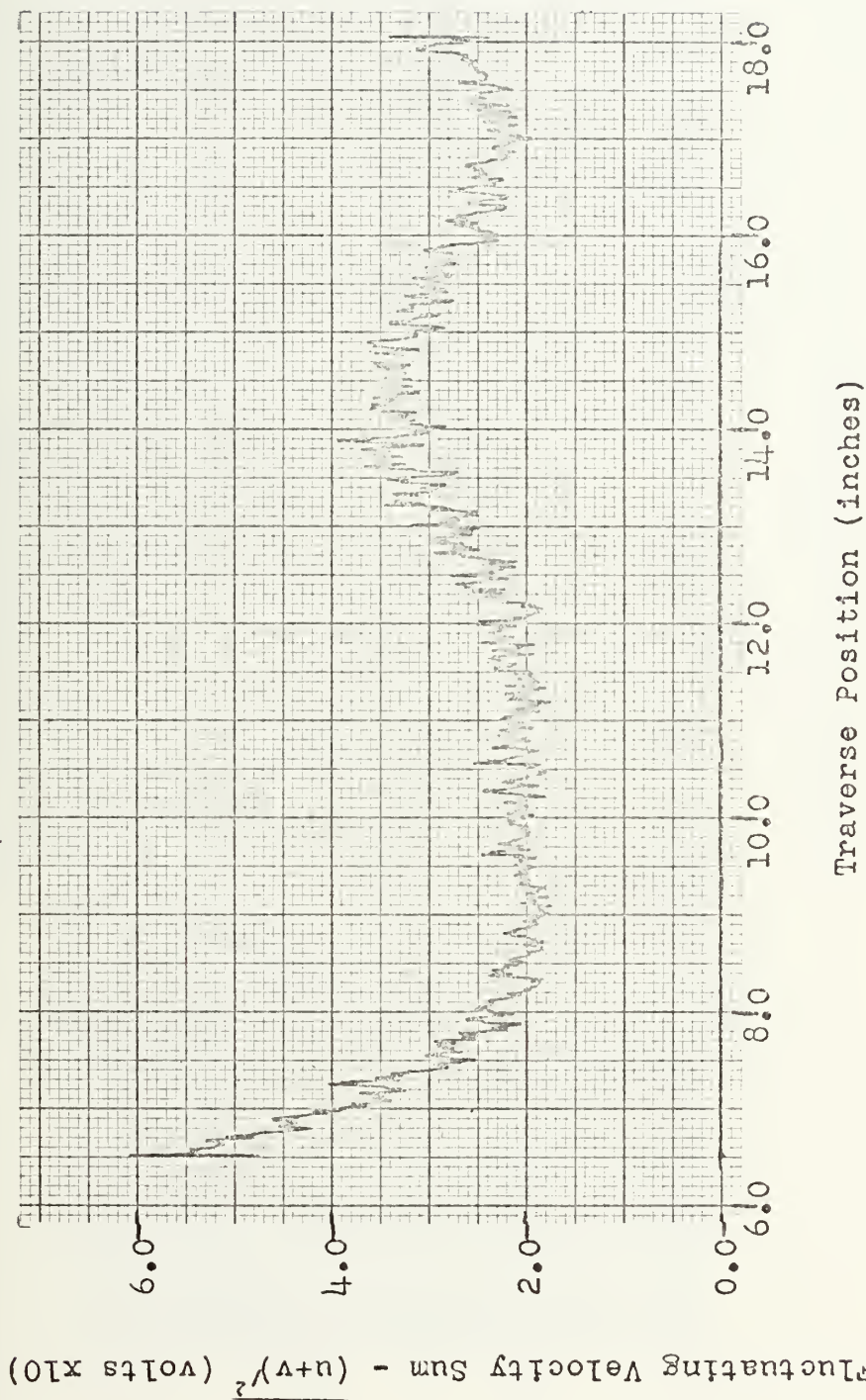


FIGURE 67

Station 7 X-Array MS Fluctuating Velocity Sum

$$\beta^2 = 174.45 \text{ ft}^2/\text{volt-sec}^2$$

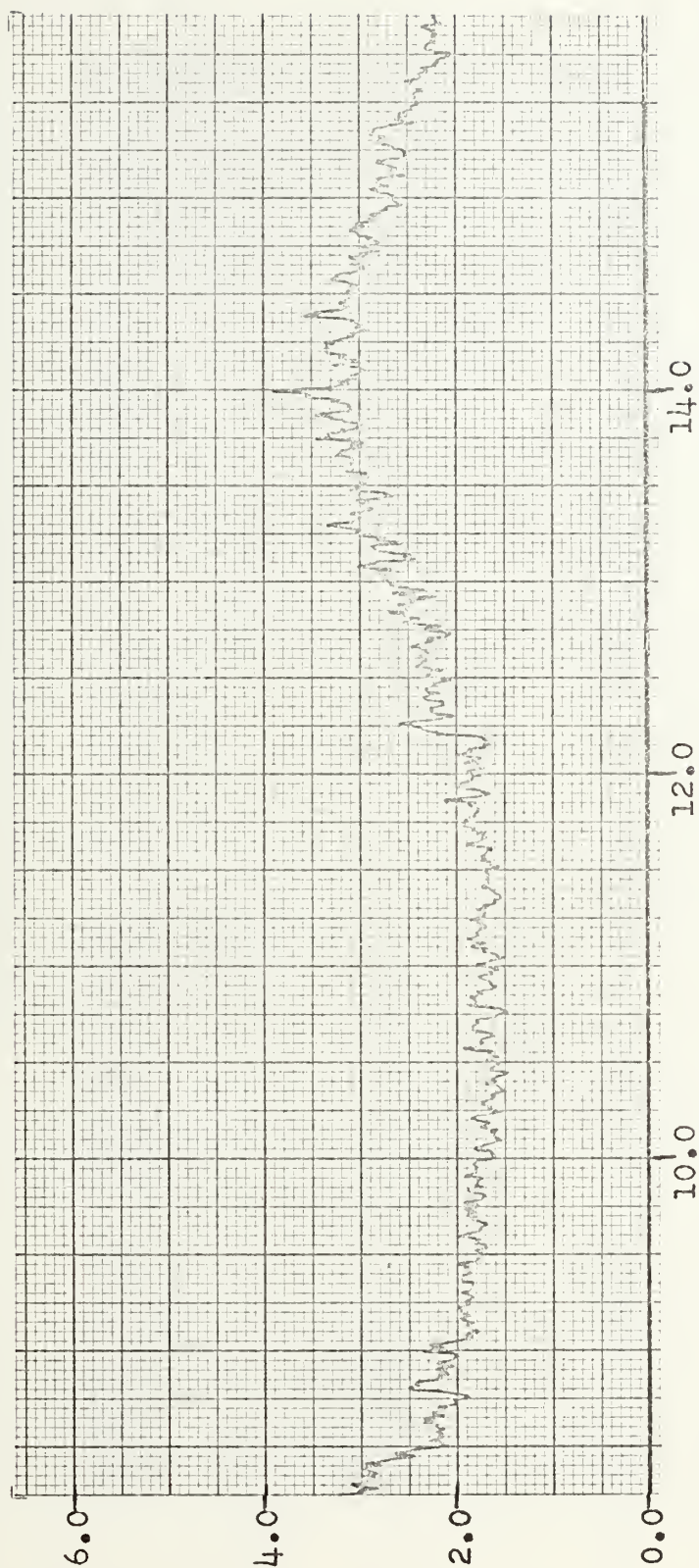


Station 8 X-Array MS Fluctuating Velocity Sum

FIGURE 68

$$\beta^2 = 165.29 \text{ ft}^2/\text{volt-sec}^2$$

MS Fluctuating Velocity Sum - $(u+v)^2$ (volts x10)

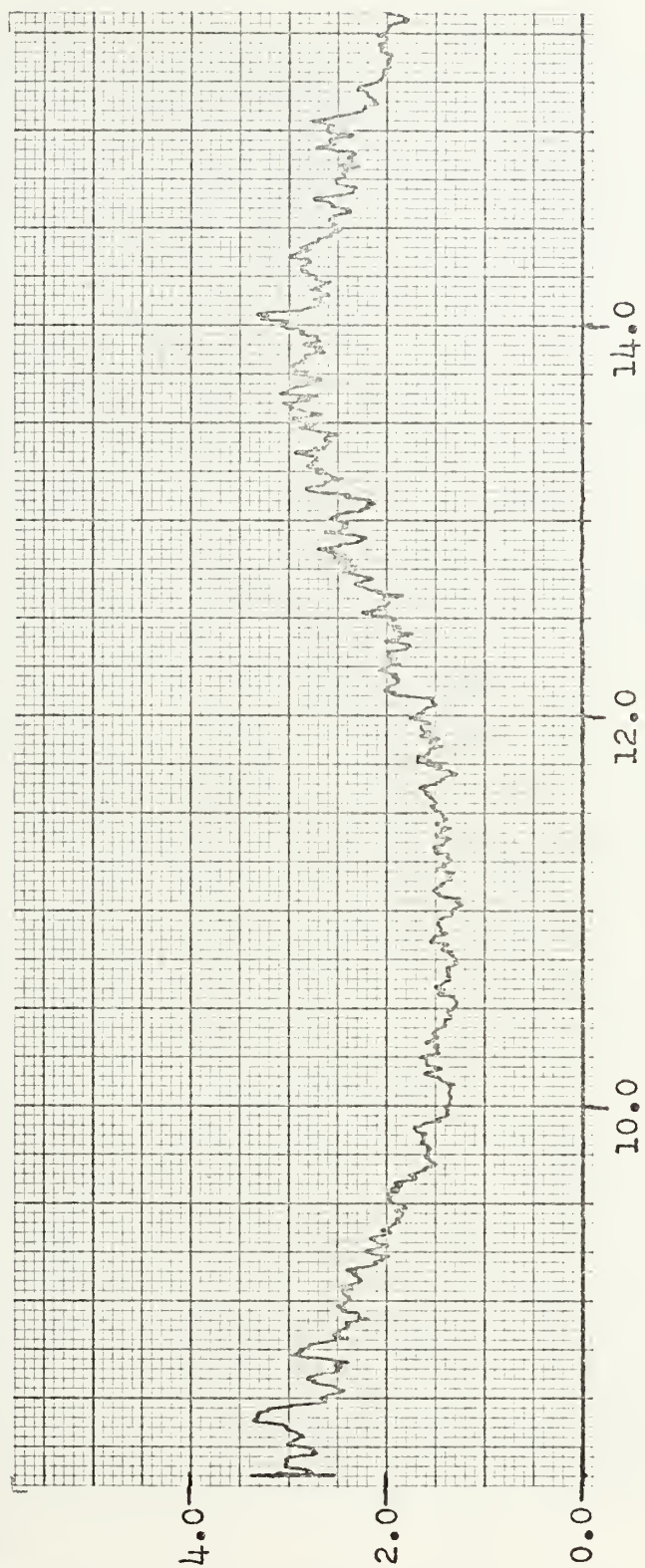


Traverse Position (inches)

FIGURE 69
Station 9 X-Array MS Fluctuating Velocity Sum

MS Fluctuating Velocity Sum - $(u+v)^2$ (volts x10)

$$\beta^2 = 164.01 \text{ ft}^2/\text{volt-sec}^2$$



Traverse Position (inches)

FIGURE 70
Station 10 X-Array MS Fluctuating Velocity Sum

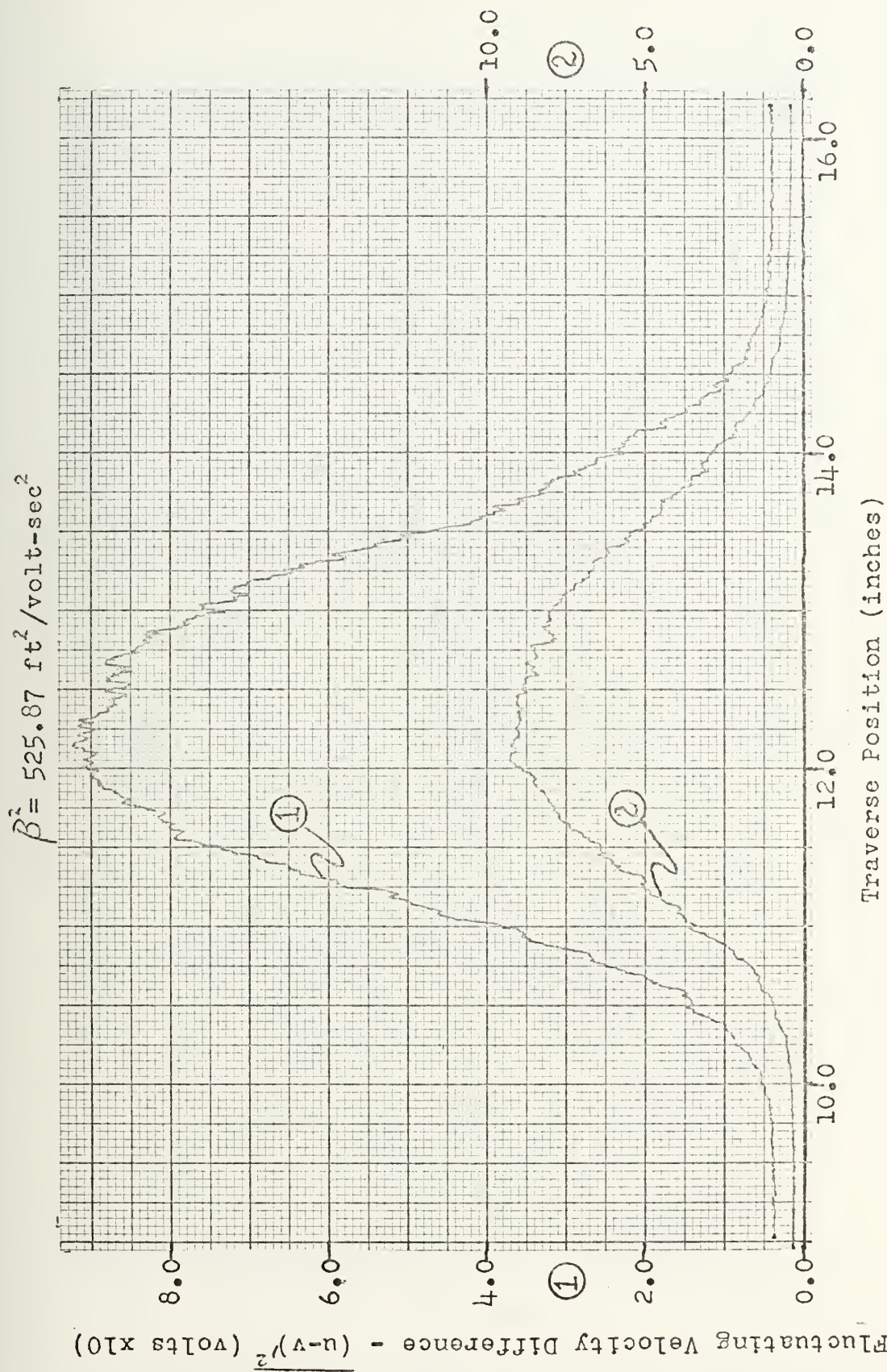
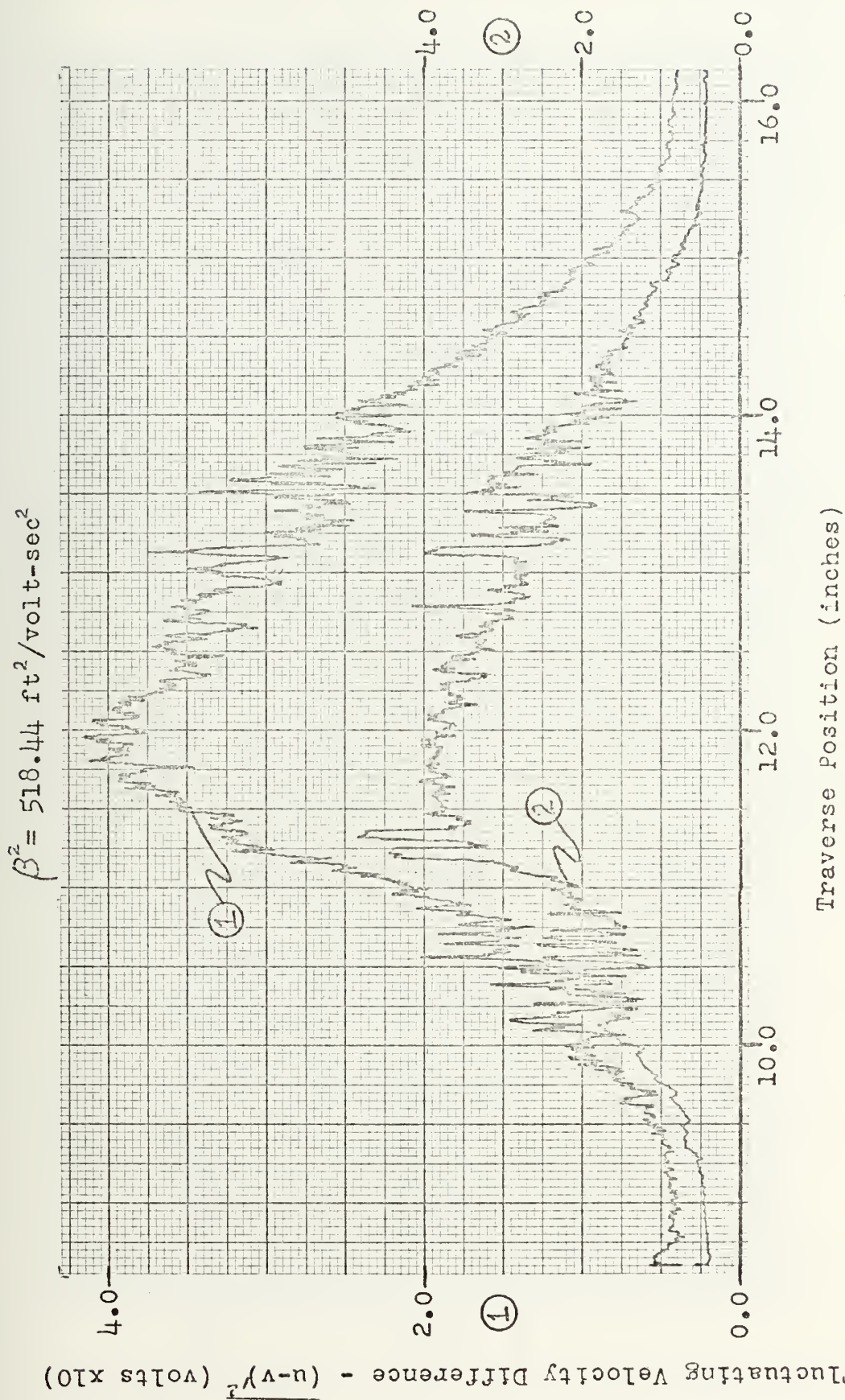
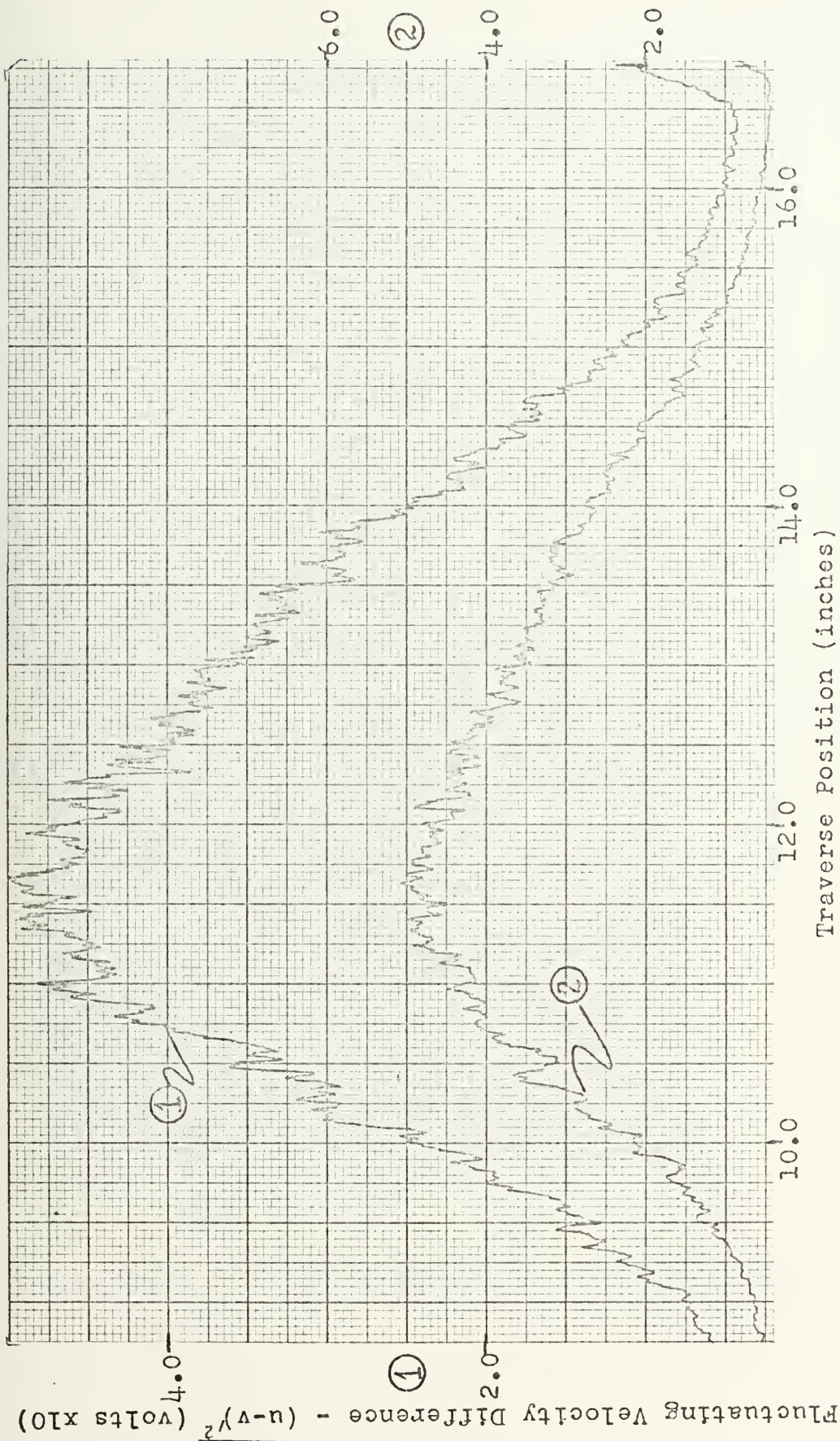


FIGURE 71
Station 1 X-Array MS Fluctuating Velocity Difference



Station 2 X-Array MS Fluctuating Velocity Difference
FIGURE 72

$$\beta^2 = 315.43 \text{ ft}^2/\text{volt-sec}^2$$



Station 3 X-Array MS Fluctuating Velocity Difference
FIGURE 73

$$\beta^2 = 153.69 \text{ ft}^2/\text{volt-sec}^2$$

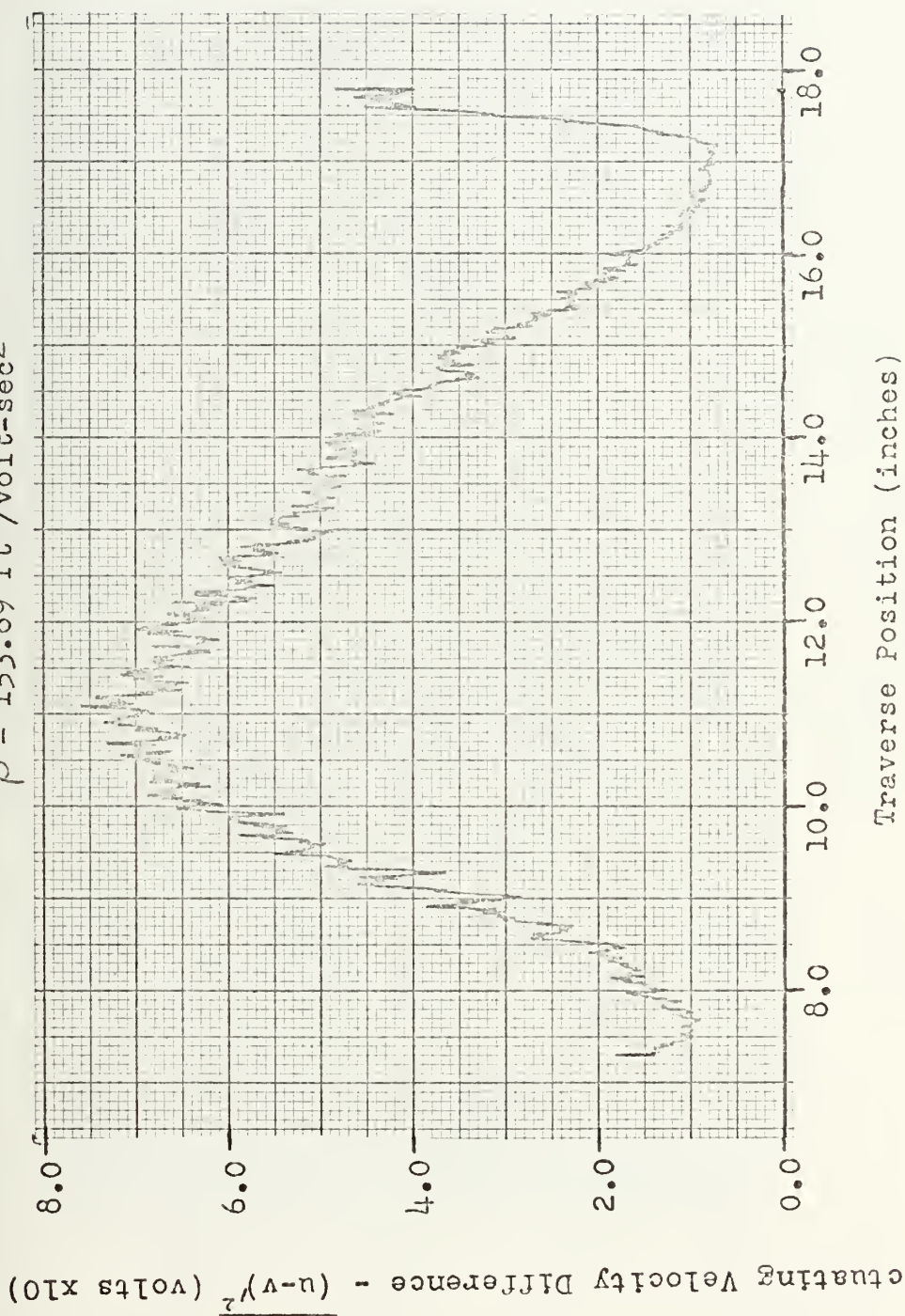
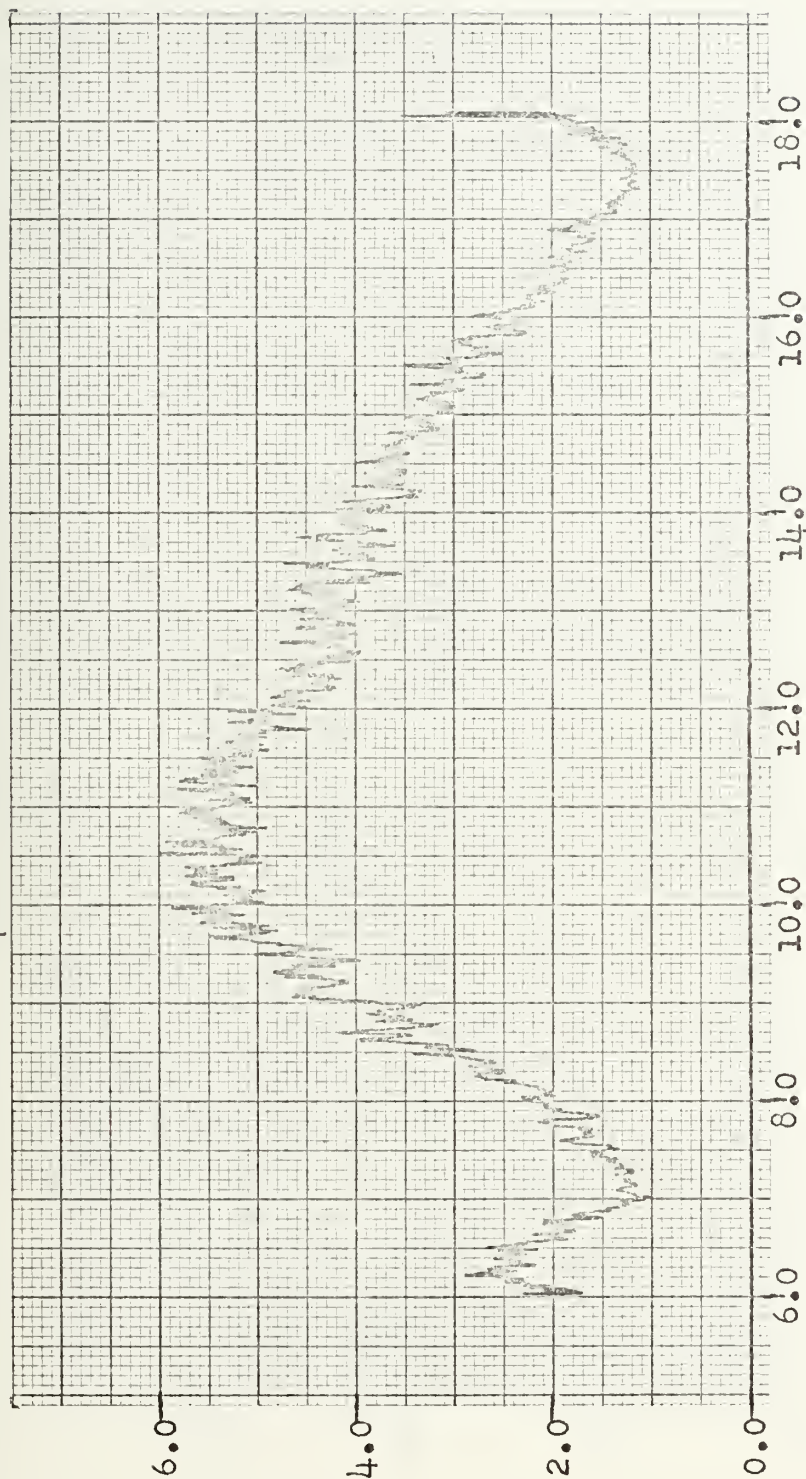


FIGURE 74
Station 4 X-Array MS Fluctuating Velocity Difference

$$\beta^2 = 178.98 \text{ ft}^2/\text{volt-sec}^2$$

MS Fluctuating Velocity Difference - $(u-v)^2$ (volts x10)

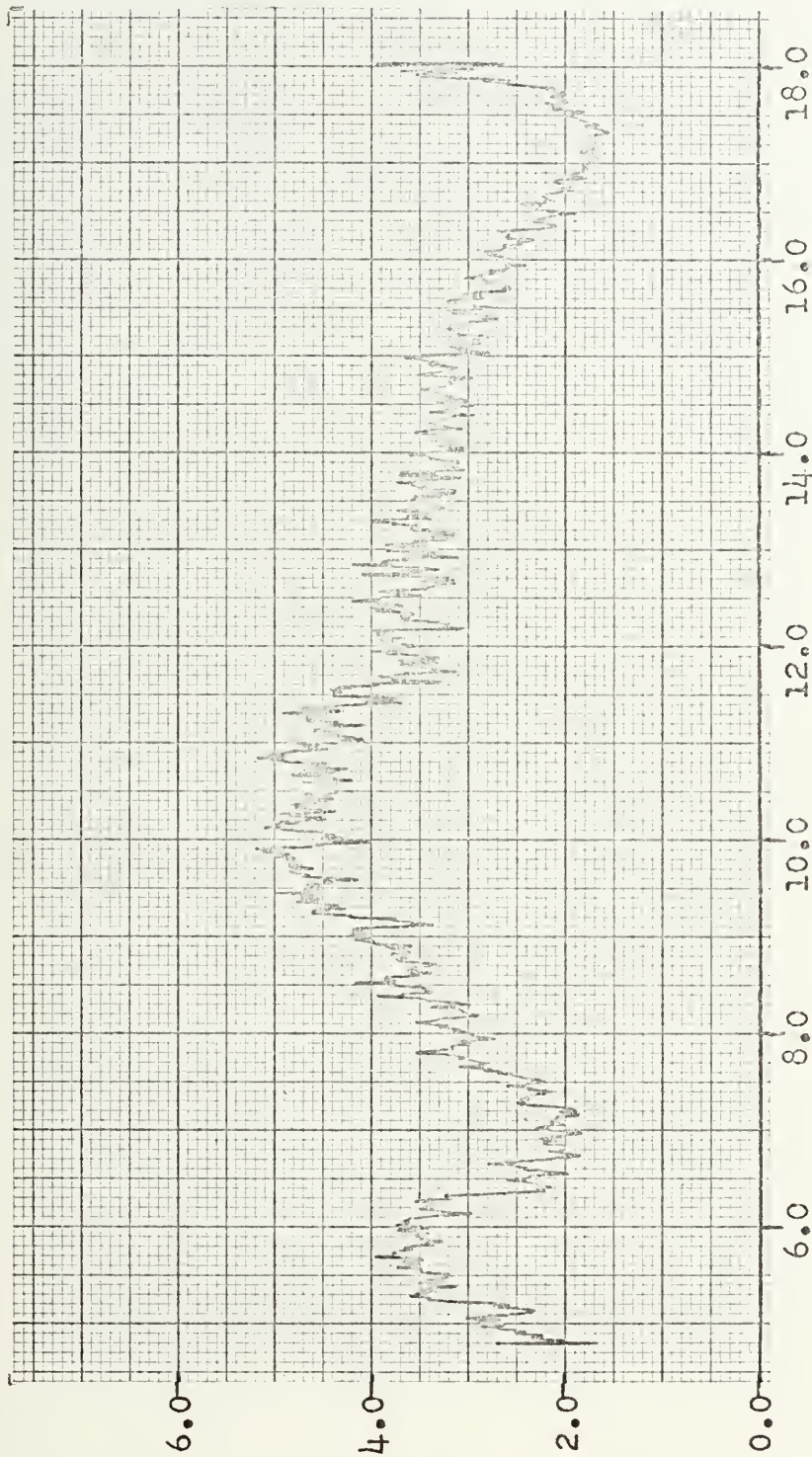


Traverse Position (inches)

FIGURE 75
Station 5 X-Array MS Fluctuating Velocity Difference

MS Fluctuating Velocity Difference - $(u-v)^2$ (volts x10)

$$\beta^2 = 181.18 \text{ ft}^2/\text{volt-sec}^2$$



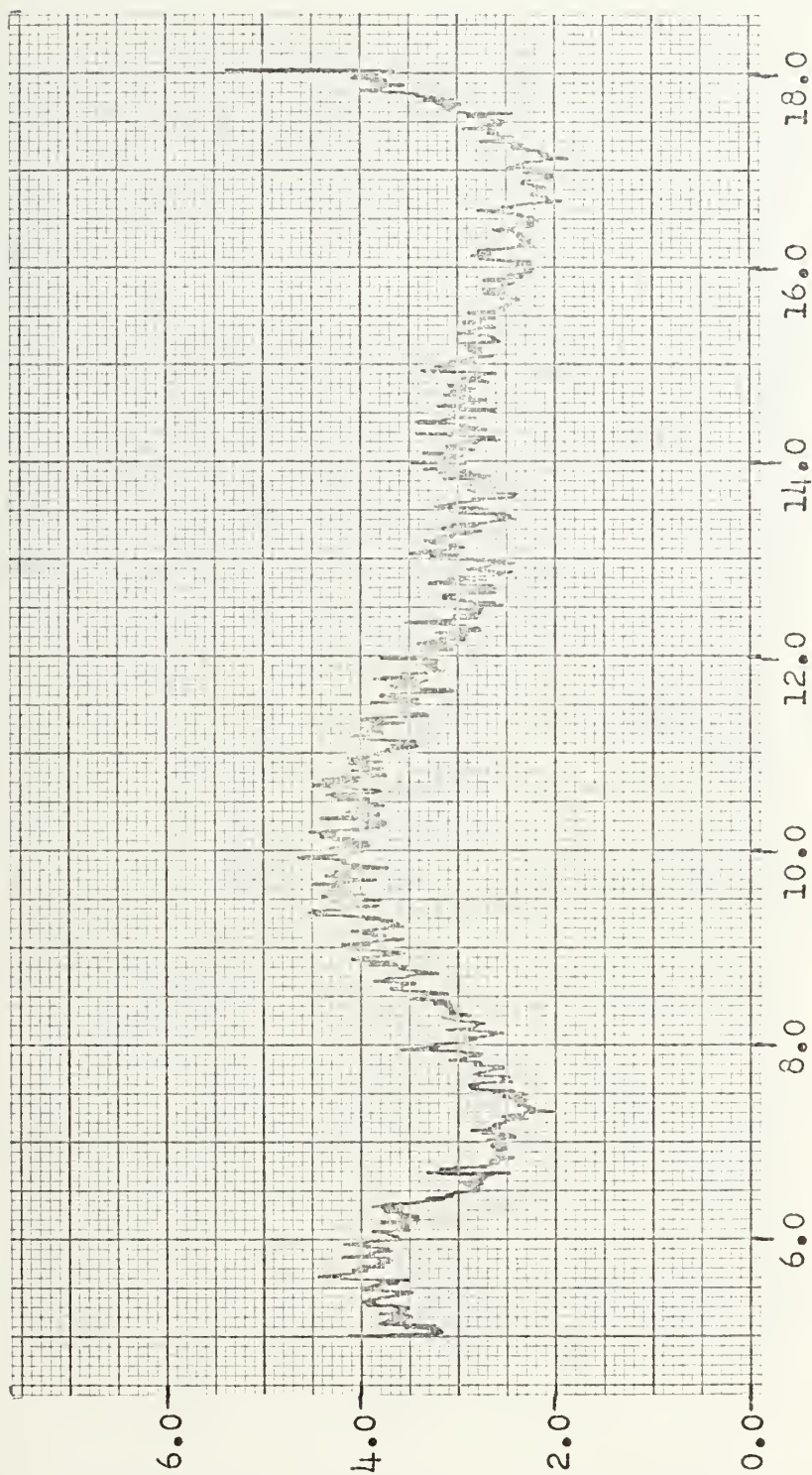
Traverse Position (inches)

FIGURE 76

Station 6 X-Array MS Fluctuating Velocity Difference

MS Fluctuating Velocity Difference - $\sqrt{(u-v)^2}$ (volts x10)

$$\beta^2 = 181.12 \text{ ft}^2/\text{volt-sec}^2$$

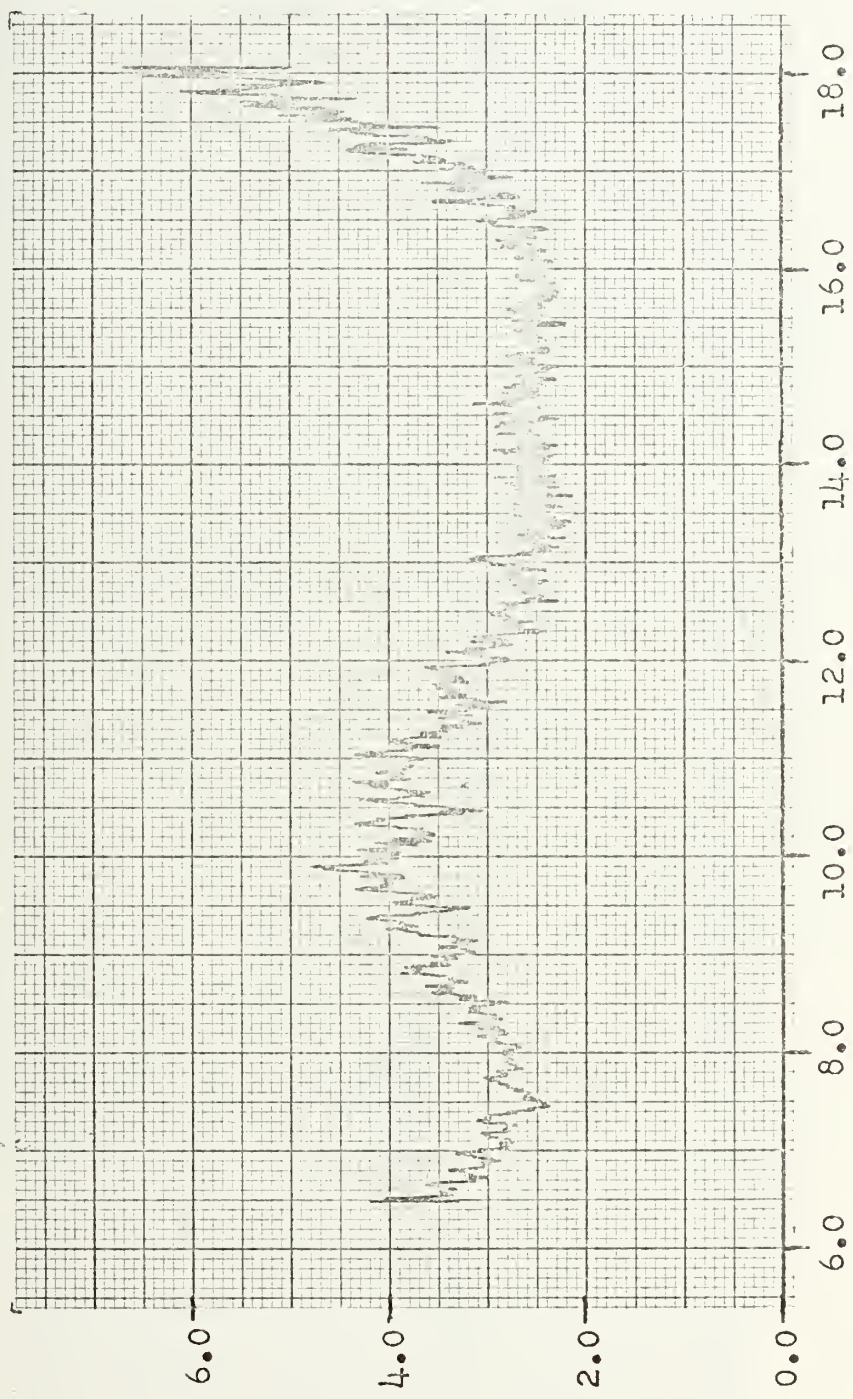


Traverse Position (inches)

Station 7 X-Array MS Fluctuating Velocity Difference
FIGURE 77

MS Fluctuating Velocity Difference - $(u-v)^2$ (volts x10)

$$\beta^2 = 174.45 \text{ ft}^2/\text{volt-sec}^2$$



Traverse Position (inches)

FIGURE 78
Station 8 X-Array MS Fluctuating Velocity Difference

MS Fluctuating Velocity Difference - $(u-v)^2$ (volts x10)

$$\beta^2 = 165.29 \text{ ft}^2/\text{volt-sec}^2$$

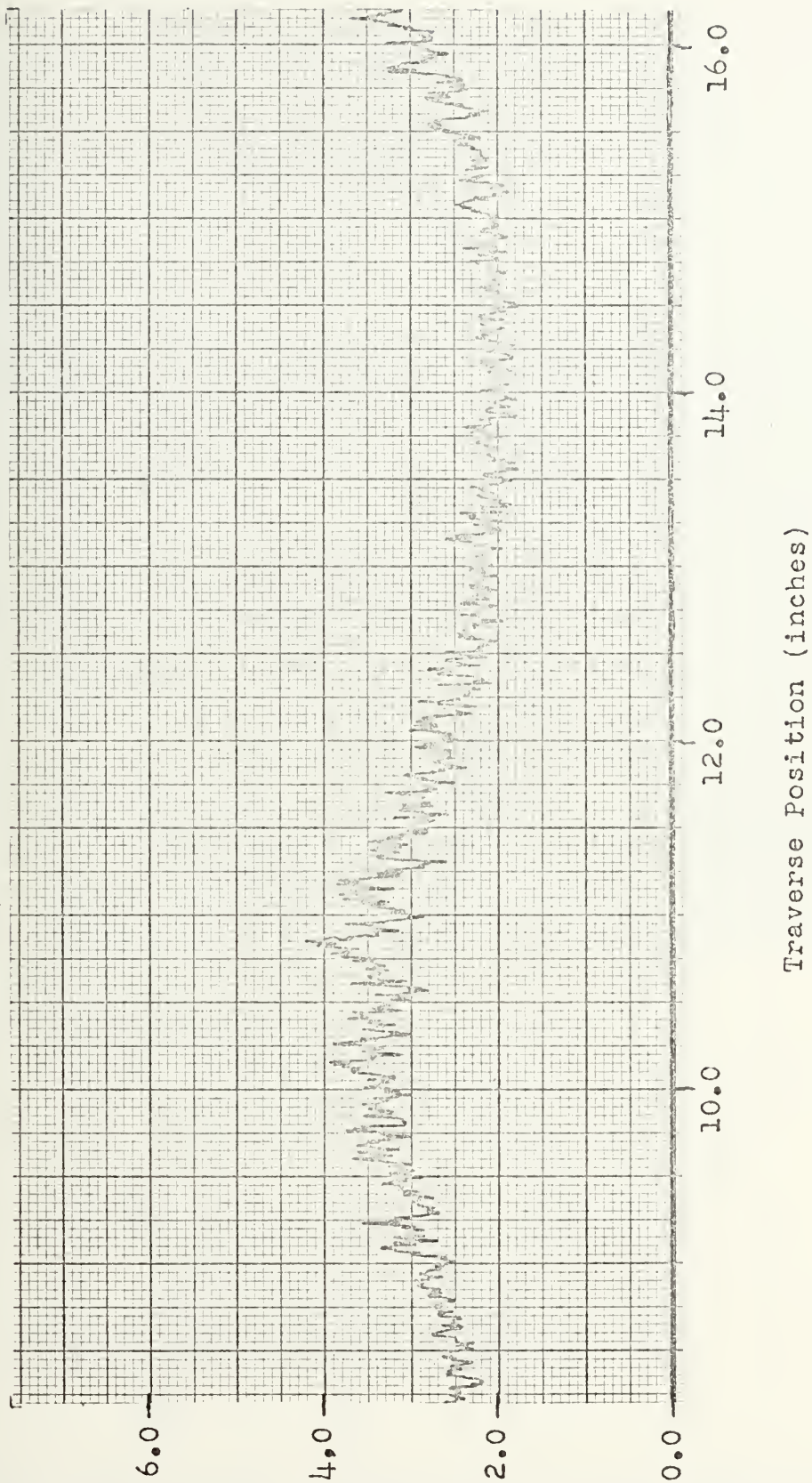
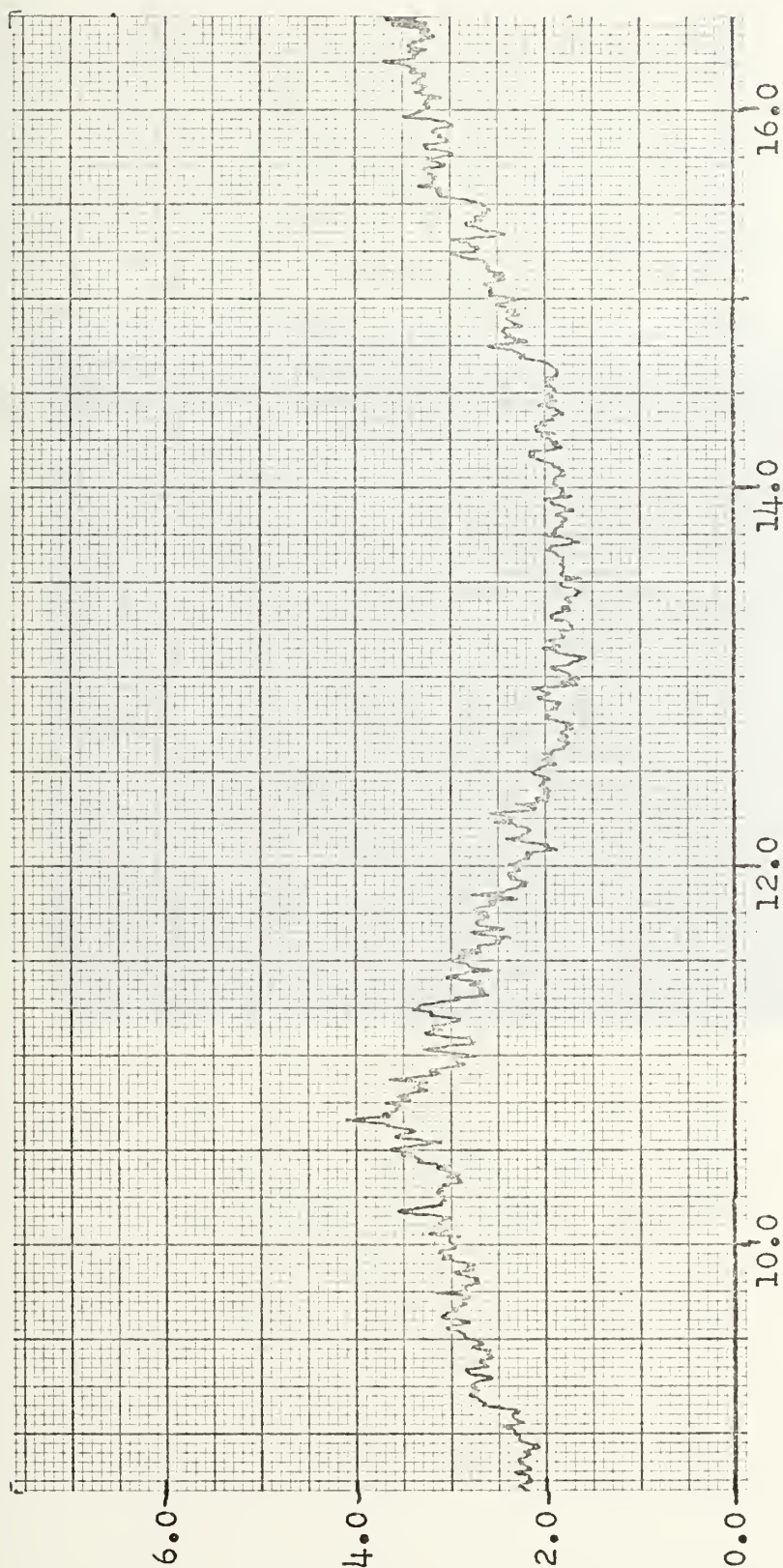


FIGURE 79
Station 9 X-Array MS Fluctuating Velocity Difference

$$\beta^2 = 164.01 \text{ ft}^2/\text{volt-sec}^2$$

MS Fluctuating Velocity Difference - $(u-v)^2$ (volts x10)



Traverse Position (inches)

FIGURE 80
Station 10 X-Array MS Fluctuating Velocity Difference

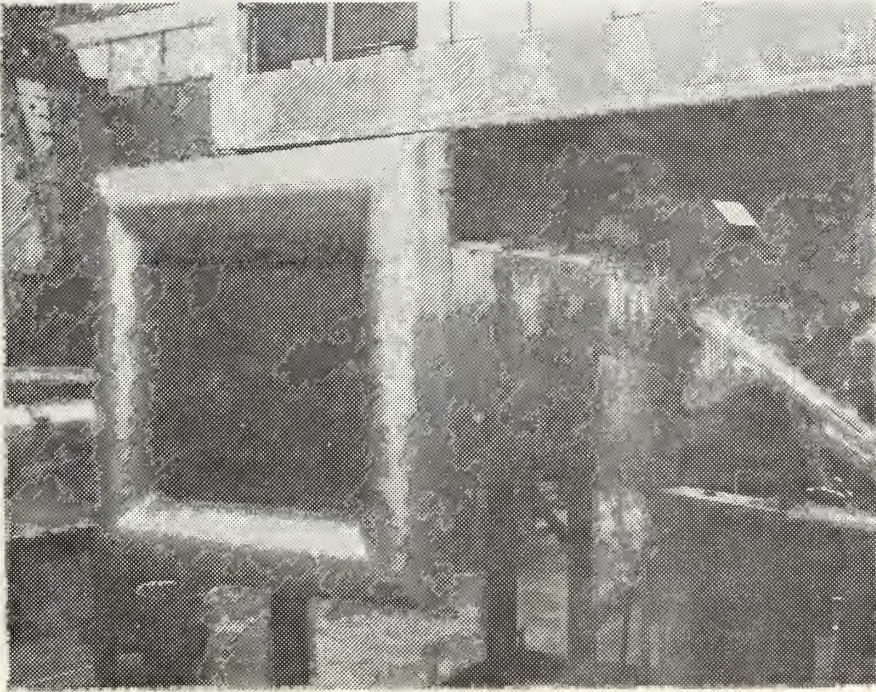


FIGURE 81
The wind Tunnel Inlet

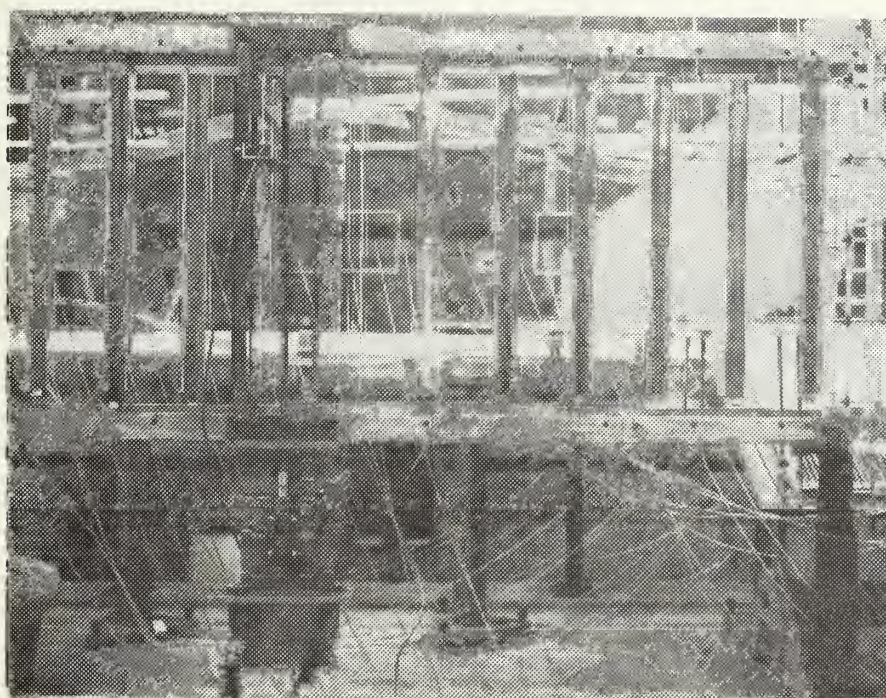


FIGURE 82

The Wind Tunnel Test Section

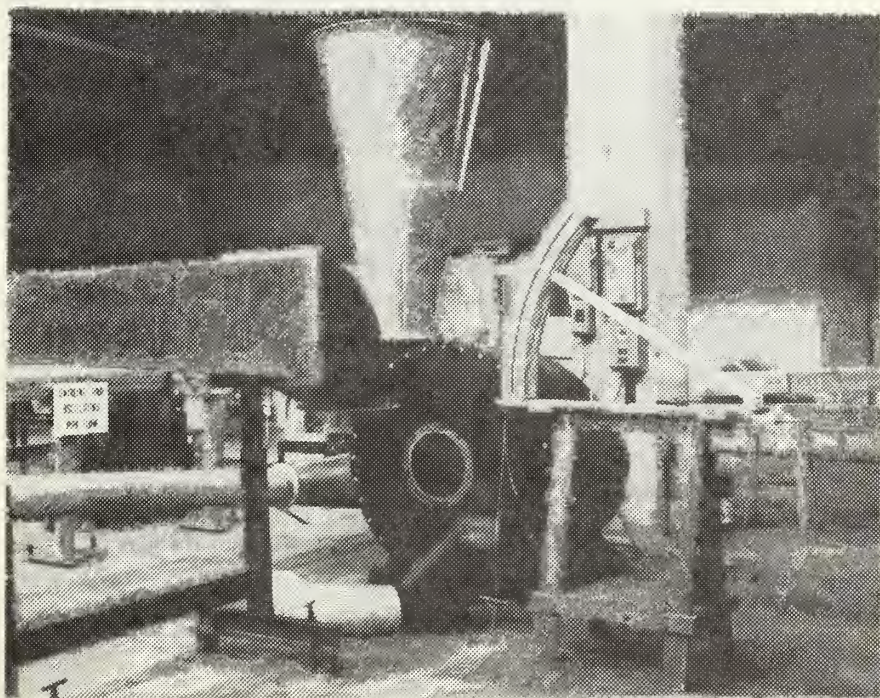


FIGURE 83

The Wind Tunnel Blower

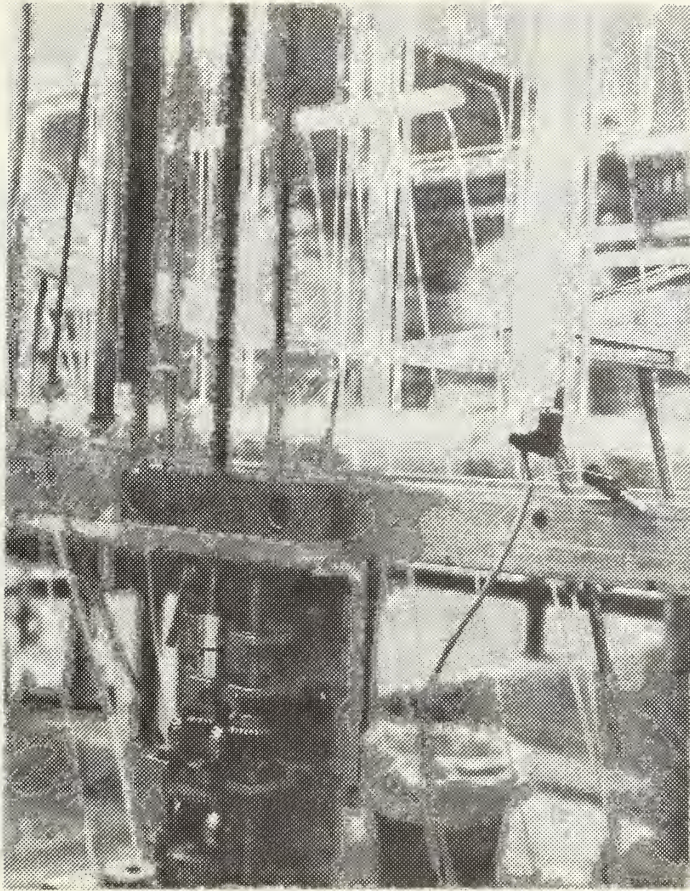


FIGURE 84

The Test Section Traverse

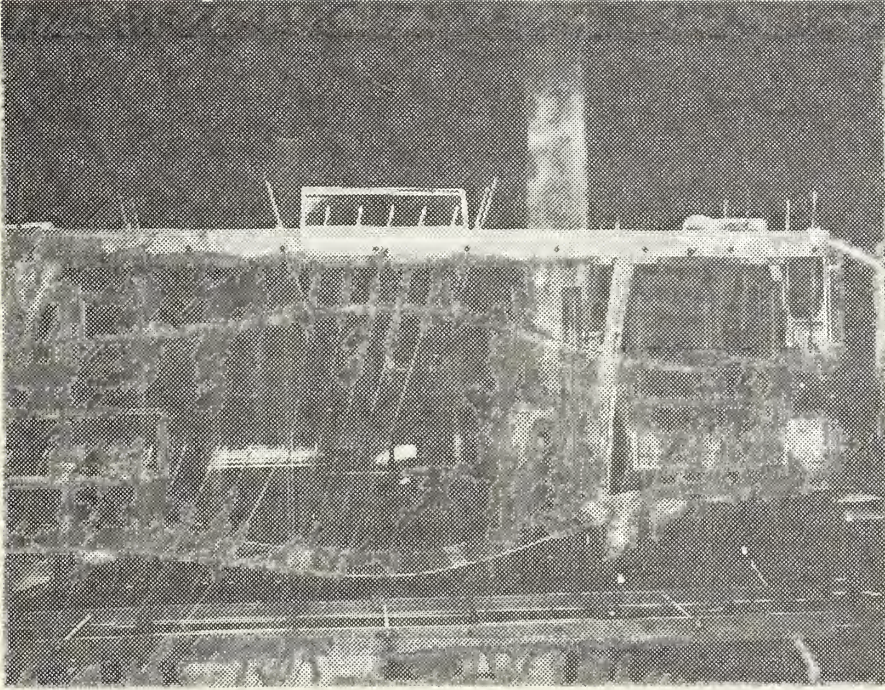


FIGURE 85

The Test Section Access Panels and
Static Pressure Ports

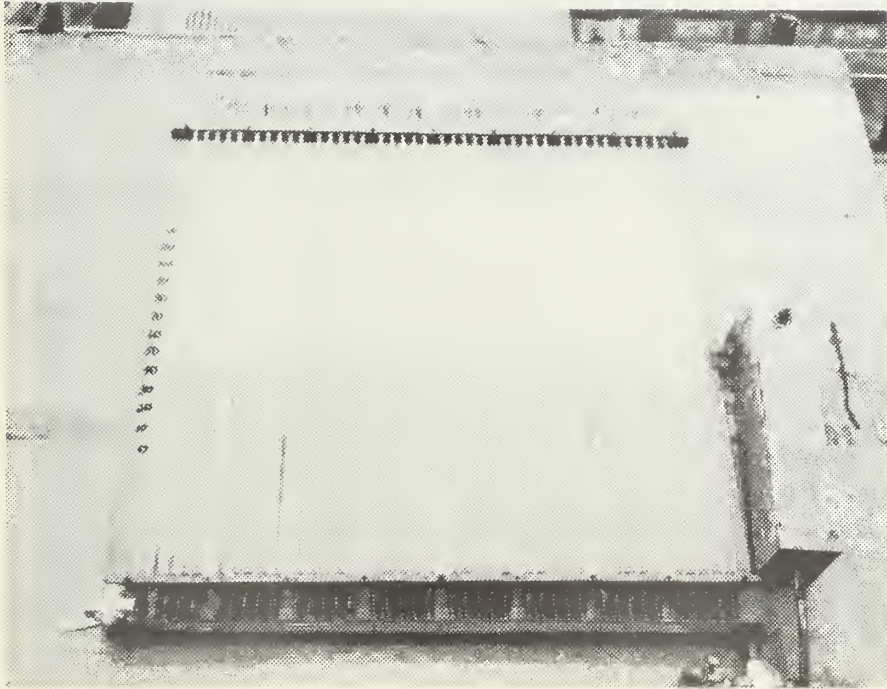


FIGURE 86

The Manometer Board

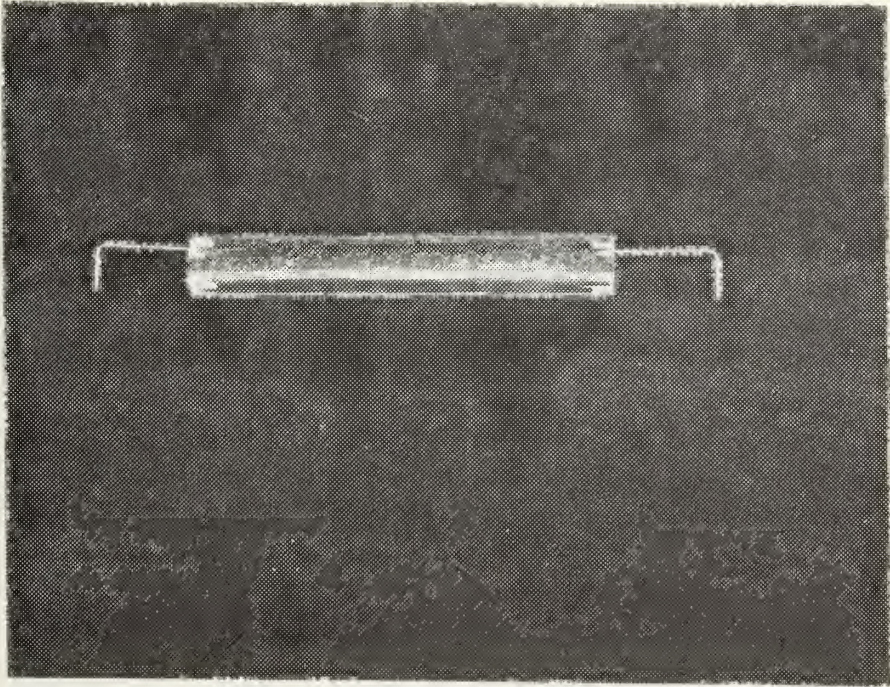


FIGURE 87

The Wake Generator
with Abrasive Strip

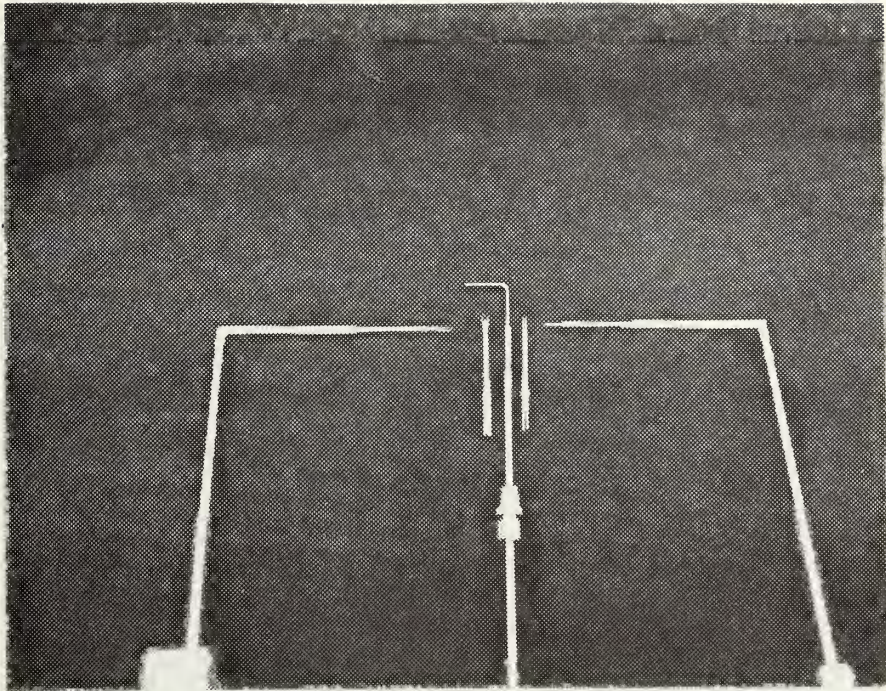


FIGURE 88

The Data Sensors

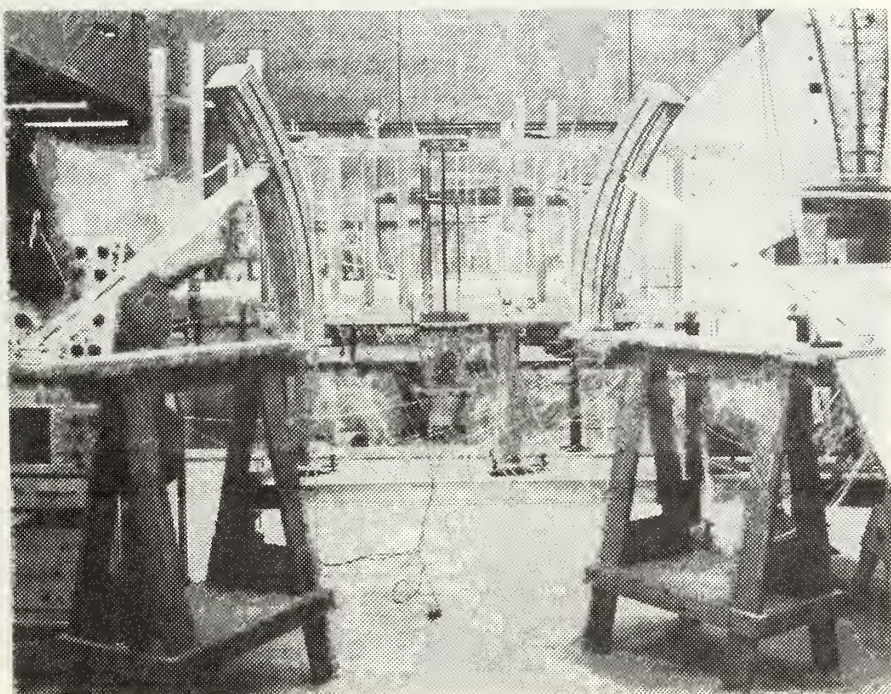


FIGURE 89

The Test Section During Phase I

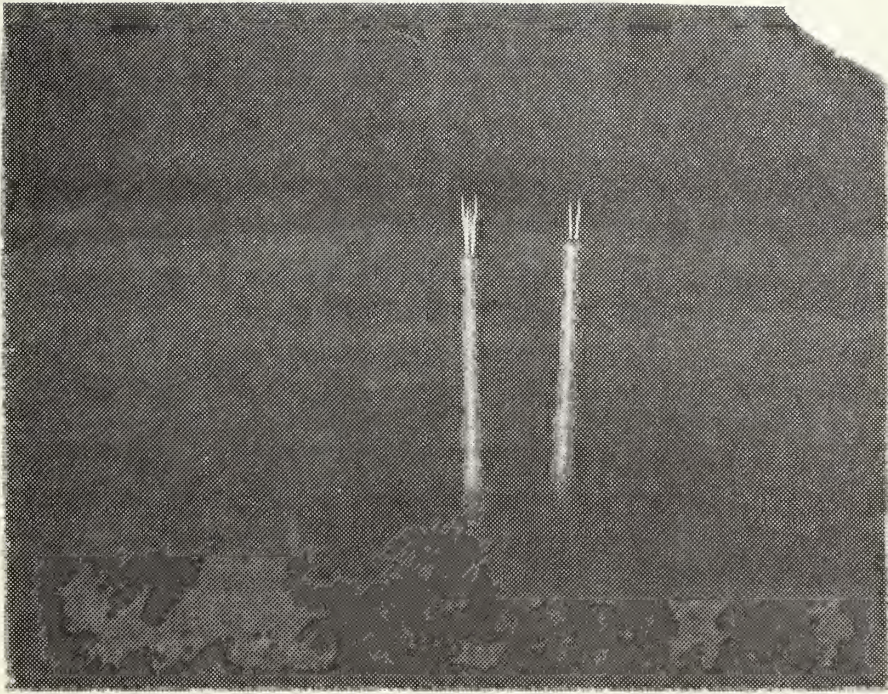


FIGURE 90

X-Array and Normal Wire
Anemometers

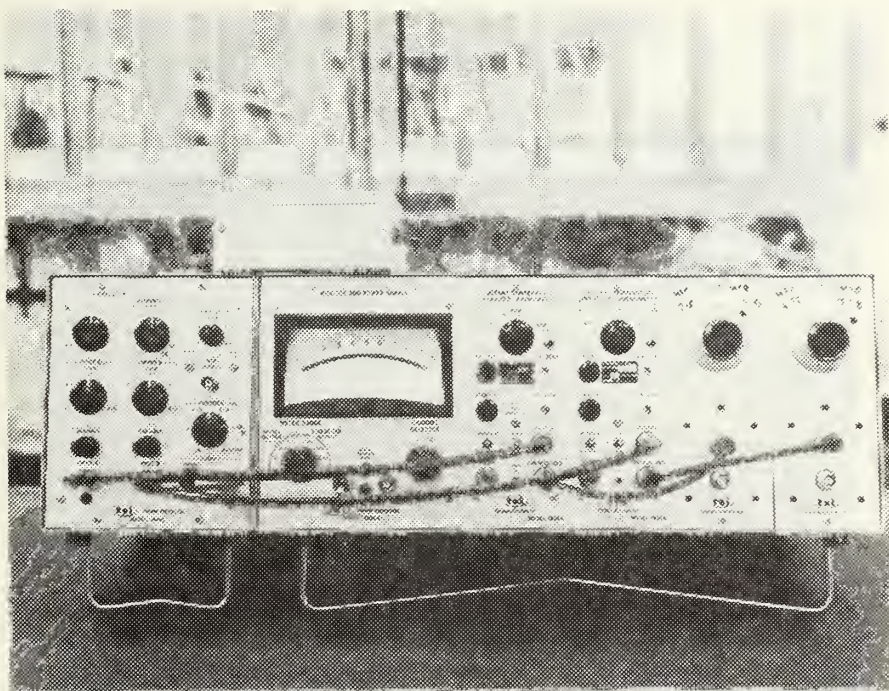


FIGURE 91

The Anemometer Modules
and Correlator

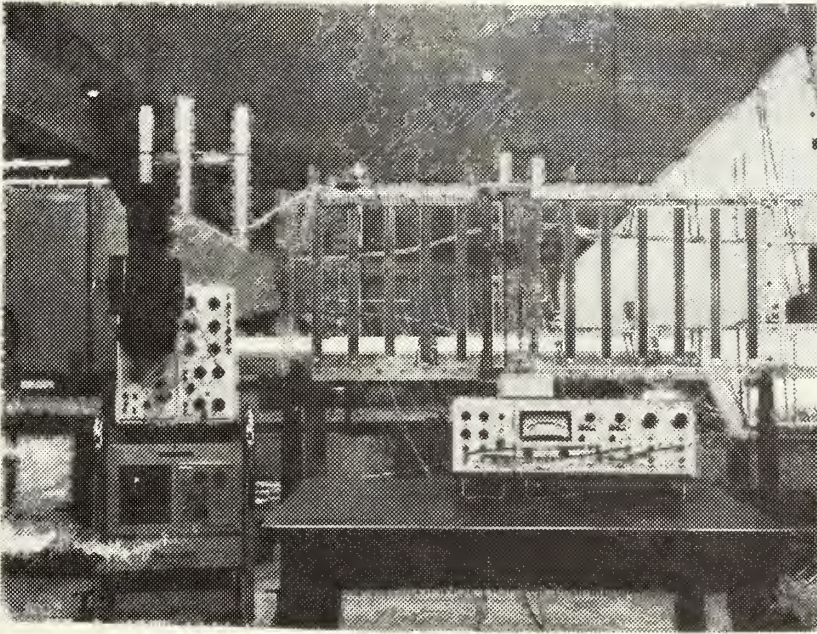


FIGURE 92

The Test Section During

Phases II and III

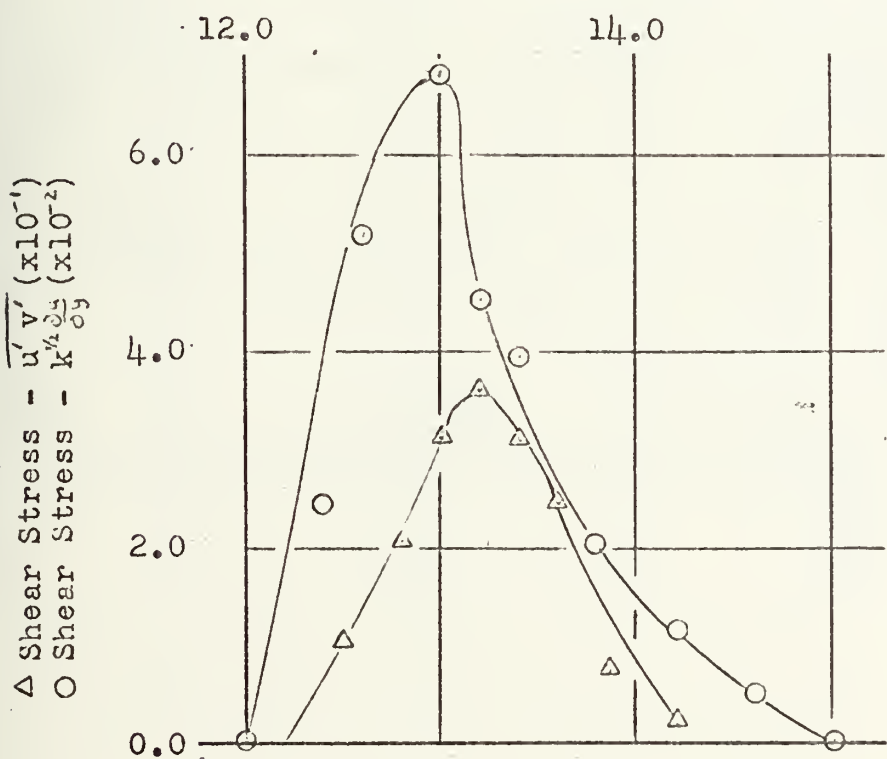
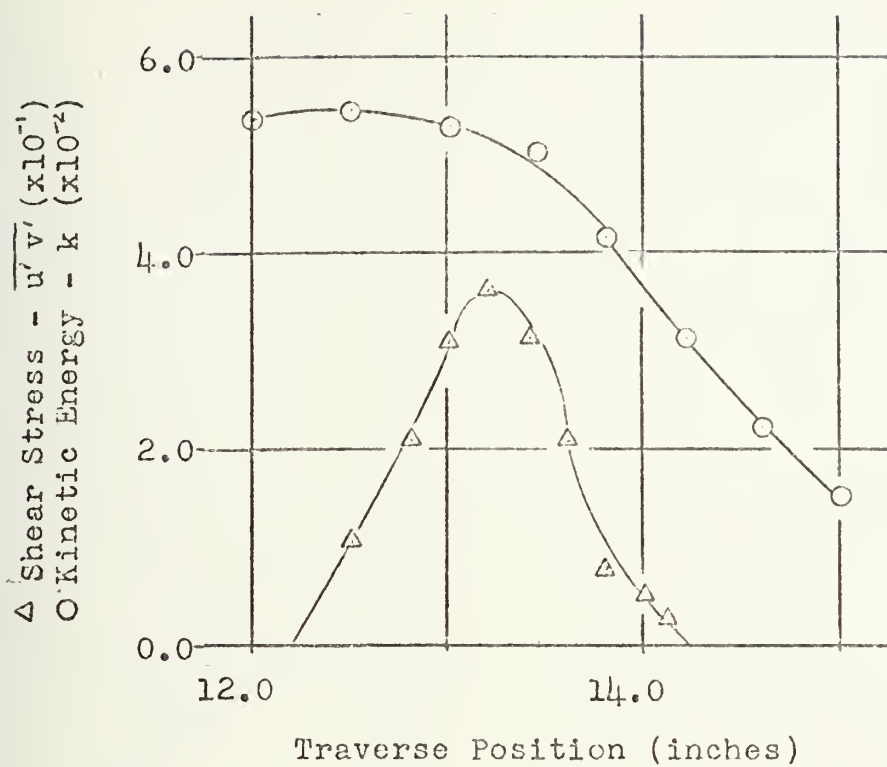


FIGURE 93

Station 2 Turbulent Stress Comparison

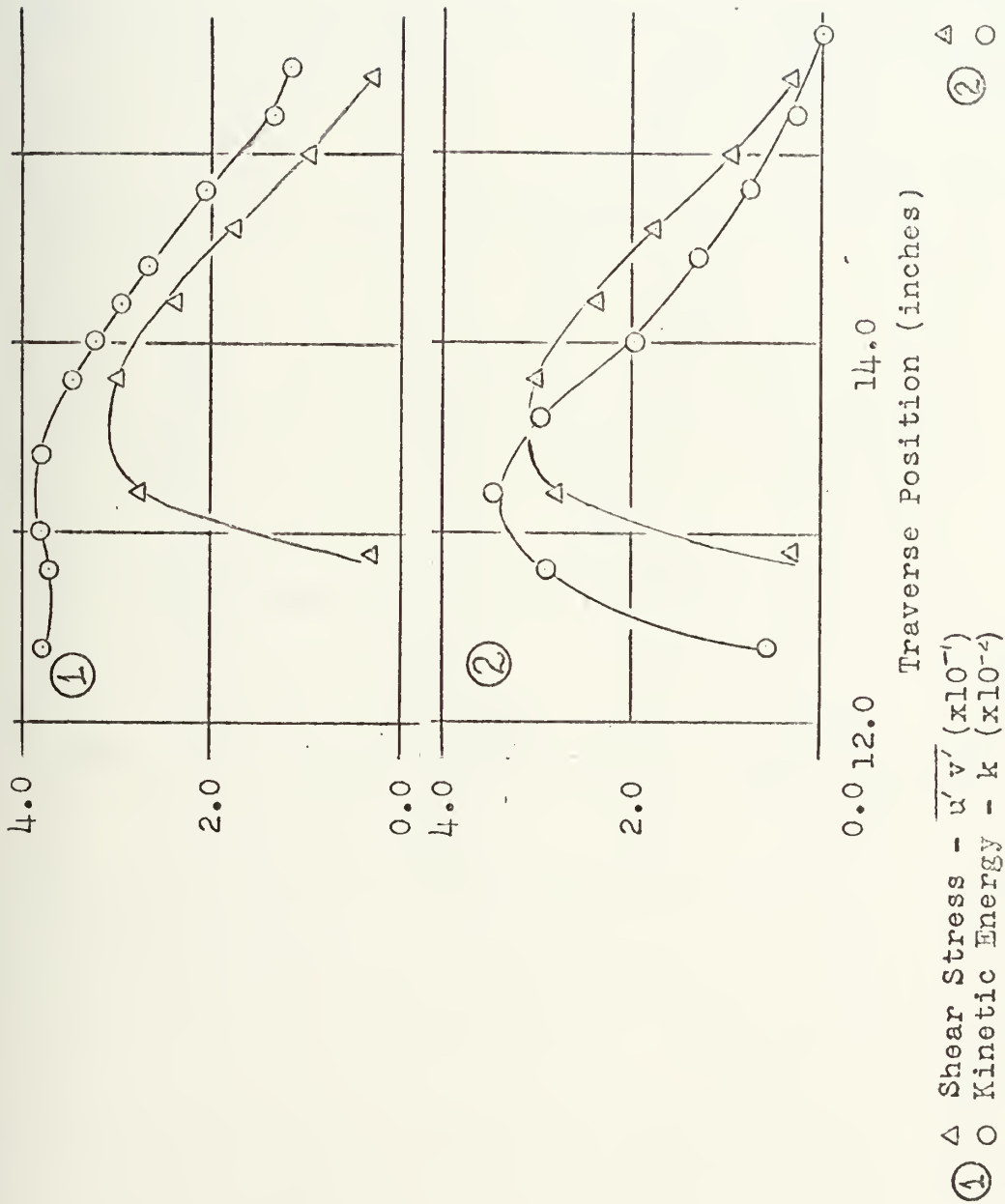
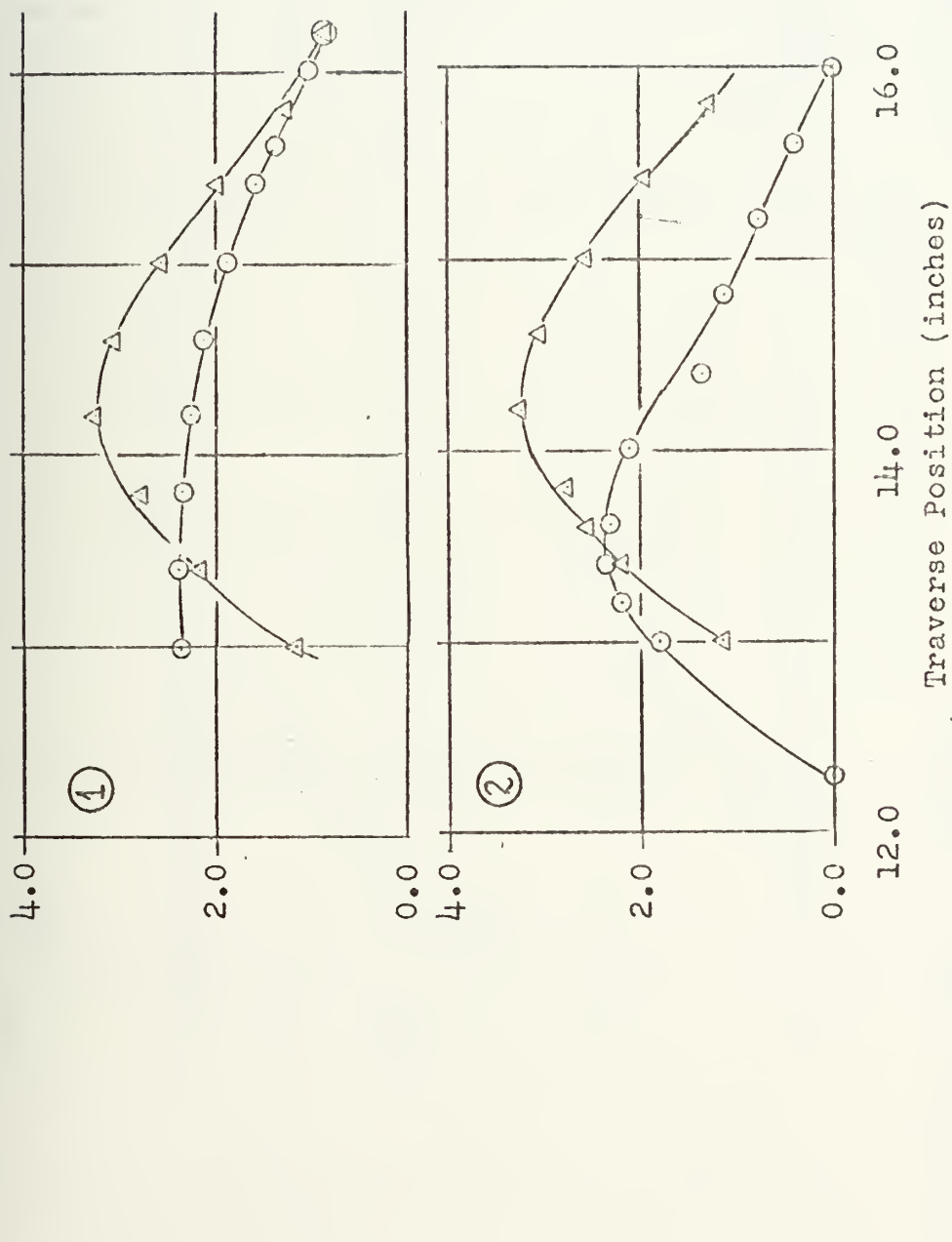


FIGURE 94
Station 3 Turbulent Stress Comparison



① Δ Shear Stress $-\overline{u'v'} (x10^{-1})$
 ○ Kinetic Energy $-k (x10^{-2})$

FIGURE 95
 Station 4 Turbulent Stress Comparison

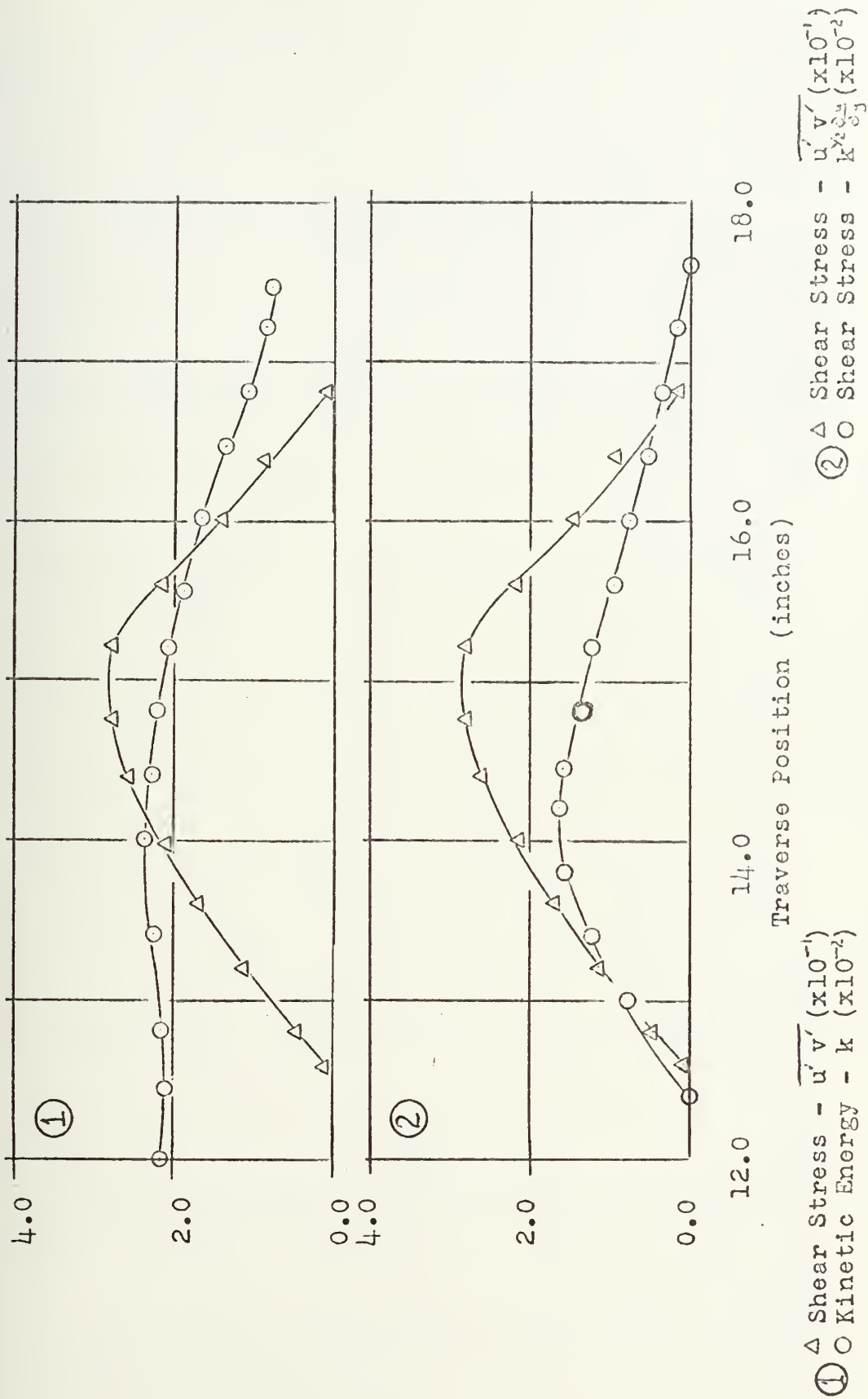


FIGURE 96
 Station 5 Turbulent Stress Comparison

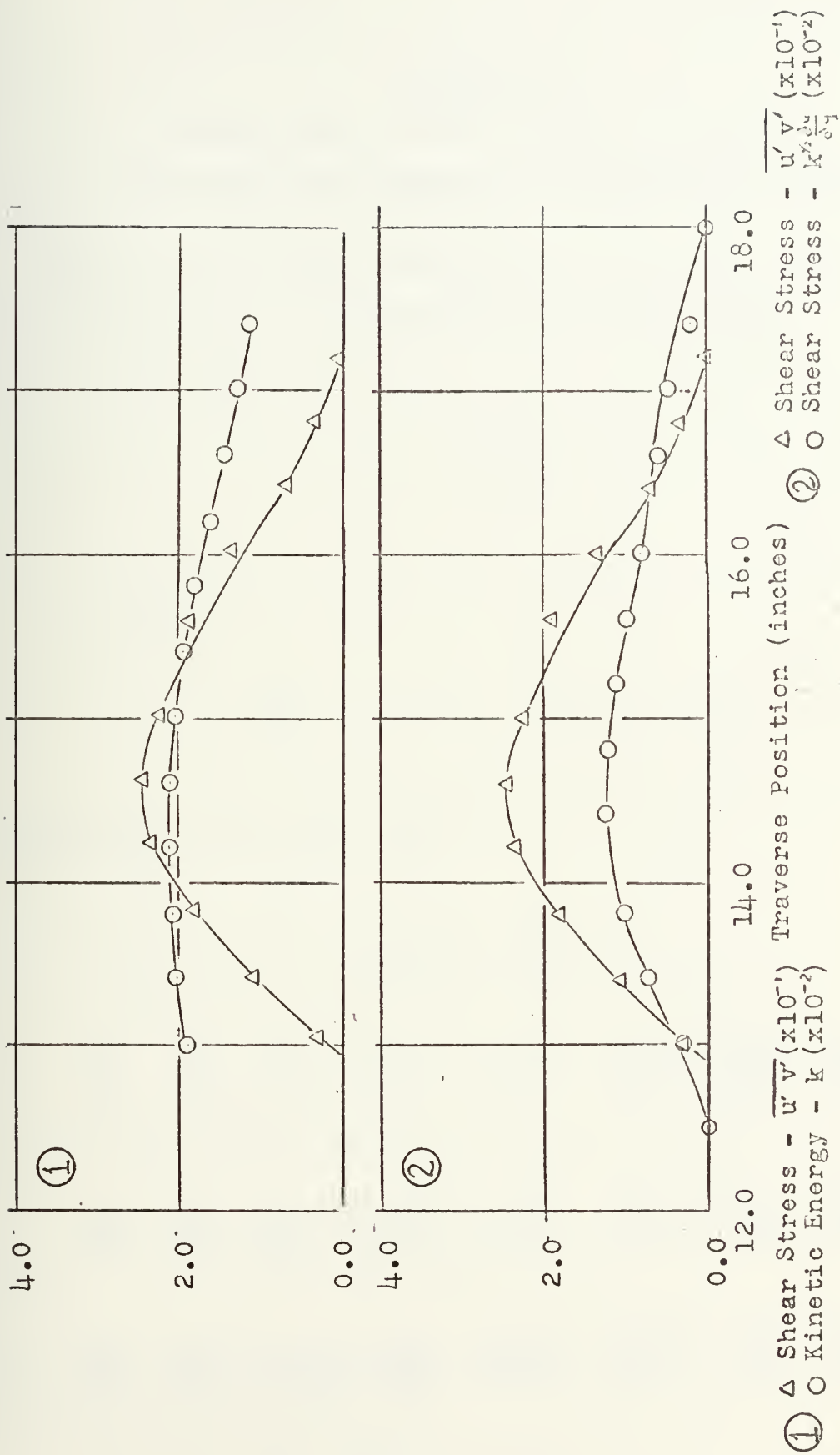


FIGURE 97
Station 6 Turbulent Stress Comparison

APPENDIX A

DEVELOPMENT OF THE GOVERNING EQUATIONS OF MOTION FOR TURBULENT INCOMPRESSIBLE FLOW

First, the following equations are the basic Navier-Stokes equation for incompressible Newtonian flow:

continuity:

$$\nabla \cdot \bar{V} = 0 \quad (A-1)$$

momentum:

$$\frac{\partial \bar{V}}{\partial t} + \bar{V} \cdot \nabla \bar{V} = -\frac{1}{\rho} \nabla P + \nu \nabla^2 \bar{V} \quad (A-2)$$

Expanding the DEL terms they are

$$\frac{\partial u}{\partial x} + \frac{\partial v}{\partial y} + \frac{\partial w}{\partial z} = 0 \quad (A-3)$$

$$\frac{\partial u}{\partial t} + u \frac{\partial u}{\partial x} + v \frac{\partial u}{\partial y} + w \frac{\partial u}{\partial z} = -\frac{1}{\rho} \frac{\partial P}{\partial x} + \nu \left(\frac{\partial^2 u}{\partial x^2} + \frac{\partial^2 u}{\partial y^2} + \frac{\partial^2 u}{\partial z^2} \right) \quad (A-4)$$

$$\frac{\partial v}{\partial t} + u \frac{\partial v}{\partial x} + v \frac{\partial v}{\partial y} + w \frac{\partial v}{\partial z} = -\frac{1}{\rho} \frac{\partial P}{\partial y} + \nu \left(\frac{\partial^2 v}{\partial x^2} + \frac{\partial^2 v}{\partial y^2} + \frac{\partial^2 v}{\partial z^2} \right) \quad (A-5)$$

$$\frac{\partial w}{\partial t} + u \frac{\partial w}{\partial x} + v \frac{\partial w}{\partial y} + w \frac{\partial w}{\partial z} = -\frac{1}{\rho} \frac{\partial P}{\partial z} + \nu \left(\frac{\partial^2 w}{\partial x^2} + \frac{\partial^2 w}{\partial y^2} + \frac{\partial^2 w}{\partial z^2} \right) \quad (A-6)$$

Now substitute equation (A-1) into (A-4), (A-5), and (A-6) to get

$$\frac{\partial u}{\partial t} + \frac{\partial}{\partial x} u^2 + \frac{\partial}{\partial y} uv + \frac{\partial}{\partial z} uw = -\frac{1}{\rho} \frac{\partial P}{\partial x} + \nu \left(\frac{\partial^2 u}{\partial x^2} + \frac{\partial^2 u}{\partial y^2} + \frac{\partial^2 u}{\partial z^2} \right)$$

$$\frac{\partial v}{\partial t} + \frac{\partial}{\partial x} uv + \frac{\partial}{\partial y} v^2 + \frac{\partial}{\partial z} vw = -\frac{1}{\rho} \frac{\partial P}{\partial y} + \nu \left(\frac{\partial^2 v}{\partial x^2} + \frac{\partial^2 v}{\partial y^2} + \frac{\partial^2 v}{\partial z^2} \right)$$

$$\frac{\partial w}{\partial t} + \frac{\partial}{\partial x} uw + \frac{\partial}{\partial y} vw + \frac{\partial}{\partial z} w^2 = -\frac{1}{\rho} \frac{\partial P}{\partial z} + \nu \left(\frac{\partial^2 w}{\partial x^2} + \frac{\partial^2 w}{\partial y^2} + \frac{\partial^2 w}{\partial z^2} \right)$$

With ρ and ν constant and using the following definitions

$$\begin{aligned} u &= \bar{u} + u' & w &= \bar{w} + w' \\ v &= \bar{v} + v' & p &= \bar{p} + p' \end{aligned}$$

equation (A-3) becomes

$$\frac{\partial}{\partial x} (\bar{u} + u') + \frac{\partial}{\partial y} (\bar{v} + v') + \frac{\partial}{\partial z} (\bar{w} + w') = 0 \quad (A-7)$$

Since the integral over time of any fluctuating quantity is zero, taking the time average of equation (A-7) results in

$$\frac{\partial \bar{u}}{\partial x} + \frac{\partial \bar{v}}{\partial y} + \frac{\partial \bar{w}}{\partial z} = 0 \quad (A-8)$$

Then subtract this from (A-7) to get

$$\frac{\partial u'}{\partial x} + \frac{\partial v'}{\partial y} + \frac{\partial w'}{\partial z} = 0 \quad (A-9)$$

Now substitute the definitions above into equations (A-4),
then

$$\begin{aligned}
 & \frac{\partial}{\partial t}(\bar{u}+u') + \frac{\partial}{\partial x}(\bar{u}+u')^2 + \frac{\partial}{\partial y}(\bar{u}+u')(\bar{v}+v') + \frac{\partial}{\partial z}(\bar{u}+u')(\bar{w}+w') \\
 &= -\frac{1}{\rho} \frac{\partial}{\partial x}(\bar{p}+p') + v \left[\frac{\partial^2}{\partial x^2}(\bar{u}+u') + \frac{\partial^2}{\partial y^2}(\bar{u}+u') + \frac{\partial^2}{\partial z^2}(\bar{u}+u') \right]
 \end{aligned} \tag{A-10}$$

and after taking the time average

$$\begin{aligned}
 & \frac{\partial \bar{u}}{\partial t} + \frac{\partial}{\partial x} \bar{u}^2 + \frac{\partial}{\partial x} \overline{u'^2} + \frac{\partial}{\partial y} \bar{u} \bar{v} + \frac{\partial}{\partial y} \overline{u'v'} + \frac{\partial}{\partial z} \bar{u} \bar{w} + \frac{\partial}{\partial z} \overline{u'w'} \tag{A-11} \\
 &= -\frac{1}{\rho} \frac{\partial \bar{P}}{\partial x} + v \left[\frac{\partial^2 \bar{u}}{\partial x^2} + \frac{\partial^2 \bar{u}}{\partial y^2} + \frac{\partial^2 \bar{u}}{\partial z^2} \right]
 \end{aligned}$$

In a similar manner, one can get

$$\begin{aligned}
 & \frac{\partial \bar{v}}{\partial t} + \frac{\partial}{\partial x} \bar{u} \bar{v} + \frac{\partial}{\partial x} \overline{u'v'} + \frac{\partial}{\partial y} \bar{v}^2 + \frac{\partial}{\partial y} \overline{v'^2} + \frac{\partial}{\partial z} \bar{v} \bar{w} + \frac{\partial}{\partial z} \overline{v'w'} \tag{A-12} \\
 &= -\frac{1}{\rho} \frac{\partial \bar{P}}{\partial y} + v \left[\frac{\partial^2 \bar{v}}{\partial x^2} + \frac{\partial^2 \bar{v}}{\partial y^2} + \frac{\partial^2 \bar{v}}{\partial z^2} \right]
 \end{aligned}$$

$$\begin{aligned}
 & \frac{\partial \bar{w}}{\partial t} + \frac{\partial}{\partial x} \bar{u} \bar{w} + \frac{\partial}{\partial x} \overline{u'w'} + \frac{\partial}{\partial y} \bar{v} \bar{w} + \frac{\partial}{\partial y} \overline{v'w'} + \frac{\partial}{\partial z} \bar{w}^2 + \frac{\partial}{\partial z} \overline{w'^2} \tag{A-13} \\
 &= -\frac{1}{\rho} \frac{\partial \bar{P}}{\partial z} + v \left[\frac{\partial^2 \bar{w}}{\partial x^2} + \frac{\partial^2 \bar{w}}{\partial y^2} + \frac{\partial^2 \bar{w}}{\partial z^2} \right]
 \end{aligned}$$

In the special case for a two-dimensional mean flow with a
steady mean, equations (A-11) and (A-12) can be written

$$\frac{\partial \overline{u^2}}{\partial x} + \frac{\partial}{\partial y} \overline{uv} = -\frac{1}{\rho} \frac{\partial}{\partial x} (\overline{p} + \rho \overline{u'^2}) - \frac{\partial}{\partial y} (\overline{u'v'}) + \nu \left[\frac{\partial^2 \overline{u}}{\partial x^2} + \frac{\partial^2 \overline{u}}{\partial y^2} \right] \quad (A-14)$$

$$\frac{\partial \overline{uv}}{\partial x} + \frac{\partial}{\partial y} \overline{v^2} = -\frac{1}{\rho} \frac{\partial}{\partial y} (\overline{p} + \rho \overline{v'^2}) - \frac{\partial}{\partial x} (\overline{u'v'}) + \nu \left[\frac{\partial^2 \overline{v}}{\partial x^2} + \frac{\partial^2 \overline{v}}{\partial y^2} \right] \quad (A-15)$$

Then applying the standard boundary layer assumptions

$$P = P(x) \quad \text{from} \quad \frac{dP}{dx} = -\rho U_e \frac{dU_e}{dx} \quad (A-16)$$

and in addition make the following approximations

$$\rho \overline{u'^2} \ll \overline{P} \quad (A-17)$$

$$\nu \left[\frac{\partial^2 \overline{u}}{\partial x^2} + \frac{\partial^2 \overline{u}}{\partial y^2} \right] \ll \frac{\partial}{\partial y} \overline{u'v'} \quad (A-18)$$

When these assumptions are substituted into (A-14), the following equation results:

$$\frac{\partial \overline{u^2}}{\partial x} + \frac{\partial}{\partial y} \overline{uv} = -\frac{1}{\rho} \frac{\partial \overline{P}}{\partial x} - \frac{\partial}{\partial y} \overline{u'v'} \quad (A-19)$$

Which can be manipulated into the form in equation (A-20) using continuity

$$\overline{u} \frac{\partial \overline{u}}{\partial x} + \overline{v} \frac{\partial \overline{u}}{\partial y} = -\frac{1}{\rho} \frac{\partial \overline{P}}{\partial x} - \frac{\partial}{\partial y} \overline{u'v'} \quad (A-20)$$

applying the Boussinesq laminarization, the turbulent shear becomes

$$-\frac{\partial}{\partial y} \overline{u'v'} = \frac{1}{\rho} \tau_y = \frac{1}{\rho} (\mu_t(x) \frac{\partial \bar{u}}{\partial y}) \quad (A-21)$$

then, $\tau = -\rho \overline{u'v'}$, is the Reynolds Stress, and $\mu_t(x)$, the Eddy Viscosity, is a function of the flow field. If (A-16) and (A-21) are substituted into (A-20) the result is

$$\bar{u} \frac{\partial \bar{u}}{\partial x} + \bar{v} \frac{\partial \bar{u}}{\partial y} = U_e \frac{dU_e}{dx} + \nu_T(x) \frac{\partial^2 \bar{u}}{\partial y^2} \quad (A-22)$$

An alternate approach to solving these equations is possible without the boundary layer assumptions (A-16, 17, & 18). Since there are three equations, (A-8), (A-14), and (A-15) and six unknowns \bar{u} , \bar{v} , \bar{p} , $\overline{u'^2}$, $\overline{v'^2}$, and $\overline{u'v'}$, three additional equations are required. By subtracting the mean equations from the full equations as shown in (A-10), three additional momentum equations for the fluctuating portion of the flow result; however, several additional unknowns also appear:

$$\overline{u'^3}, \quad \overline{v'^3}, \quad \text{and} \quad \overline{u'v'^2}.$$

One might also formulate additional equations for these variables, but higher order correlation unknowns would appear in them, and additional equations would be required

ad infinitum. It is customary at this point then to approximate $\overline{v'^2}$, $\overline{u'^2}$, and $\overline{u'v'}$ by some function of the mean flow and solve the system of equations.

APPENDIX B

DEVELOPMENT OF THE EQUATIONS FOR THE HOT-WIRE ANEMOMETER

I. Single Normal Hot-Wire

First assume the following definitions

$$e = \bar{e} + e'$$

$$u = \bar{u} + u'$$

Then, since the linearized output of the hot-wire is proportional to u

$$e = C u \quad (B-1)$$

or

$$\bar{e} + e' = C(\bar{u} + u') \quad (B-2)$$

Setting averages equal to averages, since they must be independent of the fluctuations,

$$\bar{e} = C \bar{u} \quad (B-3)$$

or solving for u

$$u = \frac{1}{C} \bar{e} = \frac{\bar{u}_e}{\bar{e}_e} \bar{e} \quad (B-4)$$

and

$$\frac{\overline{U}}{\overline{U}_e} = \frac{\overline{e}}{\overline{e}_e} \quad (B-5)$$

Now setting the fluctuations equal

$$e' = C u' \quad (B-6)$$

$$u' = \frac{1}{C} e'$$

$$\overline{u'^2} = \frac{1}{C^2} \overline{e'^2}$$

which from (B-4) becomes

$$\overline{u'^2} = \frac{\overline{U_e^2}}{\overline{e_e^2}} \overline{e'^2} \quad (B-7)$$

or

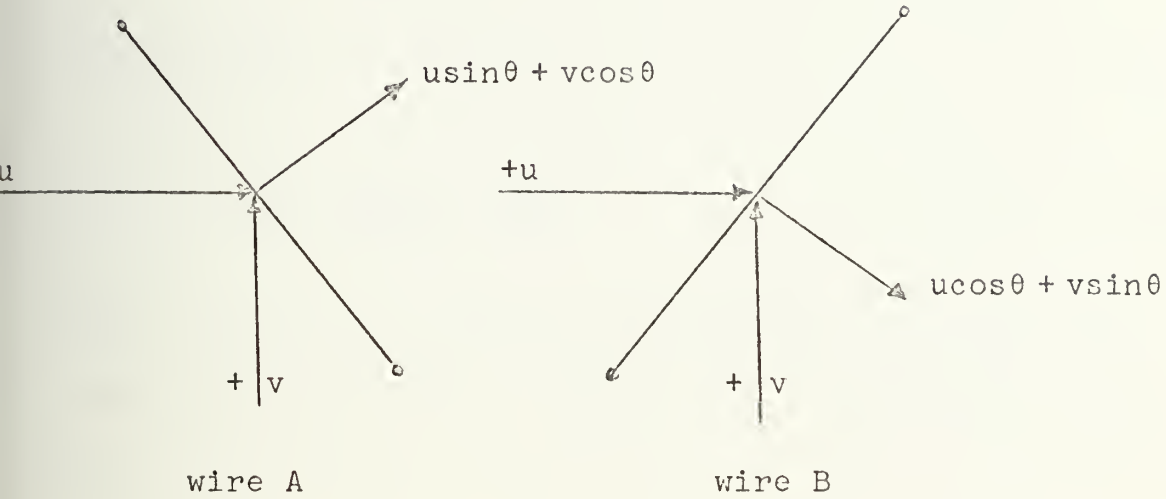
$$\frac{\overline{u'^2}}{\overline{u_e^2}} = \frac{\overline{e'^2}}{\overline{e_e^2}} \quad (B-8)$$

II. X-array Hot-Wire

Now assume in addition, that

$$v = \overline{v} + v' \quad e_A = \overline{e}_A + e_A' \quad e_B = \overline{e}_B + e_B' \quad (B-9)$$

then since the wires are separated by 90°



Now note that $\theta = 45^\circ$ so

$$\begin{aligned} e_A &= C_A (u + v) \\ e_B &= C_B (u - v) \end{aligned} \tag{B-10}$$

At the centerline of the flow the lateral velocity is approximately zero, so $e_A = e_B$ and, therefore, $C_A = C_B = C$. For this reason, once the probe is adjusted to force $e_A = e_B$ at the centerline the following relations hold

$$\begin{aligned} e_A &= C (u + v) \\ e_B &= C (u - v) \end{aligned} \tag{B-11}$$

But if these equations are summed and solved for u

$$u = \frac{1}{2C} [e_A + e_B] \quad (B-12)$$

and similarly

$$v = \frac{1}{2C} [e_A - e_B] \quad (B-13)$$

Then if $\beta \equiv 1/2 C$, and the definitions of the parameters are substituted into (B-12) & (B-13), the resulting equations are

$$\bar{u} + u' = \beta[\bar{e}_A + e_A' + \bar{e}_B + e_B'] \quad (B-14)$$

$$\bar{v} + v' = \beta[\bar{e}_A + e_A' - \bar{e}_B - e_B'] \quad (B-15)$$

As in B-I, set averages equal to averages and

$$\bar{u} = \beta[\bar{e}_A + \bar{e}_B] = \beta[\overline{e_A + e_B}] \quad (B-16)$$

$$\bar{v} = \beta[\bar{e}_A - \bar{e}_B] = \beta[\overline{e_A - e_B}] \quad (B-17)$$

setting fluctuations equal to fluctuations,

$$u' = \beta[e_A' + e_B'] = \beta[(e_A + e_B)'] \quad (B-18)$$

$$v' = \beta[e_A' - e_B'] = \beta[(e_A - e_B)'] \quad (B-19)$$

Then square and average to get

$$\overline{u'^2} = \beta^2 [\overline{(e_A + e_B)^2}] \quad (\text{B-20})$$

$$\overline{v'^2} = \beta^2 [\overline{(e_A - e_B)^2}] \quad (\text{B-21})$$

Returning to equations (B-11) and setting primes equal to primes

$$\begin{aligned} e_A' &= C(u' + v') \\ e_B' &= C(u' - v') \end{aligned} \quad (\text{B-22})$$

square and average

$$\begin{aligned} \overline{e_A'^2} &= C^2 (\overline{u'^2} + 2\overline{u'v'} + \overline{v'^2}) \\ \overline{e_B'^2} &= C^2 (\overline{u'^2} - 2\overline{u'v'} + \overline{v'^2}) \end{aligned} \quad (\text{B-23})$$

then subtract

$$\overline{e_A'^2} - \overline{e_B'^2} = 4C^2 \overline{u'v'} \quad (\text{B-24})$$

or

$$\overline{u'v'} = \frac{1}{4C^2} [\overline{e_A'^2} - \overline{e_B'^2}] \quad (\text{B-25})$$

Now add equations (B-23)

and

$$\overline{e_A'^2} + \overline{e_B'^2} = 2C^2[\overline{u'^2} + \overline{v'^2}]$$

or

$$\overline{u'^2} + \overline{v'^2} = 2\beta^2[\overline{e_A'^2} + \overline{e_B'^2}] \quad (B-23)$$

Then sum (B-20) and (B-21)

$$\overline{u'^2} + \overline{v'^2} = \beta^2[(\overline{e_A + e_B})'^2 + (\overline{e_A - e_B})'^2] \quad (B-24)$$

equating (B-23) and (B-24), and rearranging

$$\frac{2[\overline{e_A'^2} + \overline{e_B'^2}]}{(\overline{e_A + e_B})'^2 + (\overline{e_A - e_B})'^2} = 1 \quad (B-25)$$

Where

$$P_{Te} - P_e = 1/2\rho[u_e^2 + v_e^2]$$

or

$$2\left[\frac{P_{Te} - P_e}{\rho}\right] = \left(\frac{1}{2C}\right)^2 (\overline{e_A + e_B})_e^2 + \left(\frac{1}{2C}\right)^2 (\overline{e_A - e_B})_e^2$$

so

$$\beta^2 = \frac{2(P_{Te} - P_e)}{\rho[(\overline{e_A + e_B})^2 + (\overline{e_A - e_B})^2]_e}$$

and

$$\frac{2(P_{Te} - P_e)}{\rho}$$

is a known array of data from the pitot-static phase of the study.

APPENDIX C

DEVELOPMENT OF AN INTEGRATED FORM OF THE MOMENTUM EQUATION FOR THE CALCULATION OF THE LOCAL TURBULENT SHEAR COEFFICIENT

First, the basic equations of motion for a two-dimensional mean flow are

continuity:

$$u_x + v_y = 0 \quad (C-1)$$

momentum:

$$uu_x + vu_y = -\frac{1}{\rho} P_x + \frac{1}{\rho} \tau_y \quad (C-2)$$

then integrate equation (C-1) from zero to a point y

$$u_x = -v_y$$

$$\int_0^y u_x \, dy = -\int_0^y v_y \, dy$$

$$\int_0^y u_x \, dy = -[v + f(x)]_0^y$$

thus

$$v(y) = -\int_0^y u_x \, dy + v_{y=0}$$

But $v_{y=0}$ is zero, so

$$v(y) = - \int_0^y u_x \, dy \quad (C-3)$$

Now simply and multiply equation (C-1) by u and add to (C-2) to get

$$2uu_x + (vu_y + uv_y) = - \frac{1}{\rho} P_x + \frac{\tau_y}{\rho} \quad (C-4)$$

where the terms on the left can be recognized as differentials of the form

$$2uu_x = (u^2)_x$$

$$vu_y + uv_y = (uv)_y$$

thus equation (C-4) becomes

$$2uu_x + (uv)_y = - \frac{1}{\rho} P_x + \frac{\tau_y}{\rho}$$

and, since $v(0) = 0$, when this equation is integrated from $y = 0$ to an arbitrary point $y = y_\tau$,

$$\int_0^y 2uu_x \, dy + \int_0^{y_\tau} (uv)_y \, dy = \int_0^{y_\tau} 2uu_x \, dy + u(y_\tau)v(y_\tau)$$

and the result, when equation (C-3) is substituted for $v(y_\tau)$, is the following relation

$$\int_0^{y_\tau} 2u u_x dy - u(y_\tau) \int_0^{y_\tau} u_x dy = - \int_0^{y_\tau} \frac{P_x}{\rho} dy + \frac{\tau(y_\tau)}{\rho}$$

Which can be rearranged into the following form,

$$\int_0^{y_\tau} u_x [2u - u(y_\tau)] dy = - \frac{1}{\rho} \int_0^{y_\tau} P_x dy + \frac{1}{\rho} \tau(y_\tau) \quad (C-5)$$

And can be solved for the coefficient of shear at y_τ

$$(C_\tau \equiv \frac{2}{\rho u_e^2} \tau)$$

$$C_\tau(y_\tau) = \frac{1}{\rho u_e^2} \int_0^{y_\tau} P_x dy + [\frac{2}{u_e} \int_0^{y_\tau} u_x [2u - u(y_\tau)] dy] \quad (C-6)$$

An alternate approach to this development would be to substitute equation (C-3) into (C-2)

$$\bar{u} \frac{\partial \bar{u}}{\partial x} - \frac{\partial u}{\partial y} \int_0^y (\frac{\partial u}{\partial x}) dy = - \frac{1}{\rho} \frac{\partial \bar{P}}{\partial x} + \frac{1}{\rho} \frac{\partial \tau}{\partial y} \quad (C-7)$$

Then non-dimensionalize by division by the freestream velocity squared, and use the product rule of the calculus to get the following form of the momentum equation:

$$\begin{aligned} \frac{u}{u_e} (\frac{u}{u_e})_x + (\frac{u}{u_e})^2 \frac{u_{ex}}{u_e} - (\frac{u}{u_e}) \int_0^y (\frac{u}{u_e})_x dy - (\frac{u}{u_e}) (\frac{u_{ex}}{u_e}) \int_0^y (\frac{u}{u_e}) dy \\ = - \frac{1}{\rho u_e^2} P_x + (\frac{C_\tau y}{2}) \end{aligned} \quad (C-8)$$

Where $C_\tau \equiv \frac{2\tau}{\rho u_e^2}$, and the subscripts x, and y indicate partial differentiation with respect to x, and y respectively. Now, if the condition that equation (C-8) be satisfied at every point in the flow is relaxed to allow it to be satisfied on the average between $y = 0$ and an arbitrary point y_τ , then (C-8) can be integrated by parts to get the following relation for C_τ

$$\begin{aligned} \frac{C_\tau(y_\tau)}{2} = & \int_0^{y_\tau} \left[2\left(\frac{u}{u_e}\right) - \frac{u(y_\tau)}{u_e} \right] \left[\left(\frac{u}{u_e}\right)_x + \left(\frac{u}{u_e}\right)\left(\frac{u_{ex}}{u_e}\right) \right] dy \\ & + \int_0^{y_\tau} \frac{1}{2\rho u_e^2} P_x dy \end{aligned} \quad (C-9)$$

Now if the original definition of the shear term

$$\tau \equiv -\rho \overline{u'v'}$$

is substituted back into equations (C-5) and (C-9), the following relations result:

$$\overline{u'v'} = \int_0^{y_\tau} u_x [u(y_\tau) - 2u] dy - \frac{1}{\rho} \int_0^{y_\tau} P_x dy \quad (C-10)$$

$$\begin{aligned} \overline{u'v'} = & u_e^2 \int_0^{y_\tau} \left[\frac{u(y_\tau)}{u_e} - 2\left(\frac{u}{u_e}\right) \right] \left[\left(\frac{u}{u_e}\right)_x + \left(\frac{u}{u_e}\right)\left(\frac{u_{ex}}{u_e}\right) \right] dy \\ & + \int_0^{y_\tau} \frac{P_x}{2\rho} dy \end{aligned} \quad (C-11)$$

Finally, to check the validity of these equations, let y_τ go to infinity in the limit and assume that

$$P_x = -\rho u_e u_{e_x}$$

Then, equation (C-5) becomes

$$2 \int_0^\infty u u_x dy - u_e \int_0^\infty u_x dy - \int_0^\infty u_e u_{e_x} dy = 0$$

Since the shear, and therefore C_τ , is zero at ∞ and then

$$2 \int_0^\infty \left(\frac{u^2}{2}\right)_x dy - \int_0^\infty [(u_e u)_x - u u_{e_x}] dy - \int_0^\infty u_e u_{e_x} dy = 0$$

or

$$\int_0^\infty [(u^2)_x - (u_e u)_x + u u_{e_x} - u_e u_x] dy = 0$$

thus, combining terms

$$\int_0^\infty \left[u_e^2 \frac{u}{u_e} \left(\frac{u}{u_e} - 1 \right) \right]_x dy + \int_0^\infty u_e u_{e_x} \left(\frac{u}{u_e} - 1 \right) dy = 0 \quad (C-12)$$

and if the flowing parameters are defined

$$\theta \equiv \int_0^\infty \frac{u}{u_e} \left(\frac{u}{u_e} - 1 \right) dy; \quad \delta^* \equiv \int_0^\infty \left(\frac{u}{u_e} - 1 \right) dy$$

then equation (C-12) may be written

$$[u_e^2 \theta]_x + u_e u_{e_x} \delta^* = 0$$

which when the first term is differentiated becomes

$$u_e^2 \frac{d\theta}{dx} + 2 u_e u_{e_x} \theta + u_e u_{e_x} \delta^* = 0$$

or dividing by u_e^2

$$\frac{d\theta}{dx} + \frac{u_{e_x}}{u_e} [2\theta + \delta^*] = 0 \quad (C-13)$$

which is simply the well-known momentum integral equation for a boundary layer. A similar procedure will reduce equation (C-9) to (C-13) as well.

APPENDIX D

DATA CHECKS

In an experimental study, it is very important to have some idea of the quality of the data that results from the experiment. In this Appendix, several methods of checking the accuracy of the data in this study are discussed.

CONTINUITY CHECKS

Using the continuity equation, it is apparent that, since the mass flow must be constant,

$$\int_0^{\text{wall}} u dy = \text{constant} \quad (\text{D-1})$$

Therefore, this equation was added to the program described in Appendix E. The results of this check for the pitot-static data varied as much as 30% over the entire test section, yet, if the largest and smallest value are neglected the range is narrowed to $\pm 10\%$. The author believes that much of this difference is due to the inability to position the pitot-static probe near the wall in some cases, while in others, the head of the probe could be placed adjacent to the wall surface. This problem is especially critical at Station 1 where the boundary layer is thin, and mass flow near the wall, at free stream velocity, comprises a

significant part of the total mass flow in the tunnel.

See the computer output in Appendix F.

MOMENTUM CHECKS

Recall the integral momentum equation derived in Appendix C,

$$\frac{d\theta}{dx} + \frac{u_e}{u_e} [2\theta + \delta^*] = 0 \quad (C-13)$$

which is a special case for the free stream where C is zero. Taking this equation as

$$E1 = \frac{d\theta}{dx}$$

$$E2 = \frac{1}{u_e} \frac{du_e}{dx}$$

$$E3 = 2\theta + \delta$$

then the non-dimensional residual of this equation was programmed as

$$\text{Epsilon} = (E1 + E2 * E3) / (E1 - E2 * E3) \quad (D-2)$$

and its values are listed in the computer output.

In general, this ratio showed the data to correlate fairly well with the restrictions imposed by the momentum integral equation with an average residual of less than

25% and as little as +15% for most stations; however, Station 7 data was completely out of line with a residual greater than two. The primary reason for the failure of Station 7 to check satisfactorily was an inclusion of a significant portion of data at the upper portion of the traverse that reflected boundary layer interference. The inclusion of the resulting velocity decay in the calculation of the momentum, and displacement thicknesses created a large error in their values. This error is almost certainly the cause of slightly high values of Station 8 as well.

ENERGY CHECKS

Having calculated the local turbulent shear coefficient, it was possible to also integrate to the residual in the energy integral equation,

$$\frac{d}{dx}(u_e^3 \delta_3) = 2 \int_0^{\infty} \frac{\tau}{\rho} \left(\frac{\partial u}{\partial y} \right) dy \quad (D-3)$$

where the energy thickness δ_3 is defined as

$$\delta_3 \equiv \int_0^{\infty} u(u_e^2 - u^2) dy \quad (D-4)$$

Therefore taking the term on the left as A, and that on the right as B, the relation was programmed and,

$$ZETA = (A - B)/(A + B) \quad (D-4)$$

The results of this data check were inconclusive. The magnitude of one of two terms above (A and B) was so much larger than the other that the difference over the sum was due solely to an error in the programming vice an inaccuracy in the raw data.

HOT-WIRE CHECKS

In Appendix B it was shown in equation (B-25) that these terms were set equal to η , and values for η are listed in Table I. It was immediately obvious in this case that the error, although not large, was directly related to the strength of the turbulence in the flow. Thus, the magnitude of the lack of algebraic correlation in this check may have been due to an inability of the equipment to handle the rapid variations caused by severe turbulence. It is important to note here, that a change of as little as 10% in the individual values of the parameters used to calculate η would bring even the worst value of η back to within 10% of 1.0. The author felt that the data from Phase III of the experiment was well within the bounds of acceptable experimental data spread.

APPENDIX E

DATA REDUCTION COMPUTER PROGRAM

A. GENERAL

The Fortran IV computer program included in this Appendix is a revised form of that developed by the study of Reference 1. The program inputs the pitot-static data of phase I of the experiment, and a limited amount of data from phase II to calculate the wake momentum thickness, displacement thickness, energy thickness, local turbulent shear coefficient, and Eddy Viscosity.

At the inception of the present study the portion of the program dealing with the turbulent shear coefficient did not produce accurate values for C_τ . The author of Reference 1 was unable to find a reason for this error since the equations appeared correct, and there were no obvious coding errors. He postulated that the unreasonable values were a result of an inability of a forward finite difference scheme to accurately approximate the partial derivatives in equation (C-9) of Appendix C. Since this appeared to be a reasonable theory, this author attempted to obtain values for the derivatives by two additional methods:

1. A least squares polynomial approximation was fitted to the data at a given position y from the

centerline then this polynomial was differentiated.

2. A central difference scheme.

Unfortunately, these improvements resulted in no significant change in the values of τ . Thus, the values for the various derivatives were printed out in detail, and an order of magnitude analysis was carried out. At this point, it was not difficult to see that the values of the parameter U were exceptionally smooth in the x -direction, and obviously not a problem to approximate, yet the values calculated by the IBM-360 were not even similar to those calculated by hand. The author then attempted to follow the instructions programmed for the computer and quickly discovered that a subtle error was hidden in the program. Since each station had a different number of points, the index corresponding to a point y above the centerline was different at each station; therefore the arrays requiring differentiation were read into a dummy variable where $J = 1$ corresponded to the centerline for each station. This correction produced values for the local shear coefficient that were of the right order of magnitude, and the central difference scheme was considered to produce the best values for the derivative. Some of the hot-wire data was also analyzed using this program, but the values for C_τ were not very similar to those calculated from the pitot-static data. Since the pressure term was found to be the driving force of the equation for C_τ during the order of

magnitude analysis, the author felt that approximating the static pressure data with the data from phase one would be unlikely to produce realistic values for the parameters, and no additional attempt was made to use the IBM-360 to reduce the hot-wire data.

B. NOMENCLATURE

The following parameters and arrays were used in the program; their respective dimensions are shown in parenthesis:

ALV	array used to store interpolated values of dynamic pressures (feet)
AMIXL	local Prandtl mixing length in the wake (feet)
CTAU	local turbulent shear coefficient for each point in the wake
DELRAT	ratio of succeeding DELSTR's to that at the first data station
DELSTR	wake displacement thickness (feet)
DELX	axial distance between succeeding probe tip positions (feet)
DIAMTR	diameter of wake generator (inches)
EDDY	eddy viscosity
EPSIL	residual in momentum integral equation when experimental values for THETA and SHAPE are substituted into it
LABEL	label for subroutine DRAW
MN	number of data points laterally through the wake
MX	number of axial data positions
MY	number of points (always odd) into which the wake is divided

P	array of local static pressures for each point in the wake (psf)
PATM	atmospheric pressure (inches of mercury)
Q	freestream dynamic pressure (psf)
SHAPE	wake shape factor (DELSTR/THETA)
THETA	wake momentum thickness (feet)
THETAP	inclination of static pressure manometer (degrees)
THETAV	inclination of dynamic pressure manometer (degrees)
THRAT	ratio of succeeding THETA's to that at the first data station
TITLE1	title for subroutine DRAW
TITLE4	title for subroutine DRAW
U	array of velocities for each point in the wake (feet per second)
URATIO	ratio of local wake velocity to local freestream velocity
XIN	array of probe traverse positions through the wake (inches)
XOUT	interpolated probe traverse positions for each of the MY points in the wake (inches)
XPOS	probe tip position measured from downstream side of the wake generator (inches)
YOUT	interpolated manometer readings (for YQ and YPS) for each of the MY points through the wake (inches)
YPS	static pressure manometer slant distance height difference (inches)
YQ	dynamic pressure manometer slant distance height difference (inches)
MU(X)	kinematic viscosity
MM	index of the maximum velocity

MT	index of the maximum velocity in the upper half of the data
T	dummy array of U for differential
TRATIO	dummy array of URATIO for differential
ADP	dummy array of ALP for differential
D	dummy array of for calculations Eddy Viscosity
NUM	array of MN
MBM	array of MM
MAD	array of MID
MUT	array of MT
MID	index of centerline

C. SUBROUTINES

INTEG	uses Simpson's rule to numerically integrate the function F. It must be supplied with K points (always odd) equally spaced, DELX units apart
QTFE	SSP3 library subroutine for integration using trapazoidal rule
QSF	SSP3 library subroutine for integration using Simpson's Rule
FILL	used to fill in arrays to maximum dimension with freestream values
PREIN	determines midpoint of asignally dimensioned array
UTOP	determines MT, & MM
SPLIT	takes the entire array and puts the values above the centerline into a second array in the input parameters

D. USAGE

The details on the use of this program are listed in the comments at the head of the program. The deck requires 120K to compile and 230K to run.

APPENDIX E

DATA REDUCTION COMPUTER PROGRAM

A HOT-WIRE ANEMOMETER STUDY OF FREE TURBULENT MIXING
IN AXIAL PRESSURE GRADIENTS.

THIS PROGRAM WAS DESIGNED TO REDUCE PITOT-STATIC,
AND HOT-WIRE ANEMOMETER DATA TO DETAILED DATA
CONCERNING THE PHYSICAL PARAMETERS OF THE AIR FLOW.
IT WAS SPECIFICALLY DESIGNED FOR USE IN THE THESIS
PROJECT OF LT. M. E. DEARNEY IN 1972, HOWEVER, THE
PROGRAM WILL BE USEFUL TO ANYONE WHO HAS DATA OF A
SIMILAR NATURE.

TYPE OF DATA REQUIRED

EITHER PITOT STATIC, OR HOT WIRE DATA (WITH A
VELOCITY REF.) AT EQUAL INTERVALS ACROSS A PARALLEL
FLOW 2-DIMENSIONAL WIND TUNNEL. THE PROGRAM IS
PRESENTLY SET UP TO ANALYZE 3 SETS OF DATA OF 12
STATIONS EACH, THE FIRST BEING PITOT STATIC VALUES
AND THE SECOND AND THIRD, HOT-WIRE DATA. ONLY MINOR
MODIFICATIONS WOULD BE REQUIRED TO EXTEND THIS TO
MANY MORE EXPERIMENTS.

INPUT:

1. SIX TITLE DESCRIPTION CARDS
2. ONE LABEL, INTERGERS FROM 1-12
3. FIRST RUN TITLE
4. FIRST 2 LINES, NUMBER OF STATIONS
DIAMETER OF CYCLINDER(NOT REQUIRED)
5. ONE OR MORE CARDS WITH MANOMETER ANGLES
6. ONE OR MORE CARDS WITH ATMOSPHERIC
PRESSURES.
7. TITLE OF FIRST STATION, FIRST RUN
8. FIRST 3 LINES, INTERGER NUMBER OF POINTS
I<175.
9. REFERENCE VALUE OF FIRST POINT
10. DYNAMIC PRESSURES IN INCHES(Pt-PS)
11. STATIC PRESSURES IN INCHES(PS)
12. SAME DATA 7-11 FOR FOLLOWING STATIONS
11. SECOND RUN TITLE
14. NUMBER OF STATIONS
DIAMETER OF CYCLINDER
15. SAME AS 5,6, & 7
16. NUMBER OF POINTS
17. REFERENCE VALUE
18. VOLTAGE DATA
19. THEN CONTINUE FOR THE REST OF THE STATIO
THE THIRD RUN IS THE SAME AS THE FIRST.

MAJOR VARIABLES

U-VELOCITY
CTAU-COEFFICIENT OF STRESS
MU(X), VISCOSITY MODEL
P-PRESSURE
URATIO- U/U(FREE STREAM)
ALP- PSTATIC/12
ALV- PDYNAMIC/12
EDDY- EDDY VISCOSITY
AMISL- REYNOLD'S MIXING LENGTH

MAJOR SUBROUTINES

INTEG- INTEGRATE BY SIMPSON'S RULE


```

QTFE- INTEGRATE BY TRAPAZOIDAL RULE
FILL- FILL THE VELOCITY AND PRESSURE ARRAYS
      FOR COMPUTATIONAL PURPOSES.
PREIN- DETERMINE THE MIDPOINT OF THE WAKE
      DEFECT.
SM-   USED IN CONJUNCTION WITH LEAST SQUARES
      ROUTINE FOR TAKING DERIVITIVES,
      1=U, 2=DU.
SPLIT- DETERMINE THE MIDPOINT OF THE FLOW
UEE-   DETERMINE THE MAX FLOW VELOCITY

```

此後凡有關於本會之事項，請逕向本會秘書處接洽，此致。

```

IMPLICIT REAL*4 (A-H,O-Z)
REAL*8 TITLE1(12)
REAL*8 TITLE2(12)
REAL*8 TITLE4(12)
REAL*8 LABEL1/'      DELS'/'
REAL*8 LABEL2/'      THET'/'
REAL*8 LABEL3/'      SHAP'/'
REAL*4 LABEL(12)
DIMENSION YFAT(12),YFIT(12),YFOT(12),YFUT(12)
DIMENSION ALP(12,175),ALV(12,175),U(12,175),P(12,175)
DIMENSION AMU(12),MUT(12)
DIMENSION A(12,175),B(12,175),C(12,175),D(12,175)
DIMENSION EDDY(12,175),AMIXL(12,175),XOUT(12,175)
DIMENSION URAT(12,175),CTAU(12,175),YQ(175),YPS(175)
DIMENSION UR(175),UP(175),UC(175),UD(175),F(175)
DIMENSION YOUT(175),XIN(175)
DIMENSION AXIS(175)
DIMENSION DELSTR(12),THETA(12),SHAPE(12),EPSIL(12)
DIMENSION T(12,175),ADP(12,175)
DIMENSION Q(12),DELRAT(12),THRAT(12),THETAV(12)
DIMENSION THETAP(12),PATM(12),XPOS(12),DELY(12)
DIMENSION WX(12),WH(12),IW(12)
DIMENSION XFIT(12)
DIMENSION RAKE(175)
DIMENSION FAK(175),MAD(12),MBM(12)
DIMENSION NUM(12)
COMMON/A/ H
DATA GAMA/62.32/,RHO/0.002378/
H=0.1EO
Y=H/12.0

```



```

FORMAT(' ',T18,'DELSTAR=',G12.5,5X,'THETA=',G12.5,5X,
SHAPE=',G12.5,5X,'EPSILON=',G12.5)
FORMAT('////////' ',T8,'POINT',T30,'U',T48,'U/UE',T70,'P'
T88,'CTAU')
FORMAT('O',T9,I3,T24,G12.5,T44,G12.5,T64,G12.5,T84,
12.5)
FORMAT('1',T44,'***SUMMARY OF INTEGRATED WAKE PROPER',
TIES**')
FORMAT('////////' ',T3,'AXIAL',T75,'THETA'/' ',T2,'STATION
,T16,'X/D',T29,'DELSTAR',T44,'DELRATIO',T60,'THETA',
T75,'RATIO',T90,'SHAPE',T105,'EPSILON')
FORMAT('O',T4,I3,T11,G12.5,T26,G12.5,T41,G12.5,T56,
G12.5,T71,G12.5,T86,G12.5,T102,G12.5)
FORMAT('1',T49,'***REYNOLD'S MIXING LENGTH DATA***')
FORMAT('////////' ',T61,'STATION',I3///' ',T44,'POINT',
T59,'EDDY VISCOSITY',T79,'MIXING LENGTH')
FORMAT(' ',T45,I3,T60,G12.5,T80,G12.5)
FORMAT(6A8)
FORMAT('//' ', 'LAST=',I3)
FORMAT(12A4)
FORMAT(' ',T45,'MASS FLOW =',F13.5/)
FORMAT('1'////////' ',T8,'POINT',T30,'U',T48,'U/UE',T70,
T88,'CTAU')
FORMAT('1'//)
FORMAT('O',T60,'TURBULENCE CHECKS'///T10,'STATION',
15X,'ETA',12X,'MU(X)'//)
FORMAT(' ',T14,I2,11X,F12.4,5X,F12.4/)

```

```

READ(5,90) TITLE1
READ(5,90) TITLE2
READ(5,90) TITLE4
READ(5,92) LABEL

```

ZERO ALL ARRAYS BEFORE COMPUTATION BEGINS

THIS LOOP CARRIES THE PROGRAM THRU THREE SETS OF DATA

```

DO 1000 KK=1,3
Z=0.0
DO 1 I=1,12
DELSTR(I)=Z
DELSTR(I)=Z
DELY(I)=Z
EPSIL(I)=Z
PATM(I)=Z
Q(I)=Z
SHAPE(I)=Z
THETA(I)=Z
THETAP(I)=Z
THETAV(I)=Z
THRAT(I)=Z
AMU(I)=Z
XPOS(I)=Z
DO 1 J=1,175
A(I,J)=Z
B(I,J)=Z
C(I,J)=Z
CTAU(I,J)=Z
D(I,J)=Z
F(J)=Z
P(I,J)=Z
URATIO(I,J)=Z
XOUT(I,J)=Z
GO TO (36,1,1), KK
ALP(I,J)=Z
ALV(I,J)=Z
U(I,J)=Z
CONTINUE

```



```

      J7=MZ
      MZ=MZ+1
      DO 864 J=MU,175
      YPS(J)=ALP(I,ME)*12.
      YPS(J7)=YPS(MZ)
      IF(J7.EQ.1) GO TO 862
      J7=J7-1
864  CONTINUE
862  CONTINUE
      GO TO 43
      41 READ(5,56) (YPS(J),J=1,MN)
C
C      ECHO-CHECK INPUT
C
      43 WRITE(6,95)
      WRITE(6,54)
      WRITE(6,75) MN
      WRITE(6,76) (XIN(J),J=1,MN)
      WRITE(6,95)
      WRITE(6,77) (YQ(J),J=1,MN)
      WRITE(6,95)
      WRITE(6,78) (YPS(J),J=1,MN)
      MY=MN
      NUM(I)=MN
C
C      CALCULATE U VELOCITY
C
      IF(KK.GT.1) GO TO 37
      DO 3 J=1,MN
      YOUT(J)=YQ(J)
      ALV(I,J)=YOUT(J)/12.0
      U(I,J)=SQRT(2.0*GAMA*SIN(THETAV(I))*ALV(I,J)/RHO)
3  CONTINUE
      GO TO 38
      37 MM=MBM(I)
      UDUM=U(I,MM)
      CALL PREIN(YQ,MN,MID)
      MM=MID
      DO 632 J=1,MY
      632 U(I,J)=YQ(J)
      UTOP=UEE(U,MN,UMAX,MM,I,MT)
      MV=MBM(I)
      ADUM=ALV(I,MV)
      DO 39 J=1,MY
      ALV(I,J)=(ADUM*YQ(J))/YQ(MM)
      U(I,J)=(UDUM*YQ(J))/YQ(MM)
      39 CONTINUE
C
C      DETERMINE MAXIMUM FREESTREAM VELOCITY
C
C
      38 CALL PREIN(YQ,MN,MID)
      MM=MID
      UTOP=UEE(U,MN,UMAX,MM,I,MT)
      Q(I)=0.5*RHO*U(I,MM)**2
      WRITE(6,55) MID
      WRITE(6,55) MM
      WRITE(6,55) MT
      WRITE(6,53) UMAX
      WRITE(6,53) UTOP
      MAD(I)=MID
      MBM(I)=MM
      MUT(I)=MT
C
C      CONTINUITY CHECK
C
      DO 99 J=1,MY
      99 F(J)=U(I,J)
      J4=2
      CALL SPLIT(F,FAKE,MT,MID,J4)
      CALL INTEG(FAKE,J4,Y,RESULT)
      WRITE(6,93) RESULT

```



```

C
C   CALCULATE DISPLACEMENT THICKNESS
C
DO 31 J=1,MY
URATIO(I,J)=U(I,J)/U(I,MM)
F(J)=1.0-URATIO(I,J)
31 CONTINUE
J1=2
CALL SPLIT(F,FAKE,MY,MID,J1)
CALL QTFE(Y,FAKE,RAKE,J1)
DELSTR(I)=RAKE(J1)
DELRAT(I)=DELSTR(I)/DELSTR(1)

C
C   CALCULATE MOMENTUM THICKNESS
C
DO 4 J=1,MY
F(J)=URATIO(I,J)*(1.0-URATIO(I,J))
4 CONTINUE
J2=2
CALL SPLIT(F,FAKE,MY,MID,J2)
CALL QTFE(Y,FAKE,RAKE,J2)
THETA(I)=RAKE(J2)
THRAT(I)=THETA(I)/THETA(1)

C
C   CALCULATE SHAPE FACTOR IN MOMENTUM INTEGRAL
C
SHAPE(I)=DELSTR(I)/THETA(I)

C
C   CALCULATE THE PRESSURE FIELD
C
DO 5 J=1,MY
IF(KK.GT.1) GO TO 40
X=XOUT(I,J)
YOUT(J)=YPS(J)
ALP(I,J)=YOUT(J)/12.0
F(J)=URATIO(I,J)
40 P(I,J)=PATM(I)- GAMA*SIN(THETAP(I))*ALP(I,J)

C
C   5 CONTINUE
C
CALL DRAW(MN,XIN,F,0,0,LABEL,TITLE1,0,0,1,1,2,2,6, 6,1)

C
C   6 CONTINUE
C
C   FILL IN FUNCTION ARRAYS TO MAX DIMENSION FOR
C   CALCULATIONS
C
CALL FILL(NUM,1,U)
CALL FILL(NUM,1,ALP)

C
C   PREPARE DUMMY VARIABLES CENTERED ON THE FLOW
C   CENTERLINE
C
DO 711 LTB=1,2
IF(LTB.EQ.2) GO TO 712
DO 451 I=1,MX
MID=MAD(I)
DO 451 J=MID,175
JK=J-MID+1
T(I,JK)=U(I,J)
ADP(I,JK)=ALP(I,J)
451 CCNTINUE
GO TO 714
712 DO 713 I=1,MX
MID=MAD(I)
JL=MID +1
DO 713 J=MID,100

```



```

      JK=J-MID+1
      JL=JL-1
      T(I,JK)=U(I,JL)
      ADP(I,JK)=ALP(I,JL)
      IF(JL.EQ.1) GO TO 714
713  CONTINUE
714  CONTINUE

```

C
C
C CALCULATE RESIDUAL IN MOMENTUM INTEGRAL EQUATION

```

      I=1
      DELX=XPOS(I+1)-XPOS(I)
      MV=MBM(I+1)
      MM=MBM(I)
      E1=(THETA(I+1)-THETA(I))/DELX
      E2=(THETA(I)*(SHAPE(I)+2.))
      E3=(U(I+1,MV)-U(I,MM))/(DELX*U(I,MM))
      EPSIL(I)=(E1+E2*E3)/(E1-E2*E3)
      DO 7 I=2,MX1
      DELX=XPOS(I+1)-XPOS(I-1)
      M1=MBM(I-1)
      M2=MBM(I)
      M3=MBM(I+1)
      MY=NUM(I)
      E1=(THETA(I+1)-THETA(I-1))/DELX
      E2=THETA(I)*(SHAPE(I)+2.0)
      E3=(U(I+1,M3)-U(I-1,M1))/(DELX*U(I,M2))
      EPSIL(I)=(E1+E2*E3)/(E1-E2*E3)
7    CONTINUE
      I=MX
      DELX=XPOS(I)-XPOS(I-1)
      MV=MBM(I)
      MM=MBM(I-1)
      E1=(THETA(I)-THETA(I-1))/DELX
      E2=(THETA(I)*(SHAPE(I)+2.))
      E3=(U(I,MV)-U(I-1,MM))/(DELX*U(I,MV))
      EPSIL(I)=(E1+E2*E3)/(E1-E2*E3)

```

C
C
C
C
C CALCULATE LOCAL TURBULENT SHEAR COEFFICIENT IN WAKE
STATION ONE - FORWARD DIFFERENCE

```

      I=1
      MM=MBM(I)
      MY=NUM(I)-MAD(I)+1
      DELX=XPOS(I+1)-XPOS(I)
      DO 576 K=1,MY
      DO 575 J=1,K
      A(I,J)=2.*T(I,J)-T(I,K)
      B(I,J)=(T(I+1,J)-T(I,J))/DELX
      C(I,J)=(ADP(I+1,J)-ADP(I,J))/(DELX*ALV(I,MM))
575  CONTINUE
      J4=0
      DO 574 J=1,K
      J4=J4+1
574  F(J)=A(I,J)*B(I,J)
      CALL QTFE(Y,F,RAKE,J4)
      J5=0
      DO 573 J=1,K
      J5=J5+1
573  F(J)=C(I,J)
      CALL QTFE(Y,F,FAKE,J5)
      CTAU(I,K)=(2./U(I,MM)**2)*RAKE(J4)-FAKE(J5)
576  CONTINUE

```

C
C
C STATION 2 TO (MX-1) CENTRAL DIFFERENCE

```

      DO 10 I=2,MX1
      DELX=XPOS(I+1)-XPOS(I)
      MM=MBM(I)
      MY=NUM(I)-MAD(I)+1

```



```

MID=1
DO 10 K=MID,MY
DO 9 J=MID,K
MA=J-MID+1
A(I,J)=2.*T(I,J)-T(I,K)
B(I,J)=(T(I+1,J)-T(I-1,J))/(2.*DELX)
C(I,J)=(ADP(I+1,J)-ADP(I-1,J))/(2.*DELX*ALV(I,MM))
9 CONTINUE
J4=0
DO 701 J=MID,<
MA=J-MID+1
J4=J4+1
701 F(MA)=A(I,J)*B(I,J)
CALL QTFE(Y,F,RAKE,J4)
J5=0
DO 702 J=MID,K
MA=J-MID+1
J5=J5+1
702 F(MA)=C(I,J)
CALL QTFE(Y,F,FAKE,J5)
CTAU(I,K)=(2./U(I,MM)**2)*RAKE(J4)-FAKE(J5)
10 CONTINUE
IF(LTB.EQ.2) GO TO 718
DO 521 I=1,MX
MY=NUM(I)-MAD(I)+1
MID=MAD(I)
DO 521 J=1,MY
JK=J+MID-1
D(I,JK)=CTAU(I,J)
521 CONTINUE
GO TO 711
718 DO 719 I=1,MX
MY=NUM(I)-MAD(I)+1
DO 921 J=1,MY
921 F(J)=CTAU(I,J)
MY=NUM(I)
L=MAD(I)
DO 920 J=2,100
L=L-1
CTAU(I,L)=F(J)
IF(L.EQ.1) GO TO 922
920 CONTINUE
922 L=MAD(I)
DO 923 J=L,MY
923 CTAU(I,J)=D(I,J)
719 CONTINUE
711 CONTINUE
WRITE(6,79)
DO 14 I=1,MX
WRITE(6,80) I,MX
WRITE(6,81) DELSTR(I),THETA(I),SHAPE(I),EPSIL(I)
WRITE(6,82)
MY=NUM(I)
DO 13 J=1,MY
IF(J.EQ.30) WRITE(6,94)
IF(J.EQ.60) WRITE(6,94)
IF(J.EQ.90) WRITE(6,94)
IF(J.EQ.120) WRITE(6,94)
WRITE(6,83) J,U(I,J),URATIO(I,J),P(I,J),CTAU(I,J)
13 CONTINUE
14 CONTINUE
WRITE(6,84)
WRITE(6,85)
DO 15 I=1,MX
XD=12.0*XPOS(I)/DIAMTR
WRITE(6,86) I,XD,DELSTR(I),DELRAT(I),THETA(I),THRAT(I)
1,SHAPE(I),EPSIL(I)
15 CONTINUE
C
C CALCULATE THE TURBULENT KINETIC ENERGY RESIDUAL AND MU
C
DO 715 I=1,MX

```



```

MY=NUM(I)-MAD(I)+1
MID=MAD(I)
DO 715 J=1,MY
JK=J+MID-1
CTAU(I,J)=D(I,JK)
715 CONTINUE
DO 230 I=1,MX
J4=0
MID=MAD(I)
MT=MUT(I)
DO 231 J=MID,MT
J4=J4+1
MA=J-MID+1
231 F(MA)=(U(I,MT)**2-U(I,J)**2)*U(I,J)
CALL QTFE(Y,F,RAKE,J4)
YFIT(I)=RAKE(J4)*RHO
230 CONTINUE
MT=MUT(I)
MID=1
J4=0
I=1
DELX=XPOS(I+1)-XPOS(I)
MY=NUM(I)
MID=MAD(I)
DO 236 J=MID,MY
MA=J-MID+1
F(MA)=CTAU(I,MA)*2.*((U(I,J-1)-U(I,J+1))/(2.*Y))
236 J4=J4+1
CALL QTFE(Y,F,RAKE,J4)
YFOTI =RAKE(J4)-(YFIT(I)-YFIT(I+1))/DELX
YFATI =RAKE(J4)+(YFIT(I)-YFIT(I+1))/DELX
YFOT(I)=YFOTI/YFATI
DO 232 I=2,MX1
MT=MUT(I)
DELX=XPOS(I+1)-XPOS(I)
J4=0
MID=MAD(I)
DO 233 J=MID,MY
MA=J-MID+1
F(MA)=CTAU(I,MA)*2.*((U(I,J-1)-U(I,J+1))/(2.*Y))
233 J4=J4+1
CALL QTFE(Y,F,RAKE,J4)
YFOTI =RAKE(J4)-(YFIT(I-1)-YFIT(I+1))/(2.*DELX)
YFATI =RAKE(J4)+(YFIT(I-1)-YFIT(I+1))/(2.*DELX)
YFOT(I)=YFOTI/YFATI
232 CONTINUE
MT=MUT(MX)
J4=0
I=MX
MID=MAD(I)
DO 237 J=MID,MY
MA=J-MID+1
F(MA)=CTAU(I,MA)*2.*((U(I,J-1)-U(I,J+1))/(2.*Y))
237 J4=J4+1
CALL QTFE(Y,F,RAKE,J4)
YFOTI =RAKE(J4)-(YFIT(I-1)-YFIT(I))/DELX
YFATI =RAKE(J4)+(YFIT(I-1)-YFIT(I))/DELX
YFOT(I)=YFOTI/YFATI
I=1
MT=MUT(I)
DELX=XPOS(I+1)-XPOS(I)
MID=MAD(I)
J4=0
DO 581 J=MID,MT
MA=J-MID+1
F(MA)=U(I,J)**2
581 J4=J4+1
CALL QTFE(Y,F,RAKE,J4)
DER=(YFIT(I+1)-YFIT(I))/DELX
AMU(I)=DER/RAKE(J4)
DO 234 I=2,MX1
DELX=XPOS(I+1)-XPOS(I)

```



```

      MT=MUT(I)
      MID=MAD(I)
      J4=0
      DO 235 J=MID,MT
      MA=J-MID+1
      F(MA)=U(I,J)**2
235  J4=J4+1
      CALL QTFE(Y,F,RAKE,J4)
      DER=(YFIT(I+1)-YFIT(I-1))/(2.*DELX)
      AMU(I)=DER/RAKE(J4)
234  CONTINUE
      WRITE(6,96)
      DO 717 I=1,MX
717  WRITE(6,97) I,YFOT(I),AMU(I)

C
C
      CALCULATE EDDY VISCOSITY AND REYNOLD'S MIXING LENGTH

      WRITE(6,87)
      DO 17 I=2,MX
      WRITE(6,88) I
      MIN=((NUM(I)-1)/2)+10
      MAX=NUM(I)-10
      DO 16 J=MIN,MAX
      E1=ABS(D(I,J)*Q(I))
      E2=ABS(U(I,J+1)-U(I,J-1))
      E3=2.0*H
      EDDY(I,J)=(E1/RHO)/(E2/E3)
      AMIXL(I,J)=SQRT(E1/(RHO*(E2/E3)**2))
      WRITE(6,89) J,EDDY(I,J),AMIXL(I,J)
16  CONTINUE
17  CONTINUE

C
1000 CONTINUE
999  STOP
      END

```

THIS PROGRAM WAS DESIGNED TO INTEGRATE BY THE USE OF
SIMPSON'S RULE.

INPUT:

CALL INTEG(F,M,DELX,RESULT)

F- ARRAY OF VALUES OF THEINTEGRAND

M- THE NUMBER OF POINTS

DELX- THE STEP SIZE

RESULT- THE RESULT OF THE INTEGRATION

```

SUBROUTINE INTEG(F,K,DELX,RESULT)
IMPLICIT REAL*4 (A-H,O-Z)
DIMENSION F(1)
C
      INTEGRATION BY SIMPSONS RULE
      K1=K-1
      A=F(1)+F(K)
      B=0.0
      DO 1 I=2,K1,2
      SUM=4.0*F(I)
      B=B+SUM
1  CONTINUE

```



```

C=0.0
DO 2 I=3,K,2
SUM=2.0*F(I)
C=C+SUM
2 CONTINUE
RESULT=DELX*(A+B+C)/3.0
RETURN
END

```

THIS SUBROUTINE WAS DESIGNED TO FILL AND ARRAY WITH
VALUE EXISTING AT AN INDEX IN THE ARRAY.

INPUT: CALL FILL(M,N,U)

M- AN ARRAY OF INTERGER VALUES OF THE INDEX
N- A FUNCTION VARIABLE
U- A DOUBLE DIMENSIONED ARRAY OF VALUES, U(I,J)
WHERE THE INDEX M IS CONTAINED IN J.

```

SUBROUTINE FILL(NUM,MX,U)
IMPLICIT REAL*4 (A-H,O-Z)
DIMENSION NUM(1),U(12,1)
DO 2 J=1,MX
M=NUM(J)
DO 1 I=M,175
1 U(J,1)=U(J,M)
2 CONTINUE
RETURN
END

```

THIS SUBROUTINE WAS DESIGNED TO TAKE AN ARRAY AND
DETERMINE ITS MID-POINT BY MEANS OF AN ARBITRARY
FUNCTION, AND RETURN THE INDEX OF THAT POINT.

INPUT:

CALL PREIN(A,N,M)

A- THE ARRAY OF VARIABLES
N- THE LIMIT OF THE VALUES TO BE CHECKED
M- THE INDEX OF THE MID-POINT

```

SUBROUTINE PREIN(A,N,M)
DIMENSION A(1)

```

DETERMINE MIDPOINT OF MAKE DEFECT

```

DUM=1000.
N1=N-2
DO 1 I=3,N1

```



```

B=A(I-2)+A(I-1)+A(I)+A(I+1)+A(I+2)
C=AMIN1(B,DUM)
IF(C.GE.DUM) GO TO 1
DUM=B
M=I
1 CONTINUE
RETURN
END

```

THIS SUBROUTINE WAS DESIGNED TO TAKE AN ARRAY OF
VALUES AND SPLIT THEM AT AN ARBITRARY POINT, AND
PLACE THESE VALUES IN ANOTHER ARRAY.

INPUT:

CALL SPLIT(A,B,M,N,JK)

A- THE INPUT ARRAY
B- THE OUTPUT ARRAY
M- THE LIMIT OF THE SPLIT
N- THE START OF THE SPLIT
JK- THE NUMBER OF VALUES BETWEEN M, AND N

```

SUBROUTINE SPLIT(A,B,M,N,JK)
DIMENSION A(1),B(1)
IF(JK.EQ.1) GO TO 1
DO 2 I=N,M
B(I-N+1)=A(I)
2 CONTINUE
JK=M-N+1
GO TO 5
1 MD=M-N-1
DO 3 I=1,MD
IJ=N-I+1
B(I)=A(IJ)
IF(IJ.LE.1) GO TO 4
3 CONTINUE
4 JK=MD
5 RETURN
END

```

THIS FUNCTION WAS DESIGNED TO SELECT THE LARGEST VAL
ARRAY, AND THE LARGEST VALUE IN THE TOP HALF OF THAT A

INPUT:

FUNCTION UEE(U,MY,UM,MM,I,MT)

U- THE ARRAY TO BE SEARCHED
MY- THE EXTENT OF THE ARRAY TO BE
SEARCHED, AN INDEX
UM- THE MAXIMUM VALUE IN THE ARRAY
MM- THE INDEX OF THAT VALUE
I- THE INDEX OF THE FIRST DIMENSION
OF U(I,J)
MT- THE INDEX OF THE LARGEST VALUE IN
THE UPPER HALF OF THE ARRAY
UEE- THE VALUE OF THE LARGEST VALUE IN
THE TOP HALF OF THE ARRAY

```

FUNCTION UEE(J,MY,UM,MM,I,MT)
DIMENSION U(12,1)
UM=0.
M=MM
DO 1 J=1,MY
  UI=UM-U(I,J)
  IF(UI) 2,2,1
2  UM=U(I,J)
  MM=J
1  CONTINUE
  UEE=0.
  IF(MM.GT.M) GO TO 3
  DO 4 J=M,MY
    UI=UEE-U(I,J)
    IF(UI) 5,5,4
5  UEE=U(I,J)
  MT=J
4  CONTINUE
  GO TO 6
3  UEE=UM
  MT=MM
6  RETURN
END

```

THE FOLLOWING IS A PRINT OUT OF THE RAW PITOT-STATIC
DATA FOR THE STUDY

//GO.FT06F001 DD SPACE=(CYL,(1,1))


```

MM=J
1 CONTINUE
  UEE=0; GT=M) GO TO 3
  IF(MM:GT.M) MY
  DO 4 J=M,MY
  UI=UEE-U(I,J)
  IF(UI) 5,5,4
5 UEE=U(I,J)
  MT=J
4 CONTINUE
  GO TO 6
3 UEE=UM
  MT=MM
6 RETURN
  END

```

THE FOLLOWING IS A PRINT OUT OF THE RAW PITOT-STATIC DATA FOR THE STUDY

```

//GO.FT06F001 DD SPACE=(CYL,(1,1))
//GO.SYSIN DD *
A PLOT OF THE PITOT STATIC VELOCITY
VERSUS THE TRAVERSE POSITION, FIGURE
PLOT OF A CURVEFIT (KEARNEY,ME)
LT KEARNEY

```

TITL 4

[illegible]

8.48	9.01	9.04	9.17	9.30	9.43	9.60	9.78
8.98	10.21	10.46	10.76	10.95	11.31	11.70	11.80
10.00	12.15	12.18	12.43	12.17	11.96	11.81	11.53
12.02	10.98	10.67	10.43	10.17	9.93	9.74	9.52
11.21	9.21	9.13	8.98	8.86	8.80	8.79	8.78
11.36							
9.78							

57 STATION 2 PITOT STATIC DATA

9.5	7.50	7.48	7.46	7.49	7.40	7.39	7.35
7.48	7.21	7.15	7.07	6.99	6.92	6.87	6.84
7.31	6.27	6.01	5.69	5.39	5.13	4.87	4.64
6.53	4.42	4.45	4.41	4.30	4.09	3.78	3.49
4.45	4.84	5.24	5.62	5.89	6.09	6.37	6.51
4.63	6.84	6.87	6.96	7.03	7.11	7.17	7.28
6.66	7.42	7.45	7.51	7.54	7.58	7.60	7.62
7.34							
7.62	8.14	8.16	8.21	8.25	8.27	8.32	8.38
8.46	8.49	8.54	8.58	8.64	8.69	8.74	8.78
8.88	8.95	9.00	9.07	9.11	9.21	9.22	9.24
9.25	9.24	9.32	9.31	9.31	9.30	9.32	9.29
9.28	9.27	9.24	9.20	9.15	9.09	9.00	8.97
8.89	8.79	8.73	8.67	8.62	8.56	8.50	8.47
8.42	8.38	8.37	8.35	8.32	8.30	8.28	8.28

66 STATION 3 PITOT STATIC DATA

9.1	7.24	7.22	7.17	7.09	7.03	6.98	6.89
7.26	6.77	6.68	6.59	6.47	6.42	6.31	6.21
6.83	6.02	5.87	5.71	5.52	5.42	5.24	5.04
6.18	4.67	4.55	4.43	4.28	4.20	4.13	4.11
4.85	3.98	3.97	3.88	3.77	3.68	3.60	3.40
4.01	4.85	5.01	5.16	5.32	5.48	5.66	5.80
4.65	6.07	6.15	6.27	6.34	6.42	6.50	6.59
5.92	6.73	6.79	6.88	6.93	6.96	6.94	7.10
6.66	7.05	7.07	7.08	7.08	7.03	7.01	7.00
7.12	7.85	7.84	7.84	7.83	7.82	7.81	7.80
7.80	7.81	7.87	7.88	7.89	7.90	7.90	7.85
7.86	7.87	7.91	7.93	7.93	7.95	7.95	7.90
7.91	7.92	7.92	7.93	7.93	7.91	7.94	7.95
7.92	7.92	7.92	7.91	7.90	7.89	7.89	7.89
7.87	7.87	7.85	7.85	7.82	7.79	7.77	7.75
7.74	7.73	7.72	7.72	7.71	7.71	7.71	7.72
7.72							

STATION 4 PITOT STATIC DATA

5.05 STATION 6 5.04 PITOT STATIC DATA

111

7.0	57	3.53	9	5	38
3.33	30	3.22	2	3	3.06
3.33	97	3.22	2	3	3.32
3.33	60	3.22	2	3	3.32
2.22	19	3.22	2	3	3.32
1.11	56	1.56	5	1	1.66
1.11	58	1.58	5	1	1.66
1.11	79	1.79	9	1	1.66
1.11	16	1.16	6	1	1.66
2.22	57	2.57	7	2	2.04
2.22	05	2.05	5	2	2.04
3.33	37	3.37	7	3	3.33
3.33	56	3.56	6	3	3.33
3.33	46	3.46	6	3	3.33
4.44	60	4.60	0	4	4.44
4.44	50	4.50	0	4	4.44
4.44	54	4.54	4	4	4.44
4.44	60	4.60	0	4	4.44
4.44	22	4.22	2	4	4.44
4.44	61	4.61	1	4	4.44
4.44	61	4.61	1	4	4.44
4.44	60	4.60	0	4	4.44
4.44	59	4.59	9	4	4.44
4.44	55	4.55	5	4	4.44
4.44	28	4.28	8	4	4.44
4.44	47	4.47	7	4	4.44
4.44	38	4.38	8	4	4.44
4.44	38	4.38	8	4	4.44

STATION 7 PITOT-STATIC DATA

119

6.09	99	3.09	9	6	99
3.33	97	3.22	2	3	3.33
2.22	71	2.22	2	2	2.22
2.22	37	2.22	2	2	2.22
1.11	68	1.11	1	1	1.11
1.11	37	1.11	1	1	1.11
1.11	48	1.11	1	1	1.11
1.11	39	1.11	1	1	1.11
1.11	68	1.11	1	1	1.11
2.22	39	2.22	2	2	2.22
2.22	70	2.22	2	2	2.22

9.30	5.77	5.68	5.63	5.58	5.53	5.49
5.44	5.40	5.29	5.24	5.18	5.12	5.07
5.03	4.99	4.71	4.71	4.71	4.71	4.71
4.77	4.74	4.74	4.76	4.79	4.82	4.85
4.71	4.91	4.97	5.01	5.05	5.11	5.15
4.88	5.28	5.38	5.43	5.47	5.57	5.55
5.23	5.62	5.68	5.72	5.73	7.43	7.40
5.45	7.45	7.44	7.44	7.44	7.40	7.40
7.41	7.41	7.40	7.40	7.40	7.40	7.40
7.41	7.41	7.41	7.41	7.41	7.41	7.41
7.43	7.44	7.44	7.45	7.45	7.46	7.46
7.46	7.47	7.49	7.50	7.51		

5	1.0	30.0	30.0	30.0	30.0	30.0
	30.0	30.0	30.0	30.0	30.0	30.0
	29.92	29.92	29.92	29.92	29.92	29.92

71	9.0	10.80	10.80	10.80	10.80	10.80
	10.75	10.80	10.80	10.80	10.80	10.80
	10.63	10.50	10.50	10.50	10.50	10.50
	10.78	9.35	9.35	9.35	9.35	9.35
	7.42	9.26	9.26	9.26	9.26	9.26
	8.59	9.18	9.18	9.18	9.18	9.18
	10.24	10.40	10.40	10.40	10.40	10.40
	10.71	10.71	10.71	10.71	10.71	10.71
	10.68	10.63	10.63	10.63	10.63	10.63

79	8.5	10.85	10.85	10.85	10.85	10.85
	10.26	11.05	11.05	11.05	11.05	11.05
	11.08	10.82	10.82	10.82	10.82	10.82
	9.99	9.99	9.99	9.99	9.99	9.99
	8.39	7.58	7.58	7.58	7.58	7.58
	9.51	9.59	9.59	9.59	9.59	9.59
	10.97	11.00	11.00	11.00	11.00	11.00
	11.04	11.04	11.04	11.04	11.04	11.04

85

8.23	10.08	10.6	10.82	10.48	10.78	10.74	10.72
10.70	10.67	10.60	10.54	10.43	10.41	10.33	10.26
10.17	10.06	9.95	9.84	9.73	9.60	9.38	9.36
9.22	9.28	9.33	9.79	9.63	9.47	9.30	9.11
9.56	9.76	9.89	9.40	9.28	9.14	9.28	9.27
9.17	9.70	9.90	9.08	8.97	8.42	9.18	9.17
9.47	9.98	9.10	9.22	8.97	8.47	9.58	9.27
9.84	9.86	9.50	9.05	9.33	9.47	9.55	9.66
9.77	9.46	10.50	10.53	10.14	10.24	10.30	10.37
10.41	10.68	10.69	10.60	10.00	10.60	10.30	10.64
10.67	5 MEAN	10.69					
STATION	WIRE						

107

7.1	6.58	7.8	8.56	9.50	10.07	10.33	10.50
4.7	5.58	10.22	10.20	10.50	10.40	10.43	10.38
10.54	10.28	10.53	9.84	10.11	10.00	9.93	10.82
10.37	10.62	9.86	9.54	9.40	9.23	9.13	9.09
9.89	9.76	9.66	9.17	9.58	9.30	9.29	9.47
9.80	9.89	9.77	9.69	9.40	9.25	9.40	9.39
9.48	9.58	9.77	9.34	9.17	9.28	9.34	9.45
9.64	9.81	9.82	9.03	9.15	9.24	9.24	9.35
9.61	9.72	9.63	9.94	9.08	9.21	9.20	9.16
9.46	9.55	9.31	9.72	9.82	9.19	9.48	9.43
10.19	10.29	10.44	10.43	10.41	10.12	10.63	10.78
10.45	10.44	5.60					
7.79	6.70	WIRE DATA					
STATION	6 HOT						

149

5.25	1.45	1.72	9.83	2.30	3.04	3.70
1.36	1.18	6.06	1.09	8.50	9.04	7.33
9.95	1.16	10.16	9.19	10.17	9.17	10.16
10.01	9.58	9.44	9.36	9.22	9.21	9.22
9.93	9.33	9.72	9.85	9.14	9.57	9.36
9.15	9.05	9.93	9.78	9.79	9.50	9.28
9.22	9.09	7.10	9.65	9.67	9.71	9.69
9.59	9.28	9.32	9.00	9.12	9.06	9.63
9.01	9.27	9.99	9.17	9.06	9.10	9.79
9.20	9.20	9.35	9.57	9.63	9.70	9.60
9.87	9.86	9.08	9.22	9.23	9.48	9.67
9.74	9.79	9.88	9.04	9.37	9.89	9.89
9.70	9.44	9.51	9.58	9.17	9.27	9.30

AXIAL STATION IOUT OF11STATIONS

DELSTAR= 0.12447E-01 THETA= 0.10270E-01
 SHAPE= 1.2120 EPSILON= 0.56239

APPENDIX F COMPUTER OUTPUT

YPOSITION	U	U/UE	CTAU
10.500	135.93	0.99823	0.95899E-02
10.600	135.85	0.99764	0.11362E-01
10.700	135.52	0.99528	0.13215E-01
10.800	135.36	0.99409	0.15200E-01
10.900	135.12	0.99231	0.17109E-01
11.000	134.39	0.98696	0.18716E-01
11.100	134.15	0.98517	0.20302E-01
11.200	133.08	0.97736	0.21468E-01
11.300	132.76	0.97495	0.22836E-01
11.400	132.34	0.97193	0.24196E-01
11.500	131.02	0.96218	0.25231E-01
11.600	128.66	0.94489	0.25571E-01
11.700	125.83	0.92409	0.25282E-01
11.800	122.84	0.90216	0.24508E-01
11.900	119.33	0.87633	0.23064E-01

YPOSITION	U	U/UE	CTAU
12.000	113.03	0.83009	0.20437E-01
12.100	108.29	0.79530	0.16650E-01
12.200	103.76	0.76203	0.11757E-01
12.300	100.12	0.73528	0.60449E-02
12.400	99.683	0.73207	0.0
12.500	101.21	0.74325	0.58315E-02
12.600	105.85	0.77733	0.10873E-01
12.700	109.10	0.80121	0.14933E-01
12.800	113.80	0.83574	0.17985E-01
12.900	116.83	0.85800	0.19772E-01
13.000	122.49	0.89955	0.20918E-01
13.100	125.31	0.92026	0.21093E-01
13.200	128.49	0.94364	0.20839E-01
13.300	131.02	0.96218	0.19837E-01
13.400	132.10	0.97011	0.18113E-01
13.500	132.76	0.97495	0.16225E-01
13.600	133.74	0.98217	0.14341E-01
13.700	134.47	0.98756	0.12326E-01
13.800	134.72	0.98934	0.10096E-01
13.900	136.09	0.99941	0.80751E-02
14.000	135.93	0.99823	0.53339E-02
14.100	136.01	0.99882	0.27123E-02
14.200	136.17	1.0000	0.20100E-03

YPOSITION	U	U/UE	CTAU
14.300	136.09	0.99941	-0.21956E-02
14.400	136.09	0.99941	-0.42531E-02
14.500	136.09	0.99941	-0.60393E-02

AXIAL STATION 20UT OF11STATIONS

DELSTAR= 0.19818E-01 THETA= 0.16468E-01
SHAPE= 1.2034 EPSILON= 0.54603

YPOSITION	U	U/UE	CTAU
9.5000	127.81	0.99077	0.96840E-02
9.6000	127.98	0.99209	0.10285E-01
9.7000	127.81	0.99077	0.10844E-01
9.8000	127.64	0.98945	0.11506E-01
9.9000	127.38	0.98745	0.12181E-01
10.000	127.13	0.98546	0.13006E-01
10.100	127.04	0.98479	0.13804E-01
10.200	126.70	0.98212	0.14865E-01
10.300	126.35	0.97945	0.15857E-01
10.400	125.48	0.97272	0.16931E-01
10.500	124.96	0.96867	0.17780E-01
10.600	124.26	0.96323	0.18901E-01
10.700	123.55	0.95777	0.19961E-01
10.800	122.93	0.95296	0.21030E-01
10.900	121.68	0.94327	0.21995E-01

YPOSITION	U	U/UE	CTAU
11.000	120.51	0.93419	0.23070E-01
11.100	119.42	0.92572	0.23637E-01
11.200	117.02	0.90710	0.24177E-01
11.300	114.57	0.88810	0.24428E-01
11.400	111.47	0.86413	0.24557E-01
11.500	108.50	0.84104	0.24277E-01
11.600	105.85	0.82050	0.23468E-01
11.700	103.13	0.79944	0.22055E-01
11.800	100.66	0.78034	0.19893E-01
11.900	98.582	0.76419	0.17077E-01
12.000	98.249	0.76161	0.13569E-01
12.100	98.582	0.76419	0.94003E-02
12.200	98.138	0.76075	0.47806E-02
12.300	96.906	0.75120	0.0
12.400	96.680	0.74945	0.46651E-02
12.500	97.692	0.75729	0.89236E-02
12.600	99.024	0.76762	0.12665E-01
12.700	100.56	0.77949	0.15771E-01
12.800	102.81	0.79698	0.18208E-01
12.900	106.97	0.82925	0.20021E-01
13.000	110.79	0.85880	0.21100E-01
13.100	113.42	0.87918	0.21559E-01
13.200	115.33	0.89399	0.21446E-01

YPOSITION	U	U/UE	CTAU
13.300	117.11	0.90783	0.20964E-01
13.400	119.24	0.92430	0.20379E-01
13.500	120.60	0.93489	0.19451E-01
13.600	122.22	0.94744	0.18488E-01
13.700	122.49	0.94951	0.17064E-01
13.800	123.29	0.95571	0.15750E-01
13.900	123.91	0.96051	0.14334E-01
14.000	124.61	0.96596	0.12956E-01
14.100	125.13	0.97002	0.11521E-01
14.200	126.09	0.97744	0.10379E-01
14.300	126.61	0.98146	0.91705E-02
14.400	127.30	0.98679	0.81833E-02
14.500	127.55	0.98878	0.71230E-02
14.600	128.07	0.99276	0.63287E-02
14.700	128.32	0.99474	0.55048E-02
14.800	128.66	0.99737	0.48320E-02
14.900	128.83	0.99869	0.41706E-02
15.000	129.00	1.0000	0.36122E-02
15.100	129.00	1.0000	0.30116E-02

AXIAL STATION 3OUT OF11STATIONS

DELSTAR= 0.29650E-01 THETA= 0.24545E-01
 SHAPE= 1.2080 EPSILON= 0.14891

YPOSITION	U	U/UE	CTAU
9.1000	125.92	1.0000	0.66377
9.2000	125.74	0.99862	0.32624E-01
9.3000	125.57	0.99724	0.24753E-01
9.4000	125.13	0.99378	0.16500E-01
9.5000	124.43	0.98822	0.74171E-02
9.6000	123.91	0.98403	0.41703E-02
9.7000	123.47	0.98053	0.49447E-02
9.8000	122.67	0.97418	0.56491E-02
9.9000	122.13	0.96993	0.60965E-02
10.000	121.59	0.96566	0.68126E-02
10.100	120.78	0.95922	0.75033E-02
10.200	119.97	0.95274	0.82381E-02
10.300	118.87	0.94403	0.88959E-02
10.400	118.41	0.94037	0.96413E-02
10.500	117.39	0.93228	0.10381E-01

YPOSITION	U	U/UE	CTAU
10.600	116.46	0.92486	0.11153E-01
10.700	115.61	0.91814	0.11636E-01
10.800	114.66	0.91060	0.12353E-01
10.900	113.22	0.89919	0.12696E-01
11.000	111.67	0.88685	0.13104E-01
11.100	110.29	0.87591	0.13394E-01
11.200	108.80	0.86403	0.13524E-01
11.300	106.97	0.84957	0.13634E-01
11.400	104.91	0.83320	0.13575E-01
11.500	102.92	0.81734	0.13387E-01
11.600	100.99	0.80203	0.13021E-01
11.700	99.683	0.79166	0.12330E-01
11.800	98.360	0.78115	0.11243E-01
11.900	96.680	0.76781	0.99950E-02
12.000	95.772	0.76060	0.82612E-02
12.100	94.971	0.75424	0.64094E-02
12.200	94.741	0.75241	0.43508E-02
12.300	93.581	0.74320	0.21759E-02
12.400	93.230	0.74041	0.0
12.500	93.113	0.73948	0.21759E-02
12.600	94.394	0.74966	0.43508E-02
12.700	95.430	0.75788	0.64094E-02
12.800	96.114	0.76331	0.82612E-02

YPOSITION	U	U/UE	CTAU
12.900	98.026	0.77850	0.99950E-02
13.000	98.471	0.78203	0.11243E-01
13.100	100.77	0.80031	0.12330E-01
13.200	102.92	0.81734	0.13021E-01
13.300	104.60	0.83071	0.13387E-01
13.400	106.16	0.84306	0.13575E-01
13.500	107.79	0.85603	0.13634E-01
13.600	109.40	0.86880	0.13524E-01
13.700	111.18	0.88296	0.13394E-01
13.800	112.55	0.89381	0.13104E-01
13.900	113.70	0.90301	0.12696E-01
14.000	115.14	0.91438	0.12353E-01
14.100	115.89	0.92038	0.11636E-01
14.200	117.02	0.92932	0.11153E-01
14.300	117.67	0.93449	0.10381E-01
14.400	118.41	0.94037	0.96413E-02
14.500	119.14	0.94621	0.88959E-02
14.600	119.97	0.95274	0.82381E-02
14.700	120.60	0.95779	0.75033E-02
14.800	121.23	0.96281	0.68126E-02
14.900	121.77	0.96709	0.60965E-02
15.000	122.58	0.97348	0.56491E-02
15.100	123.02	0.97701	0.49447E-02

YPOSITION	U	U/UE	CTAU
15.200	123.29	0.97912	0.41703E-02
15.300	123.11	0.97771	0.74171E-02
15.400	124.52	0.98892	0.16500E-01
15.500	124.70	0.99031	0.24753E-01
15.600	124.08	0.98543	0.32624E-01

AXIAL STATION 4OUT OF11STATIONS

DELSTAR= 0.40497E-01 THETA= 0.32596E-01
 SHAPE= 1.2424 EPSILON=-0.90012E-01

YPOSITION	U	U/UE	CTAU
8.6000	109.60	0.99728	0.28348E-01
8.7000	109.50	0.99638	0.20850E-01
8.8000	109.10	0.99274	0.12808E-01
8.9000	108.60	0.98818	0.48563E-02
9.0000	108.09	0.98359	0.14801E-02
9.1000	107.38	0.97713	0.22065E-02
9.2000	106.87	0.97250	0.26959E-02
9.3000	106.05	0.96503	0.35351E-02
9.4000	105.43	0.95939	0.38840E-02
9.5000	104.60	0.95182	0.45416E-02
9.6000	103.97	0.94611	0.56118E-02
9.7000	103.45	0.94132	0.65300E-02
9.8000	102.49	0.93263	0.72837E-02
9.9000	101.85	0.92680	0.79054E-02
10.000	100.88	0.91797	0.84253E-02

YPOSITION	U	U/UE	CTAU
10.100	99.902	0.90907	0.91171E-02
10.200	99.024	0.90107	0.97816E-02
10.300	97.803	0.88997	0.10149E-01
10.400	96.793	0.88078	0.10840E-01
10.500	95.544	0.86941	0.10909E-01
10.600	94.510	0.86000	0.11050E-01
10.700	93.581	0.85155	0.11552E-01
10.800	92.525	0.84194	0.12085E-01
10.900	90.978	0.82786	0.12179E-01
11.000	89.648	0.81576	0.11283E-01
11.100	88.421	0.80460	0.11071E-01
11.200	87.303	0.79442	0.10718E-01
11.300	86.043	0.78296	0.99664E-02
11.400	85.022	0.77366	0.92704E-02
11.500	83.858	0.76307	0.85562E-02
11.600	83.335	0.75832	0.76780E-02
11.700	82.413	0.74992	0.64835E-02
11.800	81.212	0.73899	0.53499E-02
11.900	80.537	0.73285	0.42443E-02
12.000	80.537	0.73285	0.29066E-02
12.100	80.401	0.73162	0.14711E-02
12.200	79.856	0.72666	0.0
12.300	79.993	0.72790	0.14711E-02

YPOSITION	U	U/UE	CTAU
12.400	80.129	0.72914	0.29066E-02
12.500	80.672	0.73408	0.42443E-02
12.600	80.401	0.73162	0.53499E-02
12.700	80.943	0.73654	0.64835E-02
12.800	82.148	0.74751	0.76780E-02
12.900	82.810	0.75353	0.85562E-02
13.000	83.728	0.76189	0.92704E-02
13.100	85.022	0.77366	0.99664E-02
13.200	86.675	0.78871	0.10718E-01
13.300	87.802	0.79896	0.11071E-01
13.400	88.914	0.80908	0.11283E-01
13.500	91.337	0.83113	0.12179E-01
13.600	92.525	0.84194	0.12085E-01
13.700	93.230	0.84836	0.11552E-01
13.800	94.047	0.85579	0.11050E-01
13.900	95.315	0.86733	0.10909E-01
14.000	96.680	0.87975	0.10840E-01
14.100	97.468	0.88691	0.10149E-01
14.200	98.582	0.89705	0.97816E-02
14.300	99.464	0.90508	0.91171E-02
14.400	100.34	0.91304	0.84253E-02
14.500	101.31	0.92191	0.79054E-02
14.600	102.17	0.92972	0.72837E-02

YPOSITION	U	U/UE	CTAU
14.700	102.92	0.93650	0.65300E-02
14.800	103.55	0.94228	0.56118E-02
14.900	104.08	0.94706	0.45416E-02
15.000	104.81	0.95372	0.38840E-02
15.100	105.64	0.96128	0.35351E-02
15.200	106.16	0.96597	0.26959E-02
15.300	106.87	0.97250	0.22065E-02
15.400	107.38	0.97713	0.14801E-02
15.500	107.79	0.98083	0.48563E-02
15.600	108.39	0.98634	0.12808E-01
15.700	109.00	0.99183	0.20850E-01
15.800	109.20	0.99365	0.28348E-01
15.900	109.60	0.99728	0.36247E-01
16.000	109.90	1.0000	0.44146E-01

AXIAL STATION 50UT OF11STATIONS

DELSTAR= 0.62057E-01 THETA= 0.48019E-01
SHAPE= 1.2923 EPSILON=-0.99311E-01

YPOSITION	U	U/UE	CTAU
8.0000	95.201	0.98470	0.29013E-01
8.1000	94.856	0.98113	0.21579E-01
8.2000	94.394	0.97636	0.14685E-01
8.3000	94.163	0.97396	0.74734E-02
8.4000	93.931	0.97156	0.86445E-03
8.5000	93.464	0.96674	-0.28436E-02
8.6000	93.113	0.96310	-0.25159E-02
8.7000	92.525	0.95702	-0.23913E-02
8.8000	91.814	0.94967	-0.19402E-02
8.9000	91.098	0.94226	-0.64373E-03
9.0000	90.376	0.93479	-0.31501E-03
9.1000	89.891	0.92978	-0.19467E-03
9.2000	89.404	0.92474	0.22751E-03
9.3000	88.914	0.91967	0.14039E-02
9.4000	87.926	0.90945	0.17159E-02

YPOSITION	U	U/UE	CTAU
9.5000	87.303	0.90301	0.22577E-02
9.6000	86.549	0.89521	0.26050E-02
9.7000	85.406	0.88339	0.31841E-02
9.8000	84.636	0.87542	0.39863E-02
9.9000	83.335	0.86197	0.45878E-02
10.000	82.413	0.85243	0.49874E-02
10.100	81.212	0.84000	0.50012E-02
10.200	80.129	0.82880	0.51411E-02
10.300	79.307	0.82030	0.57613E-02
10.400	78.616	0.81315	0.60524E-02
10.500	77.497	0.80158	0.66503E-02
10.600	76.647	0.79278	0.69061E-02
10.700	75.931	0.78538	0.71687E-02
10.800	74.917	0.77490	0.72238E-02
10.900	74.332	0.76884	0.72426E-02
11.000	73.445	0.75967	0.74339E-02
11.100	72.548	0.75039	0.74504E-02
11.200	71.791	0.74256	0.71090E-02
11.300	71.180	0.73624	0.69998E-02
11.400	70.409	0.72827	0.65547E-02
11.500	69.472	0.71858	0.58992E-02
11.600	68.841	0.71205	0.53576E-02
11.700	68.363	0.70711	0.47808E-02

YPOSITION	U	U/UE	CTAU
11.800	68.203	0.70545	0.40954E-02
11.900	67.882	0.70213	0.32723E-02
12.000	67.073	0.69376	0.24903E-02
12.100	66.583	0.68869	0.17116E-02
12.200	66.583	0.68869	0.86933E-03
12.300	66.254	0.68529	0.0
12.400	66.583	0.68869	0.86933E-03
12.500	66.747	0.69039	0.17116E-02
12.600	66.747	0.69039	0.24903E-02
12.700	66.910	0.69208	0.32723E-02
12.800	67.398	0.69712	0.40954E-02
12.900	67.721	0.70047	0.47808E-02
13.000	68.043	0.70379	0.53576E-02
13.100	68.523	0.70876	0.58992E-02
13.200	69.472	0.71858	0.65547E-02
13.300	70.254	0.72666	0.69998E-02
13.400	70.719	0.73147	0.71090E-02
13.500	71.791	0.74256	0.74504E-02
13.600	72.548	0.75039	0.74339E-02
13.700	73.297	0.75813	0.72426E-02
13.800	74.332	0.76884	0.72238E-02
13.900	75.353	0.77941	0.71687E-02
14.000	76.218	0.78835	0.69061E-02

YPOSITION	U	U/UE	CTAU
14.100	77.214	0.79866	0.66503E-02
14.200	77.918	0.80594	0.60524E-02
14.300	78.893	0.81602	0.57613E-02
14.400	79.582	0.82315	0.51411E-02
14.500	80.672	0.83442	0.50012E-02
14.600	81.881	0.84693	0.49874E-02
14.700	82.810	0.85653	0.45878E-02
14.800	83.597	0.86468	0.39863E-02
14.900	84.248	0.87140	0.31841E-02
15.000	85.022	0.87941	0.26050E-02
15.100	85.916	0.88866	0.22577E-02
15.200	86.675	0.89651	0.17159E-02
15.300	87.553	0.90559	0.14039E-02
15.400	87.926	0.90945	0.22751E-03
15.500	88.668	0.91713	-0.19467E-03
15.600	89.526	0.92600	-0.31501E-03
15.700	90.255	0.93354	-0.64373E-03
15.800	90.497	0.93604	-0.19402E-02
15.900	91.098	0.94226	-0.23913E-02
16.000	91.814	0.94967	-0.25159E-02
16.100	92.407	0.95580	-0.28436E-02
16.200	93.113	0.96310	0.86445E-03
16.300	93.464	0.96674	0.74734E-02

YPOSITION	U	U/UE	CTAU
16.400	94.047	0.97276	0.14685E-01
16.500	94.394	0.97636	0.21579E-01
16.600	94.971	0.98232	0.29013E-01
16.700	95.315	0.98588	0.36189E-01
16.800	95.430	0.98707	0.43153E-01
16.900	95.772	0.99061	0.50521E-01
17.000	96.114	0.99414	0.57989E-01
17.100	96.454	0.99766	0.65534E-01
17.200	96.680	1.0000	0.73081E-01

AXIAL STATION 6OUT OF11STATIONS

DELSTAR= 0.82007E-01 THETA= 0.61036E-01
 SHAPE= 1.3436 EPSILON=-0.45972

YPOSITION	U	U/UE	CTAU
7.0000	88.668	1.0000	0.21442E-01
7.1000	88.298	0.99582	0.14304E-01
7.2000	87.802	0.99023	0.10441E-01
7.3000	87.303	0.98460	0.10802E-01
7.4000	86.801	0.97894	0.10953E-01
7.5000	86.549	0.97610	0.11374E-01
7.6000	86.043	0.97039	0.11416E-01
7.7000	85.916	0.96896	0.11314E-01
7.8000	85.278	0.96177	0.11695E-01
7.9000	84.893	0.95743	0.11851E-01
8.0000	84.248	0.95015	0.11767E-01
8.1000	83.858	0.94575	0.11917E-01
8.2000	83.204	0.93838	0.11910E-01
8.3000	82.810	0.93393	0.12130E-01
8.4000	82.413	0.92946	0.12167E-01

YPOSITION	U	U/UE	CTAU
8.5000	81.614	0.92045	0.12165E-01
8.6000	81.212	0.91591	0.12339E-01
8.7000	80.537	0.90830	0.12359E-01
8.8000	79.856	0.90062	0.12394E-01
8.9000	79.031	0.89132	0.12211E-01
9.0000	78.477	0.88506	0.11825E-01
9.1000	77.778	0.87718	0.11492E-01
9.2000	77.214	0.87082	0.11494E-01
9.3000	76.647	0.86442	0.11451E-01
9.4000	75.931	0.85635	0.11079E-01
9.5000	75.353	0.84984	0.10962E-01
9.6000	74.479	0.83997	0.10839E-01
9.7000	74.038	0.83500	0.10846E-01
9.8000	73.297	0.82664	0.10551E-01
9.9000	72.698	0.81989	0.10456E-01
10.000	71.791	0.80966	0.10196E-01
10.100	71.027	0.80104	0.99077E-02
10.200	69.786	0.78705	0.94778E-02
10.300	69.157	0.77996	0.90279E-02
10.400	68.523	0.77280	0.87613E-02
10.500	67.721	0.76376	0.84548E-02
10.600	66.910	0.75461	0.82124E-02
10.700	65.924	0.74349	0.78351E-02

YPOSITION	U	U/UE	CTAU
10.800	65.258	0.73598	0.74000E-02
10.900	64.754	0.73030	0.69317E-02
11.000	64.076	0.72265	0.64454E-02
11.100	63.045	0.71102	0.60206E-02
11.200	62.523	0.70514	0.55181E-02
11.300	61.821	0.69722	0.48194E-02
11.400	61.289	0.69121	0.42327E-02
11.500	60.752	0.68516	0.37085E-02
11.600	59.846	0.67495	0.30982E-02
11.700	59.112	0.66667	0.24981E-02
11.800	58.927	0.66458	0.18643E-02
11.900	58.368	0.65828	0.12487E-02
12.000	58.368	0.65828	0.63569E-03
12.100	58.368	0.65828	0.0
12.200	58.368	0.65828	0.63569E-03
12.300	58.368	0.65828	0.12487E-02
12.400	58.368	0.65828	0.18643E-02
12.500	58.368	0.65828	0.24981E-02
12.600	58.368	0.65828	0.30982E-02
12.700	58.741	0.66249	0.37085E-02
12.800	58.741	0.66249	0.42327E-02
12.900	59.112	0.66667	0.48194E-02
13.000	60.029	0.67700	0.55181E-02

YPOSITION	U	U/UE	CTAU
13.100	60.391	0.68109	0.60206E-02
13.200	60.572	0.68313	0.64454E-02
13.300	61.110	0.68920	0.69317E-02
13.400	61.821	0.69722	0.74000E-02
13.500	62.523	0.70514	0.78351E-02
13.600	63.218	0.71297	0.82124E-02
13.700	63.734	0.71880	0.84548E-02
13.800	64.416	0.72648	0.87613E-02
13.900	65.090	0.73409	0.90279E-02
14.000	66.089	0.74536	0.94778E-02
14.100	67.073	0.75645	0.99077E-02
14.200	67.882	0.76558	0.10196E-01
14.300	68.682	0.77460	0.10456E-01
14.400	69.315	0.78174	0.10551E-01
14.500	70.254	0.79232	0.10846E-01
14.600	70.873	0.79931	0.10839E-01
14.700	71.639	0.80795	0.10962E-01
14.800	72.397	0.81650	0.11079E-01
14.900	73.445	0.82832	0.11451E-01
15.000	74.185	0.83666	0.11494E-01
15.100	74.917	0.84492	0.11492E-01
15.200	75.931	0.85635	0.11825E-01
15.300	76.931	0.86763	0.12211E-01

YPOSITION	U	U/UE	CTAU
15.400	77.778	0.87718	0.12394E-01
15.500	78.477	0.88506	0.12359E-01
15.600	79.169	0.89287	0.12339E-01
15.700	79.719	0.89907	0.12165E-01
15.800	80.401	0.90676	0.12167E-01
15.900	81.077	0.91439	0.12130E-01
16.000	81.614	0.92045	0.11910E-01
16.100	82.281	0.92796	0.11917E-01
16.200	82.810	0.93393	0.11767E-01
16.300	83.466	0.94133	0.11851E-01
16.400	83.988	0.94722	0.11695E-01
16.500	84.377	0.95161	0.11314E-01
16.600	85.022	0.95888	0.11416E-01
16.700	85.534	0.96465	0.11374E-01
16.800	85.789	0.96753	0.10953E-01
16.900	86.170	0.97183	0.10802E-01
17.000	86.423	0.97468	0.10441E-01
17.100	86.927	0.98036	0.14304E-01
17.200	87.178	0.98319	0.21442E-01
17.300	87.553	0.98742	0.28880E-01
17.400	87.802	0.99023	0.36230E-01
17.500	87.926	0.99163	0.43491E-01
17.600	88.174	0.99443	0.50901E-01

YPOSITION	U	U/UE	CTAU
17.700	88.298	0.99582	0.58261E-01
17.800	88.298	0.99582	0.65568E-01
17.900	88.298	0.99582	0.72874E-01
18.000	88.298	0.99582	0.80150E-01

AXIAL STATION 70UT OF11STATIONS

DELSTAR= 0.79455E-01 THETA= 0.59835E-01
 SHAPE= 1.3279 EPSILON= -2.9388

YPOSITION	U	U/UE	CTAU
6.7000	82.148	0.99201	-0.12377E-02
6.8000	82.148	0.99201	-0.23824E-03
6.9000	82.148	0.99201	0.71903E-03
7.0000	82.015	0.99040	0.16487E-02
7.1000	81.748	0.98718	0.23760E-02
7.2000	81.480	0.98395	0.30282E-02
7.3000	81.212	0.98071	0.35627E-02
7.4000	80.808	0.97582	0.40229E-02
7.5000	80.537	0.97255	0.44790E-02
7.6000	79.993	0.96598	0.49555E-02
7.7000	79.582	0.96102	0.53310E-02
7.8000	79.169	0.95604	0.57110E-02
7.9000	78.754	0.95103	0.61139E-02
8.0000	78.616	0.94935	0.64920E-02
8.1000	77.918	0.94093	0.68763E-02

YPOSITION	U	U/UE	CTAU
8.2000	77.356	0.93414	0.72368E-02
8.3000	76.931	0.92901	0.75094E-02
8.4000	76.218	0.92040	0.78274E-02
8.5000	75.787	0.91519	0.81003E-02
8.6000	75.353	0.90996	0.83832E-02
8.7000	75.063	0.90645	0.86918E-02
8.8000	74.332	0.89763	0.90085E-02
8.9000	73.147	0.88332	0.92563E-02
9.0000	72.848	0.87971	0.94651E-02
9.1000	71.943	0.86878	0.96519E-02
9.2000	71.487	0.86326	0.97304E-02
9.3000	70.719	0.85399	0.97174E-02
9.4000	70.098	0.84650	0.97541E-02
9.5000	69.472	0.83894	0.97935E-02
9.6000	68.999	0.83323	0.98120E-02
9.7000	68.203	0.82362	0.98067E-02
9.8000	67.236	0.81193	0.97918E-02
9.9000	66.419	0.80207	0.97507E-02
10.000	65.592	0.79208	0.96684E-02
10.100	64.922	0.78400	0.95211E-02
10.200	64.076	0.77377	0.93578E-02
10.300	63.391	0.76550	0.91779E-02
10.400	62.698	0.75713	0.89408E-02

YPOSITION	U	U/UE	CTAU
10.500	62.173	0.75080	0.86147E-02
10.600	61.467	0.74226	0.82760E-02
10.700	60.572	0.73146	0.79241E-02
10.800	59.846	0.72270	0.75584E-02
10.900	59.112	0.71383	0.72158E-02
11.000	58.368	0.70485	0.68307E-02
11.100	57.993	0.70032	0.63364E-02
11.200	57.615	0.69576	0.57592E-02
11.300	57.235	0.69116	0.51747E-02
11.400	56.660	0.68422	0.46513E-02
11.500	55.884	0.67484	0.41139E-02
11.600	55.688	0.67248	0.35491E-02
11.700	55.294	0.66773	0.30172E-02
11.800	55.096	0.66534	0.24857E-02
11.900	54.898	0.66294	0.19563E-02
12.000	54.898	0.66294	0.14557E-02
12.100	54.499	0.65812	0.96901E-03
12.200	54.298	0.65570	0.48494E-03
12.300	54.699	0.66053	0.0
12.400	54.898	0.66294	0.48494E-03
12.500	54.699	0.66053	0.96901E-03
12.600	55.096	0.66534	0.14557E-02
12.700	55.294	0.66773	0.19563E-02

YPOSITION	U	U/UE	CTAU
12.800	55.294	0.66773	0.24857E-02
12.900	55.491	0.67011	0.30172E-02
13.000	55.688	0.67248	0.35491E-02
13.100	56.079	0.67720	0.41139E-02
13.200	56.660	0.68422	0.46513E-02
13.300	57.235	0.69116	0.51747E-02
13.400	57.805	0.69804	0.57592E-02
13.500	57.993	0.70032	0.63364E-02
13.600	58.741	0.70936	0.68307E-02
13.700	59.297	0.71606	0.72158E-02
13.800	59.846	0.72270	0.75584E-02
13.900	60.572	0.73146	0.79241E-02
14.000	61.289	0.74012	0.82760E-02
14.100	61.997	0.74867	0.86147E-02
14.200	62.698	0.75713	0.89408E-02
14.300	63.391	0.76550	0.91779E-02
14.400	64.076	0.77377	0.93578E-02
14.500	64.922	0.78400	0.95211E-02
14.600	65.924	0.79609	0.96684E-02
14.700	66.583	0.80405	0.97507E-02
14.800	67.236	0.81193	0.97918E-02
14.900	67.882	0.81974	0.98067E-02
15.000	68.523	0.82747	0.98120E-02

YPOSITION	U	U/UE	CTAU
15.100	69.157	0.83514	0.97935E-02
15.200	69.942	0.84462	0.97541E-02
15.300	70.564	0.85212	0.97174E-02
15.400	71.487	0.86326	0.97304E-02
15.500	72.246	0.87244	0.96519E-02
15.600	72.848	0.87971	0.94651E-02
15.700	73.445	0.88692	0.92563E-02
15.800	74.038	0.89407	0.90085E-02
15.900	74.479	0.89940	0.86918E-02
16.000	74.917	0.90469	0.83832E-02
16.100	75.498	0.91171	0.81003E-02
16.200	76.218	0.92040	0.78274E-02
16.300	76.789	0.92729	0.75094E-02
16.400	77.497	0.93584	0.72368E-02
16.500	77.918	0.94093	0.68763E-02
16.600	78.337	0.94599	0.64920E-02
16.700	78.754	0.95103	0.61139E-02
16.800	79.169	0.95604	0.57110E-02
16.900	79.856	0.96433	0.53310E-02
17.000	80.537	0.97255	0.49555E-02
17.100	80.808	0.97582	0.44790E-02
17.200	81.077	0.97908	0.40229E-02
17.300	81.480	0.98395	0.35627E-02

YPOSITION	U	U/UE	CTAU
17.400	81.881	0.98879	0.30282E-02
17.500	82.148	0.99201	0.23760E-02
17.600	82.413	0.99521	0.16487E-02
17.700	82.413	0.99521	0.71903E-03
17.800	82.545	0.99681	-0.23824E-03
17.900	82.810	1.0000	-0.12377E-02
18.000	82.545	0.99681	-0.26319E-02
18.100	82.678	0.99841	-0.68925E-02
18.200	82.281	0.99361	-0.14543E-01
18.300	81.748	0.98718	-0.18756E-01
18.400	81.480	0.98395	-0.19046E-01
18.500	80.129	0.96763	-0.20509E-01

AXIAL STATION 8OUT OF11STATIONS

DELSTAR= 0.67435E-01 THETA= 0.52687E-01
SHAPE= 1.2799 EPSILON= 0.30954

YPOSITION	U	U/UE	CTAU
7.3000	81.614	1.0000	-0.63340E-01
7.4000	81.346	0.99672	-0.57170E-01
7.5000	81.077	0.99342	-0.51119E-01
7.6000	80.672	0.98846	-0.45193E-01
7.7000	80.401	0.98514	-0.39580E-01
7.8000	79.993	0.98013	-0.34114E-01
7.9000	79.719	0.97678	-0.28668E-01
8.0000	79.169	0.97004	-0.23192E-01
8.1000	78.754	0.96496	-0.19844E-01
8.2000	78.198	0.95814	-0.18900E-01
8.3000	77.637	0.95127	-0.17841E-01
8.4000	77.073	0.94435	-0.16883E-01
8.5000	76.647	0.93913	-0.16001E-01
8.6000	76.218	0.93388	-0.14916E-01
8.7000	75.787	0.92860	-0.14019E-01

YPOSITION	U	U/UE	CTAU
8.8000	75.063	0.91973	-0.13131E-01
8.9000	74.625	0.91437	-0.12242E-01
9.0000	74.038	0.90717	-0.11520E-01
9.1000	73.297	0.89809	-0.10844E-01
9.2000	72.698	0.89075	-0.99374E-02
9.3000	72.397	0.88707	-0.90598E-02
9.4000	71.943	0.88150	-0.81930E-02
9.5000	71.334	0.87403	-0.74942E-02
9.6000	70.564	0.86460	-0.66464E-02
9.7000	69.942	0.85699	-0.59595E-02
9.8000	69.315	0.84930	-0.52870E-02
9.9000	68.682	0.84154	-0.46414E-02
10.000	67.882	0.83175	-0.41782E-02
10.100	67.073	0.82183	-0.37672E-02
10.200	66.419	0.81381	-0.32632E-02
10.300	65.592	0.80368	-0.28685E-02
10.400	65.258	0.79959	-0.23475E-02
10.500	64.754	0.79342	-0.17450E-02
10.600	64.076	0.78511	-0.14166E-02
10.700	63.218	0.77460	-0.10489E-02
10.800	62.523	0.76608	-0.79692E-03
10.900	62.173	0.76179	-0.80793E-03
11.000	61.467	0.75314	-0.73721E-03

YPOSITION	U	U/UE	CTAU
11.100	61.289	0.75096	-0.58493E-03
11.200	60.931	0.74658	-0.35559E-03
11.300	60.391	0.73996	-0.88427E-04
11.400	59.846	0.73328	-0.21659E-04
11.500	59.112	0.72429	0.52478E-04
11.600	58.741	0.71975	0.61218E-04
11.700	58.368	0.71518	0.89787E-04
11.800	57.993	0.71058	0.11539E-03
11.900	57.805	0.70827	0.12397E-03
12.000	57.615	0.70595	0.90204E-04
12.100	57.615	0.70595	0.53299E-04
12.200	57.615	0.70595	0.0
12.300	57.615	0.70595	0.53299E-04
12.400	57.615	0.70595	0.90204E-04
12.500	57.615	0.70595	0.12397E-03
12.600	57.805	0.70827	0.11539E-03
12.700	57.993	0.71058	0.89787E-04
12.800	58.181	0.71288	0.61218E-04
12.900	58.368	0.71518	0.52478E-04
13.000	58.927	0.72202	-0.21659E-04
13.100	59.297	0.72655	-0.88427E-04
13.200	60.029	0.73552	-0.35559E-03
13.300	60.572	0.74217	-0.58493E-03

YPOSITION	U	U/UE	CTAU
13.400	60.931	0.74658	-0.73721E-03
13.500	61.110	0.74877	-0.80793E-03
13.600	61.110	0.74877	-0.79692E-03
13.700	61.644	0.75531	-0.10489E-02
13.800	62.349	0.76394	-0.14166E-02
13.900	62.872	0.77035	-0.17450E-02
14.000	63.734	0.78092	-0.23475E-02
14.100	64.416	0.78927	-0.28685E-02
14.200	64.922	0.79548	-0.32632E-02
14.300	65.592	0.80368	-0.37672E-02
14.400	66.089	0.80978	-0.41782E-02
14.500	66.583	0.81583	-0.46414E-02
14.600	67.236	0.82383	-0.52870E-02
14.700	67.882	0.83175	-0.59595E-02
14.800	68.523	0.83959	-0.66464E-02
14.900	69.315	0.84930	-0.74942E-02
15.000	69.942	0.85699	-0.81930E-02
15.100	70.719	0.86650	-0.90598E-02
15.200	71.487	0.87591	-0.99374E-02
15.300	72.246	0.88522	-0.10844E-01
15.400	72.698	0.89075	-0.11520E-01
15.500	73.147	0.89626	-0.12242E-01
15.600	73.742	0.90354	-0.13131E-01

Y POSITION	U	U/UE	CTAU
15.700	74.332	0.91077	-0.14019E-01
15.800	74.917	0.91795	-0.14916E-01
15.900	75.643	0.92683	-0.16001E-01
16.000	76.218	0.93388	-0.16883E-01
16.100	76.789	0.94088	-0.17841E-01
16.200	77.356	0.94782	-0.18900E-01
16.300	77.778	0.95299	-0.19844E-01
16.400	78.337	0.95985	-0.23192E-01
16.500	78.893	0.96666	-0.28668E-01
16.600	79.307	0.97173	-0.34114E-01
16.700	79.582	0.97510	-0.39580E-01
16.800	79.856	0.97846	-0.45193E-01
16.900	80.537	0.98680	-0.51119E-01
17.000	80.943	0.99177	-0.57170E-01
17.100	81.212	0.99507	-0.63340E-01
17.200	81.212	0.99507	-0.69717E-01
17.300	81.346	0.99672	-0.76122E-01
17.400	81.346	0.99672	-0.82760E-01
17.500	81.346	0.99672	-0.89497E-01
17.600	81.346	0.99672	-0.96298E-01
17.700	81.212	0.99507	-0.10335
17.800	80.808	0.99012	-0.11096
17.900	80.265	0.98347	-0.11888

AXIAL STATION 90UT OF11STATIONS

DELSTAR= 0.47823E-01 THETA= 0.39288E-01
 SHAPE= 1.2173 EPSILON= 0.48032E-01

YPOSITION	U	U/UE	CTAU
7.7000	87.926	1.0000	-0.39580E-01
7.8000	87.802	0.99859	-0.34114E-01
7.9000	87.802	0.99859	-0.28668E-01
8.0000	87.802	0.99859	-0.23192E-01
8.1000	87.553	0.99575	-0.40279E-01
8.2000	87.178	0.99149	-0.34131E-01
8.3000	86.675	0.98577	-0.28353E-01
8.4000	86.297	0.98147	-0.22974E-01
8.5000	85.916	0.97714	-0.16867E-01
8.6000	85.662	0.97424	-0.13105E-01
8.7000	85.150	0.96843	-0.12416E-01
8.8000	84.506	0.96111	-0.11289E-01
8.9000	83.858	0.95373	-0.10272E-01
9.0000	83.335	0.94779	-0.92452E-02
9.1000	82.810	0.94181	-0.88272E-02

YPOSITION	U	U/UE	CTAU
9.2000	82.148	0.93428	-0.78797E-02
9.3000	81.614	0.92821	-0.70323E-02
9.4000	80.943	0.92057	-0.65540E-02
9.5000	80.265	0.91287	-0.55940E-02
9.6000	79.582	0.90510	-0.49410E-02
9.7000	78.893	0.89727	-0.43205E-02
9.8000	78.198	0.88936	-0.39534E-02
9.9000	77.778	0.88458	-0.38356E-02
10.000	77.073	0.87656	-0.32520E-02
10.100	76.504	0.87009	-0.28734E-02
10.200	75.787	0.86194	-0.25036E-02
10.300	75.208	0.85536	-0.17242E-02
10.400	74.479	0.84706	-0.11302E-02
10.500	73.890	0.84037	-0.95594E-03
10.600	73.147	0.83192	-0.99051E-03
10.700	72.698	0.82681	-0.69541E-03
10.800	72.246	0.82167	-0.43559E-03
10.900	71.791	0.81650	-0.16042E-03
11.000	71.180	0.80955	0.59586E-04
11.100	70.719	0.80430	0.20526E-03
11.200	70.254	0.79901	0.46175E-03
11.300	69.786	0.79369	0.56383E-03
11.400	69.315	0.78833	0.62771E-03

Y POSITION	U	U/UE	CTAU
11.500	68.841	0.78294	0.74705E-03
11.600	68.682	0.78113	0.91718E-03
11.700	68.043	0.77387	0.85716E-03
11.800	67.560	0.76837	0.70577E-03
11.900	67.398	0.76653	0.52145E-03
12.000	67.236	0.76469	0.36699E-03
12.100	67.236	0.76469	0.18904E-03
12.200	67.236	0.76469	0.0
12.300	67.236	0.76469	0.18904E-03
12.400	67.236	0.76469	0.36699E-03
12.500	67.398	0.76653	0.52145E-03
12.600	67.398	0.76653	0.70577E-03
12.700	67.398	0.76653	0.85716E-03
12.800	67.560	0.76837	0.91718E-03
12.900	68.203	0.77569	0.74705E-03
13.000	68.682	0.78113	0.62771E-03
13.100	68.999	0.78474	0.56383E-03
13.200	69.315	0.78833	0.46175E-03
13.300	69.786	0.79369	0.20526E-03
13.400	70.098	0.79724	0.59586E-04
13.500	70.564	0.80254	-0.16042E-03
13.600	71.180	0.80955	-0.43559E-03
13.700	71.791	0.81650	-0.69541E-03

YPOSITION	U	U/UE	CTAU
13.800	72.397	0.82339	-0.99051E-03
13.900	72.698	0.82681	-0.95594E-03
14.000	73.147	0.83192	-0.11302E-02
14.100	73.890	0.84037	-0.17242E-02
14.200	74.771	0.85039	-0.25036E-02
14.300	75.353	0.85701	-0.28734E-02
14.400	75.931	0.86358	-0.32520E-02
14.500	76.647	0.87172	-0.38356E-02
14.600	77.073	0.87656	-0.39534E-02
14.700	77.637	0.88298	-0.43205E-02
14.800	78.337	0.89095	-0.49410E-02
14.900	79.031	0.89884	-0.55940E-02
15.000	79.856	0.90822	-0.65540E-02
15.100	80.401	0.91442	-0.70323E-02
15.200	81.077	0.92211	-0.78797E-02
15.300	81.748	0.92973	-0.88272E-02
15.400	82.148	0.93428	-0.92452E-02
15.500	82.810	0.94181	-0.10272E-01
15.600	83.466	0.94928	-0.11289E-01
15.700	84.118	0.95669	-0.12416E-01
15.800	84.506	0.96111	-0.13105E-01
15.900	85.150	0.96843	-0.16867E-01
16.000	85.789	0.97569	-0.22974E-01



YPOSITION	U	U/UE	CTAU
16.100	86.043	0.97858	-0.28353E-01
16.200	86.423	0.98290	-0.34131E-01
16.300	86.927	0.98864	-0.40279E-01

AXIAL STATIONLOOUT OF11STATIONS

DELSTAR= 0.26115E-01 THETA= 0.23554E-01
 SHAPE= 1.1328 EPSILON= 0.17211

YPOSITION	U	U/UE	CTAU
8.9000	100.34	1.0000	-0.15654E-02
9.0000	100.12	0.99783	-0.99975E-03
9.1000	99.902	0.99565	-0.50849E-03
9.2000	99.683	0.99347	0.12028E-03
9.3000	99.134	0.98800	0.67192E-03
9.4000	98.692	0.98360	0.11427E-02
9.5000	98.249	0.97918	0.15293E-02
9.6000	97.692	0.97362	0.18550E-02
9.7000	97.131	0.96804	0.21310E-02
9.8000	96.454	0.96129	0.23839E-02
9.9000	95.886	0.95563	0.29671E-02
10.000	95.315	0.94994	0.33507E-02
10.100	94.625	0.94306	0.35611E-02
10.200	94.047	0.93730	0.37251E-02
10.300	93.230	0.92916	0.38268E-02

YPOSITION	U	U/UE	CTAU
10.400	92.525	0.92213	0.39259E-02
10.500	91.933	0.91623	0.40628E-02
10.600	91.337	0.91029	0.42053E-02
10.700	90.858	0.90551	0.41941E-02
10.800	90.376	0.90071	0.42588E-02
10.900	89.770	0.89467	0.42878E-02
11.000	89.159	0.88859	0.41045E-02
11.100	88.545	0.88246	0.39099E-02
11.200	87.802	0.87506	0.36179E-02
11.300	87.052	0.86759	0.33376E-02
11.400	86.801	0.86509	0.30554E-02
11.500	86.423	0.86132	0.26738E-02
11.600	86.297	0.86006	0.22193E-02
11.700	86.043	0.85753	0.17785E-02
11.800	85.789	0.85500	0.13468E-02
11.900	85.662	0.85373	0.92727E-03
12.000	85.662	0.85373	0.45930E-03
12.100	85.662	0.85373	0.0
12.200	85.662	0.85373	0.45930E-03
12.300	85.534	0.85246	0.92727E-03
12.400	85.662	0.85373	0.13468E-02
12.500	85.662	0.85373	0.17785E-02
12.600	85.662	0.85373	0.22193E-02

YPOSITION	U	U/UE	CTAU
12.700	85.662	0.85373	0.26738E-02
12.800	85.789	0.85500	0.30554E-02
12.900	86.043	0.85753	0.33376E-02
13.000	86.297	0.86006	0.36179E-02
13.100	86.549	0.86257	0.39099E-02
13.200	86.927	0.86634	0.41045E-02
13.300	87.303	0.87009	0.42878E-02
13.400	87.926	0.87630	0.42588E-02
13.500	88.545	0.88246	0.41941E-02
13.600	89.037	0.88737	0.42053E-02
13.700	89.648	0.89346	0.40628E-02
13.800	90.255	0.89951	0.39259E-02
13.900	90.858	0.90551	0.38268E-02
14.000	91.457	0.91148	0.37251E-02
14.100	92.052	0.91741	0.35611E-02
14.200	92.643	0.92331	0.33507E-02
14.300	93.347	0.93033	0.29671E-02
14.400	94.163	0.93845	0.23839E-02
14.500	94.741	0.94421	0.21310E-02
14.600	95.315	0.94994	0.18550E-02
14.700	95.886	0.95563	0.15293E-02
14.800	96.454	0.96129	0.11427E-02
14.900	97.019	0.96692	0.67192E-03

YPOSITION	U	U/UE	CTAU
15.000	97.580	0.97251	0.12028E-03
15.100	98.138	0.97807	-0.50849E-03
15.200	98.582	0.98249	-0.99975E-03
15.300	99.024	0.98690	-0.15654E-02
15.400	99.574	0.99238	-0.24614E-02
15.500	99.793	0.99456	-0.57225E-02
15.600	100.01	0.99674	-0.12031E-01
15.700	100.23	0.99891	-0.18452E-01

AXIAL STATION11OUT OF11STATIONS

DELSTAR= 0.15577E-01 THETA= 0.14397E-01
 SHAPE= 1.0820 EPSILON= 0.29195

YPOSITION	U	U/UE	CTAU
9.3000	112.35	1.0000	0.0
9.4000	112.25	0.99913	0.0
9.5000	111.86	0.99567	0.0
9.6000	111.38	0.99131	0.0
9.7000	110.88	0.98694	0.0
9.8000	110.39	0.98255	0.0
9.9000	109.90	0.97813	0.0
10.000	109.50	0.97459	0.0
10.100	109.00	0.97014	0.0
10.200	108.60	0.96657	0.0
10.300	108.19	0.96298	0.0
10.400	107.48	0.95667	0.0
10.500	106.97	0.95214	0.0
10.600	106.36	0.94667	0.0
10.700	105.74	0.94118	0.0

YPOSITION	U	U/UE	CTAU
10.800	105.23	0.93657	0.0
10.900	104.81	0.93287	0.0
11.000	104.39	0.92915	0.0
11.100	103.97	0.92542	0.0
11.200	103.66	0.92261	0.0
11.300	103.34	0.91979	0.0
11.400	103.02	0.91697	0.0
11.500	102.70	0.91413	0.0
11.600	102.39	0.91129	0.0
11.700	102.06	0.90844	0.0
11.800	101.74	0.90558	0.0
11.900	101.53	0.90366	0.0
12.000	101.42	0.90271	0.0
12.100	101.42	0.90271	0.0
12.200	101.42	0.90271	0.0
12.300	101.42	0.90271	0.0
12.400	101.42	0.90271	0.0
12.500	101.42	0.90271	0.0
12.600	101.42	0.90271	0.0
12.700	101.53	0.90366	0.0
12.800	101.74	0.90558	0.0
12.900	101.96	0.90748	0.0
13.000	102.28	0.91034	0.0

YPOSITION	U	U/UE	CTAU
13.100	102.60	0.91319	0.0
13.200	102.92	0.91602	0.0
13.300	103.23	0.91885	0.0
13.400	103.55	0.92167	0.0
13.500	103.87	0.92448	0.0
13.600	104.18	0.92729	0.0
13.700	104.60	0.93101	0.0
13.800	105.02	0.93472	0.0
13.900	105.64	0.94026	0.0
14.000	106.26	0.94576	0.0
14.100	106.87	0.95123	0.0
14.200	107.38	0.95577	0.0
14.300	107.89	0.96028	0.0
14.400	108.50	0.96567	0.0
14.500	108.90	0.96925	0.0
14.600	109.30	0.97281	0.0
14.700	109.70	0.97636	0.0
14.800	110.09	0.97990	0.0
14.900	110.39	0.98255	0.0
15.000	110.79	0.98606	0.0
15.100	111.08	0.98869	0.0
15.200	111.38	0.99131	0.0
15.300	111.77	0.99480	0.0

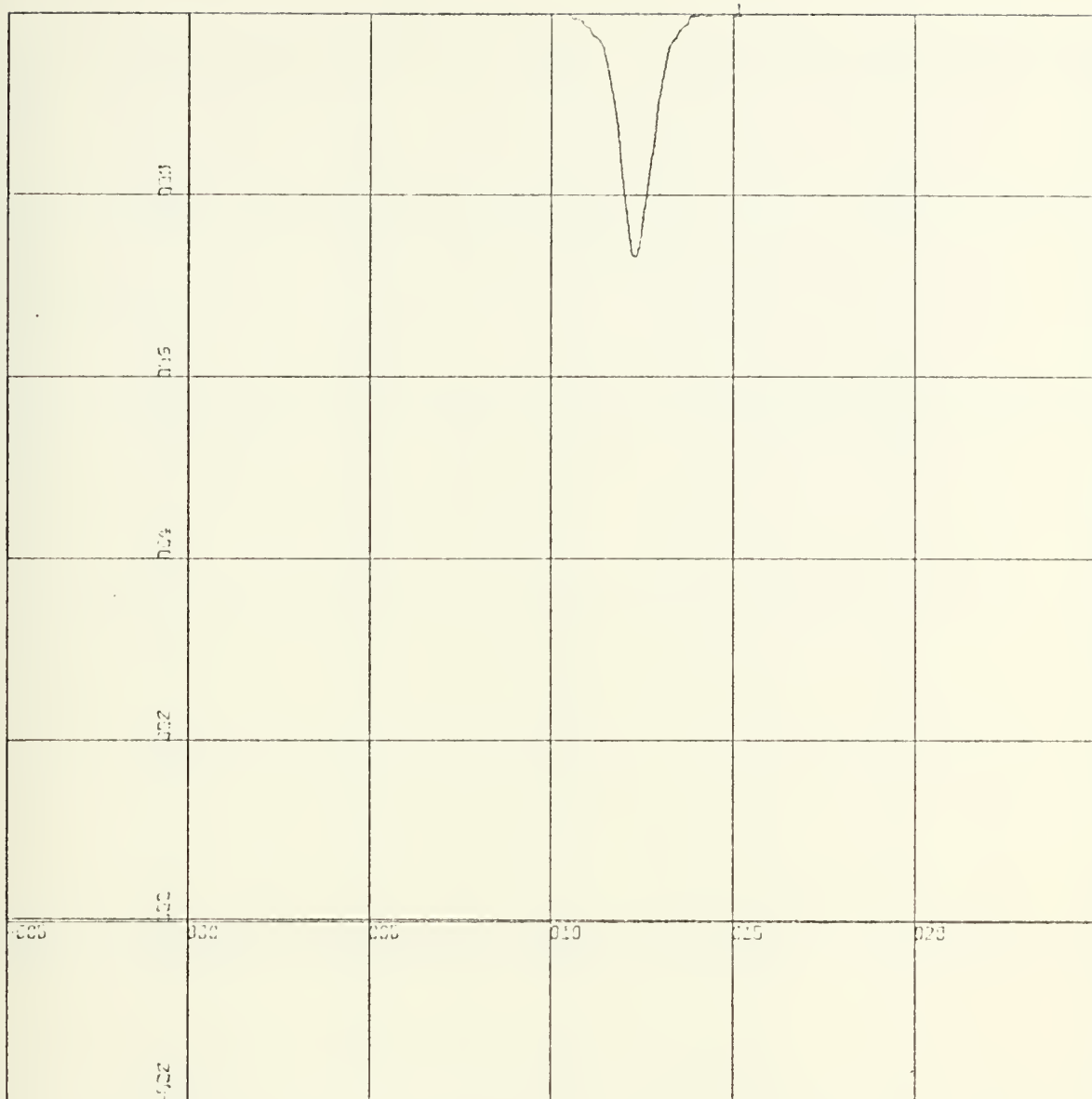
YPOSITION	U	U/UE	CTAU
15.400	111.86	0.99567	0.0
15.500	111.86	0.99567	0.0

SUMMARY OF INTEGRATED WAKE PROPERTIES

AXIAL STATION	X/D	DELSTAR	DEL RATIO	THETA	THETA RATIO	SHAPE
1	3.8125	0.12447E-01	1.0000	0.10270E-01	1.0000	1.2120
2	8.8125	0.19818E-01	1.5921	0.16468E-01	1.6034	1.2034
3	13.812	0.29650E-01	2.3821	0.24545E-01	2.3898	1.2080
4	18.812	0.40497E-01	3.2535	0.32596E-01	3.1738	1.2424
5	23.813	0.62057E-01	4.9855	0.48019E-01	4.6754	1.2923
6	28.812	0.82007E-01	6.5883	0.61036E-01	5.9429	1.3436
7	33.812	0.79455E-01	6.3833	0.59835E-01	5.8259	1.3279
8	38.813	0.67435E-01	5.4176	0.52687E-01	5.1299	1.2799
9	43.812	0.47823E-01	3.8421	0.39288E-01	3.8253	1.2173
10	48.812	0.25115E-01	2.0980	0.23054E-01	2.2447	1.1328
11	53.813	0.15577E-01	1.2515	0.14397E-01	1.4017	1.0820

TURBULENCE CHECKS

STATION	ETA	MU(X)	EPSILON	MASS FLOW
1	-0.9769	0.0424	0.5624	19.4819
2	-0.9814	0.0289	0.5460	28.2630
3	-0.9934	0.0118	0.1489	28.4597
4	-1.0009	-0.0032	-0.0900	30.9617
5	-1.0000	-0.0062	-0.0993	33.2085
6	-1.0000	-0.0187	-0.4597	36.0769
7	-1.0000	-0.0287	-2.9388	32.5661
8	-1.0000	-0.0197	0.3095	31.6917
9	-1.0000	-0.0092	0.0480	25.5959
10	-1.0002	-0.0092	0.1721	28.0386
11	-1.0000	0.0	0.2920	28.8358

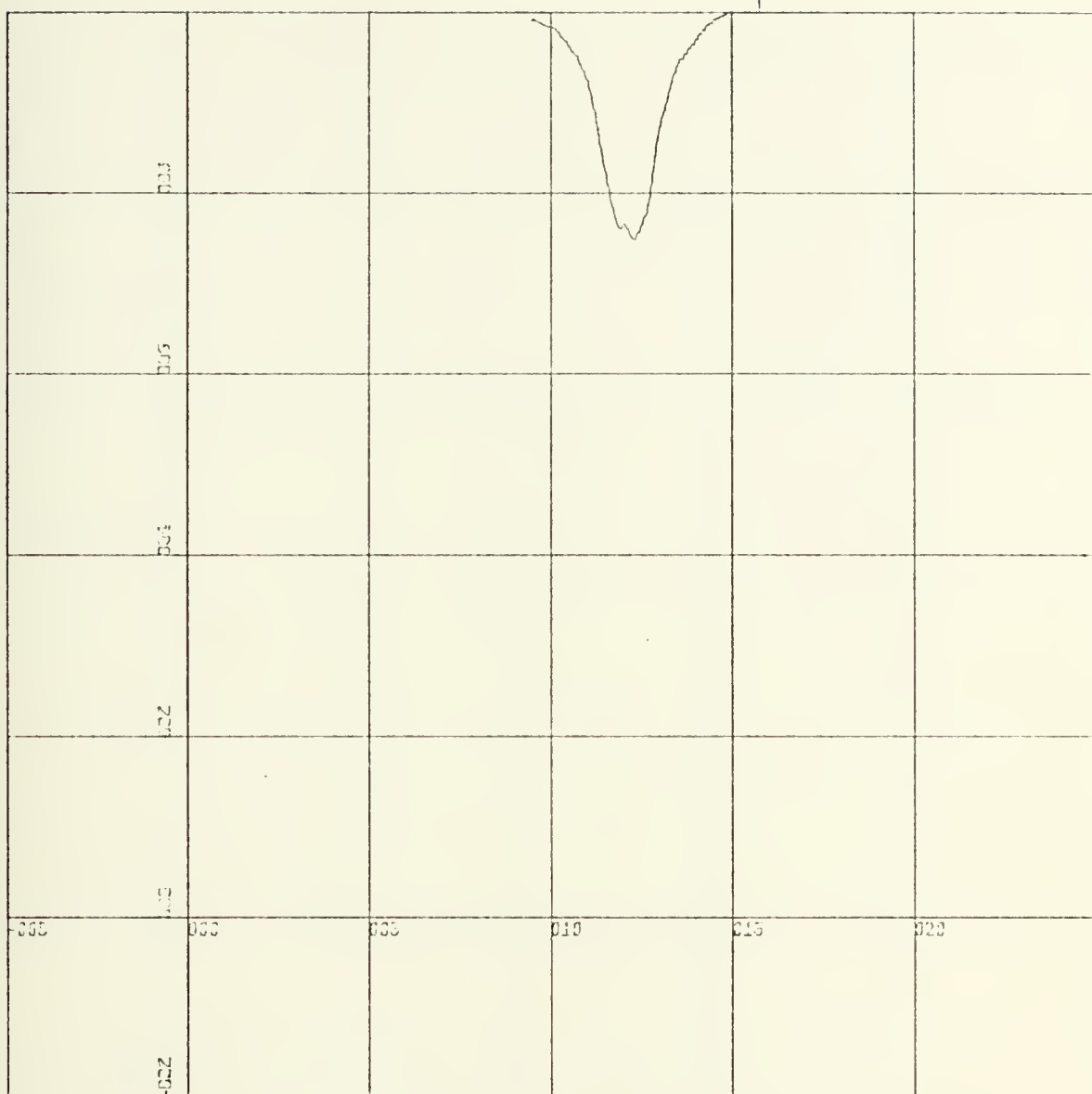


Station 1

X-SCALE=5.00E+00 UNITS INCH.

Y-SCALE=2.00E-01 UNITS INCH.

A PLOT OF THE PITOT-STATIC
VELOCITY RATIO VERSUS POSITION

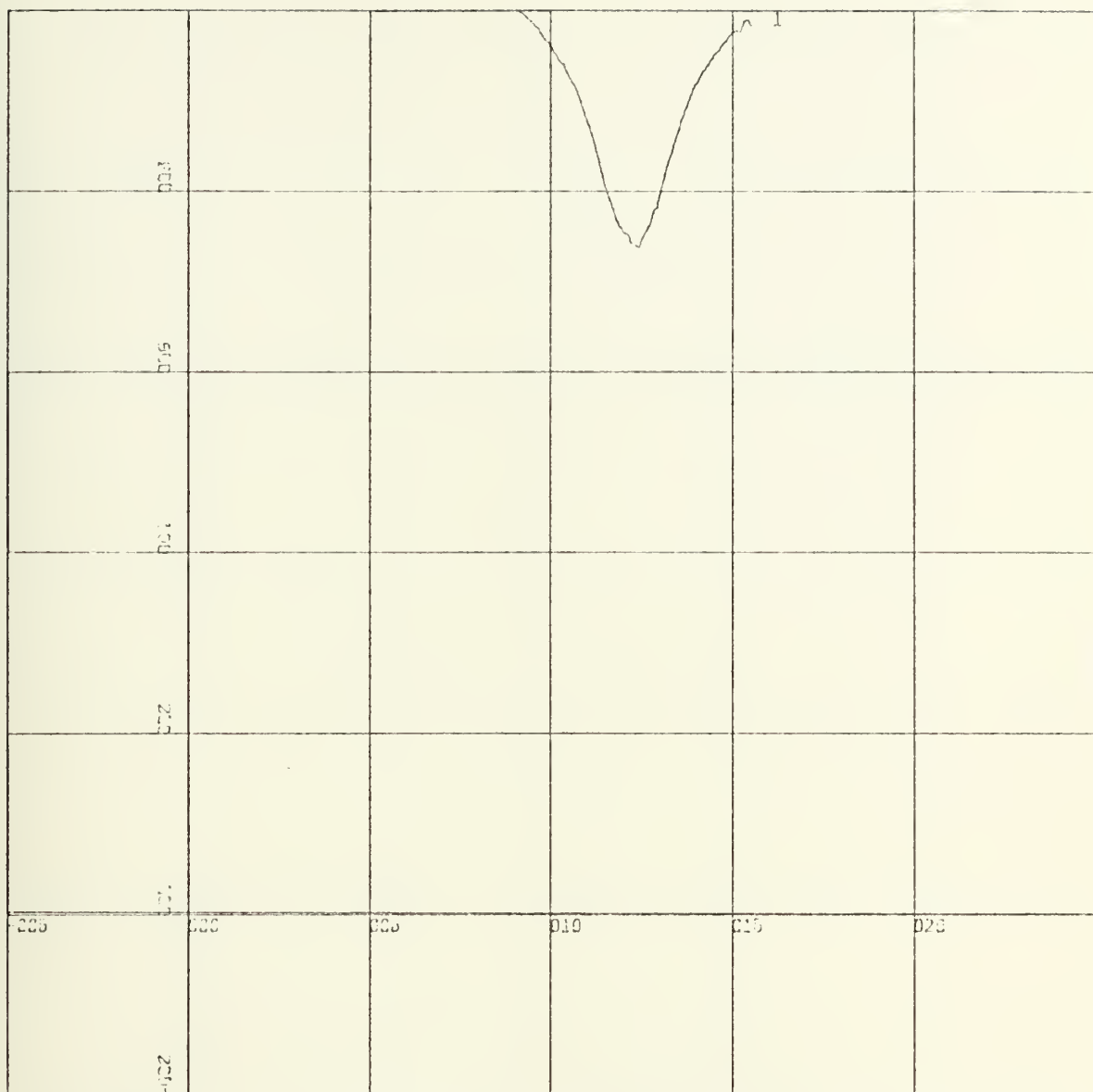


Station 2

X-SCALE:=5.00E+00 UNITS INCH.

Y-SCALE:=2.00E-01 UNITS INCH.

A PLOT OF THE PITOT-STATIC
VELOCITY RATIO VERSUS POSITION

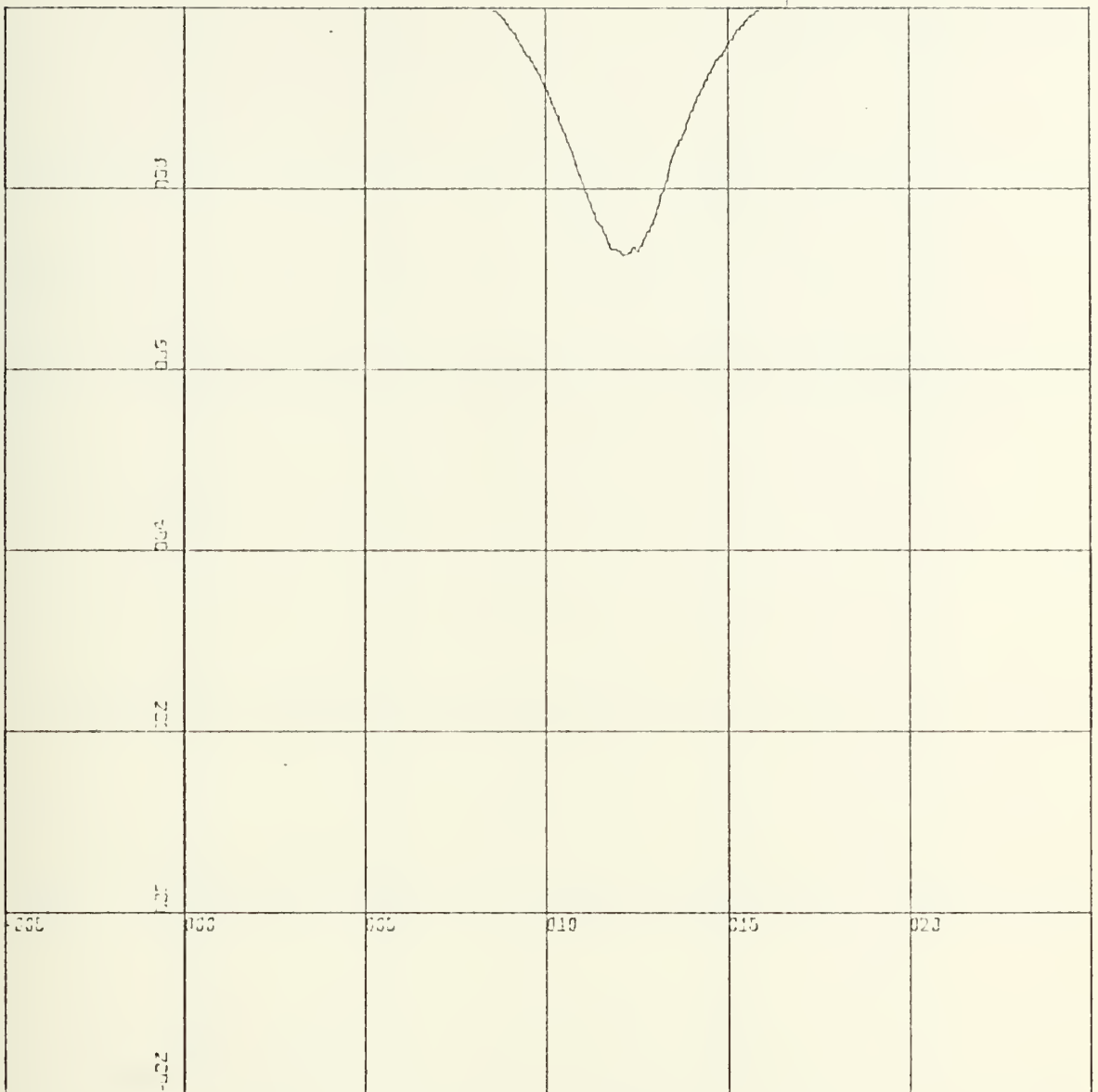


Station 3

X-SCALE=5.00E+00 UNITS INCH.

Y-SCALE=2.00E-01 UNITS INCH.

A PLOT OF THE PITOT-STATIC
VELOCITY RATIO VERSUS POSITION

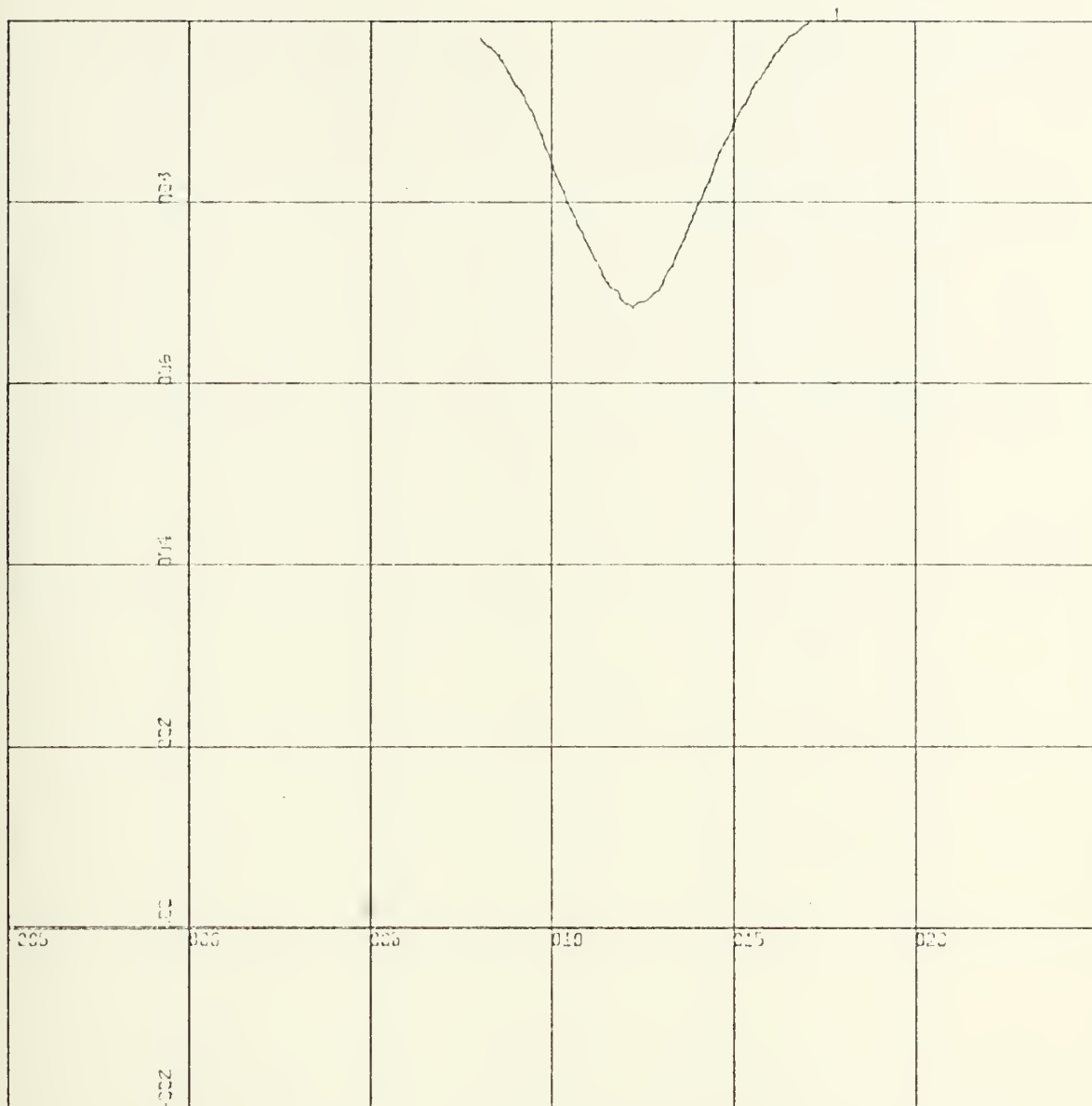


Station 4

X-SCALE=5.00E+00 UNITS INCH.

Y-SCALE=2.00E-01 UNITS INCH.

A PLOT OF THE PITOT-STATIC
VELOCITY RATIO VERSUS POSITION

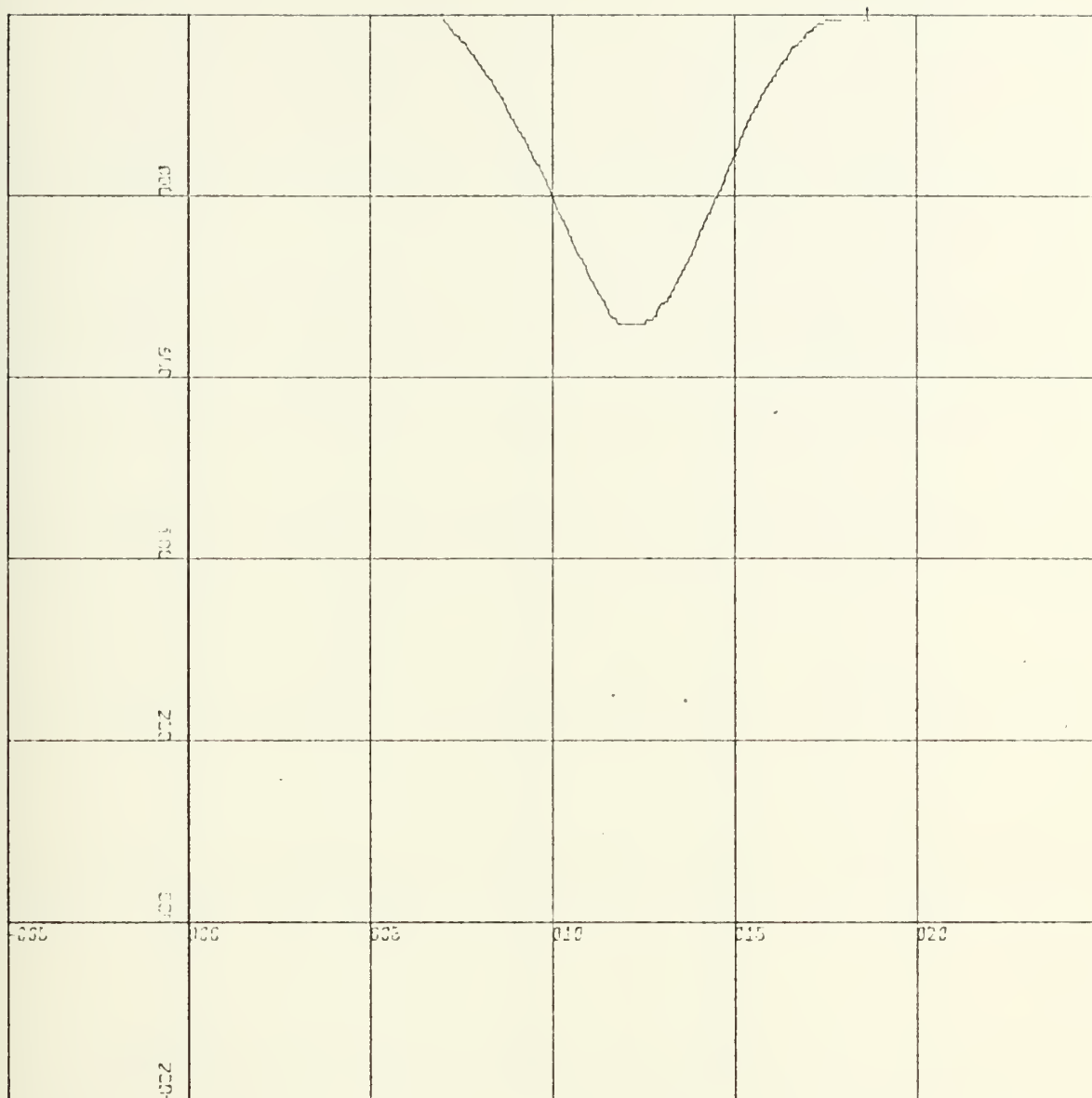


Station 5

X-SCALE: 5.00E+00 UNITS INCH.

Y-SCALE: 2.00E-01 UNITS INCH.

A PLOT OF THE PITOT-STATIC
VELOCITY RATIO VERSUS POSITION

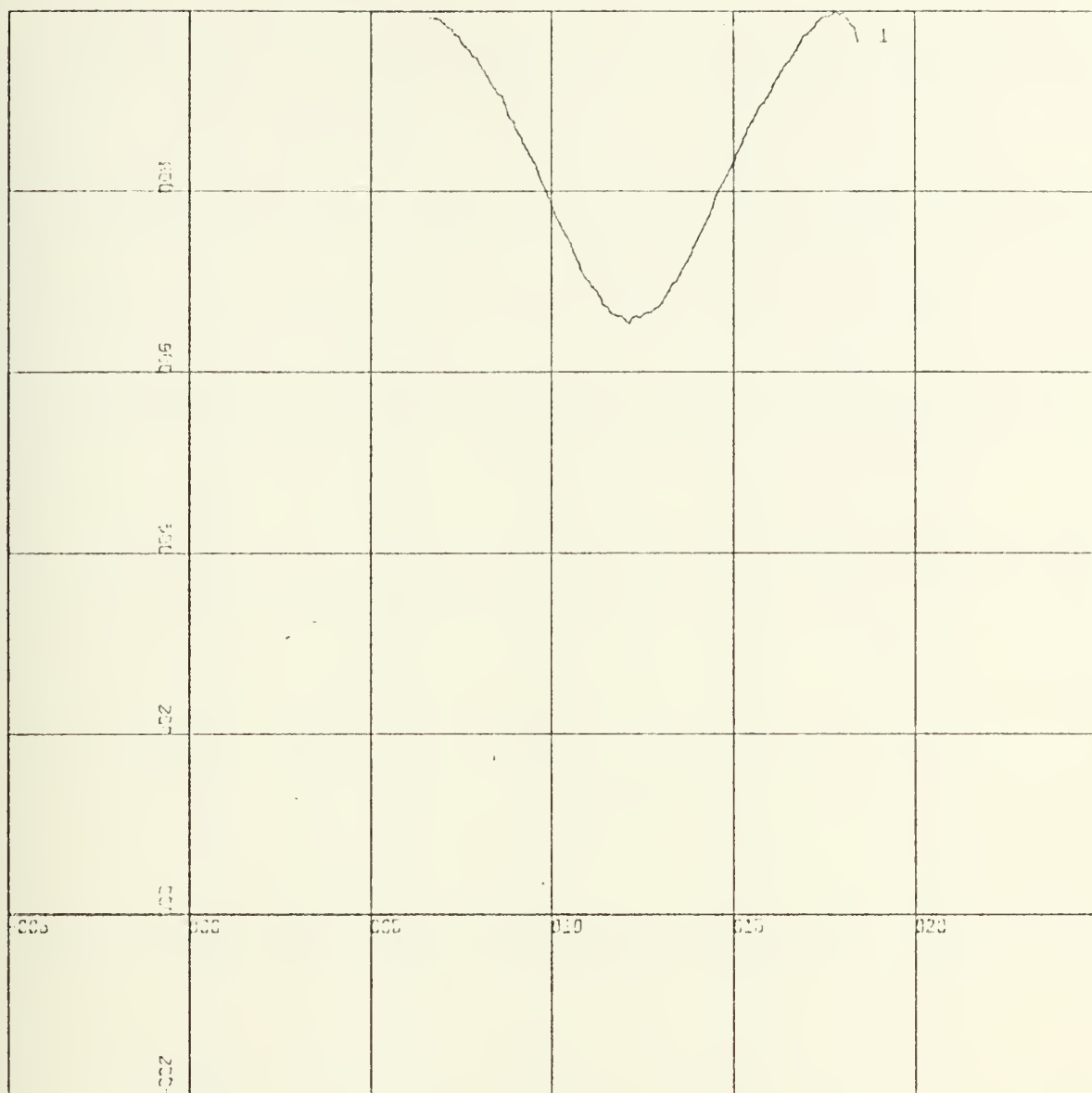


Station 6

X-SCALE=5.00E+00 UNITS INCH.

Y-SCALE=2.00E-01 UNITS INCH.

A PLOT OF THE PITOT-STATIC
VELOCITY RATIO VERSUS POSITION

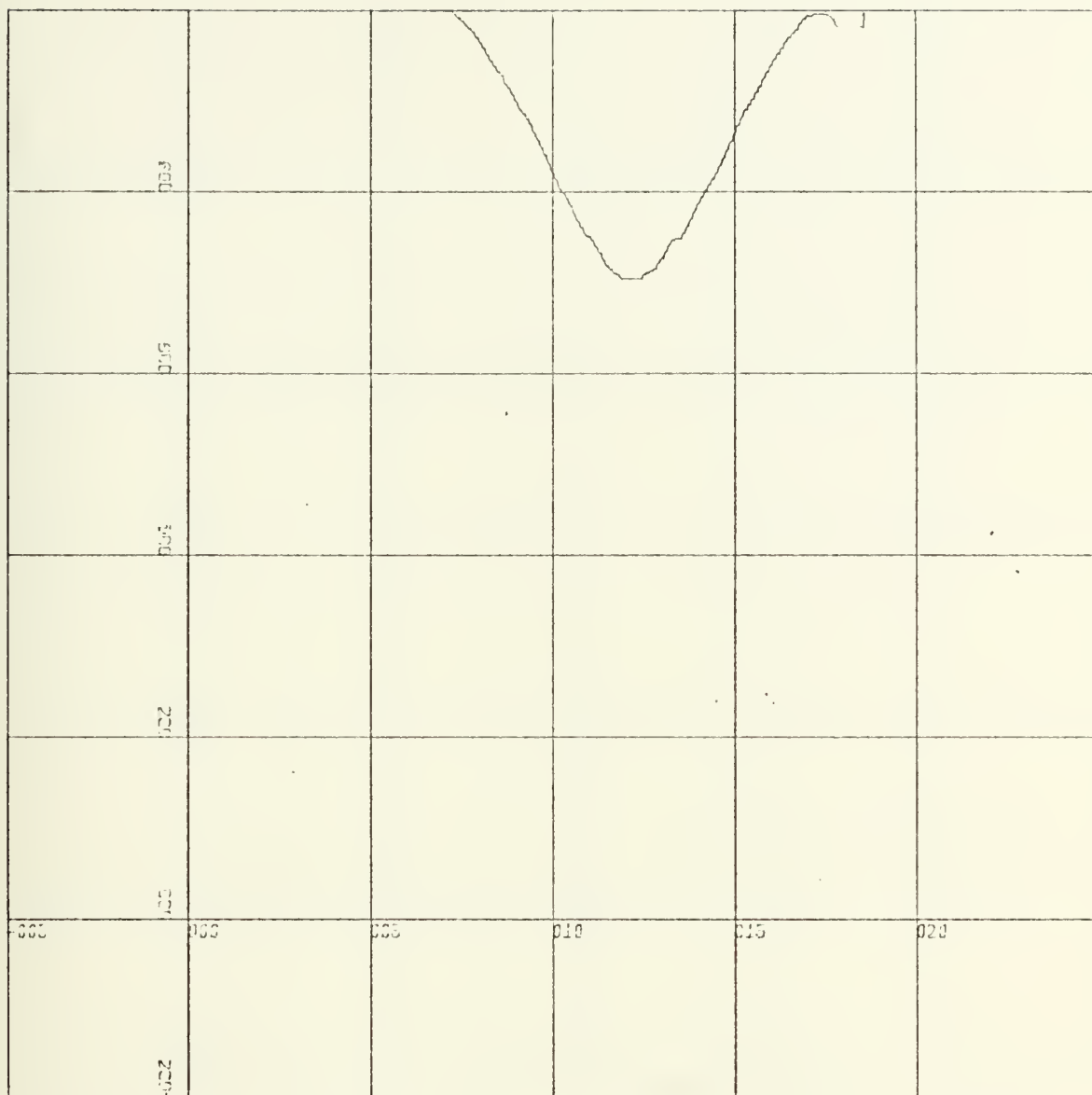


Station 7

X-SCALE=5.00E+00 UNITS INCH.

Y-SCALE=2.00E-01 UNITS INCH.

A PLOT OF THE PITOT-STATIC
VELOCITY RATIO VERSUS POSITION

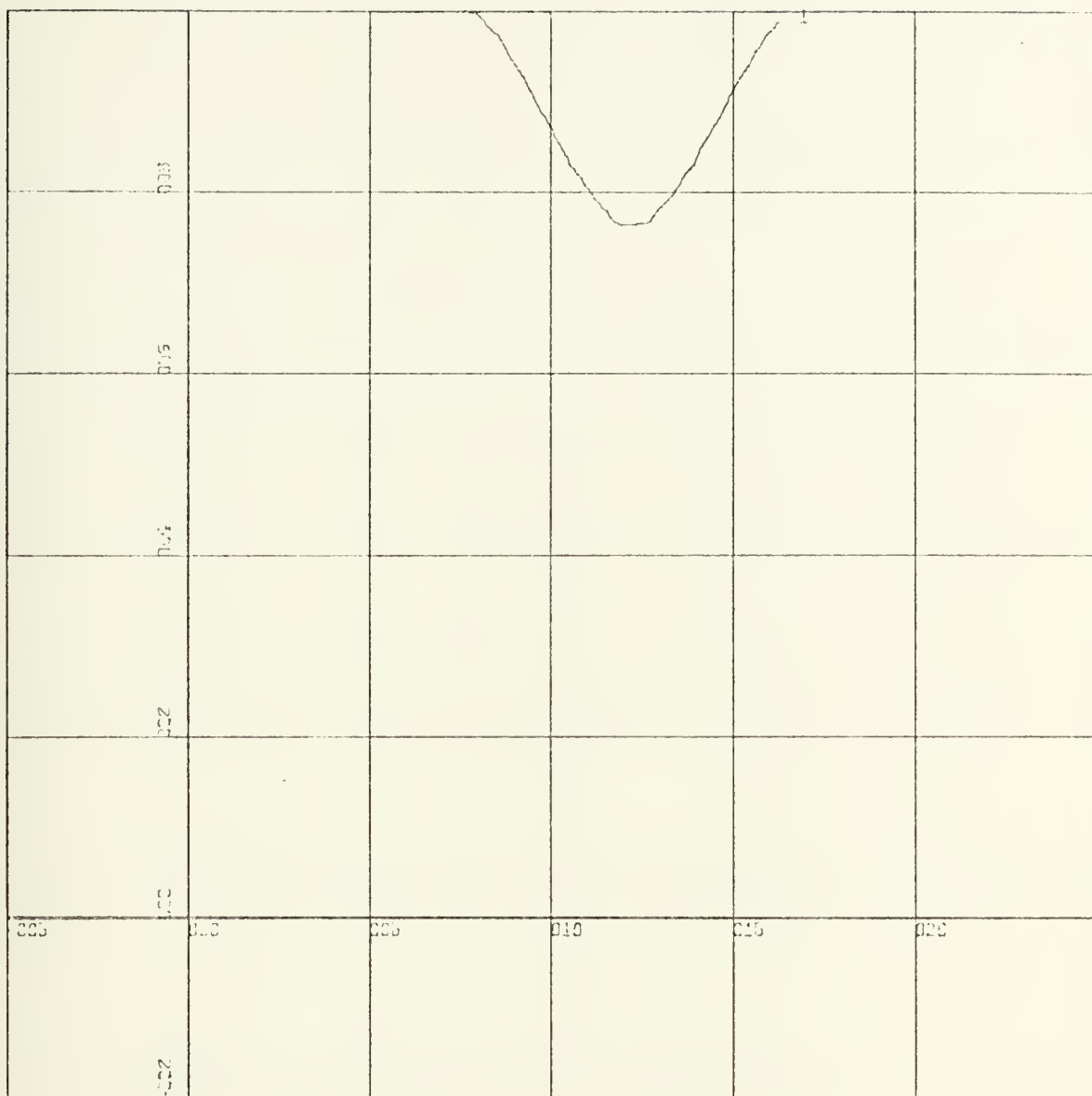


Station 8

X-SCALE=5.00E+00 UNITS INCH.

Y-SCALE=2.00E-01 UNITS INCH.

A PLOT OF THE PITOT-STATIC
VELOCITY RATIO VERSUS POSITION

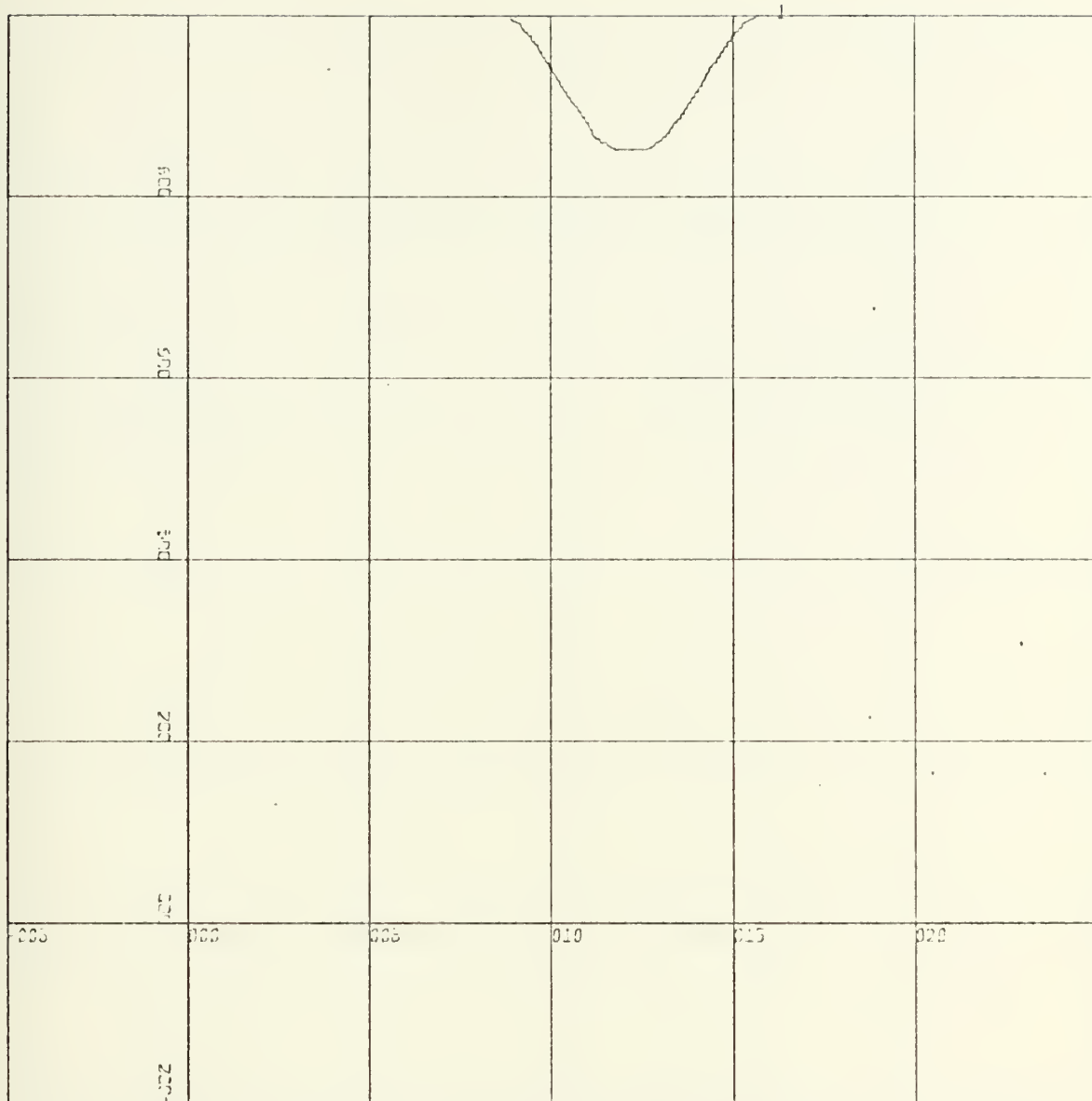


Station 9

X-SCALE=5.00E+00 UNITS INCH.

Y-SCALE=2.00E-01 UNITS INCH.

A PLOT OF THE PITOT-STATIC
VELOCITY RATIO VERSUS POSITION

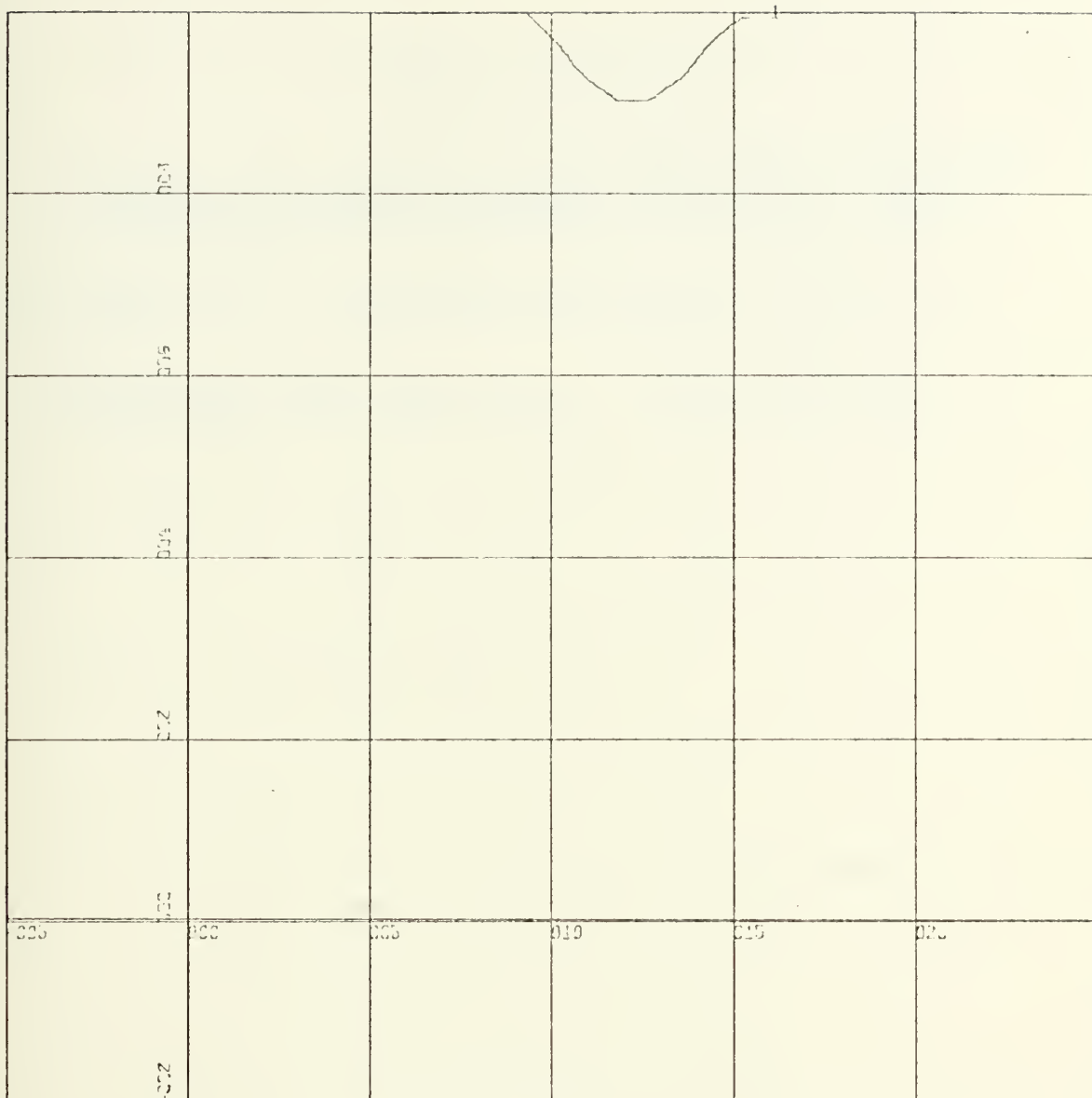


Station 10

X-SCALE=5.00E+00 UNITS INCH.

Y-SCALE=2.00E-01 UNITS INCH.

A PLOT OF THE PITOT-STATIC
VELOCITY RATIO VERSUS POSITION



Station 11

X-SCALE:-5.00E+00 UNITS INCH.

Y-SCALE:-2.00E-01 UNITS INCH.

A PLOT OF THE PITOT-STATIC
VELOCITY RATIO VERSUS POSITION

LIST OF REFERENCES

1. Anderson, T.E., A Study of Turbulent Wakes in Constant Streamwise Pressure Gradients, MSAE Thesis, Naval Postgraduate School, Monterey, California, 1972.
2. Schlichting, H., Boundary-Layer Theory, McGraw-Hill, 1968.
3. Tennekes, H. and Lumley, J. L., A First Course in Turbulence, MIT Press, 1972.

INITIAL DISTRIBUTION LIST

	No. Copies
1. Defense Documentation Center Cameron Station Alexandria, Virginia 22314	2
2. Library, Code 0212 Naval Postgraduate School Monterey, California 93940	2
3. Professor R. W. Bell, Code 57 BE Department of Aeronautics Naval Postgraduate School Monterey, California 93940	1
4. Asst. Professor G. J. Hokenson, Code 57 Hw Department of Aeronautics Naval Postgraduate School Monterey, California 93940	2
5. LT Michael E. Kearney, USN 220 W. Main St. Barstow, California	1

DOCUMENT CONTROL DATA - R & D

(Security classification of title, body of abstract and indexing annotation must be entered when the overall report is classified)

1. ORIGINATING ACTIVITY (Corporate author)

Naval Postgraduate School
Monterey, California 93940

2a. REPORT SECURITY CLASSIFICATION

Unclassified

2b. GROUP

3. REPORT TITLE

A Hot-Wire Anemometer Study of Free Turbulent Mixing in
Axial Pressure Gradients

4. DESCRIPTIVE NOTES (Type of report and, inclusive dates)

Master's Thesis; December 1972

5. AUTHOR(S) (First name, middle initial, last name)

Michael Erwin Kearney

6. REPORT DATE

December 1972

7a. TOTAL NO. OF PAGES

256

7b. NO. OF REFS

3

8a. CONTRACT OR GRANT NO.

b. PROJECT NO.

c.

d.

9a. ORIGINATOR'S REPORT NUMBER(S)

9b. OTHER REPORT NO(S) (Any other numbers that may be assigned
this report)

10. DISTRIBUTION STATEMENT

Approved for public release; distribution unlimited.

11. SUPPLEMENTARY NOTES

12. SPONSORING MILITARY ACTIVITY

Naval Postgraduate School
Monterey, California 93940

13. ABSTRACT

This report was prepared to describe the results of an experimental study of free turbulent mixing in axial pressure gradients. Both the pressure field and the velocity field were extracted using pitot-static probes and both a single normal wire and an X-array hot-wire anemometers. The resulting hot-wire data shown in Figures 1-80 present an excellent visual representation of the physical aspects of turbulent flow.

An analysis of the results of this experiment show conclusively that the Reynolds Stresses in the flow are related by some function to the turbulent kinetic energy; however, no specific function was found that would produce the relationship observed in this study.

KEY WORDS

LINK A

LINK B

LINK C

ROLE

WT

ROLE

WT

ROLE

WT

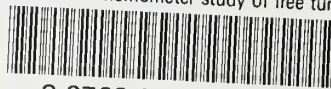
hot-wire anemometer
free turbulent mixing
axial pressure gradients

Thesis 141315
K14965 Kearny
c.1 A hot-wire anemometer
study of free turbulent
mixing in axial pressure
gradients.

Thesis 141315
K14965 Kearny
c.1 A hot-wire anemometer
study of free turbulent
mixing in axial pressure
gradients.

thesK14965

A hot-wire anemometer study of free turb



3 2768 002 11174 2

DUDLEY KNOX LIBRARY